IgE in immunotherapy of cancer

Bracher, Marguerite

IgE in immunotherapy of cancer

by

Marguerite Bracher

A thesis submitted in partial fulfilment of the
requirements for the degree of
Doctor of Philosophy in the University of London

The Randall Centre,
Division of Biomedical Sciences,
King's College London,
New Hunt's House, London, SE1 1UL

June 2005

Contents

Abstract

The focus of this thesis is to assess the ability of an IgE-isotype tumour-specific antibody, MOv18 IgE, to trigger cytotoxic immune responses against tumour cells. Currently, all tumour-specific antibodies approved by the FDA for treatment of cancer in patients, belong to IgG1 or IgG2 subclasses. It is proposed that IgE may be more effective than IgG *in vivo*, its potential having previously been underestimated due to poor performances in *in vitro* cytotoxicity assays. Results presented in this thesis suggest that IgE does in fact trigger effective immune responses against tumour cells both *in vitro* and *in vivo*. *In vitro* data has been obtained using a novel flow cytometric cytotoxicity / phagocytosis assay, the set-up of which is described. *In vivo* data has been obtained using a nude mouse xenograft model of ovarian cancer. The set-up of two new *in vivo* models is also described. These will be used to test efficacy and safety of IgE immunotherapy of cancer.

The proposed *in vivo* efficacy of tumour-specific IgE antibodies is based largely on the location of IgE-receptor-expressing cells in the body and the extremely high affinity of the interaction between IgE and its receptor FcεRI, of ~ 10^{10} M^{-1}. This high affinity interaction results in a binding half-life of IgE to FcεRI on mast cells in tissues in the order of weeks, compared to days for IgG. In allergic individuals, the effect of this tenacious retention of allergen-specific IgE on mast cells is a state of persistent hypersensitisation against allergen challenge. The IgE-FcεRI interaction is therefore a valid therapeutic target for blocking agents in allergy, a task made almost impossible however, by the large surface area of the interaction. The final aim of this thesis was to determine whether reducing the affinity of IgE binding to FcεRI could have biological effects *in vivo*. The result was that a reduction in IgE-FcεRI affinity of as little as 33-fold significantly reduced the intensity of passive cutaneous anaphylaxis *in vivo*. This result has major therapeutic implications for allergy.

Acknowledgements

The work described in this Thesis could not have been done without the contributions of so many people, to whom I am extremely grateful. Firstly, I would like to say thank you to my supervisors, Hannah Gould and Brian Sutton, for giving me the opportunity to work on this project, and for all their help, advice and enthusiasm over the last three and a half years. I have also been lucky enough to spend one year, working on this project, at the Pasteur Institute in Lille, France, where I was supervised by David Dombrowicz. Much of the work described in this Thesis has been done on a collaborative basis with David, and I would like to thank him for giving me so much time and help, to make my year in France so productive. Work described in this Thesis has also been done on a collaborative basis with the groups of Frances Balkwill, St. Bartholomew's Hospital, Charterhouse Square, London; Silvana Canevari, Istituto Tumori, Milan, Italy; and, J.-P. Kinet, Harvard, Boston. I would like to thank all of those involved, from all three groups, for their contributions.

I would like to thank Sophia Karagiannis for all her help and advice with work performed as part of the MOv18 IgE project, and for allowing my use of her IL-4-treated U937 data, as well as for her immunofluorescent imaging, in this Thesis. I would also like to say thank you to Jianguo Shi for making the R334S mutant used for this work, as well as to James Hunt for the Biacore data he has contributed, and for the many helpful discussions regarding this work. Thanks also to Andrew Beavil, James Hunt and Melissa Corbett for the contributions they have made towards the purification of antibodies used in this project.

I would also like all those in Group 17 at the Randall, to know how much I appreciate their help, advice and friendship over the last few years. I would like to thank in particular, Rebecca and Andrew Beavil, Natalie McCloskey, Lyn Smurthwaite and James Hunt, who have each always been there to offer support and advice with so many different things. I am also grateful for the support given to me by members of David's group, at the Pasteur Institute Lille. I am particularly grateful to Sébastien Fleury, who enabled the continuation of the anaphylaxis work after I left Lille, as well as Gaetane Wöerly and Veronique Décot for their instruction in eosinophil purification, and Kohei Honda for his instruction on animal handling. I would also like to thank all of you who so generously gave me your blood for my experiments. Financial support for this project was provided by a King's College London Medical School grant, and my year in Lille was made possible by a Marie-Curie Fellowship.

List of Figures

List of Tables

List of Abbreviations

Abbreviation	Full name
ACD	Acid citrate dextrose
ADCC	Antibody-dependent cell mediated cytotoxicity
ADCP	Antibody-dependent cell mediated phagocytosis
ADCCP	Antibody-dependent cell mediated cytotoxicity and or phagocytosis
BCR	B cell receptor
CFSE	Carboxy-fluorescein succinyl ester
CSF	Colony stimulating factor
DMEM	Dulbecco's Modified Eagles Medium
EGF	Epidermal growth factor
EGFR	Epidermal growth factor receptor
FcεRI	High affinity Fc receptor for IgE
FcγR	Receptors for the Fc region of IgG, including FcγRI (CD64), FcγRII (CD32) or FcγRIII (CD16)
$F(ab')_2$	Fragment antigen-binding, created by pepsin digestion of an antibody
FBP / FR	Folate binding protein / Folate receptor
Fc	Fragment crystallisable, created by papain digestion of an antibody
FCS	Foetal calf serum
FCM	Flow cytometry
FDA	Food and Drug Administration
FITC	Fluorescein isothiocyanate
GM-CSF	Granulocyte macrophage colony stimulating factor
HIF-2α	Hypoxia-inducible factor-2α
HPLC	High performance liquid chromatography
hFcεRI Tg	Transgenic mouse expressing FcεRI composed of human α-chain in addition to mouse β and or γ_2-chains
IFN-γ	Interferon-γ
Ig	Immunoglobulin
IL	Interleukin
ITAM	Immuno-receptor tyrosine-based activation motif
ITIM	Immuno-receptor tyrosine-based inhibition motif
LDH	Lactate dehydrogenase
LTC_4	Leukotriene C_4

mAb	Monoclonal antibody
MCP-1	Monocyte chemotactic protein-1
MCSF	Macrophage colony stimulating factor
MHC	Major histocompatability complex
NIP(5)BSA	Bovine serum albumin coated with 5 molecules of the hapten, NIP
NK	Natural killer
PAF	Platelet activating factor
PBMC	Peripheral blood mononuclear cells
PBS(-T)	Phosphate-buffered saline (with Tween)
PCA	Passive cutaneous anaphylaxis
PE	Phycoerythrin
PGE_2	Prostaglandin-E_2
PI	Propidium Iodide
R1 / R2 / R3	Region 1 / Region 2 / Region 3
RBL-2H3	Rat basophilic leukaemia cells, clone 2H3
SCID	Severe combined immune deficiency
SDS-PAGE	Sodium dodecyl-sulphate polyacrylamide gel electrophoresis
SPR	Surface plasmon resonance
TAA	Tumour-associated antigen
TAM	Tumour-associated macrophage
TCR	T cell receptor
TGF-β	Transforming growth factor-β
TNF-α	Tumour-necrosis factor-α
VEGF	Vascular endothelial growth factor
WAG	Wistar Albino Glaxo

CHAPTER 1:

Introduction

Chapter 1: Introduction

Work described in this Thesis has been performed as part of a novel, ongoing study into the proposal that tumour-specific antibodies of the IgE isotype could be used to initiate a powerful immune response towards tumour cells in cancer patients. The immune response triggered by IgE is most commonly encountered in the form of a futile, allergic response towards innocuous allergens, although it is also known to offer protection from parasite infection. For many years it has been clear that the interaction between IgE and one of its receptors, FcεRI, is of extremely high affinity (Metzger, 1986). As discussed below, this high affinity interaction confers on IgE the ability to bind FcεRI tenaciously; this enables FcεRI-expressing mast cells in tissues and basophils in blood to respond immediately to a specific multivalent allergen (or cell-bound tumour antigen) challenge. Results of experiments described in this Thesis suggest that the high affinity of this interaction may also make a more direct contribution to the intensity of the cellular response, triggered by antigen-induced FcεRI cross-linking, as I have found a relationship between the affinity with which IgE binds FcεRI and the intensity of the subsequent cellular response. To aid discussion of these experiments, I have introduced the IgE-system, cancer, and the immunotherapeutic treatment of cancer with monoclonal antibodies. To highlight the challenge faced by anti-cancer antibodies in their role as tools for manipulating the immune system to kill tumour cells, I also discuss the nature of the complex relationship that exists between cancer cells and the immune system.

1.1 Cancer

It is very desirable that new approaches to cancer therapy be rapidly explored, as statistics provided by Cancer Research UK show that cancer causes more than one quarter of all deaths in the UK population (http://www.statistics.gov.uk). For men, cancers of the lung, prostate, colon and oesophagus are the four main causes, and for women, it is lung, breast, bowel and ovary.

1.1.1 The relationship between cancer and the immune system

It is a slow process by which a normal cell transforms into a malignant one, potentially taking many years. A transformed cell may arise from a small population of rapidly dividing, genetically unstable cells, through the acquisition of mutation(s) that prevent it from being eliminated by the immune system (Hanahan and Weinberg, 2000). The immune-resistant nature of this tumour cell leaves it free to develop into a mass of tumour cells until its increasing size dictates that nutritional and oxygen supplies be increased or

causes damage to surrounding normal host tissue; these are stress signals which initiate an innate, followed by an adaptive, immune response (Dunn *et al.*, 2002). This immune response may be unproductive for one of two reasons, despite, in some cases, expression of a unique tumour antigen. Firstly, a tumour may have already 'tolerised' T cells towards it; as tumour cells are essentially 'self', they do not send out distress signals or microbial immune-recognition patterns normally used by the immune system to recognise 'danger' (Matzinger, 1998). In this way, tumour cells avoid stimulating expression of co-stimulatory signals on either themselves, or local professional antigen-presenting cells (Janeway *et al.*, 4th edition). Co-stimulation is necessary to prevent T cell anergy or tolerance induction occurring upon interaction of a specific T cell receptor with tumour-antigen in the context of MHC. Alternatively, a tumour may be able to actively evade an immune response mediated towards it by one of a number of methods, discussed below. The immune system, therefore, inadvertently acts to select tumour cells with immune-resistant phenotypes. For a review of the process by which tumours develop under immunological pressure, see Dunn *et al.*, 2002.

Mechanisms used by tumour cells to avoid immune elimination (in addition to those used by normal host cells to avoid autoimmune attack) include methods for 'hiding' from, or actively manipulating immune responses. Examples include the loss or down-regulation of MHC class I antigens, in combination with mechanisms to inhibit NK cell function, loss of tumour antigen expression or the expression of defective death receptors. Alternatively, a tumour may secrete immunosuppressive cytokines that negatively affect maturation and function of immune cells, or induce apoptosis in tumour-specific activated T cells (for a review see Khong *et al.*, 2002). The outcome of an unproductive anti-tumour immune response is often a tumour infiltrated with many components of an immune response, with which it has a dynamic relationship, as discussed below.

1.1.2 Tumour-infiltrating leukocytes

A dominant tumour-infiltrating cell type is the macrophage. The relationship between tumour cells and tumour-associated macrophages (TAMs) has recently been reviewed by Pollard, 2004; earlier reviews have been made by Mantovani *et al.*, 1986 and 1992, and by Bingle *et al.*, 2002. Most TAMs are derived from peripheral blood monocytes, recruited from the circulation, although there is evidence for local macrophage proliferation (McBride, 1986). Paradoxically, although monocyte recruitment is mediated by the host as part of an anti-tumour immune response, it is also mediated by the tumour itself. Signals for monocyte recruitment include monocyte chemotactic protein-1 (MCP-1) and macrophage colony stimulating factor (M-CSF) (Pollard, 2004; Mantovani *et al.*, 1992). Other cell-types found infiltrating tumours include mast cells, eosinophils and neutrophils; these cell types

accumulate in response to both tumour- and TAM-derived chemoattractants, and are discussed below.

In the majority of cases, macrophage infiltration is associated with poor prognosis. This highlights the success of the tumour in suppression of anti-tumour macrophage functions. A tumour may create an immunosuppressive environment through secretion of IL-10 and TGF-β1. In addition, secretion of soluble CSF-1 and IL-6 may occur; these cytokines can act together to block the maturation of TAMs into antigen-presenting dendritic cells (Pollard, 2004). Moreover, tumours may actually 'educate' TAMs to perform roles supportive in tumour growth and progression. For example, the release of stress-signals by tumour cells, *e.g.*, hypoxia-inducible factor-2α (HIF-2α), has been shown to stimulate TAMs to 'help' the tumour, as they might help normal cells in distress. The HIF-α2 signal triggers production of a wide variety of growth factors including those that aid directly in tumour growth, *e.g.*, epidermal growth factor (EGF), and those which act indirectly, *e.g.*, vascular endothelial growth factor (VEGF). VEGF enables angiogenesis to occur, allowing the tumour to satisfy its increased requirements for nutrients and oxygen, and thus increase in size (Pollard, 2004). An increase in tumour vasculature also facilitates the escape of metastatic cells.

Tumour-associated eosinophilia has also been associated with both tumour-protective (Goldsmith *et al.*, 1987; Kapp *et al.*, 1983; Lowe *et al.*, 1984a; Lowe *et al.*, 1984b; Pretlow *et al.*, 1983) and tumour-promoting (Chang *et al.*, 1993; Elovic *et al.*, 1990; Horiuchi *et al.*, 1993; Wong *et al.*, 1990) functions. The role of these tumour-infiltrating eosinophils is not fully understood, nor is the role of those eosinophils found infiltrating sites of allergic challenge or helminthic infections; it is clear, however, that eosinophils are highly cytotoxic and able to mediate significant host cell damage in all three disease states (Weller, 1991). In a number of animal models, it has been possible to manipulate eosinophils for tumour cell destruction: Tepper *et al.*, 1989 and 1992, found tumour cells transfected to secrete IL-4 were significantly less tumourigenic than untransfected tumour cells, and the anti-tumour immune response was dependent upon the recruitment and infiltration of eosinophils. Perhaps also by an IL-4-dependent mechanism, Reali *et al.*, 2001, showed that the specific targeting of tumours with IgE led to tumour rejection by a mechanism involving eosinophils. Interestingly, a study involving subcutaneous treatment of small-cell lung carcinoma patients with recombinant human IL-2 resulted in marked peripheral eosinophilia (Rivoltini *et al.*, 1993); when purified, these eosinophils were shown to mediate significant IgG1-dependent tumour-cell death in an *in vitro* chromium-release assay. In contrast, eosinophils purified from the same patients before IL-2-therapy showed no significant IgG1-dependent tumour

cell killing. These results implicate eosinophils in the mechanism behind the survival advantage conferred by IL-2 therapy.

Like macrophages and eosinophils, tumour-infiltrating mast cells have both positive and negative effects on tumour growth. Although classical mast cell degranulation as occurs in allergic disease might be detrimental to tumour growth, tumour-associated mast cells appear to have the capacity to 'selectively' degranulate. Selective degranulation may involve the release of mediators which aid in tumour growth (*e.g.*, VEGF), and retention of those detrimental to tumour growth (*e.g.*, IL-4) (a phenomenon reviewed in Theoharides and Conti, 2004).

1.2 Monoclonal antibody therapy for cancer

1.2.1 The structure and function of antibodies

Antibodies are one of three classes of specific antigen-recognition molecules in the immune system; the other two being the T cell receptor and the class I and II molecules of the major histocompatability complex (MHC). Antibodies are produced by B cells; they may be tethered in B cell membrane where they act as the B cell receptor, or secreted by terminally differentiated B cells, termed plasma cells. A monomeric antibody is composed of two identical heavy chains, and two identical light chains. The heavy chains may be one of five different isotypes or subclasses therein, IgD, IgM, IgG1, IgG2, IgG3, IgG4, IgA1, IgA2, or IgE. The light chains may be either kappa or lambda class. The variable regions of each pair of heavy (V_H) and light (V_L) chains constitute the two identical antigen-binding sites. Each pair of V_H and V_L, together with their adjacent C_H1 and C_L domains constitute one of two Fab (**F**ragment **a**ntigen **b**inding) regions of the antibody, which may be cleaved from the whole structure by papain digestion, or as one $F(ab')_2$ unit by pepsin digestion. The remaining heavy chain constant domain pairs (C_H2-C_H3 for IgD, IgA and IgG or C_H2-C_H4 for IgE and IgM) constitute the Fc region (**F**ragment **c**rystallisable). Heavy and light chains are cross-linked and stabilised by interchain disulphide bonds and non-covalent interactions. The five different antibody isotypes are shown schematically in Figure 1.1.

As mentioned above, antigen binds within the cleft between the variable regions of each pair of heavy and light chains. The exquisite specificity of this region is determined by the amino acid sequence of three discrete, hypervariable, antigen-binding regions, termed complementarity-determining regions (CDRs) in each V_H and V_L region. The sequence of the CDRs, and thus their antigen specificity, is determined during lymphocyte development by a complex process of gene rearrangement. However, during an immune response, by the process of somatic hypermutation, a dividing B cell will produce progeny with mutations in these CDRs, some of which will confer the antibody with enhanced affinity binding to its

antigen. The amino acid sequence found between the CDRs provides the structural framework of the variable domains. Details of the development, structure and function of antibodies in the immune system can be found in Chapter 9 of Janeway *et al.*, 4th Edition.

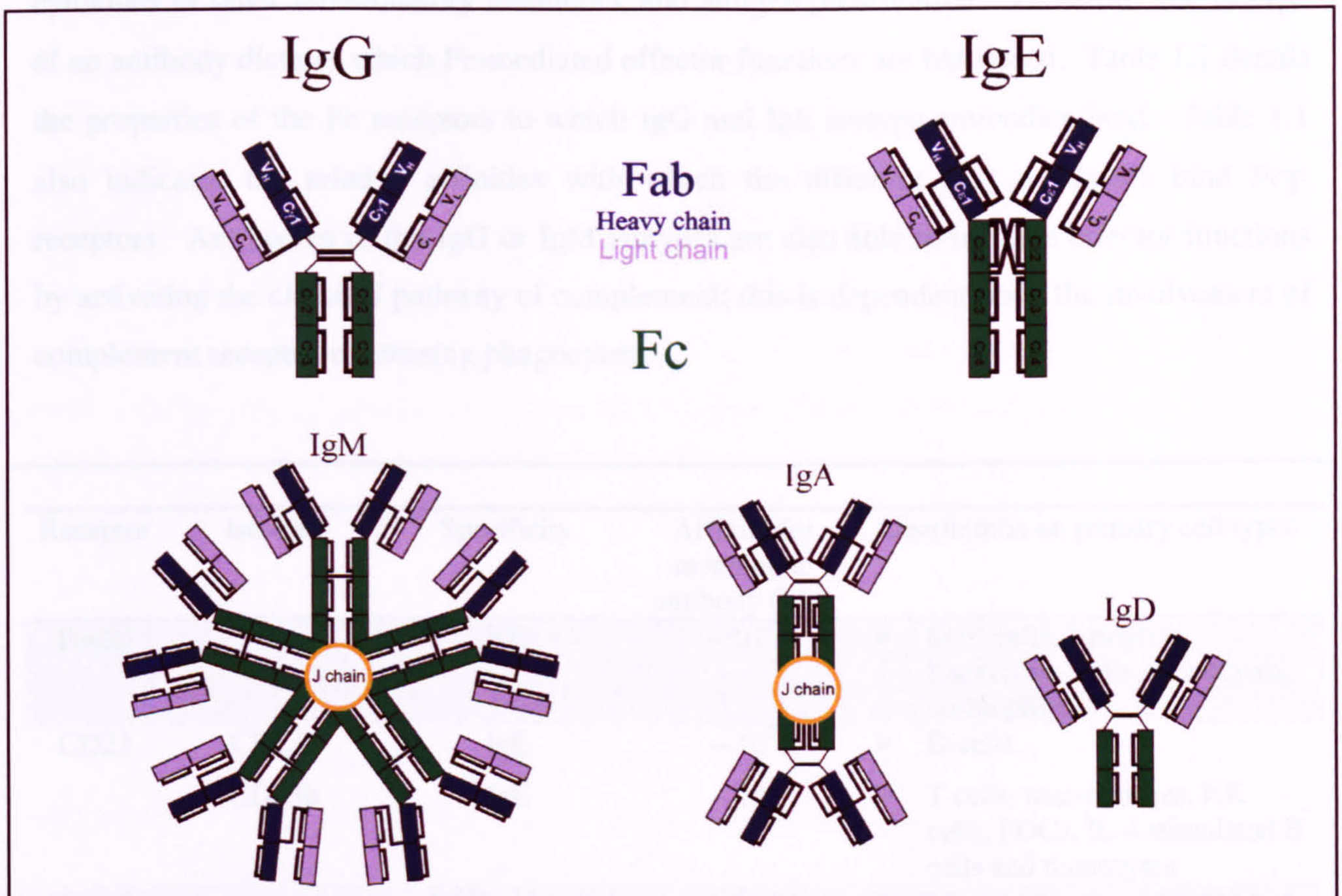

Figure 1.1: Schematic representation of the five different antibody isotypes found in the human body. Each Fab region contains three complementarity-determining regions that determine the antigen specificity of that antibody. The Fc region of each antibody mediates effector functions; one mechanism of Fc-mediated effector function is through binding to isotype-specific Fc receptors. The class of Fc-receptor to which an antibody binds, determines the cellular effector mechanisms available to that antibody isotype.

An antibody is able to act in conjunction with cellular effectors by binding via its Fc-region to an isotype-specific Fc receptor expressed by the effector cell. Each antibody isotype binds to one or more specific Fc receptors. Each class of Fc receptor has a specific cellular expression profile and displays characteristic binding affinity for specific antibody. Classically, it is through the cross-linking and aggregation of two or more Fc receptors by specific antibody-antigen immune complexes that an Fc-receptor expressing cell becomes activated (Metzger, 1992). The signalling response initiated by receptor aggregation may trigger stimulatory or inhibitory responses depending on the nature of the signalling pathways

with which an Fc receptor is linked. Although the final cellular response mediated by Fc receptor aggregation with specific antibody-antigen complexes will depend upon the cell type, effector functions may include ADCC, phagocytosis, endocytosis, release of inflammatory cytokines or other inflammatory mediators, and antigen presentation. Therefore, the isotype of an antibody dictates which Fc-mediated effector functions are harnessed. Table 1.1 details the properties of the Fc receptors to which IgG and IgE isotype antibodies bind. Table 1.1 also indicates the relative affinities with which the different IgG subclasses bind Fcγ-receptors. Antibodies of the IgG or IgM isotypes are also able to mediate effector functions by activating the classical pathway of complement; this is dependent upon the involvement of complement receptor-expressing phagocytes.

Receptor	Isoform	Specificity	Affinity for monomeric antibody (M^{-1})	Distribution on primary cell types
FcεRI	-	IgE	~ 10^{10}	➢ Mast cells, basophils, Langerhans cells, monocytes, eosinophils
CD23	CD23a	IgE	~ 10^{7}	➢ B-cells
	CD23b	IgE	~ 10^{7}	➢ T cells, macrophages, NK cells, FDCs, IL-4 stimulated B cells and monocytes
FcγRI	-	IgG1 = 3 > 4	~ 10^{8} -10^{9}	➢ Monocytes, macrophages and IFN-γ-stimulated neutrophils and eosinophils
FcγRII	FcγRIIa (stimulatory)	IgG1 ≥ 1 = 2	< 10^{7}	➢ Monocytes, macrophages, neutrophils, Langerhans cells (eosinophils?)
	FcγRIIb (inhibitory)	IgG1 ≥1 >2 > 4		➢ Monocytes, macrophages and B cells (eosinophils?)
FcγRIII	FcγRIIIa (stimulatory)	1 = 3 > 2 = 4	~ 10^{6}	➢ Macrophages, NK cells, monocytes, γδ T cells

Table 1.1: Details of IgE and IgG Fc receptors. This table is adapted from Woof *et al.*, 2004. Antibody affinities are taken from Ravetch and Kinet, 1991 and were determined using cell binding assays.

1.2.2 Background to monoclonal antibody therapy for cancer

In 1975, a letter written by Köhler and Milstein was published in *Nature*, reporting the technical feasibility of producing continuous cell lines from mice, expressing mouse antibodies of a single, chosen specificity. The advent of this hybridoma technology made real the possibility of generating large amounts of monoclonal tumour-specific antibody that could be used as a tool for the passive induction of a highly specific, anti-tumour immune response. This potential for highly selective tumour cell killing was a great advance on the indiscriminate cell killing of chemotherapy and radiotherapy. Since Köhler and Milstein's publication in 1975, many more technical barriers have been overcome and these mouse antibodies have been replaced by chimaeric or 'humanised' tumour-specific antibodies, to minimise the immunogenicity of therapeutic mouse antibodies in humans (the implications of which are discussed below, in section 1.2.4). Chimaeric antibodies are composed of human constant regions and murine variable regions, whereas a 'humanised' antibody is almost entirely human with only the CDRs of murine origin.

Those anti-cancer antibodies that have been approved by the FDA for the treatment of cancer in humans are shown in Table 1.2; these antibodies can be divided into two broad categories. The first group includes those which rely on the manipulation of natural immune responses and or interference of tumour-antigen signalling pathways for their anti-tumour activity. The second group includes those which use the antibody as a vector for highly specific delivery of a toxic modality, to tumour cells. The potential mechanism by which an anti-cancer antibody of the former group may harness natural immune responses for tumour-cell killing, are discussed in section 1.2.3. Two important determinants of their success in immune manipulation are highlighted as being the nature of the tumour target antigen and the isotype of the antibody. However, the most effective isotype and specificity of an antibody reliant on immune manipulation for its activity may be quite different from those of a toxin-conjugate. For example, although a tumour-antigen that is internalised might make an inappropriate target for an antibody attempting to cross-link the antigen-expressing tumour cell with a cytotoxic effector cell, this same antigen may be successfully manipulated for internalisation of a toxin-conjugate. Similarly, where an antibody of the IgG1 isotype may effectively recruit cytotoxic effector cells by its high affinity binding to Fc receptors on these cell types, a toxin-conjugate of the same isotype may result in unwanted killing of these FcγR-expressing cells.

Antibody Name	Isotype	Nature	Target	Treatment for
Rituximab	IgG1	Chimaeric	CD20	Non-Hodgkin's lymphoma
Trastuzumab	IgG1	Humanised	Her-2/neu	Metastatic breast cancer
Campath-1H	IgG1	Humanised	CD52	Chronic lymphocytic leukaemia
Cetuximab	IgG1	Chimaeric	EGFR	Metastatic colorectal carcinoma
Gemtuzumab	IgG4	Humanised toxin conjugate	CD33	Relapsed acute myeloid leukaemia
Tositumomab	IgG2a	Mouse radionuclide conjugate	CD20	Rituximab-failed, Non-Hodgkin's lymphoma
Ibritumomab tiuxetan	IgG1	Mouse radionuclide conjugate	CD20	Rituximab-failed, Non-Hodgkin's lymphoma

Table 1.2: FDA-approved anti-cancer antibodies which directly target antigens expressed by tumour cells. The top four antibodies in this table are described in section 1.2.2 as belonging to 'group 1' and the remaining, lower three antibodies, as belonging to 'group 2'. This table combines data found in Glennie and van de Winkel, 2003, and Segota and Bukowski, 2004.

1.2.3 Mode of anti-cancer antibody action: Influence of target antigen and antibody isotype

The original vision for anticancer antibodies was that they should be used as a precise way of exposing tumour cells to the immune system for killing. It was proposed that, following opsonisation, tumour cell killing would occur by Fc-mediated activation of complement pathways or recruitment of cytotoxic effector cells, as represented diagrammatically in Figures 1.2A and B, below. Although dependence on Fc-mediated tumour-cell killing mechanisms has been shown (Clynes *et al.*, 1998), it was later realised that significant tumour cell death can be mediated independently of the antibody Fc region (Tutt *et al.*, 1998), depending on the nature of the target antigen. Potential mechanisms by which an anti-cancer antibody may kill tumour cells independently of its Fc portion are shown diagrammatically in Figure 1.2C. These include, blocking the uptake of a vital growth factor in the case of growth factor receptor target antigens, or direct interference with cellular

signalling pathways to induce apoptosis or prevent proliferation. Anti-cancer antibodies that mediate a significant proportion of their function through Fc-independent mechanisms include Trastuzumab, Rituximab and anti-idiotype antibodies. Cross-linking of the target antigen of each of these antibodies, Her-2/neu, CD20 and the idiotype of the B cell receptor respectively, results in the generation of intracellular signals that negatively influence the survival of the cell (reviewed in Cragg and Glennie, 1999). Trastuzumab binding to Her-2/neu also leads to the blocking and down regulation of this receptor, preventing EGF uptake, which is critical for cell survival.

Adding further weight to the importance of target antigen choice is the impact its properties have on the efficacy of Fc-mediated killing mechanisms. A high density of target antigen expression, and a high affinity of $F(ab')_2$ binding to target antigen, have been shown to correlate with effective ADCC (Xia *et al.*, 1993; Coney *et al.*, 1994). The valency of a tumour antigen and whether or not it is internalised or shed will also impact on an antibody's efficacy; whether or not these factors impact positively or negatively may depend upon the properties of the antibody (*e.g.*, its isotype and whether its functioning is dependent upon recruitment of natural immune effector mechanisms or the action of a conjugated toxic modality). The anatomical location of the tumour may also influence the type of immune response triggered, bearing in mind the selective distribution of the different antibody isotypes in the body (Janeway *et al.*, 4th edition).

The other critical determinant of anti-cancer antibody efficacy is its isotype. As discussed above, an antibody may be one of five different isotypes found in the human body, or subclasses therein, with each different isotype mediating a unique immune response. Rituximab, Trastuzumab, CAMPATH-1H and Cetuximab are all chimaeric IgG1 antibodies (see Table 1.2). The dominance of the IgG1 isotype among FDA-approved antibodies can be explained by the original theory that the mechanism of anti-cancer antibody action was dependent on recruitment of cellular effector mechanisms and complement activation. This theory was based on *in vitro* studies, which showed mouse IgG2a and rat IgG2b to be the most effective subclasses in mediating ADCC of tumour cell targets *in vitro* (Herlyn and Koprowski, 1982; Seto *et al.*, 1983; Denkers *et al.*, 1985; Hale *et al.*, 1985 and Kaminski *et al.*, 1986). These *in vitro* studies showing the efficacy of rat IgG2b, were supported by *in vivo* models (Dyer *et al.*, 1989). Chimaeric or humanised IgG1 antibodies were therefore chosen on the basis of their known ability to recruit cellular effectors, through their high affinity for FcγR expressed by cytotoxic effector cells (see Table 1.1). IgG1 was subsequently shown to be the most effective IgG subclass in mediating ADCC of tumour cells by human effector cells by *in vitro* ADCC assays with human peripheral blood mononuclear cells (PBMC) as effectors (Steplewski *et al.*, 1988).

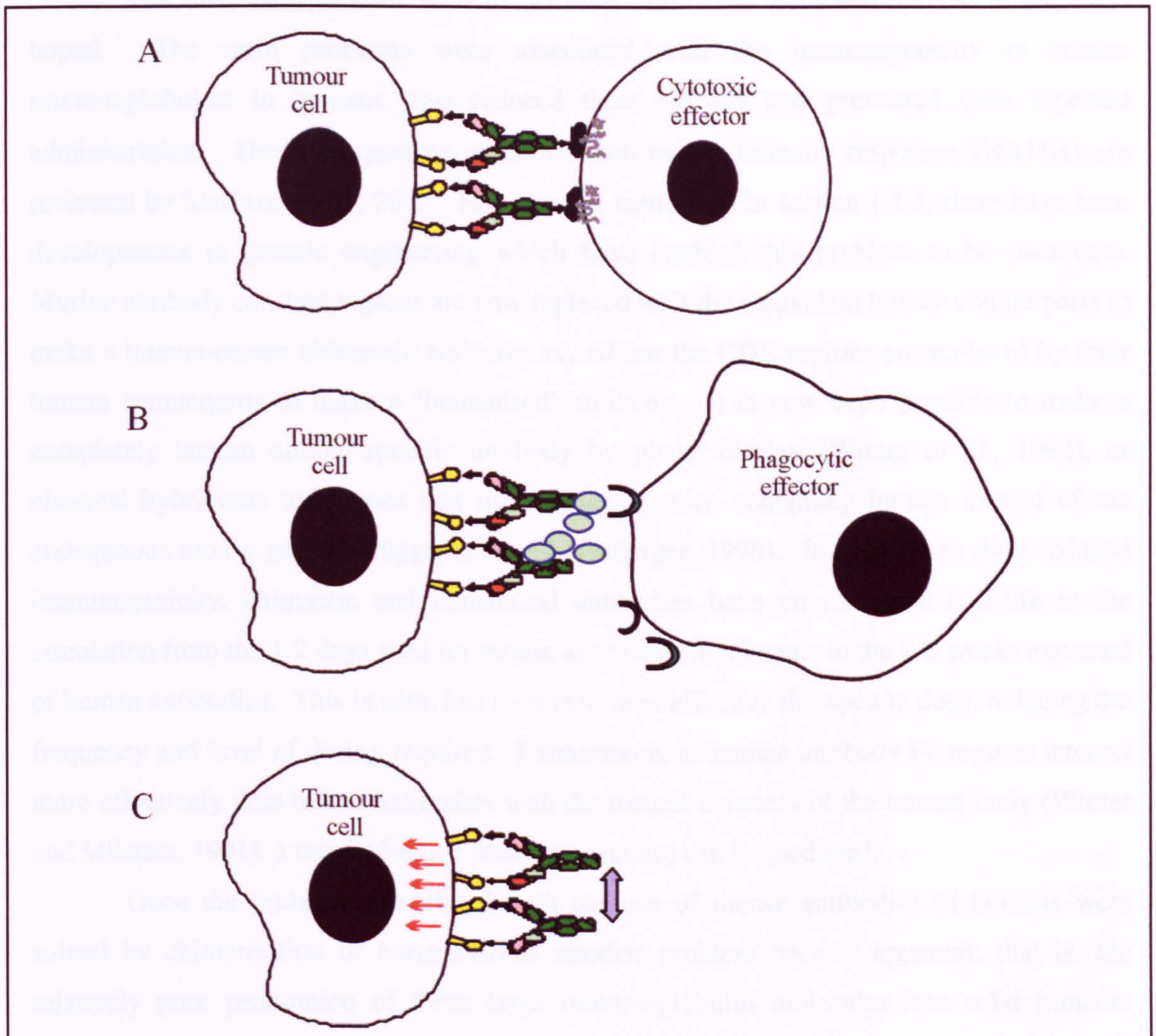

Figure 1.2: Potential mechanisms by which a tumour-specific antibody may mediate tumour-cell death. In each case the tumour-specific antibody binds a tumour-associated antigen via its $F(ab')_2$ regions. (A) The Fc regions interacts specifically with Fc receptors expressed by cytotoxic effector cells, such as NK cells or monocytes, to mediate ADCC of the tumour cell target. (B) Where an anti-tumour antibody is of the IgG or IgM isotype, the Fc region may activate the classical pathway of complement for tumour cell killing, or bind to complement-receptor expressing effector cells (such as macrophages) to mediate phagocytosis. (C) Depending on the nature of the tumour antigen, cross-linking of tumour antigens by $F(ab')_2$ regions may interfere with normal cell signalling to induce apoptosis, slow or stop cell growth or proliferation. Signalling through tumour antigen may be enhanced by cross-linking of antibody Fc regions, using a Fc-receptor-expressing cell as a multivalent platform upon which to cross-link.

1.2.4 Improving the clinical efficacy of anti-cancer antibodies

The early clinical trials with monoclonal antibodies were less successful than was hoped. The main problems were associated with the immunogenicity of mouse immunoglobulins in humans; this reduced their efficacy and prevented their repeated administration. The consequences of human anti-mouse immune responses (HAMA) are reviewed by Merluzzi *et al.*, 2000. However, as mentioned in section 1.2.2, there have been developments in genetic engineering which have enabled this problem to be overcome. Murine antibody constant regions are now replaced with the equivalent human counterparts to make a human-mouse chimaeric antibody, or, all but the CDR regions are replaced by their human counterparts to make a 'humanised' antibody. It is now even possible to make a completely human tumour-specific antibody by phage display (Winter *et al.*, 1994), or classical hybridoma techniques that use transgenic mice containing human instead of the endogenous mouse genes (Brüggemann and Neuberger, 1996). In addition to their reduced immunogenicity, chimaeric and humanised antibodies have an increased half-life in the circulation from the 1-2 days seen for mouse antibodies in humans, to the 2-3 weeks expected of human antibodies. This in turn, has increased their effective therapeutic dose, reducing the frequency and level of dosing required. Furthermore, as human antibody Fc regions interact more effectively than rodent antibodies with the natural defences of the human body (Winter and Milstein, 1991), a more effective immune response can be mediated.

Once the problems associated with the use of mouse antibodies in humans were solved by chimerisation or humanisation, another problem became apparent; that is, the relatively poor penetration of these large immunoglobulin molecules into solid tumours (Carter, 2001). This is reflected in the fact that those anti-cancer antibodies that have been approved by the FDA are most successful in the treatment of tumours of haematopoietic origin, where such penetrative capacity is not required. One method of assisting antibody penetration into solid tumours is to remove the constant regions of an antibody, to make $F(ab')_2$, Fab or single chain antibody variable region (scFv) fragments (Hudson and Souriau, 2003). However, many benefits are lost by removing the Fc portion of an antibody. These include, a lower affinity for target antigen, a shorter half-life and a restriction in the range of effector functions that antibody is able to mediate; these fragments are therefore reliant on the tumour-target antigen being involved in a signalling pathway, which, when disrupted, negatively affects cell viability or proliferation.

The efficacy of IgG1 in the treatment of cancers of haematopietic origin is in accordance with the known role of this antibody class in immunosurveillance and mediation of effector functions in the circulation. Indeed, each antibody isotype possesses unique properties that allow it to act more effectively at particular anatomical locations. For

example, IgA mediates its effector functions in mucosal secretions, which it is able to effectively penetrate by interaction of its dimeric IgA-J-chain complex with secretory component receptor on epithelial cells (Janeway *et al.*, 4th edition). In contrast, IgE mediates its effector functions predominantly in solid tissues, which relates to the presence of FcεRI-expressing mast cells in this location, and the high affinity of IgE for FcεRI; the reported role of CD23 in IgE transport may facilitate the entry of IgE into tissues, and this is discussed in more detail in section 1.4. Therefore, it may be that the isotype of tumour-specific antibody able to trigger the most effective anti-tumour immune response will vary according to the anatomical location of the tumour. Another factor likely to play an important role in the *in vivo* efficacy of anti-cancer antibodies, which was not directly assessed in the original experiments leading to the selection of the IgG1 isotype, is the affinity of an antibody for its Fc receptor(s); this will dictate the half-life for which the antibody remains bound to its receptor(s) on effector cells in serum and tissue. Clearly, the efficacy of an anti-cancer antibody depends upon a multiplicity of properties determined by the target antigen, antibody isotype, anatomical location of the tumour, and the immune context of the interaction between effector and target cells.

1.2.5 IgE isotype anti-cancer antibodies?

IgE has the capacity to trigger a powerful cell mediated immune response involving a range of cytotoxic effector cell types which occurs most obviously towards innocuous allergens (Gould *et al.*, 2003). Despite the well-recognised role of IgE in triggering such a powerful cell-mediated immune response, this isotype has rarely been included in comparisons of different isotypes of tumour-specific antibodies, in mediating specific target cell death. Where IgE has been included, it has performed less well than other isotypes in *in vitro* ADCC assays (Brüggemann *et al.*, 1987; Gould *et al.*, 1999). This poor performance of IgE *in vitro*, where the effector cell populations were PBMCs (and thus primarily lymphocytes and monocytes), most likely reflects the relatively low number of IgE-receptor-expressing effector cells in the circulation and the fact that, in the PBMC donors, who are frequently allergic and have high IgE levels, the IgE receptors expressed by the cells are already occupied with endogenous allergen-specific IgE (Karagiannis *et al.*, 2003). It has been proposed that this naturally tissue-based IgE-mediated immune response might be manipulated for the killing of tumours of solid tissues in patients (Gould *et al.*, 1999; Reali *et al.*, 2001; Karagiannis *et al.*, 2003). This is a particularly important area of cancer therapy to target, as the majority of human cancers are carcinomas arising from the epithelial cell layers (Rangarajan *et al.*, 2003). The IgE-mediated immune response is described below, so that in

section 1.4 a more detailed rationale for the proposed use of IgE in cancer therapy can be made.

1.3 The IgE-mediated immune response

1.3.1 The IgE antibody

IgE shares the basic architecture of all antibody isotypes (described in section 1.2.1) in having two identical heavy and two identical light chains, of epsilon and kappa or lambda class, respectively (Bennich and Johansson, 1968), linked by disulfide bonds and non-covalent interactions (see Figures 1.1 and 1.3). It is the presence of the Cε2 domain pair that principally distinguishes the IgE (and IgM) isotype from IgG, IgA and IgD. The equivalent position in IgG (between the $F(ab')_2$ and Fc regions), where the Cε2 domains are found in IgE, is occupied by a flexible hinge region; this hinge region differs in length between each IgG subclass. The presence of the Cε2 domains in IgE has a profound impact on IgE's physical properties through their effect on the shape acquired by free IgE in solution and, consequently, the kinetics of IgE binding to its receptor FcεRI (as discussed in section 1.3.3). In addition to FcεRI, IgE is a ligand for both CD23 (FcεRII) and epsilon-binding protein (εBP). The role of CD23 in the immune system has been extensively studied and is discussed below in section 1.3.6. Less is known of εBP, and it is discussed only briefly, in section 1.3.8.

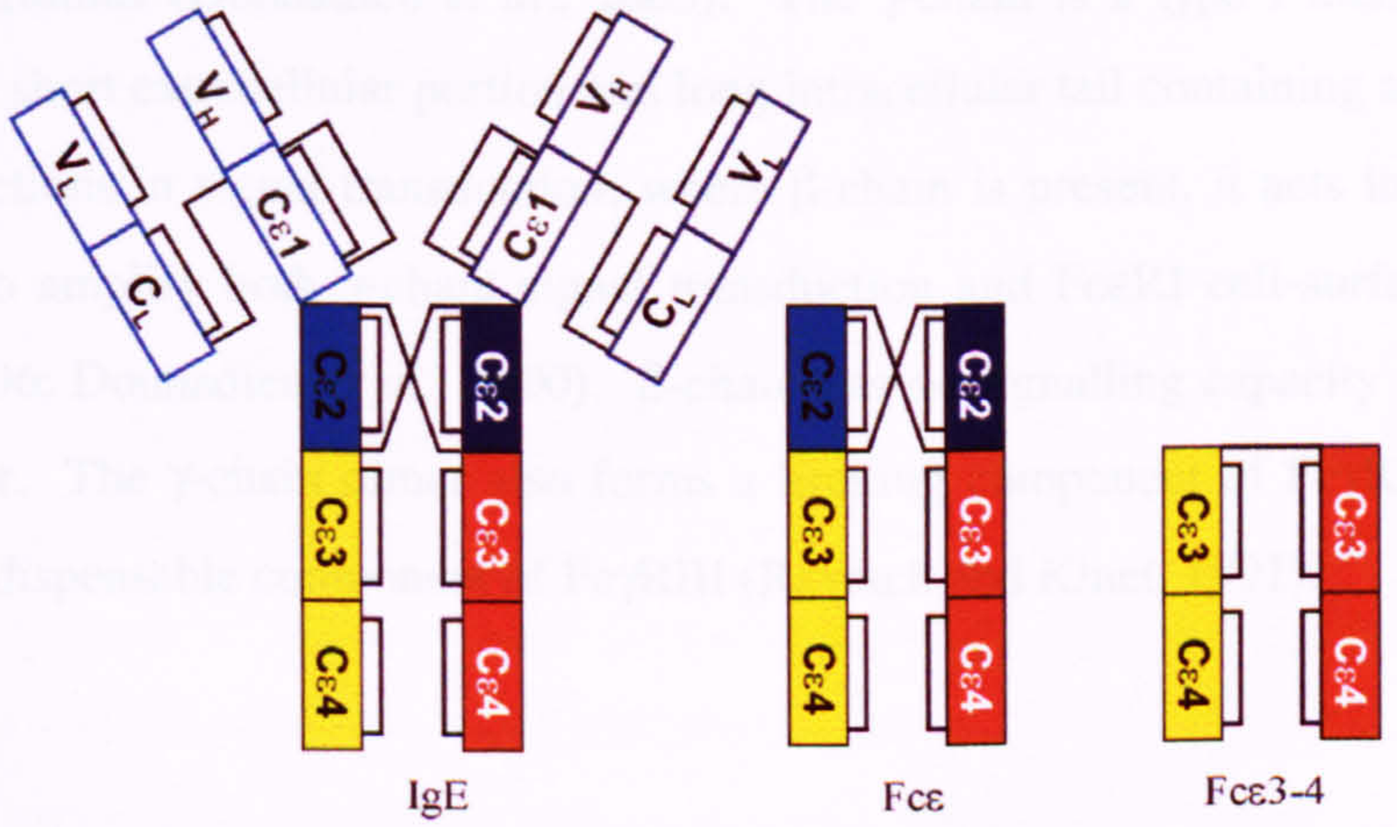

Figure 1.3: Schematic representation of IgE, IgE Fc and an IgE Fcε3-4 fragment. The Fc region (filled rectangles) is composed of the Cε2-4 domains of each of two heavy-chains. The $F(ab')_2$ region (open rectangles) is composed of light-chain (variable (V_L) and constant (C_L) domains) and heavy-chain variable regions (V_H) in addition to Cε1 domains. Inter-chain and intra-domain disulphide bridges are represented by black lines.

1.3.2 FcεRI

FcεRI is the IgE receptor best known for its role in the immediate activation of mast cells upon exposure to allergen in sensitised individuals. FcεRI is a member of the immunoglobulin superfamily. The structure of FcεRI may be tetrameric or trimeric. Tetrameric FcεRI is composed of a single α-chain, single β-chain and a disulphide-linked γ-chain dimer (Figure 1.4A). For trimeric FcεRI expression, α-chain associates with the γ_2-dimer in the absence of a β-chain (Figure 1.4B). For human and rat, but not mouse FcεRI-expression, β-chain presence is dispensable and thus humans and rats express both isoforms, and mice only the tetrameric form (Blank *et al.*, 1989; Miller *et al.*, 1989). The necessity of β- for α-chain expression in mice is thought to be due to the presence of an additional endoplasmic reticulum dilysine retention motif in the intracellular portion of mouse α-chain which can only be masked by β, whereas human α-chain has a single retention motif, effectively masked by steric hindrance upon assembly with γ-chain alone (Blank *et al.*, 1990; Letourneur *et al.*, 1995; Donnadieu *et al.*, 2000).

It is the α-chain, a type I integral membrane protein, to which IgE binds. It consists of an extracellular sequence which is expressed as two immunoglobulin domain folds at the cell surface, in addition to a single transmembrane and a short cytoplasmic region. The β-chain spans the membrane four times such that the amino and carboxy termini are intracellular, with an aypical immuno-receptor tyrosine-based activation motif (ITAM) near the carboxy terminus (Donnadieu *et al.*, 2003). The γ-chain is a type I membrane protein consisting of a short extracellular portion and long intracellular tail containing an ITAM. The γ_2-subunit functions in signal transduction; where β-chain is present, it acts in synergy with the γ_2-dimer to amplify both γ-chain signal transduction and FcεRI cell-surface expression (Lin *et al.*, 1996; Donnadieu *et al.*, 2000). β-chain has no signalling capacity in the absence of the γ_2-dimer. The γ-chain dimer also forms a limiting component of FcγRI and FcγRIII, and β-chain a dispensable component of FcγRIII (Ravetch and Kinet, 1991).

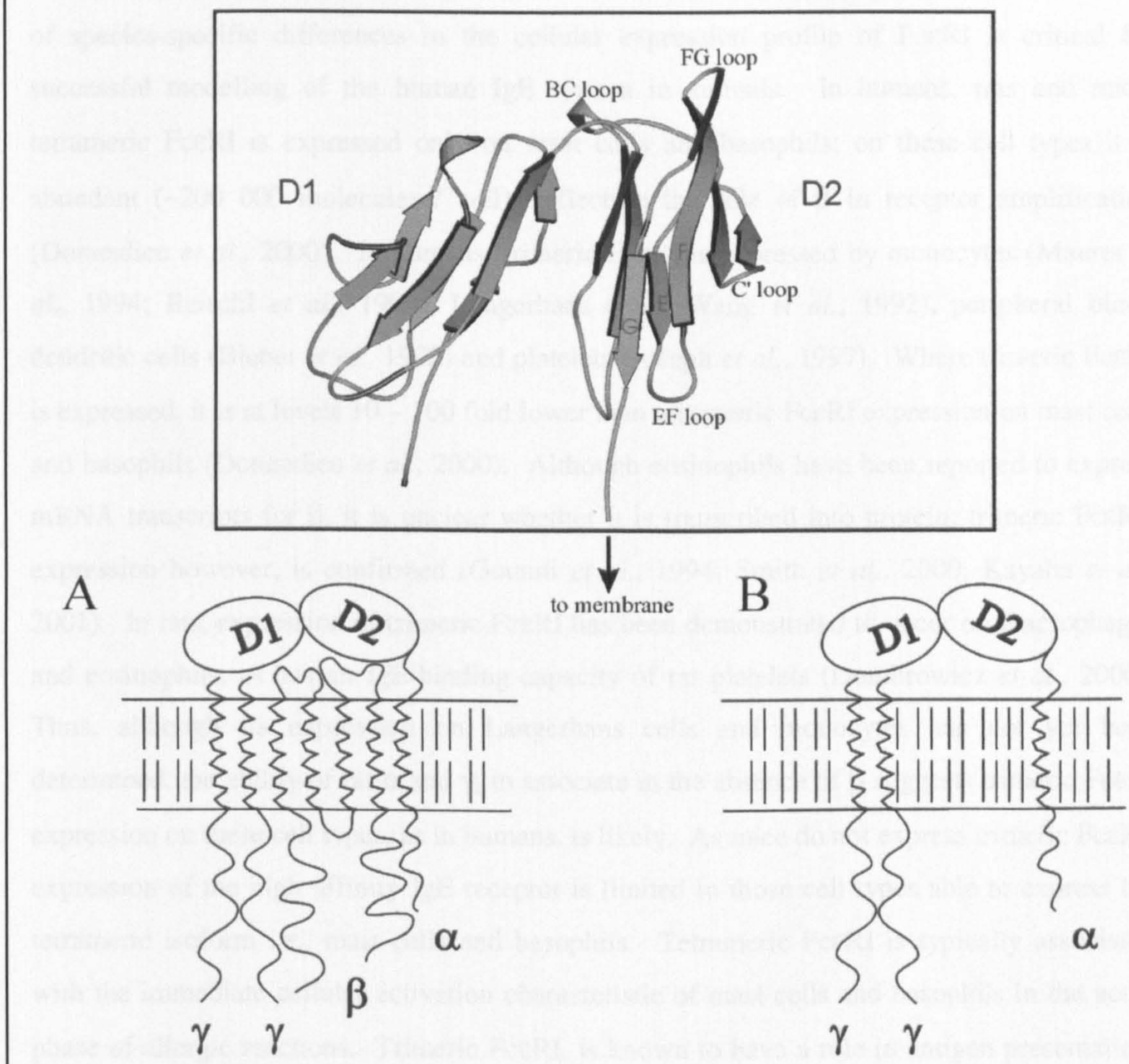

Figure 1.4: Schematic representation of the structure of FcεRI in (A) tetrameric and (B) trimeric isoforms. The (predominantly extracellular) IgE-binding α-chain is composed of two immunoglobulin domains D1 and D2. Both trimeric and tetrameric FcεRI include a γ-chain dimer involved in signal transduction. Tetrameric FcεRI additionally includes a single (predominantly cytoplasmic and transmembrane) β-chain, which functions to upregulate FcεRI expression, and to amplify γ-chain signalling. Inset shows ribbon representation of FcεRI α-chain, based on crystal structures: this is provided for reference with section 2.1.2.

Tetrameric and trimeric FcεRI isoforms have different cellular expression patterns, consistent between species and associated with different IgE-effector functions. Knowledge of species-specific differences in the cellular expression profile of FcεRI is critical for successful modelling of the human IgE system in animals. In humans, rats and mice, tetrameric FcεRI is expressed only on mast cells and basophils; on these cell types it is abundant (~200 000 molecules / cell), reflecting the role of β in receptor amplification (Donnadieu *et al.*, 2000). In humans, trimeric FcεRI is expressed by monocytes (Maurer *et al.*, 1994; Reischl *et al.*, 1996), Langerhans cells (Wang *et al.*, 1992), peripheral blood dendritic cells (Bieber *et al.*, 1992) and platelets (Joseph *et al.*, 1997). Where trimeric FcεRI is expressed, it is at levels 10 – 100 fold lower than tetrameric FcεRI expression on mast cells and basophils (Donnadieu *et al.*, 2000). Although eosinophils have been reported to express mRNA transcripts for β, it is unclear whether it is transcribed into protein; trimeric FcεRI-expression however, is confirmed (Gounni *et al.*, 1994; Smith *et al.*, 2000; Kayaba *et al.*, 2001). In rats, expression of trimeric FcεRI has been demonstrated to occur on macrophages and eosinophils, as has an IgE-binding capacity of rat platelets (Dombrowicz *et al.*, 2000). Thus, although its expression on Langerhans cells and monocytes has not yet been determined, the ability of rat α and γ_2 to associate in the absence of β suggests trimeric FcεRI expression on these cell types, as in humans, is likely. As mice do not express trimeric FcεRI, expression of the high affinity IgE receptor is limited to those cell types able to express the tetrameric isoform *i.e.*, mast cells and basophils. Tetrameric FcεRI is typically associated with the immediate cellular activation characteristic of mast cells and basophils in the acute phase of allergic reactions. Trimeric FcεRI, is known to have a role in antigen presentation, with internalisation of antigen-IgE complexes leading to presentation of antigen in the context of MHC class II at the cell surface (Novak *et al.*, 2001). The effector functions that are triggered by cross-linking of FcεRI expressed by different cell types are discussed in section 1.3.5 and reviewed in Gould *et al.*, 2003.

1.3.3 The IgE-FcεRI interaction

A defining feature of the interaction between IgE and FcεRI is its extremely high affinity (Metzger *et al.*, 1986). Cell binding assays have determined this to be in the order of ~10^{10} M^{-1} (Ishizaka *et al.*, 1986; Miller *et al.*, 1989; Young *et al.*, 1995; and Keown *et al.*, 1997). The crystal structures of IgE-Fc (Wan *et al.*, 2002), FcεRI (Garman *et al.*, 2001) and an IgE-Fcε3-4 fragment complexed with FcεRI (Garman *et al.*, 2000) have allowed the structural basis for this high affinity interaction to be understood in more detail. In brief, as demonstrated in Figure 1.5, the D1 and D2 domains of FcεRI α-chain (Figure 1.4) are

essentially 'wedged' between the two Cε3 domains of IgE. The generation of this high affinity interaction is discussed below and has been reviewed in detail in Wurzburg and Jardetzky, 2001, and Gould *et al.*, 2003.

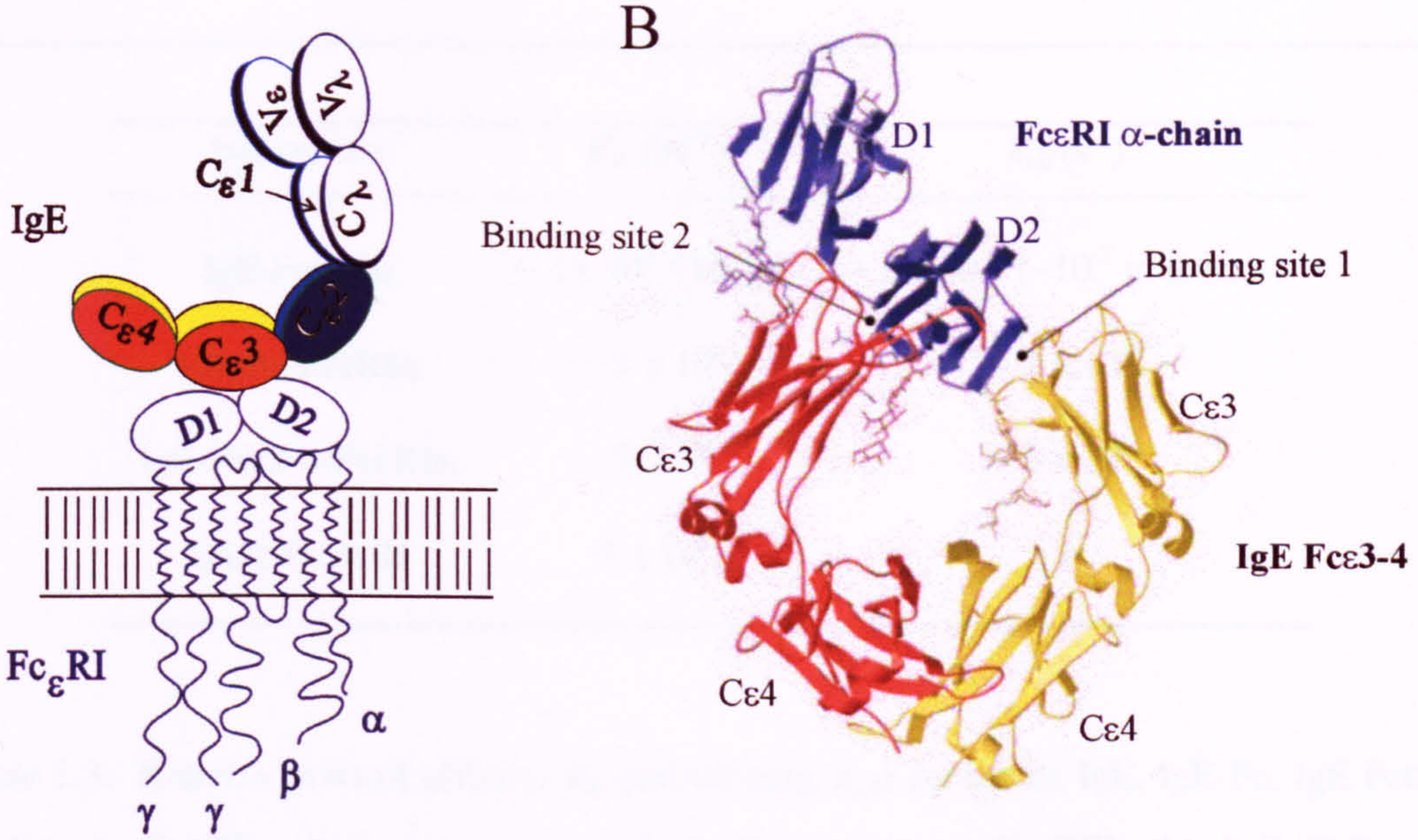

Figure 1.5: (A) Schematic representation of the interaction between whole IgE and FcεRI, showing that the interaction occurs between (predominantly D2 of) FcεRI α-chain and (predominantly the Cε3 domains of) IgE-Fc. (B) Ribbon representation based on the crystal structure of the interaction between an IgE Fcε3-4 fragment (shown schematically in Figure 1.3) and FcεRI α-chain.

It can be seen from Table 1.3 below, that there is little difference between the overall affinities of whole IgE, IgE-Fc and an IgE Fcε3-4 fragment, for FcεRI, with neither Cε4 domain making direct contact with FcεRIα (although they are required for maintenance of the Cε3 domains in a conformation suitable for receptor binding). It is the Cε3 domains which contribute the majority of the binding energy to the interaction. Indeed a large contact surface area has been shown to be involved in the interaction between Cε3 and FcεRIα, involving twenty-two residues from IgE in total, making direct contacts with FcεRIα. Of those residues involved from each Cε3 domain, only four are common to both; these include H424, R334,

G335 and V336. The importance of the arginine residue at position 334 (in the Cε2-Cε3 linker region) was identified by mutatagenesis studies, prior to elucidation of the crystal structure of the IgE-Fcε3-4:FcεRIα complex, as being critical for high affinity binding of IgE to FcεRI (Henry *et al.*, 1997). Some direct contacts are also made between the Cε2 domains and FcεRIα (McDonnell *et al.*, 2001).

Interaction	K_A (M^{-1})	k_{off} (s^{-1})
IgE-FcεRIα	~ 1x 10^9 (10^{10})*	~ 2 x 10^{-4} (~10^{-7} in tissues)
IgE Fc-FcεRIα	~ 1 x 10^9	~ 2 x 10^{-4}
IgE-Fcε3-4-FcεRIα	~ 3 x 10^8	~ 3 x 10^{-3}
IgG1-FcγRIII	5 x 10^5	1

Table 1.3: Kinetics (overall affinity, K_A and off-rate, k_{off}) for whole IgE, IgE-Fc, IgE Fcε3-4 binding to FcεRIα, and comparison with IgG1 binding to FcγRIII, the IgG FcR most homologous to FcεRI. Affinity constants are representative of comparable surface plasmon resonance (SPR) experiments (McDonnell *et al.*, 2001 and Maenaka *et al.*, 2001). Each K_A is a weighted average of the affinity of both phases of the biphasic interaction between IgE and FcεRI. The affinity of whole IgE for FcεRI shown in brackets and marked with a star represents that obtained in cell binding assays, which typically give higher affinities than SPR.

It is proposed that for IgE to bind FcεRI with full affinity it must undergo a dramatic conformational change upon receptor interaction. In solution, IgE adopts a compact and acutely bent structure, which, from comparison of the crystal structures of free IgE-Fc and the IgE-Fcε3-4:FcεRI complex, occludes receptor access to a number of residues required for direct interaction with FcεRI. This bent structure of uncomplexed IgE results from the two Cε2 domains, bending at the Cε2-Cε3 linker region, folding back asymmetrically against IgE-Fc, such that Cε2 of heavy-chain A (indicated in Figure 1.6A) makes a number of direct contacts with Cε3 and even Cε4 of heavy chain B; in addition, Cε2 of chain B, also makes a few additional contacts with Cε3, but not Cε4, of chain A (Wan *et al.*, 2002). The

conformational change, shown schematically in Figure 1.6D, is proposed to involve the dissociation of Cε2 from these contacts with Cε3 and Cε4 and an opening out of IgE into a conformation with more space between the two Cε3 domains.

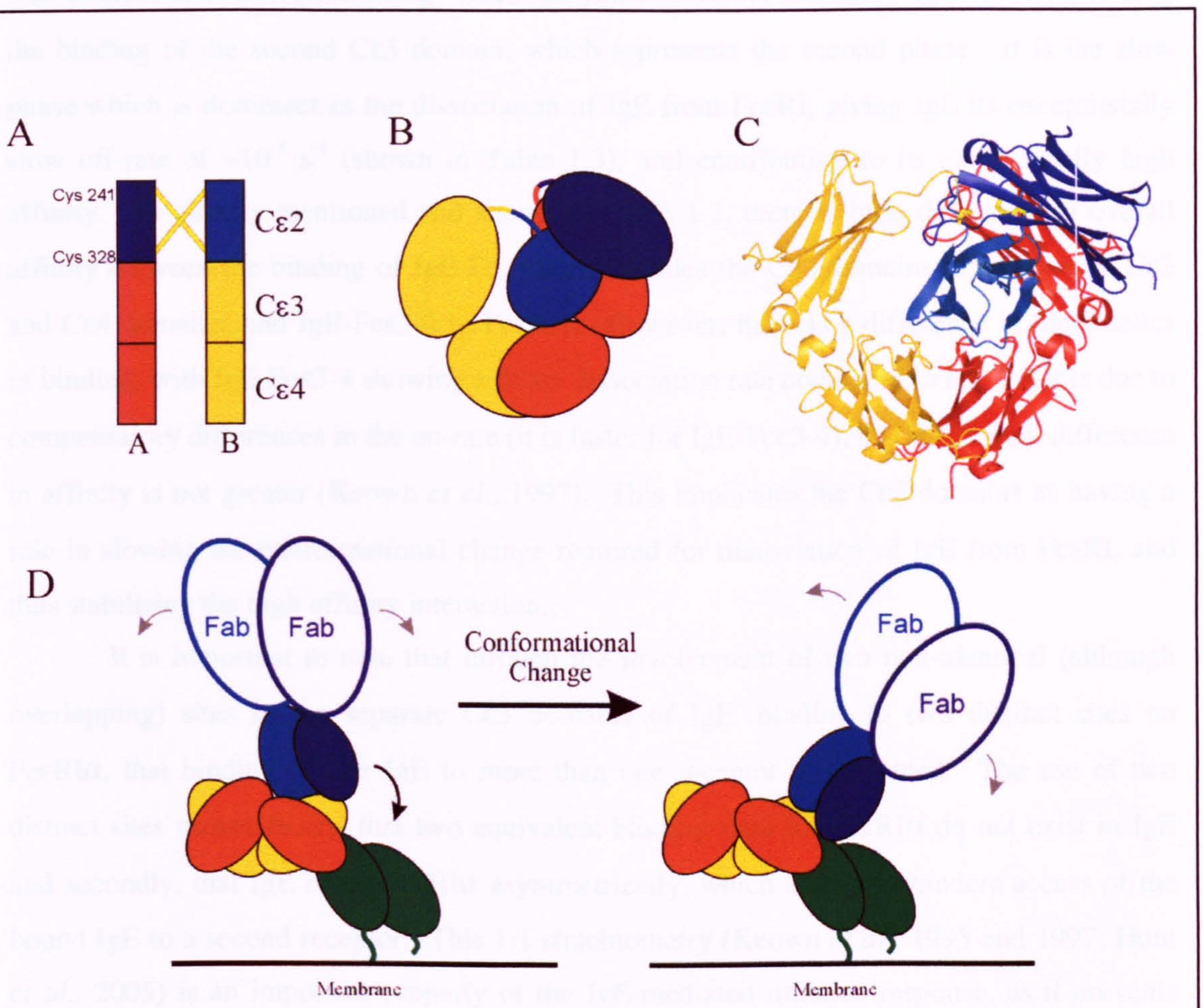

Figure 1.6: (A) schematic representation of an IgE Fcε2-4 fragment. (B) Domain structure of IgE Fcε2-4 showing the acute bend in the Cε2-3 linker region leading to the folding back of the Cε2 domains (blue) against Cε3 and Cε4 domains (red and yellow); (C) Ribbon representation of the crystal structure showing the acute bend represented in (B). (D) Schematic representation of the conformational change that occurs in IgE upon interaction with FcεRI (green), allowing the D2 domain of FcεRI α-chain to access all receptor-binding sites in IgE. Figure adapted from Wan *et al.*, 2002.

It is this conformational change in IgE which is thought to explain the biphasic binding kinetics seen in its interaction with FcεRI, manifest as one slow and one fast association phase and one slow and one fast dissociation phase (Henry *et al.*, 1997). It is proposed that the first phase of IgE's association with FcεRI represents the binding of one Cε3 domain to FcεRIα, following which the conformational change in IgE occurs, allowing the binding of the second Cε3 domain, which represents the second phase. It is the slow phase which is dominant in the dissociation of IgE from FcεRI, giving IgE its exceptionally slow off-rate of ~10^{-5} s^{-1} (shown in Table 1.3), and contributing to its exceptionally high affinity. As already mentioned and shown in Table 1.3, there is little difference in overall affinity between the binding of IgE Fc, which includes the Cε2 domains in addition to Cε3 and Cε4 domains, and IgE-Fcε3-4 to FcεRIα. However, there is a difference in the kinetics of binding, with IgE-Fcε3-4 showing a faster dissociation rate compared to IgE-Fc; it is due to compensatory differences in the on-rate (it is faster for IgE-Fcε3-4), that the overall difference in affinity is not greater (Keown *et al.*, 1997). This implicates the Cε2 domains as having a role in slowing the conformational change required for dissociation of IgE from FcεRI, and thus stabilising the high affinity interaction.

It is important to note that through the involvement of two non-identical (although overlapping) sites in the separate Cε3 domains of IgE, binding to two distinct sites on FcεRIα, that binding of one IgE to more than one receptor is prevented. The use of two distinct sites means firstly, that two equivalent binding sites for FcεRIα do not exist in IgE and secondly, that IgE binds FcεRIα asymmetrically, which sterically hinders access of the bound IgE to a second receptor. This 1:1 stoichiometry (Keown *et al.*, 1995 and 1997; Hunt *et al.*, 2005) is an important property of the IgE-mediated immune response, as it prevents cross-linking of FcεRI and thus cellular activation occurring in the absence of antigen.

1.3.4 Biological consequences of the high affinity interaction between IgE and FcεRI

The large surface area of interaction between IgE and FcεRI in combination with the extremely slow rate of IgE:FcεRI dissociation, together, make the interaction extremely high affinity. This high affinity interaction confers IgE, and thus the IgE-mediated immune response, with unique properties; the ability to bind FcεRI in monomeric form, without the need to first complex with antigen, and to remain tenaciously bound for long periods of time. This creates an unusual situation for an antibody-mediated immune response, whereby FcεRI-expressing cells adopt the antigenic specificity of the prevalent IgE repertoire in the absence of antigen, such that cells are persistently sensitised for an immediate response upon antigen exposure and cross-linking of the receptor-bound IgE by allergen. Local synthesis of allergen-specific IgE contributes to this sensitisation (Smurthwaite *et al.*, 2001).

It has been calculated (using cell binding assays) that the half-life of IgE bound to FcεRI expressed by cells in serum is approximately 16 hours (off-rate of ~ 10^{-5} s^{-1}) (Young *et al.*, 1995; Wan *et al.*, 2002). In tissues, however, the diffusion of IgE would be restricted, and this is expected to slow the rate of dissociation of IgE from FcεRI, to ~10^{-7} s^{-1}, increasing the half-life of binding to the order of weeks (calculated in Wan *et al.*, 2002, from data in Geha *et al.*, 1985). Indeed, IgE has been shown to remain in human skin for a half-life of approximately 13 days (Cass and Anderson, 1968). This restricted diffusion in tissues is also likely to lead to the re-binding of IgE to FcεRI (and CD23) expressed by the same, or nearby, cells. Therefore, for the duration for which IgE persists in tissues, association, dissociation and re-association with FcεRI, is likely to occur.

The IgG Fc receptor most homologous to FcεRI, is FcγRIII. IgG1 binds FcγRIII with an affinity of 5 x 10^5 M^{-1}, and a half-life of binding to cells in serum of only hours (determined in surface plasmon resonance experiments in Maenaka *et al.*, 2001, comparable to those used to determine the kinetics of IgE binding to FcεRI, discussed above). As for IgE, restricted diffusion of IgG in the tissues is likely to increase the half-life of IgG binding to FcγRIII, to approximately one day (Wan *et al.*, 2002), although it may persist in tissue for longer as a result of re-binding to Fcγ receptors expressed by the same, or nearby cells, as is the case for IgE. It has been shown by Tada *et al.*, 1975, that the half-life of rat IgE in rat skin, is 7.4 days, compared to only 2.4 days for rat IgG2a.

The longer half-life of free IgG in serum, over IgE, can be explained by the ability of the former but not latter, to bind the neonatal Fc receptor, FcRn; this Fc receptor was first identified for its role in the gastrointestinal absorption of IgG from orally administered mothers milk into the systemic circulation of the neonate, as suggested by its name (Junghans, 1997). However, in adults, FcRn is proposed to provide protection for IgG from degradation

(Lobo *et al.*, 2004). The normal mechanism of antibody catabolism is involves the uptake of antibody into endosomes of catabolic cells by fluid-phase pinocytosis. The antibody is then subject to a decreasing pH in the endosome upon fusion with a lysosome, resulting in its proteolytic degradation. The affinity of FcRn for IgG-Fc has been shown to increase with decreasing pH; thus, a high affinity interaction between IgG and FcRn tethered to the inner leaflet of the endosome, protects the former from degradation. Subsequent fusion of the endosome with the plasma membrane and the associated return to physiologic pH allows the release of IgG from what is now cell surface FcRn, back into the extracellular medium. The role of FcRn in recycling of IgG, has been recently reviewed by Lencer and Blumberg, 2004.

1.3.5 IgE-FcεRI mediated effector functions in an allergic reaction

As mentioned above, the IgE-FcεRI interaction is central to the mediation of allergic immune responses. The basis of allergic disease is reviewed in Gould *et al.*, 2003. An allergic immune response can only occur once an individual has produced allergen-specific IgE, in the 'sensitisation' phase; this requires Langerhans cells at the site of exposure to internalise allergen, migrate to local lymph nodes and present it to cognate T cells in the context of MHC class II. Following this, allergen-specific T helper cells provide the co-stimulation necessary in the lymph node, but subsequently also at the site of allergen exposure, for mature allergen-specific B cells to differentiate to plasma cells producing allergen-specific IgE. This IgE binds to FcεRI on mast cells 'sensitising' them towards subsequent challenge with the same allergen. Mast cells are the effector cells of the immediate response to allergen; their activities are said to 'orchestrate' the subsequent allergic immune response (shown below in Figure 1.7).

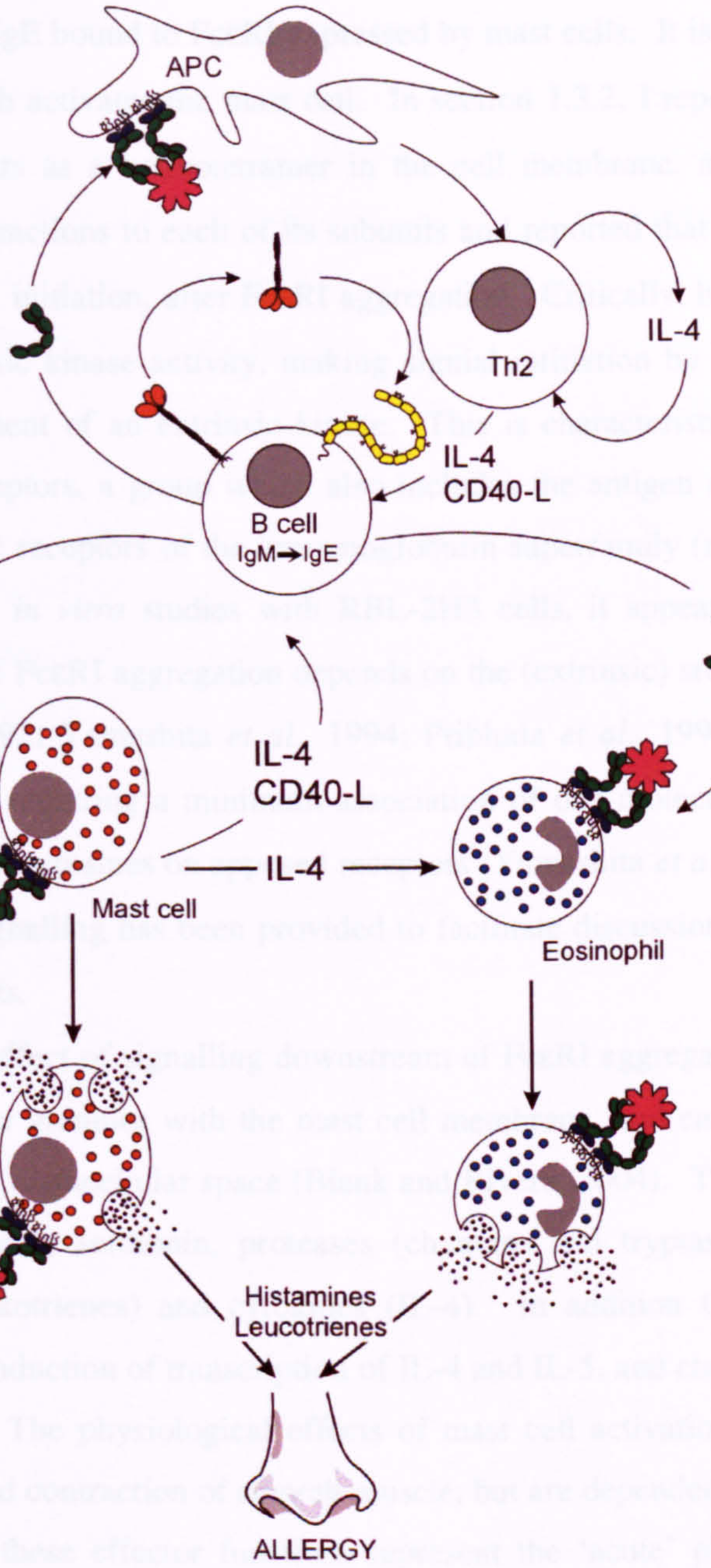

Figure 1.7: Allergic immune response. In the sensitisation phase, allergen is taken up by Langerhans cells which migrate to local lymph nodes and present antigen to cognate T cells. Activated T helper cells then produce IL-4, triggering B cells to switch and differentiate into IgE-producing plasma cells. Allergen-specific IgE binds to FcεRI on mast cell and is cross-linked, aggregating FcεRI, upon subsequent challenge with multivalent antigen: mast cell degranulation results in symptoms, according to the site of allergen provocation, characteristic of the acute phase of the allergic reaction. In addition, eosinophils, amongst other cell types, are recruited, and these mediate the late phase of the allergic reaction.

When a sensitised individual is exposed to multivalent allergen, the allergen binds to, and cross-links, specific IgE bound to FcεRI expressed by mast cells. It is this aggregation of two or more FcεRI which activates the mast cell. In section 1.3.2, I reported that mast cell and basophil FcεRI exists as a heterotetramer in the cell membrane, and I discussed the devolution of different functions to each of its subunits and reported that they include a role for the γ_2-dimer in signal initiation, after FcεRI aggregation. Critically, however, no subunit of FcεRI includes intrinsic kinase activity, making signial intitiation by FcεRI aggregation, dependent upon recruitment of an extrinsic kinase. This is characteristic of all multichain immuno-recognition receptors, a group which also includes the antigen receptors of T cells and B cells, and other Fc receptors of the immunoglobulin superfamily (reviewed in Keegan and Paul, 1992). From *in vitro* studies with RBL-2H3 cells, it appears that initiation of signalling downstream of FcεRI aggregation depends on the (extrinsic) src-family kinase Lyn (Eiseman and Bolen, 1992; Yamashita *et al.*, 1994; Pribluda *et al.*, 1994), with one newly formed FcεRI-aggregate requiring a minimum association of one molecule of Lyn to allow for transphoshorylation of tyrosines on apposed receptors (Yamashita *et al.*, 1994). This brief introduction to FcεRI signalling has been provided to facilitate discussion of work described in Chapter 7 of this Thesis.

The immediate effect of signalling downstream of FcεRI aggregation in mast cells is the fusion of intracellular granules with the mast cell membrane, and ensuing release of the granule contents into the extracellular space (Blank and Rivera, 2004). The contents of these granules include histamine, serotonin, proteases (chymase and tryptase), lipid mediators (prostaglandins and leukotrienes) and cytokines (IL-4). In addition to release of stored granule proteins, is the induction of transcription of IL-4 and IL-5, and chemokines, including eotaxin and RANTES. The physiological effects of mast cell activation include increased vascular permeability and contraction of smooth muscle, but are dependent upon the local site of allergen challenge: these effector functions represent the 'acute' phase of the allergic reaction, occurring within minutes of allergen challenge. When allergen is introduced directly into the blood stream of sensitised individuals, anaphylactic shock may occur; the consequences are severe and may be fatal (a recent review on the definition and management of systemic anaphylaxis can be found in Sampson *et al.*, 2005).

As well as mediating the acute phase of an allergic reaction, mast cell activation products also provide the signals for generation of the chronic, late, phase response, which manifests 4 to 8 hours after the initial reaction, and is dependent on the influx of T cells, monocytes, eosinophils and basophils; indeed eosinophil infiltration is a hallmark of allergic disease. The influx of these cell types is mediated by the IL-4, secreted from mast cells; this

serves to upregulate VLA-4 on the local epithelium, which interacts with the VCAM-1 expressed by T cells, monocytes, eosinophils and basophils, to mediate their extravasation to sites of allergen provocation. Other non-specific chemoattractants present in allergic tissues include platelet-activating factor (PAF), complement factors, leukotrienes and IL-8. Both eotaxin and IL-5, secreted from mast cells, act as specific chemotactic signals for eosinophil recruitment from blood into tissues; eotaxin also acts on basophils. Local IL-5 and eotaxin production is enhanced by IL-4, IL-13 and IL-9, increasing eosinophil recruitment further (Dombrowicz and Capron, 2001). The specific inhibition of eosinophil apoptosis by IL-5 also contributes to tissue eosinophilia (Simon *et al.*, 1995).

In the eosinophil cytoplasm are granules containing major basic protein, eosinophil peroxidase, eosinophil-derived neurotoxin and eosinophil cationic protein (Seminario *et al.*, 1998). Eosinophil immediate cytotoxic effector functions, manifest in the late phase of the allergic reaction, are therefore also mediated predominantly by degranulation. Pro-inflammatory functions are also mediated through the synthesis and release of lipid mediators (PAF, leukotriene C_4 and prostaglandin E_2), oxygen metabolites and cytokines, including IL-2 and IFN-γ (Wardlaw *et al.*, 1995). Eosinophils may also act as immunoregulatory cells through expression and secretion of IL-10, IL-13, IL-4 and TGF-β. Furthermore, the ability of eosinophils, recruited to airways in allergic subjects, to home to regional lymph nodes following internalisation of IgE-antigen complexes, and present antigen to $CD4^+$ T-cells in the context of MHC class II in the presence of co-stimulation, has been demonstrated (reviewed in Shi, 2004).

The pathogenesis of allergic reactions is enhanced by the involvement of several positive feedback loops (Gould *et al.*, 2003). Firstly, the increased levels of allergen-specific IgE produced locally in response to allergen challenge and its binding to FcεRI, serves to both increase FcεRI levels at the cell membrane by protecting it from proteolysis (Borkowski *et al.*, 2001), and also to prolong the survival of these FcεRI-expressing cells (reviewed in Kawakami and Galli, 2002). Increased levels of IgE bound to FcεRI may also allow for enhanced FcεRI-dependent presentation of antigen by Langerhans cells, monocytes, eosinophils and mast cells, to cognate T cells, and consequently enhanced secretion of IL-4 and IL-5 from T helper cells. Secretion of IL-4 has the effect of stimulating B cells to switch to production of IgE-isotype allergen-specific antibodies (Gould *et al.*, 2003). IL-4 will also serve to increase the numbers of infiltrating eosinophils, T cells, monocytes and basophils (Figure 1.7).

1.3.6 CD23

CD23 is the second of IgE's well-characterised receptors, and has been reviewed in Gould *et al.*, 1997. CD23 is a 45 kDa type-II integral membrane protein with a calcium-dependent (C-type) lectin-like domain at its extracellular C-terminus, giving it homology to members of the C-type lectin superfamily. This makes IgE the only immunoglobulin isotype to bind to a receptor that is not a member of the immunoglobulin superfamily. As shown in Figure 1.8A, CD23 is composed of a single polypeptide chain. Its C-type lectin domain 'head' is separated from a single transmembrane region by a 15 nm long, α-helical coiled-coil stalk. The stalk of human CD23 is composed of three homologous repeats of 21-amino acids, which together contain a periodic pattern of heptads, with hydrophobic residues at the first and fourth positions. This structure allows CD23 to oligomerise to form homodimers or homotrimers in the cell membrane (Beavil *et al.*, 1992). In addition to IgE, CD23 interacts with complement receptors 2 (CR2 / CD21), 3 (CR3 / CD18 / CD11b) and 4 (CR4 / CD18 / CD11c) and vitronectin (Gould *et al.*, 1997).

Although CD23 is typically referred to as the 'low affinity' receptor for IgE, the affinity of the interaction is actually quite high. The binding of IgE to a monomeric lectin domain head of CD23 occurs with an affinity of ~ 10^6 M^{-1} (Gould *et al.*, 1997). This affinity is increased to ~ 10^7 M^{-1} when IgE binds to CD23 in its native, homotrimeric form in the cell membrane (Gould *et al.*, 1997). This increase in affinity is likely due to the specific binding of two different CD23 lectin domain heads to two non-identical sites in IgE, proposed to lie within the Cε3 domains, and avidity effects conferred by the involvement of three polypeptide chains, each with IgE-binding capacity. The interaction between CD23 and IgE is unusual for ligand binding to a C-type lectin family member, as CD23 recognises protein and not carbohydrate moieties, in IgE (Gould *et al.*, 1997).

Two different isoforms of CD23 have been identified, CD23a and CD23b; these differ by 7 and 6 amino acids in their N-terminal cytoplasmic regions respectively, generated by the use of two alternative transcription-initiation sites and splicing of a short first exon to a common second exon. The primary impact of the sequence difference in the N-terminal tails of these isoforms appears to be on the intracellular trafficking properties of CD23a and CD23b; CD23a is associated with enodocytosis of IgE-coated particles, whereas CD23b is not efficiently internalised, and is instead associated with phagocytosis of IgE-coated particles (Yokota *et al.*, 1992). CD23a and CD23b have different cellular expression profiles; the former is expressed on mature activated (μ^+/δ^+) B cells prior to heavy-chain class switching and differentiation to plasma cell. The latter is expressed on B cells and monocytes, following IL-4 stimulation, in addition to Langerhans cells, follicular dendritic cells, T cells,

and tissue eosinophils. CD23b expression has also been detected on airway (Campbell *et al.*, 1994) and intestinal epithelial cells (Montagnac *et al.*, 2005).

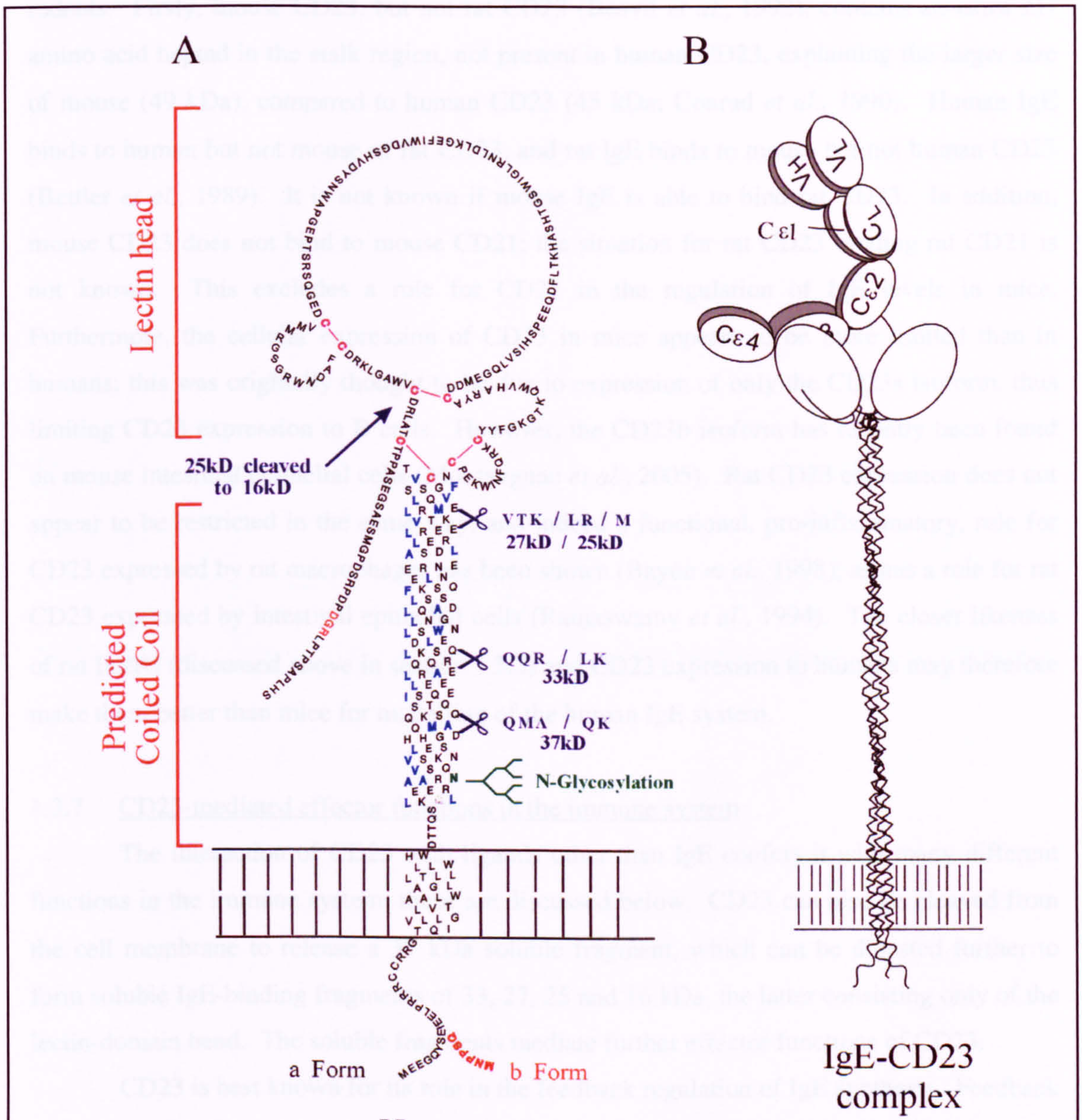

Figure 1.8: (A) The primary sequence of CD23. Sequences of both CD23a and CD23b, differing only by 6 and 7 amino acids, respectively, in their N-terminal, intra-cellular cytoplasmic regions, are shown. The sites of the α-helical stalk, which can be cleaved by endogenous proteases, are shown in blue along with the sizes of the fragments released. The single N-glycosylation site is shown in green, and disuphide bonds in magenta. (B) Schematic representation of IgE binding to trimeric CD23 in the cell membrane.

As for FcεRI, there are a number of differences between human, mouse and rat CD23 structure and expression, which complicate the modelling of the human IgE system in rodents. Firsly, mouse CD23, but not rat CD23 (Beavil *et al.*, 1992), contains an extra 21-amino acid heptad in the stalk region, not present in human CD23, explaining the larger size of mouse (49 kDa), compared to human CD23 (45 kDa; Conrad *et al.*, 1990). Human IgE binds to human but not mouse or rat CD23, and rat IgE binds to mouse but not human CD23 (Bettler *et al.*, 1989). It is not known if mouse IgE is able to bind rat CD23. In addition, mouse CD23 does not bind to mouse CD21; the situation for rat CD23 binding rat CD21 is not known. This excludes a role for CD21 in the regulation of IgE levels in mice. Furthermore, the cellular expression of CD23 in mice appears to be more limited than in humans; this was originally thought to be due to expression of only the CD23a isoform, thus limiting CD23 expression to B cells. However, the CD23b isoform has recently been found on mouse intestinal epithelial cells (Montangnac *et al.*, 2005). Rat CD23 expression does not appear to be restricted in the same way, and indeed a functional, pro-inflammatory, role for CD23 expressed by rat macrophages has been shown (Bayón *et al.*, 1998), as has a role for rat CD23 expressed by intestinal epithelial cells (Ramaswamy *et al.*, 1994). The closer likeness of rat FcεRI (discussed above in section 1.3.2) and CD23 expression to humans may therefore make them better than mice for modelling of the human IgE system.

1.3.7 CD23-mediated effector functions in the immune system

The interaction of CD23 with ligands other than IgE confers it with many different functions in the immune system; these are discussed below. CD23 can also be cleaved from the cell membrane to release a 37 kDa soluble fragment, which can be digested further to form soluble IgE-binding fragments of 33, 27, 25 and 16 kDa, the latter consisting only of the lectin-domain head. The soluble fragments mediate further effector functions of CD23.

CD23 is best known for its role in the feedback regulation of IgE synthesis. Feedback regulation of IgE synthesis is reviewed in Gould *et al.*, 2001, and shown schematically in Figure 1.9. The feedback system is required to counteract the positive feedback loop of IgE synthesis: IL-4 and ligation of CD40 provide the signals for a B cell to switch to secretion of IgE isotype antibodies; IgE binds to mast cells allowing for their activation upon antigen challenge resulting in further IL-4 secretion and thus increased IgE secretion. The role of CD23 in negative feedback of IgE is highlighted by CD23-knockout mice, which overexpress IgE, whereas mice overexpressing CD23 are deficient in IgE (Lamers and Yu, 1995; Payet and Conrad, 1999). Binding of IgE to CD23 leads to down-regulation of IgE synthesis. Co-ligation of membrane IgE with CD23 on B cells by allergen-IgE complexes also has a role in downregulation of IgE synthesis. Soluble CD23 fragments and CD21 also serve to regulate

IgE synthesis, with binding of soluble CD23 fragments larger than 25 kDa to CD21 expressed by B cells up-regulating IgE synthesis. As CD23 is protected from proteolysis when IgE is bound, the binding of the excess IgE to membrane CD23 prevents the release of soluble CD23 fragments, and thus these soluble CD23 fragments are unable to stimulate IgE synthesis further.

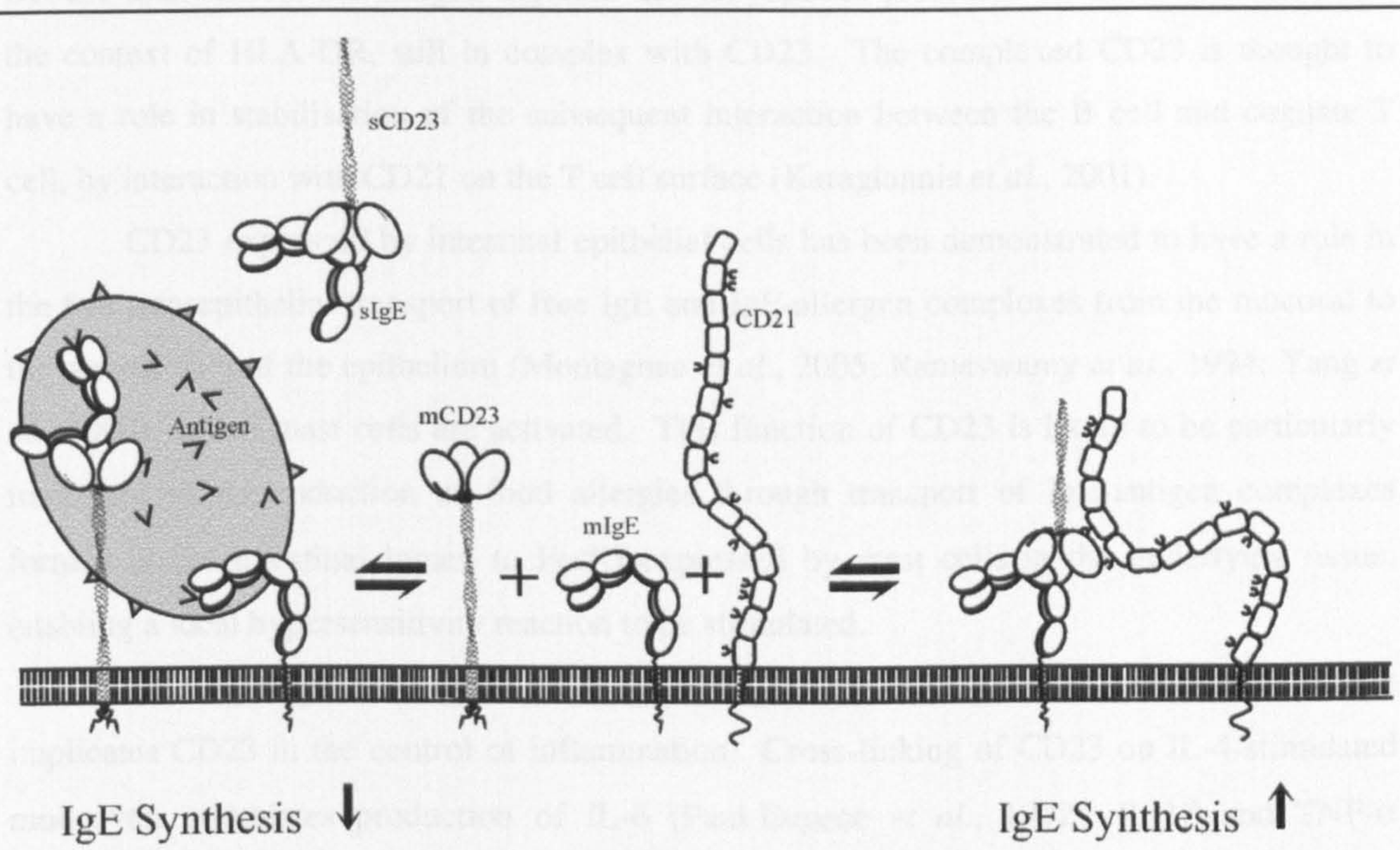

Figure 1.9: Bi-directional switch in IgE regulation by CD23: Interactions between IgE, CD23 and CD21 that lead to an increase in IgE synthesis, are shown on the right-hand side of this diagram. These include the co-ligation of membrane IgE and CD21 by oligomeric soluble CD23 fragments. Interactions between IgE, CD23 and antigen that lead to a decrease in IgE synthesis are shown on the left-hand side of this diagram. These include the co-ligation of membrane IgE and CD23 by antigen-IgE complex in addition to the binding of secreted IgE (sIgE) to soluble CD23 fragments (sCD23), which compete with CD23 binding to membrane IgE. The binding of IgE to CD23 also provides protection from proteolysis of CD23 into soluble fragments, which would normally serve to upregulate IgE synthesis.

The role of CD23 expressed by follicular dendritic cells in the apical light zone of the germinal centre in lymphoid tissue is the rescue of germinal centre B cells (centrocytes) from apoptosis; interaction of CD23 with CD21 on the B cell surface, induces expression of the Bcl-2 oncogene. This interaction may provide a second survival signal following the primary survival signal in the basal light zone, of a productive BCR interaction with antigen held as immune complexes on the surface of the FDC (Bonnefoy *et al.*, 1993; Liu *et al.*, 1991).

CD23 is not expressed by these germinal centre B cells but, as mentioned above, CD23a is expressed by mature, unswitched, B cells, where it has a role in the enhancement of IgE-dependent presentation of antigens to T cells. CD23 is non-covalently associated with the MHC class II antigen, human leukocyte antigen (HLA)-DR, in the B cell membrane. When an antigen-IgE complex binds to CD23, the antigen-IgE-CD23 complex and associated HLA-DR are internalised, the antigen digested and its peptides presented on the B cell surface in the context of HLA-DR, still in complex with CD23. The complexed CD23 is thought to have a role in stabilisation of the subsequent interaction between the B cell and cognate T cell, by interaction with CD21 on the T cell surface (Karagiannis *et al.*, 2001).

CD23 expressed by intestinal epithelial cells has been demonstrated to have a role in the fast transepithelial transport of free IgE and IgE-allergen complexes from the mucosal to the serosal side of the epithelium (Montagnac *et al.*, 2005; Ramaswamy *et al.*, 1994; Yang *et al.*, 2000), where mast cells are activated. This function of CD23 is likely to be particularly important in the induction of food allergies through transport of IgE-antigen complexes formed in the intestinal lumen to FcεRI expressed by mast cells in the underlying tissue, enabling a local hypersensitivity reaction to be stimulated.

Finally, expression of CD23 on cells of the mononuclear phagocyte lineage implicates CD23 in the control of inflammation. Cross-linking of CD23 on IL-4-stimulated monocytes stimulates production of IL-6 (Paul-Eugene *et al.*, 1992), IL-1β and TNF-α (Borish *et al.*, 1991) and superoxide anions (Kikutani and Kishimoto, 1990). Ligation of CD23 on the U937 monocyte cell line is also associated with the production of pro-inflammatory mediators, in addition to an increase in cell size, induction of oxidative metabolism and promotion of CD14 and LFA-1expression (Ouaaz *et al.*, 1993).

1.3.8 Epsilon-binding protein

Epsilon-binding protein (εBP) is a 31 KDa member of the soluble (S)-type lectin superfamily originally discovered in rat basophilic leukeamia cells by Liu *et al.*, in 1985, as a protein with IgE-binding capacity. εBP, as an example of S-type mammalian lectins, is reviewed in Liu *et al.*, 1993. The structure of εBP conforms to the highly conserved two-domain structure of S-type mammalian lectins; the carboxy-terminal domain contains consensus sequences shared by other β-galactoside-binding soluble lectins and the amino-terminal domain contains a highly conserved repetitive sequence. Human, rat and mouse εBP are highly homologous. εBP is secreted by mast cells and macrophages in response to inflammatory stimuli. One function of εBP in the allergic immune response is proposed to be the modulation of mast cell activation. It is through the ability of εBP to self-associate to

form oligomers by which it is able to cross-link FcεRI, or IgE bound to FcεRI, at the mast cell surface. This suggests that εBP might contribute to the amplification of IgE-mediated inflammatory responses. However, the ability of εBP to bind cell surface glycoproteins means εBP found in the extracellular medium may be expressed at the surface of cell types other than those from which it is secreted. Therefore, although the ability of εBP to bind both IgE and FcεRI implicates it with a role in allergic immune responses, it is likely to have a broad spectrum of functions in the immune system.

1.4 IgE and cancer

In the sections above I have introduced cancer, its relationship with the immune system and treatment with tumour antigen-specific monoclonal antibodies. I have also described IgE, its receptors, FcεRI, CD23, and εBP, and the allergic immune response. I now describe the features of this immune response which may make it a suitable arm of the immune system to be manipulated for tumour cell killing, particularly of solid-tissue-tumours.

1.4.1 Rationale for use of tumour-specific IgE in cancer immunotherapy

Throughout section 1.2, I have emphasised the underlying causes of the high affinity interaction formed between IgE and FcεRI, and highlighted the biological consequence of this high affinity interaction as being a long half-life for which monomeric IgE remains bound to FcεRI. For cancer immunotherapy, an IgE isotype tumour-specific antibody may therefore be well-retained on effector cells such as mast cells, eosinophils and monocytes, leaving them primed to mediate an anti-tumour-immune response immediately upon exposure to tumour cells expressing specific antigen. The long half-life of the IgE-FcεRI interaction should therefore reduce need for frequent treatment doses. Moreover, as mast cells are extremely sensitive to activation mediated through IgE-dependent cross-linking of FcεRI, with IgE-antigen-induced formation of FcεRI dimers shown to be sufficient for cellular activation (Segal *et al.*, 1977), this suggests that the size of the treatment doses required would also be minimised.

It is only possible to take advantage of this high affinity interaction for the treatment of cancers of solid tissues by virtue of the anatomical location of IgE receptor-expressing cytotoxic effector cells. Firstly, there is the presence of FcεRI-expressing mast cells throughout the tissues of the body and infiltrating tumours (as discussed in section 1.1.2). Mast cells initiate a powerful inflammatory immune response, as exemplified by their role as primary effector cells in allergic reactions, discussed in section 1.3.5. Furthermore, the effector mechanisms of mast cells are mediated in a highly specific manner, with localised

receptor aggregation causing localised degranulation (Lawson *et al.*, 1978). This highly sensitive and specific route of mast cell activation may also be the answer to the killing of those few, but potentially fatal, malignant cancer cells that remain in minimal residual disease following surgery, or those metastatic cells, isolated and distant from primary tumour sites.

In addition to mast cells with their well-recognised role in the allergic immune response and confinement to tissues, monocytes, macrophages and eosinophils are also potential cytotoxic, IgE-receptor-expressing effector cells (as discussed in section 1.3.5). The latter two cell types are found not only throughout tissues of the body, but actively infiltrating tumours of solid tissues and sites of inflammation, following receipt of specific signals to mediate their recruitment (as discussed in section 1.1.2). Those eosinophils and macrophages, resident within tissues, are perfectly positioned such that their sensitisation with tumour-specific anti-IgE antibody may trigger them to mediate a passive, specific, anti-tumour immune response.

As mentioned in section 1.2.3, a major barrier to successful of treatment of solid tumours with anti-cancer antibodies is their poor ability to penetrate such tissues. An intact IgG molecule has been shown to take 54 hours to move 1 mm into a solid tumour (Jain *et al.*, 1988). Also mentioned in section 1.2.3 is the fact that although penetration of solid tissues with antibody Fab fragments may be faster, 16 hours for movement of 1 mm (Jain *et al.*, 1988), the efficacy of this antibody fragment is reduced not only by its inability to recruit Fc-mediated effector mechanisms, but by their poor retention in the target tissue, making frequent dosing necessary. Use of IgE isotype antibodies may overcome this problem: it is well known that IgE is rapidly sequestered from the circulation to the tissues (Waldmann *et al.*, 1976) until all IgE binding sites are occupied (Strober *et al.*, 1978). The mechanism of this transport into tissues is likely to involve binding of monomeric IgE to FcεRI and CD23 on cells in the circulation, enabled by the high affinity of the interactions, and then the movement of these cells into the tissues. Furthermore, CD23b expression has been demonstrated to occur on intestinal epithelial cells where it has a role in transcellular transport of free IgE (discussed in section 1.3.7). It therefore follows that a comparable process might operate to mediate the uptake of intravenous IgE, a potential route of exogenous tumour-specific IgE administration, into tissues containing tumour cells.

Finally, treatment of cancer with IgE isotype tumour-specific antibodies may lead to the development of an acquired tumour-specific immune response. As mentioned in section 1.3, both FcεRI expressed by Langerhans cells, eosinophils and monocytes, and CD23 expressed by B cells, have a role in antigen presentation. Tumour antigen bound to tumour-specific IgE, itself bound to FcεRI (or CD23 on B cells), may be internalised and subsequently presented in the context of MHC class II to cognate T cells. The inflammatory

environment created by the local activation of mast cells during MOv18 IgE therapy, will hypothetically provide the signals for the expression of co-stimulatory molecules and stimulation of productive anti-tumour T cell responses.

1.4.2 MOv18 IgE and its antigen: Folate binding protein

The tumour-specific antibody used to assess the efficacy of IgE-isotype antibodies in mediating immune responses against tumour cells in this Thesis is MOv18 IgE. MOv18 IgE is a chimaeric IgE antibody specific for the ovarian carcinoma tumour-associated antigen, Folate Binding Protein (FBP) (Gould *et al.*, 1999; Coney *et al.*, 1991). The original MOv18 monoclonal antibody, murine MOv18 IgG1, was generated by immunisation of mice with a surgical specimen of ovarian cancer, as described in Miotti *et al.*, 1987. The murine γ1-heavy chains and κ-light chains of this original MOv18 IgG1 antibody were switched for human γ1-heavy chains and κ-light chains to make chimaeric MOv18 IgG (Coney *et al.*, 1994) and, subsequently, the human γ1-constant regions were switched for human ε constant regions to make the chimaeric MOv18 IgE (Gould *et al.*, 1999). The affinity of MOv18 IgE for FcεRI is as expected for native IgE at ~ 10^{10} M^{-1} (Gould *et al.*, 1999).

FBP is stably expressed on the cell surface of the majority of malignant as well as benign non-mucinous epithelial ovarian tumour cells. FBP is involved in the uptake of folate, from the extracellular environment and, accordingly, is also referred to as Folate Receptor (FR). The level of FBP expression has been shown to relate to clinical severity (Campbell *et al.*, 1991; Toffoli *et al.*, 1998), with high expression levels (~ 10^6 molecules / cell) associated with poor prognosis (Coney *et al.*, 1994), perhaps due to the proliferative advantage FBP expression confers (Bottero *et al.*, 1993). The affinity of MOv18 IgE for FBP is high at ~ 4 x 10^9 M^{-1} (Gould *et al.*, 1999). Expression of FBP on normal tissue is restricted to low levels, predominantly on adult oviduct epithelium and kidney proximal and distal tubules (Buist *et al.*, 1985). Only weak reactivity of a radiolabelled MOv18 IgG was seen with normal tissues in a Phase I study of intraperitoneal treatment of ovarian cancer patients with chimaeric MOv18 IgG (Molthoff *et al.*, 1997).

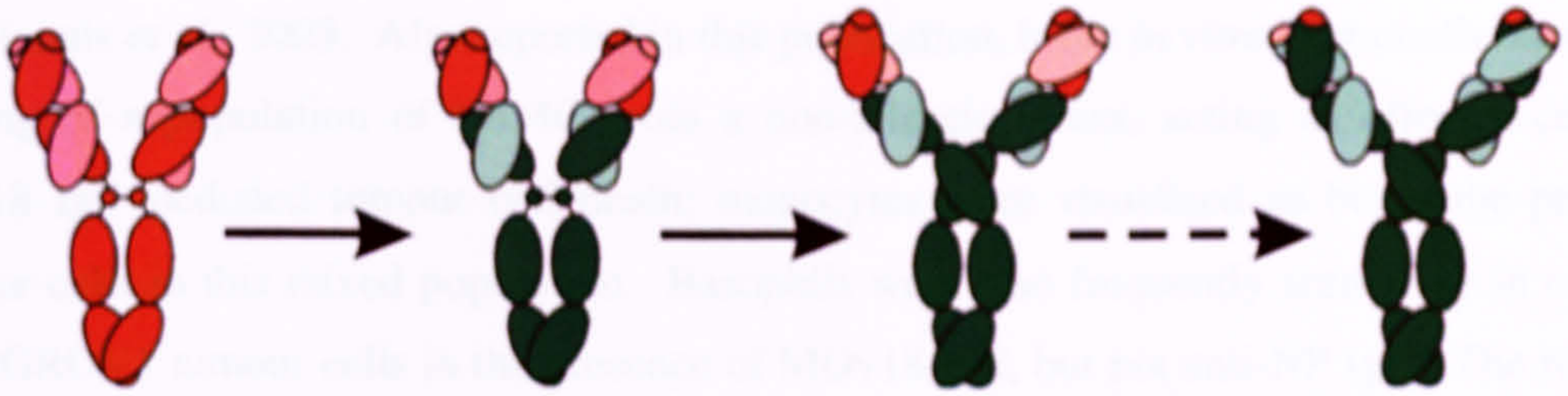

Figure 1.10: Schematic representation of the structure of murine MOv18 IgG, human-mouse chimaeric MOv18 IgG, human-mouse chimaeric MOv18 IgE and humanised MOv18 IgE. Murine regions are shown in pink and red, and human regions shown in dark and light green. Chimaeric antibodies can be seen to contain only murine variable regions, and humanised antibodies to contain only murine CDRs.

1.4.3 Evidence supporting the use of IgE in cancer so far

There have been two studies, referred to throughout this Thesis, which document research performed with MOv18 IgE to date: Gould *et al.*, 1999 and Karagiannis *et al.*, 2003. *In vitro* work described in the earlier of these two studies, includes the demonstration of histamine release by purified human peripheral blood basophils sensitised with MOv18 IgE, but not anti-NP IgE or MOv18 IgG1, upon stimulation with the FBP-expressing ovarian cancer cell line, IGROV1 (also used in this Thesis and described in sections 2.2.1 and 3.3). In addition, MOv18 IgE-sensitised platelets were activated by FBP-expressing IGROV1 cells, with the effect of bystander killing of schistosome larvae; this killing could be blocked by pre-incubation of the platelets with $F(ab')_2$ fragments of the monoclonal antibody 15-1, against FcεRI (described in section 2.1.2), confirming the involvement of FcεRI in MOv18 IgE effector function. Gould *et al.*, 1999, also report that purified human peripheral blood leukocytes act as effector cells in MOv18 IgG1 but not MOv18 IgE mediated tumour cell death *in vitro*. However, *in vivo*, when MOv18 IgE was injected with human PBMC, it provided significantly longer-lasting protection than MOv18 IgG1 plus human PBMC, from growth of a subcutaneous IGROV1 tumour in SCID mice. One dose resulted in at least 35 days protection with MOv18 IgE, compared to 19 days for MOv18 IgG.

The enhanced *in vivo* activity of MOv18 IgE over MOv18 IgG has been reproduced in a second model, a nude mouse model, described in this Thesis (section 6.2) and Karagiannis *et al.*, 2003. Also reported in this publication, is the *in vitro* immunofluorescence imaging of a population of PBMC from a non-allergic donor, acting as effector cells of MOv18 IgE-mediated tumour cell death; monocytes were visualised as being the primary effector cells in this mixed population. Basophils were also frequently seen to be in contact with IGROV1 tumour cells in the presence of MOv18 IgE, but not anti-NP IgE. The role for monocytes was supported by immunohistochemical staining of tumour sections taken from HUA-tumour bearing nude mice, HUA is a human ovarian cancer xenograft expressing human FBP (described in detail in section 2.3.3 of this Thesis), which had been treated with human PBMC alone or PBMC plus MOv18 IgE; monocytes were shown to be the primary infiltrating cells in the latter group. Furthermore, we demonstrated that a pure population of monocytes have the capacity to act as MOv18 IgE-mediated effector cells in the killing of IGROV1 tumour cells *in vitro*.

Reali *et al.*, 2001, provide another particularly important study addressing the potential for use of IgE in cancer therapy. *In vivo* models used in this study assess the efficacy of IgE in its ability to trigger passive anti-tumour immune responses against syngenic mouse tumours in immunocompetent mice, and compare this to IgG. This model involved transplantion of C57BL/6 mice with the syngeneic tumour, MC38-CEA-2. Tumours were then targeted indirectly, with IgE. Treatment with tumour-targeted IgE conferred mice with a significant survival advantage over both untreated control mice, and, IgG-treated mice. Furthermore, experiments performed in this study also addressed whether or not the local inflammatory response accompanying tumour destruction, following treatment with tumour-specific IgE, has the capacity to initiate an active anti-tumour immune response. To this end, C57BL/6 mice were inoculated with a low dose of MC38-CEA-2 tumour cells, which were pre-loaded with IgE. Control mice were inoculated in the same way, but tumour cells were IgE-negative. Subsequently, all mice were re-challenged with IgE-negative MC38-CEA-2 tumour cells. What they found was that when mice were first 'vaccinated' with IgE-bearing tumour cells, they were conferred with significant protection from tumour growth resulting from tumour re-challenge; these mice survived significantly longer than mice 'vaccinated' with IgE-negative tumour cells.

In the study reported by Reali *et al.*, 2001, and described above, the protection conferred to C57BL/6 mice by inoculation with IgE-bearing tumour cells, from tumour-growth occurring in response to re-challenge with the same tumour (not bearing IgE) at a later date, was shown to be dependent upon eosinophils, $CD4^+$ and $CD8^+$ T cells. Indeed, tumour-specific CTLs could be isolated from the spleens of protected mice, showing protection from

tumour growth, and used to elicit tumour cell killing *in vitro*. Tumour-specific CTLs could not be similarly isolated from mice bearing progressively growing tumours. IgE antibodies are already known to have a role in the capture and processing of antigen by professional antigen-presenting cells (Beiber *et al.*, 1997). These data suggest that treatment of cancer with tumour-specific antibodies of the IgE isotype may lead to the generation of active, anti-tumour immunity.

1.5 The aims of this Thesis

The aims of this Thesis are two-fold.

- The first is to assess the efficacy of MOv18 IgE in triggering immune responses against tumours, both *in vitro* and *in vivo*, work described in Chapters 3 to 6 of this Thesis.

- The second is to address how the affinity of the IgE-FcεRI interaction impacts on the intensity of IgE-mediated immune responses *in vivo*, work described in Chapter 7 of this Thesis.

CHAPTER 2:

Materials and Methods

Chapter 2: Materials and Methods

2.1 Materials

2.1.1 General Reagents

Details of all the general reagents used for experimental work described in this Thesis, are tabulated below (Table 2.1). The supplier name and catalogue number is given for each product. Where relevant, the chemical formula and molecular weight is provided.

Name, chemical formula, formula weight	Supplier	Catalogue #
Acetic acid, glacial (CH_3CO_2H)	Sigma	A9967
Acid citrate-dextrose	Sigma	C3821
Acrylamide, 30% (w/v) acrylamide / 0.8% (w/v) NN'-methylenebis-acrylamide stock solution	Severn Biotech Ltd	20-2100-05
Ammonium Chloride, 53.49	Sigma	A-215666
Ammonium persulphate, $(NH_4)_2S_2O_8$, 228.2	Sigma	A-3678
Bovine Serum Albumin (BSA)	Sigma	A-2153
CFSE, $C_{29}H_{19}NO_{11}$, 557.47	Molecular Probes	C-1157
Coomassie brilliant blue R250, purified	Electran	44418 2M
D-Glucose, $C_6H_{12}O_6$, 180.16	Sigma	G7528-1KG
DMEM	Gibco	11966-025
Dimethyl sulfoxide (DMSO)	Sigma	D2650
Ethanol	Sigma	45-983-6
EDTA disodium salt, $C_{10}H_{14}N_2O_8Na_2.2H_2O$, 372.2	Sigma	E-5134
Evans blue dye	Sigma	E-2129
Ficoll-Paque™ PLUS	Amersham Biosciences	17-1440-03
Foetal Calf Serum	Gibco	10106-169
Formaldehyde	Sigma	F8775
Formamide	Sigma	F7503
Geneticin, 50 mg/ml	Gibco	10131-027
Glycerol	Sigma	G-6279
Glycine, $C_2H_5NO_2$, 75.07	Sigma	G-7403
Goat serum, normal	Gibco	16210-072
HEPES	Sigma	H-3375
Histopaque®-1077, density = 1.077 ± 0.001	Sigma	1077-1
HT Supplement (50 x)	Gibco	41065-012
Hydrochloric Acid, HCl, 2.0 N	Sigma	251-2
IGEPAL CA-630	Sigma	9036-19-5
MACS CD16 MicroBeads	Miltenyi Biotech	130-045-701
MACS CS Depletion Columns	Miltenyi Biotech	130-041-305
Magnesium Chloride, $MgCl_2$	FSA Laboratory Supplies	M/0600
Marvel, dried skimmed milk	Premier International Foods, UK	

2-mercaptoethanol, C_2H_6OS, 78.13	Sigma	M-7522
Neuraminidase	Sigma	N2133
NIP-BSA	Biosearch Technologies	N-5040-10
NONIDET P-40	Sigma	N-6507
o-Phenylenediamine tablets, 5 mg per tablet	Sigma	P-6912
Penicillin, Streptomycin, Glutamine	Gibco	10378-016
Percoll™, density = 1,130 g/ml	Amersham Biosciences	17-0891-01
Phosphate buffered saline, sterile	Gibco	14190-094
Phosphate-citrate buffer with sodium perborate capsule	Sigma	P-4922
Poly-$_D$-lysine, lyophilised	Sigma	P-7405
Potassium Chloride, KCl, 74.55	Sigma	P-9333
Potassium Phosphate, KH_2PO_4, 136.1	Sigma	P-0662
Propidium Iodide Nucleic Acid Stain, 1mg/ml in water	Molecular Probes	P-3566
Protease inhibitor cocktail tablets	Roche Diagnostics	1 873 580
RAL 555 Kit	Reactifs RAL	361550-0000
Recombinant human IL-5	R&D Systems	205-IL
Recombinant human IL-4	R&D Systems	204-IL
RosetteSep™ human monocyte enrichment cocktail	Stemcell Technologies	15028
RPMI 1640	Gibco	31870-025
Sodium Azide, NaN_3, 65.01	Sigma	S-2002
Sodium Chloride, NaCl, 58.44	Sigma	S-9625
Sodium Hydrogen Carbonate, $NaHCO_3$, 84.01	BDH Chemicals	30151
Sodium Pyruvate, 100 mM	Gibco	11360-039
Sucrose, $C_{12}H_{22}O_{11}$, 342.3	Sigma	S-7903
TMED, N,N,N',N'tetramethylethylenediamine, $C_6H_{16}N_2$	Sigma	T-9281
Trypsin-EDTA solution (10 x)	Gibco	35400-027
Trizma® base, $C_4H_{11}NO_3$, 121.14	Sigma	T1503-5KG
Trypan blue solution, 0.4 %	Sigma	T8154
Tween20 (polyoxyethylene(20)sorbitan monolaurate)	Sigma	P-5927
Xanthine, sodium salt, 174.1	Sigma	X-3672

Table 2.1: Supplier details for general reagents.

2.1.2 Antibodies

All antibodies used in this project are described in Table 2.2 below. Antibodies specific for different epitopes of a single antigen have been used in some cases. Each antibody has been given a specific reference number to make clear which was used for which experiment. All antibodies are specific for human antigens unless specified otherwise. Table 2.2 excludes details of chimaeric MOv18 IgE, chimaeric MOv18 IgG, human wild type anti-NP IgE and R334S anti-NP IgE, which were all produced in-house as described below, in section 2.2.2. Additional details of those antibodies against human IgE, FcεRIα and CD23 are given below Table 2.2.

Ref. #	Specificity	Conjugate	Host Species	Supplier and Code
1	CD14	PE	Mouse, IgG2a, κ	Dako, R0864
2	CD16	-	Mouse IgG1, κ	Dako, M7006
3	CD23, BU38	-	Mouse IgG1	The Binding Site, AP271
4	CD23, BU38	-	Mouse IgG1	Produced in-house (Dr. N. McCloskey)
5	CD23, IDEC-152	-	Monkey	IDEC, 3002G990
6	CD23, IDEC-152 $F(ab')_2$	-	Monkey	IDEC
7	CD23, Tu1	-	Mouse IgG3, κ	SouthernBiotech, 9580-01
8	CD32	-	Mouse IgG1, κ	Dako, M7190
9	CD49d	PE	Mouse IgG1, κ	BD Pharmingen, 555503
10	CD64	-	Mouse IgG1, κ	Dako, M7218
11	CD89	PE	Mouse IgG1, κ	BD Pharmingen, 555686
12	Dual Negative	FITC	Mouse IgG1	Dako, X0949
		PE	Mouse IgG2a	
13	FcεRIα (15–1/ 3G6)	-	Mouse ascities	Upstate Biotechnology, 05-491
14	FcεRIα (15-1)	-	Mouse IgG	Produced in-house (M. Corbett)
15	FcεRIα (15A5)	-	Mouse IgG1	Provided by Dr. A. Gilfillan, NIH
16	IgE, 4.15	-	Mouse IgG1, κ	Produced in-house (Dr. L. Smurthwaite)
17	IgE	HRP	Polyclonal rabbit	Dako, P 0295
18	IgE	FITC	Goat	Vector Laboratories, F1-3040
19	IgE	Biotin	Goat	Vector Laboratories, BA-3040
	(Reference 19 used with:	Streptavidin-PE		Dako, R 0438)
20	IgE, α-γ fusion protein	-	Human IgG_4	Produced in-house (Dr. S. Karagiannis)
21	IgG	FITC	Rabbit $F(ab')_2$	Dako, F0315
22	IgG1, Mouse	PE	Rat	BD Pharmingen, 550083
23	Isotype control	PE	Mouse IgG1, κ	Dako, X0955
24	Isotype Control	-	Mouse IgG1, κ	Dako, X 0931
25	Isotype Control	-	Mouse IgG3, κ	BD Pharmingen, 556657
26	Mouse immunoglobulins	FITC	Goat $F(ab')_2$	Dako, F0479
27	MOPC 21	-	Mouse IgG1, κ	Sigma

Table 2.2: Details of antibodies used for experiments described in this Thesis.

Anti-human IgE antibodies: Antibodies used against human IgE in this project, include those with reference numbers 16-20 in Table 2.2. Antibody number 16, anti-human IgE of clone 4.15 (Hassner and Saxon, 1984), was produced from the CIA-E-4.15 hybridoma (ATCC: HB-235), and provided by Dr. Lyn Smurthwaite. 4.15 has been used to coat ELISA plates for the detection of human IgE (described in section 2.3.1, below). 4.15 binds to an epitope between amino acids 218 and 301 in the Cε2 domains, of IgE-Fc (information available in the ATCC specification sheet for the CIA-E-4.15 hybridoma). The HRP-

conjugated polyclonal rabbit anti-human IgE antibody from Dako, code P 0295 (Table 2.2; reference 17) was used as a detection antibody in the same anti-human IgE ELISAs.

The FITC-conjugated goat-anti-human IgE antibody from Vector (Table 2.2; reference 18) has been used to detect endogenous IgE, MOv18 IgE and anti-NP IgE, bound to IgE receptors on (both primary and U937) monocytes (Chapter 3). An equivalent goat anti-human IgE antibody (Table 2.2; reference 19, also from Vector Laboratories) conjugated to biotin, was used in combination with streptavidin-PE, to detect IgE (again endogenous, MOv18 IgE and anti-NP IgE) bound to IgE receptors on eosinophils (Chapter 3). The purpose of using the biotin-streptavidin-PE detection method instead of FITC was to amplify the signal from the low level of IgE receptors expressed by eosinophils; an anti-human IgE antibody directly conjugated to PE was not available.

The structure of the anti-IgE construct, α-γ fusion protein (reference number 20, in Table 2.2), is that of an IgG_4 antibody with its two Fab arms, each replaced with a soluble fragment (the IgE-binding, extracellular region) of the FcεRIα chain: IgG_4-Fc-$(sFc\varepsilon RI\alpha)_2$, as described in Shi *et al.*, 1997. When α-γ fusion protein is amine coupled to Sepharose beads (via its Fc region), the extremely high affinity (and specificity) of the FcεRIα:IgE interaction can be exploited for the specific isolation of IgE antibodies from cell culture supernatants, as indeed has been its role in this project (protein purification by affinity chromatography is described in section 2.3). α-γ fusion protein itself is purified from cell culture supernatants using a standard Protein G-Sepharose column.

Antibodies against FcεRIα: Those antibodies with specificity for FcεRI α-chain, which were used in this project, include 15-1 (Table 2.2; reference numbers 13 and 14) and 15A5 (Table 2.2; reference number 15). Antibody 15-1 was originally described in Wang *et al.*, 1992, and 15A5 in Riske *et al.*, 1991. What 15-1 and 15A5 have in common, is that they both bind to a site in FcεRIα, which is overlapping with, but non-identical to, the IgE binding site. The site in FcεRI to which IgE binds includes the B-C, C'-E and F-G loops of the D2 domain of FcεRI α-chain (shown in Figure 1.4). The 15-1 binding site has been localised to residues 110-120 of the BC loop (Rigby *et al.*, 2000). The 15-1 binding site was originally thought to also involve direct interactions with valine 155 and tryptophan 156 in the FG loop (Nechansky *et al.*, 1998). However, Rigby *et al.*, 2000 suggest mutation of these residues to leucine and alanine, respectively, are likely to have prevented 15-1 binding through an indirect effect on the conformation of the BC loop and not through direct disruption of the FcεRIα:15-1 interaction. The site in FcεRIα to which 15A5 binds has also been localised to D2, specifically, within residues 125-140 (Riske *et al.*, 1991). The consequence of 15-1 and

15A5 binding to sites in FcεRIα which are cross-reactive with the IgE binding site, is that IgE is unable to bind receptors to which antibody is pre-bound, and likewise, 15-1 and 15A5 are unable to bind receptors to which IgE is bound. Therefore, 15-1 and 15A5 can only directly detect those FcεRI unoccupied by IgE. The affinities of the 15-1 and 15A5:FcεRI interactions are similar to IgE:FcεRI. 15-1 has a slightly slower off-rate than IgE (Nechansky *et al.*, 2001) and 15A5 a slightly faster off-rate (Riske *et al.*, 1991).

Antibodies against CD23: Anti-human CD23 antibodies used in this project include clone BU38 (Table 2.2; references 3 and 4), clone Tu1 (Table 2.2; reference 7) and IDEC-152 (Table 2.2; reference 5). Two different supplies of BU38 were used; one was made in house and kindly provided by Dr. Natalie McCloskey and the other was purchased from a commercial source (The Binding Site). BU38 recognises the lectin domain of CD23 (Gabriel Grundy, PhD Thesis), blocking IgE binding. The anti-human CD23 antibody, Tu1 (Southern Biotechnology), also blocks binding of IgE to CD23, but the site in which Tu1 binds to in CD23 to mediate this effect has not been characterised. It is not reported in the available literature regarding IDEC-152, to which epitope of CD23 IDEC-152 binds; however, it is known to be cross-reactive with the IgE binding site (Mavromatis and Cheson., 2001; Rosenwasser *et al.*, 2003; Mavromatis *et al.*, 2004, and personal communication with IDEC Pharmaceuticals).

2.1.3 Buffers and Solutions

Suppliers and details of the chemicals used in the recipes listed below are detailed in Table 2.1. Ultrapure water was obtained from a MilliQ UF Plus machine supplied by Triple Red (Thame, UK) and used at a purity of 18.2 mΩ / cm. Buffers and solutions were prepared as follows:

APS: APS was prepared as a 10 % (w/v) solution in MilliQ water.

Carbonate coating buffer: 15 mM sodium carbonate, (1.59 g / litre), 35 mM sodium hydrogen carbonate, (2.93 g / litre) prepared in 1 litre MilliQ water and pH adjusted to 9.6.

Coomassie blue stain: 0.05% Coomassie brilliant blue R was dissolved in methanol, distilled water and acetic acid mixed at a 5:5:1 ratio.

Coomasssie destain: 0.05 % methanol 7.5 % acetic acid in deionised water.

FACS Buffer: PBS supplemented with 5 % normal goat serum.

FACS Fix: FACS buffer supplemented with 1 % paraformaldehyde.

Fekete solution (Fekete, 1938): A bleaching solution used for the identification of tumour metastases on rodent lung tissue. This is composed of 70 % ethanol, 15 % MilliQ water, 10 % formaldehyde and 5 % glacial acetic acid.

Glycine: 2 M glycine (15 g / litre of MilliQ water), pH adjusted to 2.5.

Lysis Buffer A: For lysis of red blood cells in granulocyte pellets during eosinophil purification. 155 mM ammonium chloride, (8.29 g / litre), 10 mM $NaHCO_3$, (0.84 g / litre) and 0.1 mM EDTA (0.37 g / litre) prepared in 1 litre MilliQ water. Filter sterilised and pH adjusted to 7.4.

Lysis Buffer B: For homogenisation of mouse ear tissue. To make 50 ml, 2.5 ml 2 M NaCl (100 mM), 0.5 ml 1 M Hepes (10 mM), 0.075 ml 1 M $MgCl_2$ (1.5 mM), 0.5 ml 1 M KCl (10 mM) in addition to 12.5 ml 100 % glycerol (25 %) and 0.25 ml 100 % NP40 (0.5 %) were added to 33.675 ml MilliQ water. The MilliQ water included a protease inhibitor cocktail prepared by dissolving one 'complete' tablet in 2 ml of MilliQ water to make a 25 times stock solution of which 1.407 ml was included in the 33.675 ml of MilliQ water.

MACS Buffer: 2 mM EDTA (0.74 g / litre) and 0.5 % BSA (5 g) dissolved in 1 litre of PBS.

OPD Buffer: 0.05 M phosphate-citrate buffer was made by dissolving the contents of one phosphate-citrate buffer capsule into 100 ml of milliQ water. OPD buffer was made by dissolving 1 o-Phenylenediamine tablet into 10 mls of phosphate-citrate buffer.

Percoll, density = 1.082 g / ml: Percoll was made to a density of 1.082 g / ml for density gradient fractionation of whole blood for eosinophil isolation. First, a 90 % solution of percoll was made by diluting 9 parts percoll with 1 part sodium chloride 9 % (9 g NaCl / 100 ml MilliQ water, filter sterilised). For the percoll d = 1.082, to make 100 ml, 66.3 ml of percoll 90 % was mixed with 33.7 ml sodium chloride 0.9 % (0.9 g NaCl / 100 ml MilliQ water, 0.2 μm filter sterilised).

Phosphate Buffered Saline: 0.14 M NaCl, 2.7 mM KCl, 1.5 mM KH_2PO_4, 8.0 mM Na_2HPO_4 pH 7.4 in MilliQ water.

Phosphate Buffered Saline-(Tween): PBS with the addition of 0.05 % Tween 20 (0.5 ml / litre PBS).

Run buffer for gel filtration: Standard buffer used in both preparative and analytical gel filtration. 0.5 M Tris-HCl, 250 mM NaCl 0.05 % NaN_3; degassed and 0.2 μm filtered pH 7.2.

Run buffer for SDS-PAGE: A 10x stock solution was made by dissolving 30 g Tris and 144g Glycine in 100 ml 10 % SDS. One part stock solution was added with 9 parts MilliQ water immediately before use.

Sample buffer: A 5 x stock solution was made by making 3.125 ml 1 M Tris (pH 6.8), 5 ml Glycerol and 0.25 g SDS and 1 ml β-mercaptoethanol to 10 ml with water. 20 μl sample was mixed with 5 μl sample buffer to make a final buffer concentration of 1 x.

Selection media A: Used in the selection of J558L cell colonies, successfully transfected with R334S anti-NP IgE heavy chain. This selection media is composed of 84 ml DMEM, 4 ml HT supplement (50x), 4 ml Xanthine (12.5 mg / ml; made in 0.2 M NaOH), 8 ml Mycophenolic Acid (250 μg / ml; made in 0.1 M NaOH) and 0.6 ml HCl (2 N).

Selection media B: Used in the selection of J558L cell colonies, successfully transfected with R334S anti-NP IgE heavy chain. This selection media is composed of 92 ml DMEM, 2 ml HT supplement (50x), 2 ml Xanthine (12.5 mg / ml; made in 0.2 M NaOH), 4 ml Mycophenolic Acid (250 μg / ml; made in 0.1 M NaOH) and 0.3 ml HCl (2 N).

Tris Buffered Saline: A 10 x TBS stock was made by dissolving 48.46 g of Trizma base (200 mM) with 116.88 g of Sodium Chloride (1 M) and 20 g of Azide (1 %) in 2 litres of water. The pH was reduced to 8.2. 200 ml of stock solution was diluted with MilliQ water to 2 litres immediately before use and the pH of 8.2 confirmed.

Tris: 1 M tris was made by dissolving 121.14 g of Trizma base in 1 litre of MilliQ water and adjusting the pH to 8.2.

2.1.4 Animals

All animals were housed in a specific pathogen-free facility at room temperature, excluding nude mice, which were housed in sterile isolators at 20 °C (La Calhene, Ltd., United Kingdom). All animals had continuous access to food and water.

Balb/c mice: Balb/c mice were purchased from Iffa-Credo, France. All mice were 8-12 weeks old at the start of experiments, and of either gender.

Nude mice: Female *nu/nu* mice from a colony of mixed genetic background (purchased by Frances Balkwill, Translational Oncology, St. Bartholomew's Hospital, Charterhouse Square, London) were used at 8-12 weeks old. Nude mice are born athymic (and free of hair). This phenotype results from a nonsense mutation in the ***w***inged-***h***elix-***n***ude gene which encodes a member of the forkhead / winged-helix transcription factor family. Expression of *whn* is restricted to epithelial cells of the thymus and skin, where it normally functions to direct cell-fate decisions, maintaining the balance between growth and differentiation. Without the thymic microenvironment, developing T cells are unable to make the cellular interactions they need to undergo positive or negative selection and the effect of the *whn* defect is therefore an almost complete absence of T-cells (T cells are not completely absent, as some are able to mature in the periphery).

Human FcεRI transgenic (hFcεRITg) mice: The generation of hFcεRITg mice, mutant for the murine FcεRI α-chain gene and carrying a transgene for human FcεRI α-chain, is described in detail in Dombrowicz *et al.*, 1996 and 1998. In brief, transfected human α-chain associates with mouse FcεRI β-chain and γ_2-dimer or γ_2-dimer alone, to form complete tetrameric or trimeric FcεRI complexes at the cell surface. Receptors have been demonstrated to be functional *in vitro* by the triggering of an intracellular calcium influx and serotonin release in IL-3-cultured BMMCs from hFcεRI transgenic mice but not control animals, when loaded with human anti-NP IgE and cross-linked by NIP-BSA. Functionality *in vivo* has been demonstrated by passive induction of cutaneous and systemic anaphylaxis following sensitisation with human IgE and subsequent antigen challenge. 'Humanisation' of these mice is conferred not only through expression of a form of FcεRI which binds to human IgE, but by a move from a tissue-specific distribution of FcεRI characteristic of mice (tetrameric FcεRI on mast cells and basophils) to a tissue-distribution characteristic of humans (tetrameric FcεRI on mast cells and basophils in addition to trimeric FcεRI on monocytes, eosinophils, langerhans cells and platelets) (Dombrowicz *et al.*, 1998). This is a consequence

of both transfection of the human FcεRI promotor (Dombrowicz *et al.*, 1996) and the fact that the γ-subunit alone is sufficient for expression of human but not mouse α-chain, which also requires the presence of β-chain (Ra *et al.*, 1989), as discussed in section 1.3.2. Expression of hFcεRIα was checked prior to my receipt of the mice by Southern blot (as described in Dombrowicz *et al.*, 1996).

Wistar Albino Glaxo (WAG) rats: Female inbred rats of strain WAG/RijHsd were purchased from Harlan, France. All rats were used between 10 and 12 weeks of age.

2.2 Tissue culture

All tissue culture was perfomed under sterile conditions in a laminar flow hood (Howorth, Crowthorne Hi-tec.). Cells were grown in a humidified atmosphere at 37 °C in 5 % CO_2 (in a Nuaire DH Autoflow incubator, Triple Red Ltd.). All culture media was supplemented with 10 % FCS (not heat inactivated), 2 mM $_L$-glutamine, penicillin (5000 U / ml) and streptomycin (100 µg / ml) unless otherwise specified. For storage, aliquots of 10 x 10^6 cells were prepared to a total volume of 1 ml using 950 µl of freezing media (90 % FCS and 10 % cell-specific standard culture media) plus 50 µl DMSO and kept in liquid nitrogen after a progressive shift of temperature.

2.2.1 Culture of cell lines

The relevant phenotypic characteristics of the cell lines described below are discussed in more detail in Chapter 3 of this Thesis. In this section, details of the origin and maintenance of each cell line are given. In all cases, cell lines were maintained for a maximum of 100 passages. To passage, adherent cell lines were detached by removal of media, rinsing of the monolayer in PBS, followed by incubation in the minimal amount of Trypsin-EDTA necessary to cover the monolayer, for the minimal amount of time possible at 37 °C in 5 % CO_2. When all cells were detached (as judged by light microscopy), they were washed in the culture media in which they were normally grown (as were cells which grew in suspension). Washing of all cell lines involved centrifugation for 5 – 8 minutes at 1200 rpm in a Sorval RT 6000D centrifuge, fitted with a H1000B rotor. After centrifugation, supernatant was poured off and the cells reconstituted at the required split ratio, or specific concentration.

U937 monocyte cell line: The U937 monocyte cell line was originally derived (as reported in Sunstrom and Nilsson, 1976) from the pleural effusion of a patient with histiocytic

lymphoma. The wild type myelomonocytic U937 cell line used in this Thesis was kindly provided by Dr. J.-P. Kinet. U937s were grown in the standard culture media described above, and maintained at a density between 1 x 10^5 - 2 x 10^6 cells / ml. Where U937 monocytes were cultured in IL-4, this involved supplementation of the standard culture media with 320 U / ml of recombinant human IL-4, four days prior to use of the U937 monocytes in an experiment (this protocol for IL-4 culture of U937 monocytes was optimised for maximal upregulation of CD23 expression, by Dr. Sophia Karagiannis).

IGROV1 tumour cell line: The human ovarian cancer cell line IGROV1 (Bénard *et al*, 1985) was used as the standard tumour-target in *in vitro* killing assays. The IGROV1 cell line originates from a stage III ovarian carcinoma of a 47-year-old woman. Histological analysis of the original tumour diagnosed it to be a glandular and polymorphous ovarian epithelioma with multiple differentiations, primarily endometrioid, with some serous clear cells and undifferentiated foci. Since establishment in tissue culture, the IGROV1 cell line has been maintained in monolayer where it exhibits a 20-hour doubling time and retains its epithelial morphology. IGROV1 cells were maintained in RPMI 1640 with standard additives and passaged as described above thrice weekly, at a ratio of 1:3 or 1:4.

For some experiments (indicated where relevant), it was required that IGROV1 cells be killed. This was perfomed using the Dako fixation / permeabilisation kit, according to the manufacturer's instructions. This involved treatment of a pellet of IGROV1 cells (up to 1 million, in no more than 500 µl of FACS buffer), with 50 µl of 'Buffer A' for 30 minutes at 4 °C. Cells were then washed once in FACS buffer, and 50 µl of 'Buffer B' was added to the pellet, again for 30 minutes at 4 °C.

C26 cells: The Balb/c colon carcinoma cell line C26 was maintained in Dulbecos Modified Eagles Medium with standard additives. C26 cells grow as an adherent monolayer. C26 cells transfected to express human FBP, and termed C26tFR, were cultured in the same media as for wild type C26 cells, additionally supplemented with 0.8 mg / ml G418. C26tFR cells were grown in the absence of G418 for 5 days prior to injection into mice. Cells were split approximately 1:6 every 3 days by standard trypsinisation, as described above. Both wild type and C26tFR cells were kindly provided by Dr. S. Canevari.

CC531 cells: Dr. S. Canevari also kindly provided the CC531-tumour cell line, which was originally derived from a chemically induced adenocarcinoma of the colon of a WAG rat (Marquet *et al.*, 1984). Wild type CC531 cells were grown in RPMI 1640 with standard additives. For the purposes of work described in Chapter 6 of this Thesis, Dr. S. Canevari

also kindly provided CC531 cells transfected to express human FBP, termed CC531tFR. Three different clones of CC531tFR were received, clones 2, 11 and 16, each expressing FBP at high, medium and low levels, respectively. Transfected CC531 cells were grown in the same medium as wild type cells, additionally supplemented with 0.4 mg / ml G418. Wild type and FBP-transfected CC531 clones were split approximately 1:6 every 3 days by standard trypsinisation as described above. The normal appearance of CC531 cells is of visibly granular adherent cells, with some cells in suspension.

2.2.2 Hybridoma culture

Culture media for all hybridoma cell lines was supplemented with standard additives and grown in a humidified atmosphere at 37 °C in 5 % CO_2, as described above. When a total volume of 250 ml was reached by culture in flasks, cells and media were transferred to roller bottles in which they were grown for up to two weeks. During roller bottle growth, cells were gassed with sterile 5 % CO_2 in air for one minute every other day. Cell counts were carried out regularly by haemocytometer using 2 % w/v trypan blue. Supernatant was harvested by centrifugation at 10 000 rpm (in a Sorval RC-5B Plus centrifuge fitted with fixed-angle rotor) for ten minutes to remove cell debris. Supernatant was subjected to 0.2 μm filtration and stored at 4 °C after supplementation with sodium azide to a final concentration of 0.05 % to inhibit bacterial growth. Purification of antibodies from hybridoma supernatants is described in section 2.3.1.

JW8 hybridoma: The cell line JW8, secreting wild type, human anti-NP IgE, was kindly provided by Dr. M. Neuberger (Bruggemann *et al.*, 1987). This consisted of the J558L λ-light chain-secreting mouse myeloma permanently transfected with the construct for human anti-NP IgE heavy chain. Cells were grown in Dulbecco's Modified Eagles Medium with standard supplements and kept between 3 and 9 x 10^5 cells / ml.

R334S hybridoma: Human anti-NP IgE mutated in the Cε3 domain of each heavy chain by substitution of the arginine residue at position 334 for serine (R334S NIP IgE), was constructed by Dr. Jianguo Shi for the purpose of work described in Chapter 7 of this Thesis. Dr. J. Shi used the following protocol: Wild type human anti-NP IgE heavy chain construct was transformed into *Escherichia coli* (XL1-blue) and the plasmid DNA was purified with QIAGEN™ purification kit and mapped with restriction enzymes according to the manufacturer's instructions. The DNA was then sequenced using a reverse primer, IgE-S2 (5' cca ggt cag gtt cag g 3', between amino acid residues 369-374). Using the obtained sequence, two primers (R334S-FOR and R334S REV) were designed and synthesised by

MWG-biotec. The mutant R334S was generated using Quickchange XL site-directed mutagenesis kit (Stratagene) according to the manufacturers instructions. The colonies obtained were screened and mapped. Two of the positive colonies were sequenced to judge the site of mutagenesis. The R334S human anti-NP IgE heavy chain construct was transfected into J558L cell line (a human λ light chain-secreting mouse myeloma). Transfection was performed by electroporation; 1 x 10^7 cells were washed and resuspended in a final volume of 0.7 ml of ice cold PBS and 15 µg of linearised R334S anti-NP IgE was added to the cells and mixed well in a 0.4 cm electroporation cuvette (Bio-Rad). Electroporation was performed with two 0.1 second pulses of 1500 V at a capacity of 3 µF. The samples were left on ice for 30 minutes then diluted in 70 ml of DMEM and plated in seven 96-well flat-bottomed plates at 100 µl / well. After 24 hours of growth, 'selection media A' was added, which was replaced after 5 days with 'selection media B' (the details of which are described in section 2.1.3). Four positive colonies were obtained. After ELISA and western blotting analysis, one colony was selected due to its faster growth rate and higher production of R334S anti-NP IgE. J558L cells expressing the R334S anti-NP IgE protein were grown in DMEM with standard supplements and kept between 3 to 9 x 10^5 cells / ml.

Chimaeric MOv18 IgG1: The construction of chimaeric MOv18 IgG was originally described in Coney *et al.*, 1994. SP2/0 cells transfected to express chimaeric MOv18 IgG were grown in Iscove's Modified Dulbeccos Medium supplemented in addition to standard additives, with 1 mM pyruvate. The concentration of FCS in the media was reduced during culture firstly to 5 % by splitting 1:1 in serum free media, then 1:1 again in 5 % low IgG FCS, so that the final concentration of regular FCS and low IgG FCS is each at 2.5 %, reducing the IgG which is not MOv18 IgG in the supernatant.

Chimaeric MOv18 IgE: Construction of the chimaeric MOv18 IgE expression vector and its transfection into the murine melanoma cell line SP2/0 is described in Gould *et al.*, 1999. To express chimaeric MOv18 IgE, SP2/0 cells were cultured in Iscove's Modified Dulbeccos Medium, supplemented in addition to standard additives, with 1 mM pyruvate. Chimaeric MOv18 IgE is described in more detail in Chapter 3 of this Thesis.

2.2.3 Isolation and culture of primary cells

Isolation of primary cells: Primary monocytes and peripheral blood mononuclear cells (PBMC) which were to used as effector cells in *in vitro* assays of tumour cell killing were purified from the peripheral blood of donors with no history of allergic symptoms. Those

monocytes to be used as effector cells in *in vivo* assays of MOv18-mediated tumour cell killing were purified from human volunteers whose atopic status was determined on the basis of negative skin prick tests for 11 aeroallergens, and total serum IgE levels of 30 – 150 ng / ml, with allergen specific IgE levels, below 0.3 IU / ml. The reasoning for selection of non-atopic donors is discussed in Chapter 3. Any donor was used for eosinophil donation, regardless of atopic status. As standard, blood was venous and treated immediately with 1 ml of acid citrate-dextrose (ACD) per 10 ml whole blood.

Peripheral blood mononuclear cells: To isolate an enriched population of mononuclear cells from whole peripheral blood, ACD-treated blood was diluted 3 parts blood to 5 parts PBS and 8 parts of this diluted blood was layered onto 3 parts Histopaque-1077. For gradient separation of PBMC, the layered blood was centrifuged at 2000 rpm for 20 minutes at room temperature, with the brake off. Buffy coat, containing the PBMC, was transferred to a new sterile tube using a Pasteur pipette and washed by resuspension in PBS and centrifugation at 1500 rpm for 10 minutes at room temperature, following which the cell pellet was resuspended to 10 million cells in 1 ml PBS. Lyophilised neuraminidase was made to 1 ml in PBS to make a stock solution of 10 neuraminidase units per ml PBS. Aliquots of 30 µl containing 0.3 units were then made and stored at – 20 °C. PBMC were incubated with one aliquot of neuraminidase per 1 ml cell suspension for 30 minutes at 37 °C, as was previously determined to be optimal (Karagiannis *et al.*, 2003). The purpose of neuraminidase treatment was to digest the carbohydrate groups (sialyl Lewis x), shown to be present on the cell membrane which, likely through their proximity to FcεRI, sterically hinder IgE binding (Wank *et al.*, 1983 and Reischl *et al.*, 1996). After neuraminidase incubation, PBMC were washed once in the solution in which they were to be finally resuspended, and centrifuged at 1200 rpm for 10 minutes at room temperature.

Monocytes: For each ml of ACD-treated whole blood, 10 µl of 100 mM EDTA (1 mM final) and 50 µl RosetteSep™ human monocyte enrichment cocktail was added. This preparation was left to stand for 20 minutes at room temperature in sterile conditions. RosetteSep™ cocktail includes antibodies against cells expressing CD2, CD3, CD8, CD19, CD56 or CD66b, and anti-glycophorin A for red blood cells. Unwanted cells are cross-linked to red blood cells, creating tetrameric antibody complexes that increase their density relative to monocytes and allow their separation. The blood preparation was then diluted 1:1 with PBS and subjected to gradient separation by layering at a ratio of 4 parts blood/PBS mix onto 3 parts Ficoll, followed by centrifugation at 2000 rpm for 20 minutes with the brake off, at room temperature. The buffy coat, containing predominantly monocytes was isolated and

transferred to a new sterile tube, using a Pasteur pipette. This monocyte preparation was washed twice by resuspension in a solution of PBS containing 2 % FCS and 1 mM EDTA and centrifugation at 1500 rpm for 10 minutes. The supernatant was poured off and the cell pellet made to 1 ml with PBS and counted; cells were resuspended to 10 million per ml PBS. One freshly-thawed aliquot of neuraminidase, containing 0.3 U, as described above, was added per 1 ml monocyte suspension, and the suspension was incubated for 30 minutes at 37 °C. Following neuraminidase incubation, for *in vitro* killing assay use, monocytes were washed in RPMI containing 10 % FCS and 2 mM $_L$-glutamine, penicillin (5000 U / ml) and streptomycin (100 µg / ml), in which they were also resuspended. For injection into nude mice, monocytes were washed and resuspended in PBS. Monocyte preparations isolated in this way were on average 70 – 80 % pure as judged by FACS analysis of the proportion of cells staining positive for CD14 (a monocyte marker) in the final cell population.

Eosinophils: Throughout the eosinophil purification procedure, cell preparations and buffers were kept at 4 °C, which kept eosinophils inactive and thus prevented them from degranulating. Whole blood diluted 1:1 with sterile PBS was layered at a 2:1 ratio onto a Percoll gradient (density 1.082 g / ml) and centrifuged at 2000 rpm for 20 minutes with the brake off at room temperature. The granulocyte pellet containing mainly neutrophils and eosinophils was harvested and transferred into a clean falcon tube to avoid contamination by mononuclear cells adhering to the tube sides. Erythrocytes were depleted with a 25 minute hypotonic saline lysis. This involved a 15 minute incubation of no more than 10 ml of granulocyte pellet reconstituted to a total volume of 50 ml with lysis buffer A, followed by centrifugation of the cell / lysis buffer suspension for 8 minutes at 1500 rpm, and replacement with fresh lysis buffer for a further 10 minute incubation. The granulocyte pellet was washed once in ice cold PBS and resuspended to 1 x 10^6 cells / ml in MACS buffer followed by incubation for 30 minutes with 8 µl of anti-CD16-coated immunomagnetic beads per 1 million granulocytes, at 4 °C. CD16 (FcγRIII) is expressed at high levels on neutrophils but is absent on ~ 94 % of eosinophils (Seminario *et al.*, 1999). Neutrophils were then removed by passage of the cells through the field of a permanent magnet. After isolation, a cytospin was performed and eosinophils were established to be a minimum of 95 % pure by RAL 555, May Grünwald Giemsa staining kit, and at least 99 % viable by trypan blue exclusion.

Culture of primary cells: Where indicated, eosinophils were cultured for 4 days at 1 million cells per 1 ml of RPMI 1640 medium containing standard culture media supplements. Flasks (25 cm^2) containing 5 ml cells were additionally supplemented with 2.5 ng / ml of recombinant human IL-5, either alone or in combination with either 10 µg / ml anti-NP IgE or

MOv18 IgE. This concentration of IgE was chosen based on work described in Kayaba *et al.*, 2001, which demonstrated that this was the minimal amount of IgE required for maximal upregulation of FcεRI. IL-5 was included in all eosinophil culture as, without it, the number of cells viable after 4 days of culture was less than 50 %, as judged by trypan blue exclusion.

2.3 Methods

2.3.1 Protein Methods

Antibody purification: Antibodies produced in-house included MOv18 IgE, MOv18 IgG, wild type anti-NP IgE and R334S anti-NP IgE. Individual hybridoma cell lines were grown as described in section 2.2.2. All antibodies were purified from cell culture supernatants by affinity chromatography. Purification of wild type and R334S anti-NP IgE for use in *in vivo* passive cutaneous anaphylaxis experiments also included a second step of gel filtration, using HPLC (analytical and preparative). Affinity chromatography and HPLC was always performed with the help of either Dr. Andrew Beavil or Dr. James Hunt.

Affinity chromatography: Purification of IgG isotype antibodies (MOv18 IgG and 15.1) was performed using a Protein G column, purchased in a ready-to-use form from Amersham Biosciences. The specific ligand used for purification of IgE isotype antibodies (MOv18 IgE, wild type and R334S anti-NP IgE) was the α-γ fusion protein, amine coupled to Sepharose beads and packed into a glass column. The structure of α-γ fusion protein is described in section 2.1.2, and originally in Shi *et al.*, 1997. All affinity chromatography steps described below were performed using automated peristaltic pump apparatus passing fluid over the column at a rate of 0.5 ml / minute. The first step involved repeated cycling of the pH adjusted supernatant (pH 8.6) over the column to allow for binding of antibody to ligand until column saturation. Unbound material was removed by thorough washing of the column with TBS, pH 8.6. Captured antibody was eluted using 0.2 M glycine, pH 2.5, and the eluate immediately neutralised by addition of 1 M Tris, pH 8. The column was re-equilibrated by cycling of TBS.

Gel filtration: The purpose of the additional gel filtration step in both wild type and R334S anti-NP IgE purification, was to ensure these preparations were free of aggregated material to avoid activating cells in the absence of antigen in passive cutaneous anaphylaxis experiments, described in Chapter 7. Gel filtration provides a suitable method for removing aggregated protein by separating proteins on the basis of size. Aggregated molecules and other contaminants larger than the monomeric antibody pass more quickly through the porous bead

matrix, allowing them to be separated from the pure monomeric antibody fraction which travels more slowly, due to transient trapping in smaller pores of the matrix. Gel filtration was perfomed on a Gilson HPLC system using a Superdex^{TM} 200 column (Amersham Pharmacia Biotech), which is suitable for separation of proteins with molecular weights between 10 - 600 kDa.

Final preparations: Eluted protein was concentrated using 80 ml Centricon Plus-80 centrifugal filter units (Millipore) containing ultrafiltration membranes with a molecular weight cut off of 100 kDa. Centricon Plus units were spun in a Sorvall RC-5B Plus superspeed centrifuge (Du Pont) with a swinging-bucket rotor at a maximum centrifugal force of 3 000 rpm. For small volumes (up to 3.5 ml), Microsep^{TM} microconcentrators were spun in a Sorval RC-5B Plus fixed-angle rotor at 2 000 rpm. Before use, antibodies were dialysed against PBS to remove azide. To determine the concentration (mg / ml) of the antibody, the optical density at 280 nm was measured in a Cary 1E UV visible spectrophotometer using a 1 cm path length quartz cell. The optical density was divided into the extinction coefficient for the antibody (1.3 M^{-1} cm^{-1} for IgE and 1.4 M^{-1} cm^{-1} for IgG) and multiplied by the path length of the cell (1 cm).

SDS-PAGE: Antibody purity was assessed on the basis of size by sodium dodecyl sulphate polyacrylamide gel electrophoresis (SDS-PAGE), according to the discontinuous buffer system described by Laemmli (Laemmli, 1970); Atto system gel apparatus was used. Twelve-well 4-20 % Tris-glycine gradient gels were purchased from Invitrogen. A 5 – 8 % gradient gel electrophoresis was performed by Dr. R. Beavil (and is shown in Figure 3.1A); this gel was prepared according to a standard recipe. After placement in the gel tank, the tank was filled with running buffer, the comb removed and 20 µl of each sample in combination with 5 µl of 5 x sample buffer, was loaded after boiling for 2 minutes, alongside 10 µl SeeBlue^{TM} Plus2 pre-stained standard marker (Invitrogen). Samples were run at 150 V until the dye had reached the bottom of the gel plate. The gel plates were then separated, the stacking gel removed and the gel transferred to Coomassie blue for 2 hours for visualisation of proteins. Gels were then washed with water and incubated overnight with destain.

ELISA Procedure: ELISA was used for detection of human IgE in mouse ear homogenisation extracts and for estimation of the amount of antibody present in cell culture supernatants to determine expected yields before purification by affinity chromatography. A standard procedure was followed as described below. Plates were sealed under polythene for all incubations. Incubations at 37 °C took place in a humidified atmosphere. Plate washing

was performed using an Anthos fluido ELISA plate washer (Jencons PLS) programmed to wash 4 times in PBS-T. For detection of human IgE, Nunc flat-bottomed ELISA plates were coated with either NIP(5)BSA at 1 μg / ml or 4.15 anti-IgE (antibody with reference number 16 in Table 2.2) at 10 μg / ml, diluted in carbonate coating buffer (50 μl / well, 4 °C overnight). Without washing, non-specific antigen binding was blocked by addition of 2 % Marvel in PBS-T (200 μl / well, 2 hours at 37 °C). Unadsorbed coating antibody and blocking solution were removed by standard washing. Test samples were then added to relevant wells (50 μl / well, 4 °C overnight). Bound material was detected by the addition of the HRP-conjugated secondary anti-human IgE antibody P 0295 (antibody with reference number 17 in Table 2.2), diluted 1:2000 in PBS (50 μl / well, 1 hour at 37 °C). Following washing, chromogenic substrate solution (OPD buffer) was added (50 μl / well) and left for colour to develop at room temperature in the dark. The colour reaction was stopped by addition of 3 M HCl (50 μl / well). The absorbance of each well at 492 nm was measured using an automatic ELISA plate reader (Titertek multiskan, Flow), linked to a computer employing Ascent software. For quantification of MOv18 IgE or anti-NP IgE in cell culture supernatants, a standard curve was generated using a World Health Organisation IgE standard provided by Dr. L. Smurthwaite. For detection of wild type and R334S anti-NP IgE in mouse ear homogenates, dilutions of both wild type and R334S anti-NP IgE of known concentration were used to confirm equal detection of both wild type and R334S anti-NP IgE and to enable adjustment for differences in signal between plates.

Surface plasmon resonance using Biacore: A Biacore 3000 instrument was used to obtain kinetic information about the interaction between both wild type and R334S anti-NP IgE with FcεRIα. In a Biacore, the ligand, in this case FcεRIα in the form of the α-γ fusion protein IgG_4-Fc-$(sFc\varepsilon RI\alpha)_2$ (described in section 2.1), is immobilised on a sensor chip. The sensor chip consists of a glass slide, coated on one side with a thin gold film, itself covered with a covalently bound matrix to which the ligand is attached. This chip forms one wall of a 'micro-flow cell', positioned such that the ligand face is parallel to the flow of a solution containing the analyte, in this case anti-NP IgE (Figure 2.1). Changes in the concentration of analyte in contact with the sensor chip surface can then be measured in real-time using the optical phenomenon, surface plasmon resonance (SPR).

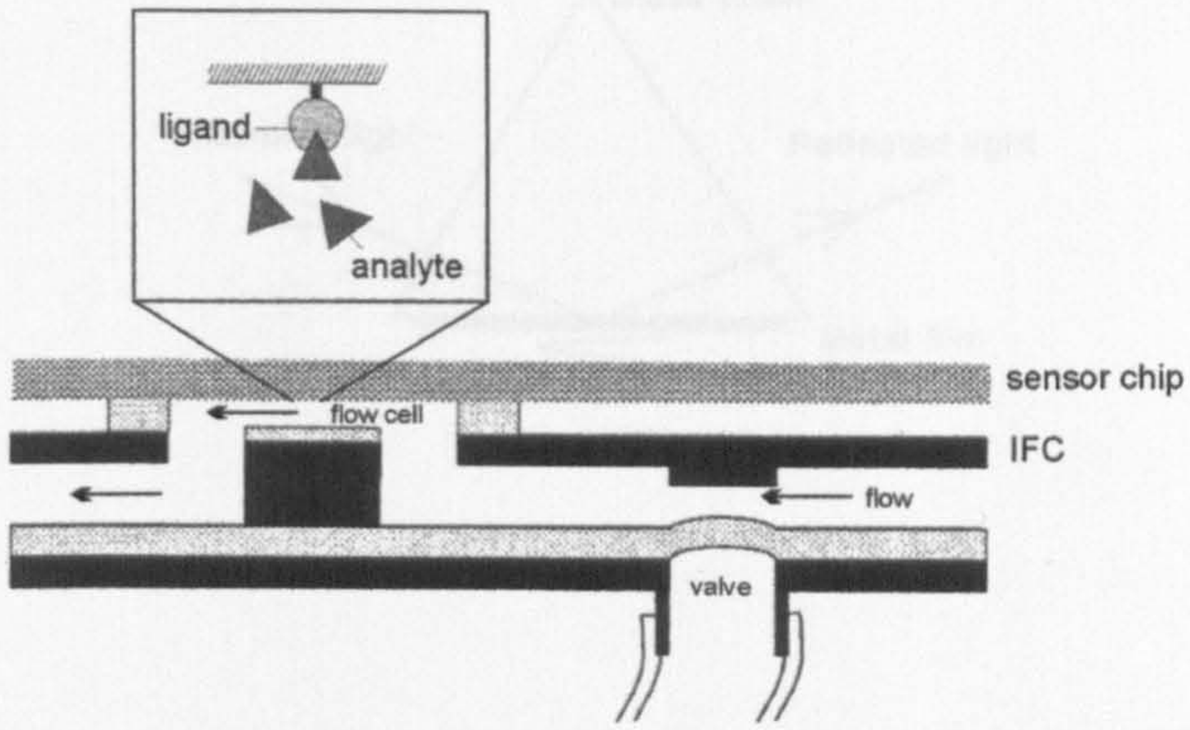

Figure 2.1. Diagrammatic representation of a vertical section through the flow cell, showing how the sensor chip ligand-binding face forms one wall of the flow cell such that analyte is able to bind as part of a continuous flow of fluid through the cell. Inset shows direct immobilisation of ligand on the sensor surface, which is able to interact with the analyte free in solution.

The term SPR describes the effect that occurs when light energy interacts with a thin metal film at the interface between two transparent media of high and low relative refractive index respectively, through which the light passes. SPR is dependent upon the light being monochromatic, polarised such that the electric vector component is parallel to the plane of incidence and above a critical angle of incidence, so that total internal reflection occurs. Under these conditions, when the light meets the interface between the two different media and is reflected, an evanescent wave is generated. This is an electromagnetic field component which penetrates a short distance into the lower refractive index medium (Figure 2.2A). Energy from the evanescent wave excites surface plasmons in the metal film, causing them to resonate. The effect of SPR is the absorption of the reflected light at a critical angle. This angle is dependent on the refractive index of the second media through which the light passes on the non-illuminated side of the metal film.

In a Biacore the glass slide of the chip represents the first transparent medium and the second transparent medium is represented by the aqueous layer of analyte immediately adjacent to the gold ligand-coated surface of the sensor chip. The refractive index is therefore dependent on the state of ligand-analyte interaction.

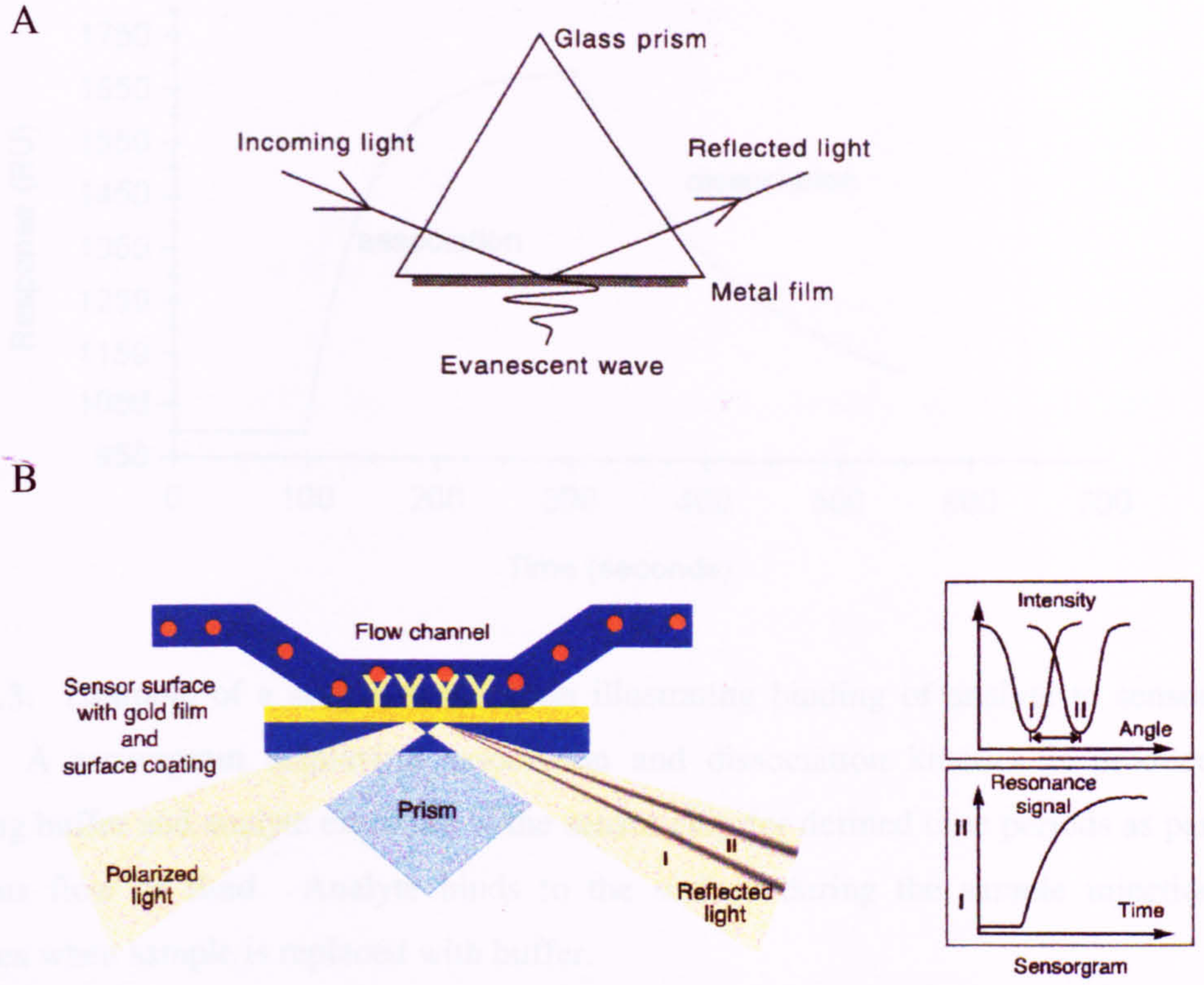

Figure 2.2: A: Diagrammatic representation of the evanescent wave propagated into the medium of lower refractive index on the non-illuminated side of the metal film. This occurs under conditions of total internal reflection. B: Diagrammatic representation of surface plasmon resonance occurring when light penetrates the gold film of the sensor chip after first passing through the glass slide. The change in resonance angle can be plotted as resonance units as a function of time to obtain a sensorgram, displaying the progress of the interaction.

Therefore, when sample and buffer are flowed in alternation for defined time-periods over the sensor chip as part of a continuous flow of fluid, such that analyte binds ligand during sample injection, and dissociates when sample injection is stopped and replaced with buffer, kinetic analysis of the interaction can be performed. The flow of analyte must not be slower than the rate of diffusion of analyte from the laminar flow to the ligand on the chip (mass transport) or it will limit the analyte-ligand interaction and incorrect binding kinetics will be observed. A trace termed a sensorgram is produced, plotting the change in resonance angle as a function of time such that the rise and fall in resonance angle reflects the association and dissociation phases of analyte (Figure 2.3). Kinetic information can then be extracted from the rate of change of the association and dissociation signals.

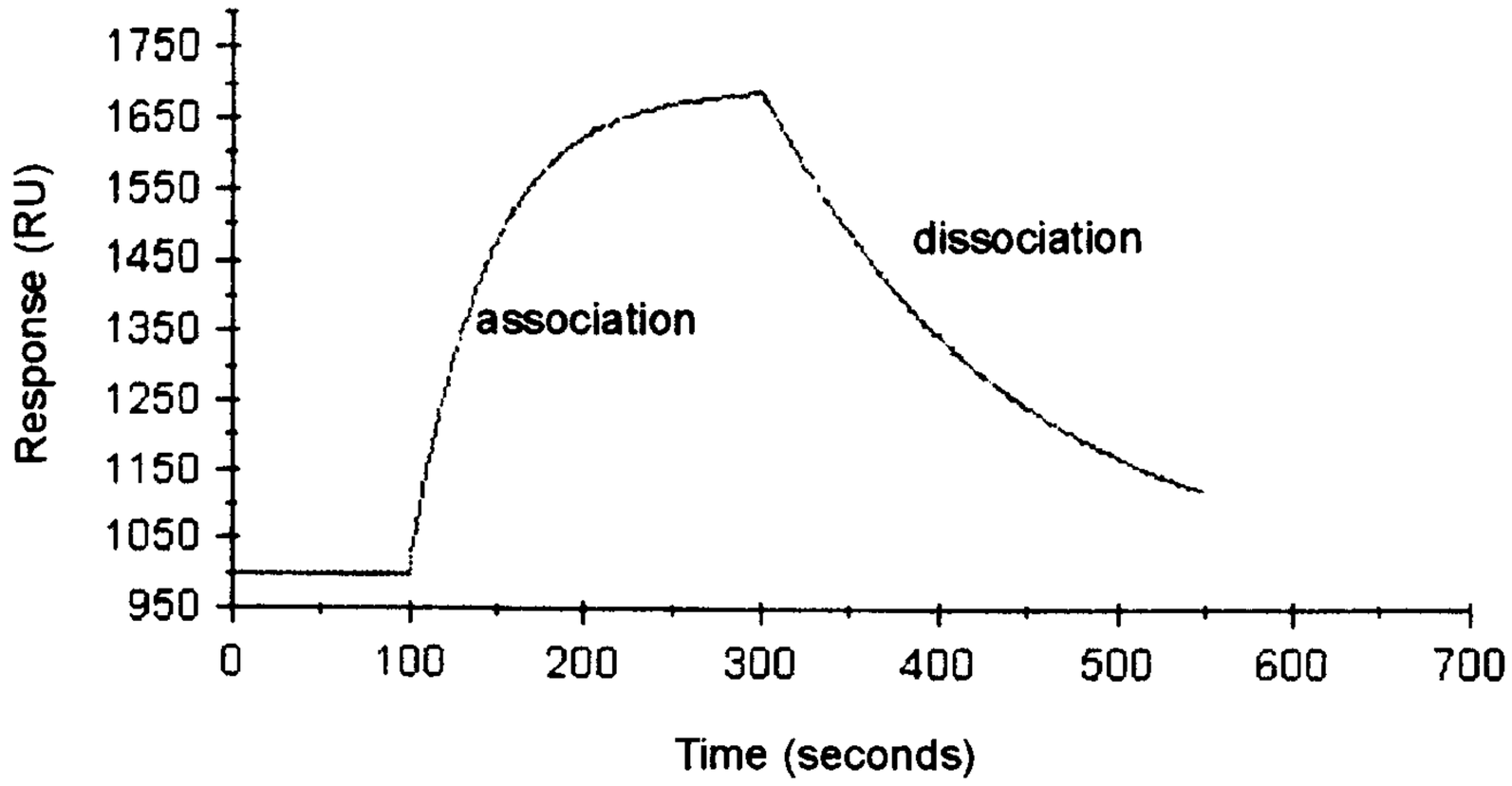

Figure 2.3: Example of a simple sensorgram illustrating binding of analyte to sensor chip surface. A sensorgram displaying association and dissociation kinetics is produced by alternating buffer and analyte exposure to the sensor chip for defined time periods as part of a continuous flow of fluid. Analyte binds to the surface during the sample injection and dissociates when sample is replaced with buffer.

Protocol used for measurement of binding kinetics: All Biacore experiments documented in this Thesis were performed by Dr. James Hunt. Assays were performed on a Biacore 3000 instrument (Pharmacia Biosensor), at 24 °C. The IgG_4-Fc-$(sFc\varepsilon RI\alpha)_2$ fusion protein was immobilised on a CM5 sensor chip using the amine coupling kit (Biacore) according to the manufacturer's instructions. Coupling density was restricted to less than 500 RU. Non-specific binding was assessed by preparation of a control surface of IgG_4-Fc, in an identical manner. Samples of wild type and R334S anti-NP IgE were diluted in HBS, pH 7.4 (supplied by Pharmacia Biosensor) and injected over the sensor chip at a flow rate of 20 µl / min. A 420 s association phase was followed by a 420 s dissociation phase. Data were collected for both wild type and R334S anti-NP IgE in a concentration range of 12.5 to 100 nM. The sensor surface was regenerated by three 60 s pulses of 0.2 M glycine-HCl, pH 2.5. The data were analysed using the BIAevaluation analysis package (version 3.2, Pharmacia Biosensor). Non-specific binding was subtracted from the specific binding prior to kinetic analysis.

Previous Biacore analysis and structural studies of the interaction between IgE and FcεRI have shown it to be biphasic. The biphasicity of the binding kinetics between IgE and FcεRI can be explained by the occurrence of an interaction with 1:1 stoichiometry, involving

two distinct interaction sites (as discussed in section 1.3.3). The BIAevaluation software includes a model which describes this biphasic interaction:

$$A + B \leftrightarrow AB$$

plus:

$$C + B \leftrightarrow CB$$

Where A and C represent the two different modes of IgE binding and B represents FcεRI. From this the following differential rate equations can be derived:

$$\frac{dR_1}{dt} = k_{a1} \cdot C_A \cdot \left(R_{max} - R_1 - R_2\right) - k_{d1} \cdot R_1 \cdot$$

$$\frac{dR_2}{dt} = k_{a2} \cdot C_c \cdot \left(R_{max} - R_1 - R_2\right) - k_{d2} \cdot R_2 \cdot$$

The total response is derived from the sum of the two individual components:

$$R = R_1 + R_2$$

These equations are solved by the computer.

2.3.2 Cellular biology methods

Cytotoxicity/phagocytosis assay: A flow cytometric assay was set up for quantification of tumour cell death induced by MOv18 IgE or IgG, encompassing a method for detection of the proportion of cells that are phagocytosed by effector cells and those killed by cell-mediated cytotoxicity. The design and optimisation of this assay are described in detail in Chapter 4. Tumour cell targets and cytotoxic effector cells are distinguished by CFSE and PE-labelling respectively, and dead cells are labelled with propidium iodide (PI). After incubation of effector and target cells with MOv18 or control antibody, tumour cell targets that have been phagocytosed by effector cells can be recognised as a CFSE/PE double positive population and tumour cell targets killed externally can be recognised as a CFSE/PI double positive population. This assay is explained schematically in Figure 4.1.

Experimental method: Tumour cell targets were stained with CFSE approximately 24 hours prior to performing the killing assay; cells were trypsinised and washed once in standard culture media, followed by one wash in serum-free culture media before resuspension to 50 x 10^6 cells / ml in PBS. Cells were warmed to 37 °C before addition of 20 µl of 0.5 mM CFSE per 1 ml of cell suspension, and incubated at 37 °C for 10 minutes, mixing every two minutes to improve the uniformity of staining. Staining was stopped with one wash in ice-cold standard culture media. Normal culture conditions were resumed until use in killing assay, whereupon CFSE-stained tumour cell targets were trypsinised and washed in standard culture and re-suspended to 130 000 cells / 200 µl culture media. Effector cells were washed and resuspended to the same concentration. 200 µl aliquots of each effector and target cells were mixed together in FACS tubes. Where relevant, blocking antibodies were added for 30 minutes prior to normal incubation for 2.5 hours at 37 °C in the presence of either PBS or defined amounts of test antibody (anti-NP IgE, MOv18 IgE, MOPC or MOv18 IgG). After incubation, cells were washed once in 2 ml ice-cold FACS buffer and effector cells were identified by staining with 4 µl of anti-CD89-PE (primary and U937 monocytes) or anti-CD49d-PE (primary eosinophils) per tube, for 30 minutes, 4 °C. PE-staining was followed by one wash in 2 ml ice-cold FACS buffer and staining of dead cells with 5 µl of 10 µg / ml PI for 15 minutes, 4 °C. Cells were washed once in 2 ml ice-cold FACS buffer and resuspended to 200 µl in FACS buffer for immediate analysis with a Becton Dickinson FACScan flow cytometer. Quantification of tumour cell death by MOv18 in the absence of effector cells was performed as above but excluding steps for effector cell addition and effector cell labelling.

Analysis method: Calculations for quantification of tumour cell death as contributed by cytotoxicity or phagocytosis were made using CellQuest™ software on a FACScan flow cytometer (BD Biosciences). Two dot plots, were created following the acquisition of 20 000 events from each tube; representative dot plots are shown in Figure 2.4 (and reproduced in Chapter 4 as Figure 4.5B). A detailed description of the logic behind this calculation is given in section 4.2.5. Each cytotoxicity assay was performed in triplicate. The mean number of events in region 'R1' (indicated in Figure 2.4, left-hand plot, large green gate) was calculated for three control tubes containing effector and target cells, but no antibody, and the resulting value termed the 'R1 ratio control'. From this number, the number of events in region R1 for each 'test' tube was subtracted. The resulting value was added to the number of events in region 'R3', divided into the R1 ratio control value and multiplied by 100. This number represents the percentage of target cells of those originally added to the tube, which have been killed by cytotoxic mechanisms. The number of target cells killed by phagocytosis is

calculated by dividing the number of events in 'R2' into the R1 ratio control and multiplying by 100.

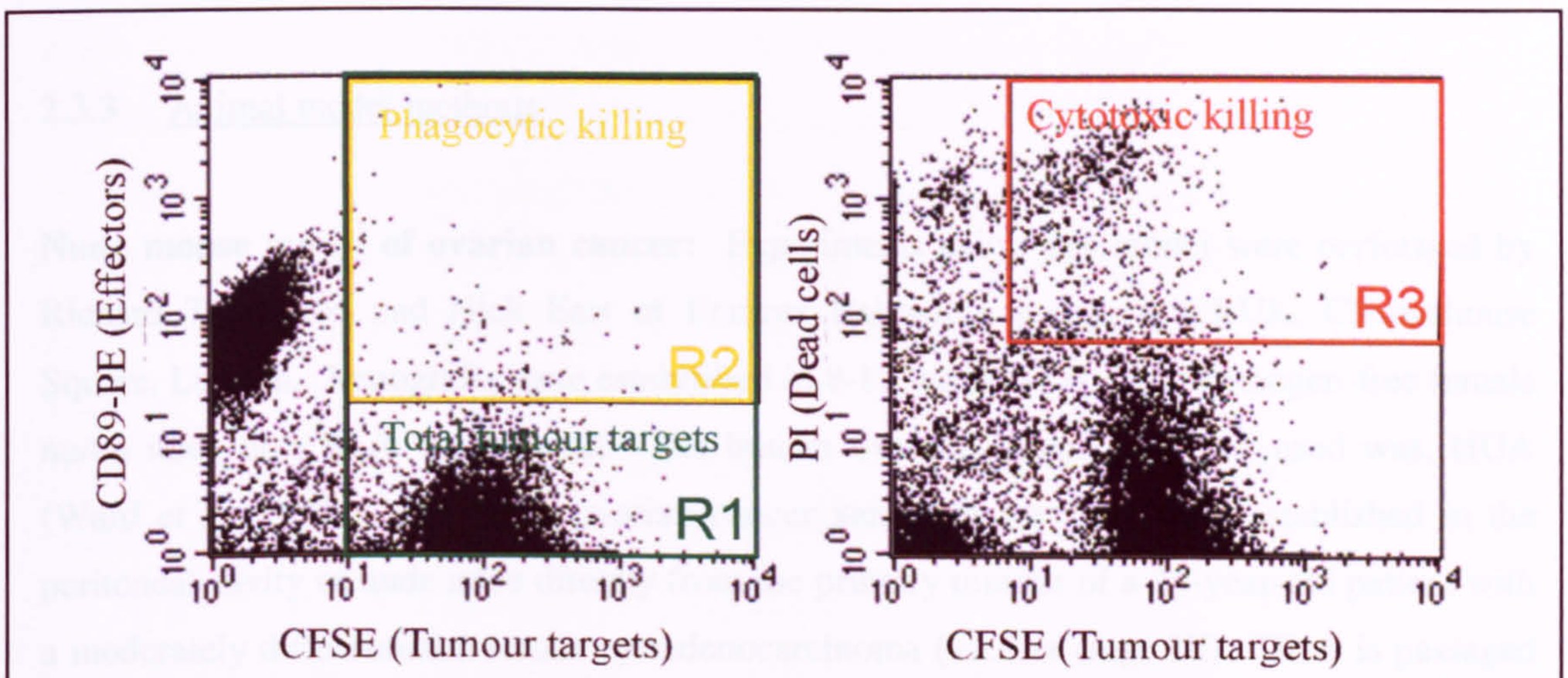

Figure 2.4: Dot plots showing the gates used to calculate antibody dependent cytotoxicity (ADCC) and phagocytosis (ADCP) in the killing assay described in Chapter 4 of this Thesis, and used for experiments described in Chapter 5 of this Thesis. Region 1 (R1, large green gate) contains all $CFSE^+$ IGROV1 cells acquired. Region 2 (R2, yellow gate) contains those IGROV1 cells which are also positive for PE and represent phagocytosed IGROV1 cells. Region 3 (R3, red gate) contains those $CFSE^+$ IGROV1 cells that are also PI^+, and thus represent IGROV1 cells killed by cytotoxicity. This figure is reproduced in Chapter 4, as Figure 4.5B, where the calculation made using the values defined by these gates is described in more detail.

Immunofluorescence imaging of killing: In order to confirm that the populations assumed to represent killing of IGROV1 tumour cells by cytotoxic and phagocytic mechanisms in the novel ADCCP assay described above, Dr. Sophia Karagiannis performed immunofluorescence imaging of killing, according to the protocol described below. In brief, 130 000 $CFSE^+$ IGROV1 tumour cells (CFSE stained according to the protocol described above) were incubated with 130 000 U937 cells, either untreated or cultured for 4 days prior to the assay in standard U937 culture media supplemented with 320 U / ml recombinant human IL-4, in glass chamber slides (Lab-Tek II, SLS, Nottingham, UK) for 2.5 hours at 37 °C, 5 % CO_2. Following this incubation, cells were washed twice by gently pipetting ice-cold FACS buffer onto the slide, which was immediately tipped off. U937 effector cells were then stained with anti-CD89-PE by addition of 14 µl of anti-CD89-PE to each chamber, and

incubation for 25 minutes at 4 °C. Cells were then washed twice with ice-cold FACS buffer (as before), fixed in 1 % paraformaldehyde and mounted in fluorescence preserver (DAKO) under a cover-slip for analysis using a Carl Zeiss microscope at a magnification of 200 x.

2.3.3 Animal model methods

Nude mouse model of ovarian cancer: Experiments using this model were performed by Richard Thompson and Nick East of Frances Balkwill's group, at CRUK, Charterhouse Square, London. Xenografts were established in 8-12 week old specific pathogen-free female nu/nu mice of a BL/6 background. The human ovarian cancer xenograft used was, HUA (Ward *et al*, 1987). The HUA ovarian cancer xenograft was originally established in the peritoneal cavity of nude mice directly from the primary tumour of a 23-year-old patient with a moderately differentiated serous cystadenocarcinoma (ascities stage III). HUA is passaged in mice whilst retaining its human phenotype. The passage cycle time of the HUA tumour is 20-22 days when transferred from one nude mouse to another by intraperitoneal injection of 200 µl ascities (Ward *et al*, 1987). Immunohistochemical staining of tumour sections with MOv18 IgE revealed that HUA tumour cells express the folic acid receptor (Karagiannis *et al.*, 2003). To implant the HUA tumour mice were injected intraperitoneally with 0.2 ml HUA tumour ascities on day 1.

In the first experiment, the ability of an effector cell population of human PBMC plus MOv18 IgE was compared to human PBMC plus MOv18 IgG1, to mediate improved survival of HUA-bearing nude mice. To this end, the HUA tumour was transplanted into a total of 16 mice; these 16 mice were divided into 4 groups of 4 (termed groups A, B, C and D). Mice in all groups were treated on days 1, 7, 14 and 21 with the following treatments: Each mouse in Group A was treated identically with 200 µl of PBS, each mouse in Group B was treated identically with 200 µl of PBS containing 4 million human PBMC, each mouse in Group C was treated identically with 200 µl of PBS containing 4 million human PBMC in addition to 100 µg of MOv18 IgE and each mouse in Group D was treated identically with 200 µl of PBS containing 4 million PBMC in addition to 100 µg of MOv18 IgG. In all experiments, the first treatment dose was given on the same day of tumour transplant, a minimum of five hours later. PBMC for this experiment were obtained from the same donor, on all treatment doses. This experiment was repeated, using an additional 5 mice per group, and a different, single, PBMC donor. The results shown in Figure 6.1, represent the compiled results of both experiments.

The second experiment performed using this model, involved transplant of the HUA tumour into a total of 20 mice; these 20 mice were divided into 5 groups of 4 (Groups A – E). On days 1 and 15, each mouse in group A was treated with 200 µl of PBS; each mouse in group B with 200 µl of PBS containing 4 million PBMC; each mouse in group C with 200 µl of PBS containing 4 million monocytes; each mouse in group D with 200 µl of PBS containing 4 million PBMC plus 100 µg of MOv18 IgE; and each mouse in group E with 200 µl of PBS containing 4 million monocytes plus 100 µg of MOv18 IgE. A single blood donor was used for this experiment, from which both PBMC and monocyes were purified, on both treatment dates.

The third experiment performed using this model, involved transplant of the HUA tumour into a total of 15 mice; these 15 mice were divided into three groups of 5 (Groups A – C). On days 1 and 15, each mouse in group A was treated with 200 µl of PBS; each mouse in group B was treated with 200 µl of PBS containing 4 million U937 monocytes; and each mouse in group C was treated with 200 µl of PBS containing 4 million U937 monocytes plus 100 µg of MOv18 IgE. This experiment was repeated by Dr. S. Karagiannis, therefore, the results of this experiment, shown in Figure 6.3, represent the compiled results from both experiments, therefore n = 9.

The fourth experiment performed using this model, involved transplant of the HUA tumour into a total of 30 mice; these 30 mice were divided into three groups of 10 (Groups A – C). On day 1, each mouse in group A was treated with either 200 µl of PBS; each mouse in group B was treated with 200 µl of PBS containing 3.6 million human eosinophils; each mouse in group C was treated with 200 µl of PBS containing 3.6 million eosinophils with 100 µg of MOv18 IgE (Group C). On day 15, these treatments were repeated, but where eosinophils were included, the number was reduced to 2.6 million per mouse, due to a lower yield from the same volume of blood, from the same donor.

In all experiments, mice were killed by cervical dislocation when the abdomen became distended to an extent to which the original body weight was increased by no more than 10 %, and ascities was removed under sterile conditions into liquid nitrogen or folmol saline for 24 hours for immunohistochemical processing at a later date.

'Humanised' mouse model of lung metastases: Experiments in this model involved the growth of C26tFR tumour cells as superficial metastases on the lungs of syngenic mouse strains. *In vitro* culture of C26tFR cells was performed in the absence of G418 for 5 days prior to injection. Before injection, cells were washed twice in PBS in which they were also re-suspended. In all cases, tumour cells were injected intravenously into the tail vein, using a

26 Gauge needle, in a total volume of 400 µl. For tumour cell injection, mice were placed under ether anaesthetic and restrained in a small ventilated box from which the tail protruded. Sacrifice was by cervical dislocation either when mice showed dyspnea or on a specific date prior to this. In all cases, lungs were analysed for metastases using the following procedure: A midline incision from below the diaphragm to above the throat followed by an incision through the salivary glands was used to expose the trachea before opening of the chest cavity. Great care was taken to avoid even minor damage to the lungs. Approximately 1 ml of a solution of 15 % India ink in water was infused into the lungs by inserting a syringe (to which a p200 Gilson pipette tip was attached) into the trachea via the mouth to fill the alveolar spaces and stain all lobes deep black. The lungs were then dissected *en bloc*, from the thoracic cage and placed in a beaker of distilled water for at least 5 minutes to remove excess ink. The organ was then placed in Fekete solution (a bleach preservative, see section 2.1.3) for 48 hours, after which tumours were visible as white nodules on a black normal lung tissue surface (Wexler *et al*, 1966).

C26tFR tumour cells were first tested for their ability to grow in hFcεRI Tg mice. This was performed by intravenous injection of 10^4 C26tFR tumour cells into each of four hFcεRI Tg mice as described above. This number of tumour cells was chosen for injection based on work documented in Rodolfo *et al.*, 1998, where injection of 10^4 C26tFR tumour cells resulted in dyspnea from lung metastases between days 20 and 40. Differences in the growth rate of C26tFR cells between Balb/c mice and different strains of hFcεRI Tg mice (FcεRI Tg $h^{+/+}$ $m^{-/-}$, $h^{-/-}$ $m^{+/+}$ and $h^{-/+}$ $m^{-/+}$) was tested for by intravenous injection of 10^4 C26tFR cells in a volume of 400 µl into a minimum of 4 mice of each strain. Mice were sacrificed by cervical dislocation when they showed dyspnea, and the number of survival days between tumour injection and sacrifice noted. For set-up of 'metastases counting' experiments, the optimal number of tumour cells required for injection and optimal date of sacrifice for a high number of superficial lung metastases to have developed was determined. Forty-five, eight-week-old Balb/c mice received intravenous injection of either; 5 x 10^3, 10^4 or 10^5 C26tFR tumour cells, resuspended to 400 µl in PBS. Three mice from each group were sacrificed on days 15, 17, 19, 21 and 23 by cervical dislocation, and metastases quantified as described above.

WAG rat model of lung metastases: To determine the optimal number of CC531tFR cells for injection in survival experiments, 10-week-old WAG rats, under isofluorane anaesthesia, were injected intravenously in the lateral tail vein with CC531tFR tumour cells (clone 16) grown for 5 days prior to injection in G418-deficient media and resuspended to 1 ml in PBS.

Rats received a single dose of 2.5 x 10^6, 5 x 10^6, 10 x 10^6, 25 x 10^6 or two or three doses of 5 x 10^6 CC531tFR cells. Rats were sacrificed by overdose of carbon dioxide gas when they showed dyspnea. Lungs were removed and metastases detected using the same method described above for mice.

Passive cutaneous anaphylaxis model: A mouse model of passive cutaneous anaphylaxis was used based on work described in Dombrowicz *et al.*, 1993 and 1996, which itself is based on original work by Wershil *et al.*, 1987. This model was used to compare the ability of wild type to R334S anti-NP IgE to sensitise FcεRI-expressing cells for IgE-specific antigen-activation. A local anaphylactic reaction (local fluid extravasation, fibrin deposition and tissue swelling) is induced by intradermal injection of IgE into the dorsal surface of the mouse ear, followed by an intravenous antigenic challenge. Specifically, hFcεRITg mice (see section 2.1.4) were injected under ether anaesthesia with 20 µg, in a 20 µl volume, of wild type anti-NP IgE in one ear, and mutant (R334S) anti-NP IgE or PBS in the other ear of the same mouse. At defined time-points following sensitisation (48 or 96 hours), animals were injected in the tail vein with 200 µl of PBS containing 100 µg of NIP-BSA and 2 % Evans blue dye. Evans blue dye binds serum proteins and so remains largely in the circulation until the change in vascular permeability associated with anaphylaxis allows its extravasation. Thus, quantification of extravasated Evans blue dye into the IgE-sensitised area following intravenous antigen challenge is representative of the intensity of the local anaphylactic reaction. As such, animals were sacrificed 1.5 h after intravenous antigen challenge, ears were amputated, cut to identical sizes and Evans blue dye extracted into 1 ml formamide by mincing followed by incubation at 80 °C until all dye was extracted. The Evans blue dye in 300 µl of formamide was measured by absorbance at 620 nm after filtration to remove ear debris.

Quantification of human IgE in the ear tissue: For experiments measuring the rate of IgE diffusion out of ears, 14 µg of anti-NP IgE in a 20 µl volume was injected into the dorsal surface of the mouse ear. Mice were sacrificed either 24, 48 or 96 hours later without antigen challenge or Evans blue dye injection, and ears removed and cut to identical sizes as above. IgE was extracted from ear tissue by homogenisation of each individual ear in Lysis buffer B. Four sequential extractions from each ear were made by homogenisation of the chopped ear in 400 µl of Lysis buffer B using an Anachem cordless motor (Part number K-749540-0000) with disposable homogenisation attachment. This was followed by four sequential sets of each a 30-minute incubation at 4 °C with gentle shaking, centrifugation at 14 000 rpm (using

an ALC Airspeed refrigerated centrifuge (model PK121R) fitted with a fixed angle ALC T527 rotor), at 4 °C for 30 minutes, removal of 300 µl of supernatant followed by replacement of 300 µl fresh Lysis buffer B. Supernatants containing IgE-extracts were stored at –70 °C until quantification of IgE by ELISA.

2.3.4 Statistical tests

Students *t*-test: Significance of differences between effector cell populations acting either alone or in combination with MOv18 IgE or anti-NP IgE in killing tumour cells or mediating improved survival of nude mice, was calculated using 2-tailed, un-paired *t*-tests unless otherwise indicated. P values greater than 0.05 were deemed to be insignificant, and those equal to or less than 0.05 deemed to be significant. Calculations were performed using Microsoft Excel software.

CHAPTER 3:

Characterisation of cells and antibodies central to work discussed later in this Thesis: Cytotoxic effector cells, tumour cell targets, MOv18 IgE and MOv18 IgG1

3.1 Introduction

In this project, I have assessed the ability of MOv18 IgE and MOv18 IgG1 to trigger different Fcε- and Fcγ-receptor-expressing effector cell populations to kill (Folate Binding Protein (FBP)-expressing) tumour targets, both *in vitro* and *in vivo*. The *in vitro* assay I have used is a novel flow cytometric assay designed to distinguish and quantify tumour cell death as it occurs by both cytotoxicity and phagocytosis. The set-up and optimisation of this assay is described in Chapter 4, and results from experiments using this assay are documented in Chapter 5. Work described in Chapter 6, a nude mouse model of human ovarian cancer, assessed the efficacy of those same effector cell populations, in triggering MOv18 IgE-mediated tumour cell death *in vivo*. Additionally described in Chapter 6, is the set-up of two new, more clinically relevant *in vivo* models in which the safety and efficacy of MOv18 IgE can be tested in the future. The purpose of this chapter is to provide an introduction to those effector cells, tumour target cell lines and MOv18 IgE and MOv18 IgG1 antibodies used for experiments described in Chapters 4 to 6 of this Thesis.

3.2 MOv18 IgE and MOv18 IgG1 antibodies

Both the MOv18 IgE and MOv18 IgG1 used in this project are chimaeric human antibodies. Chimaeric-human MOv18 consists of human constant regions and murine antigen-binding variable regions (as described in sections 1.4.2 and 2.2.2 and shown schematically in Figure 1.10). MOv18 IgE and MOv18 IgG1 were purified from cell culture supernatants by affinity chromatography using an αγ-fusion protein and Protein G column respectively (see section 2.3.1). SDS-polyacrylamide gel electrophoresis of the affinity purified MOv18 IgE and MOv18 IgG1 under non-reducing conditions, is shown in Figure 3.1A (this 5 - 8 % SDS-PAGE gradient gel, was kindly performed by Dr. Rebecca Beavil). This revealed that the products are of the expected molecular mass of approximately 190 000 Da and 150 000 Da, respectively, and of high purity. That MOv18 IgE and MOv18 IgG1 could bind FBP was confirmed by positive binding to IGROV1 tumour cells, which do not express IgE or IgG Fc receptors and thus cannot bind anti-NP IgE or control human IgG. The ability of MOv18 IgE and MOv18 IgG1 to bind Fcε- and Fcγ-receptors respectively was determined by positive binding to the U937 monocyte cell line, which does not express FBP (Figure 3.1B). In both cases, MOv18 IgE and MOv18 IgG1 binding was detected using a FITC-conjugated anti-IgE or anti-IgG secondary antibody. The isotype control antibodies for MOv18 IgE was anti-NP IgE, raised against the hapten NP, but also binding NIP. MOPC was used as the control antibody for MOv18 IgG1 in cytotoxicity assays. Anti-NP IgE and MOPC were both unable to bind IGROV1 cells, but bound U937 monocytes, as expected (Figure 3.1B)

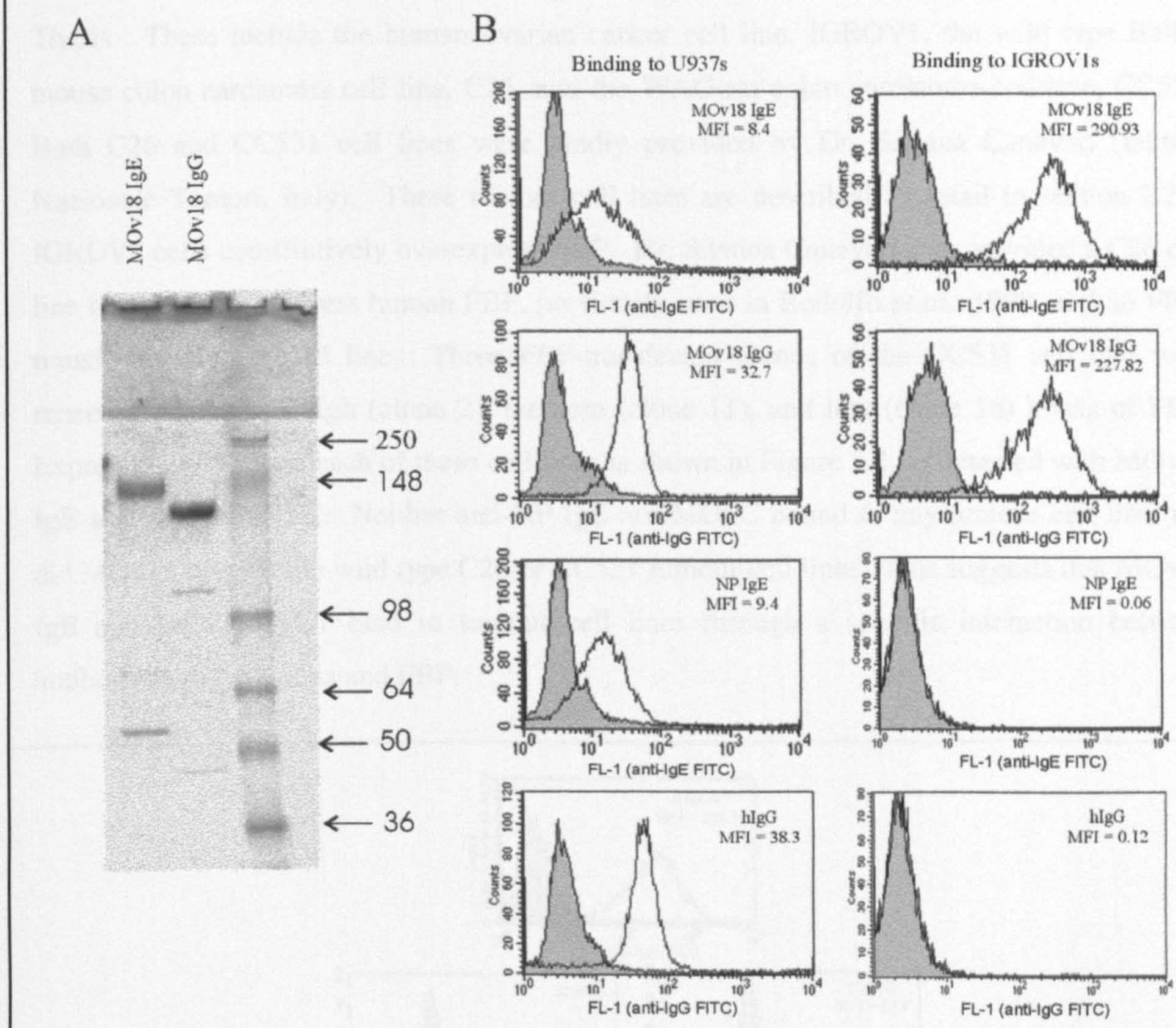

Figure 3.1: (A) 5 - 8 % SDS-PAGE gradient gel of MOv18 IgE and MOv18 IgG1 showing products of approximately 190 kDa and 150 kDa, respectively, performed by Dr. Rebecca Beavil. (B) FACS histograms showing binding of MOv18 IgE and MOv18 IgG1 to both U937 monocytes and IGROV1 tumour targets implying functional $F(ab')_2$ and Fc regions. Anti-NP IgE and control hIgG bound to U937 but not IGROV1 cells, as expected. The grey shaded area represents the negative control (anti-IgE-FITC or anti-IgG-FITC alone), and open curves represent the test antibody and secondary antibody. The mean fluorescence intensity (MFI) given is representative of the difference between the negative control and test antibody.

3.3 Tumour-target cell lines

3.3.1 Folate binding protein expression

Three different *in vitro* maintained tumour-target cell lines have been used in this Thesis. These include the human ovarian cancer cell line, IGROV1, the wild type Balb/c mouse colon carcinoma cell line, C26, and the WAG rat colon carcinoma cell line, CC531. Both C26 and CC531 cell lines were kindly provided by Dr. Silvana Canevari (Istituto Nazionale Tumori, Italy). These tumour cell lines are described in detail in section 2.2.1. IGROV1 cells constitutively overexpress FBP. Dr. Silvana Canevari also provided a C26 cell line transfected to express human FBP, previously used in Rodolfo *et al.*, 1998, and an FBP-transfected CC531 cell line. Three FBP-transfected clones of the CC531 cell line were received, expressing high (clone 2), medium (clone 11), and low (clone 16) levels of FBP. Expression of FBP on each of these cell lines is shown in Figure 3.2, as detected with MOv18 IgE and anti-IgE FITC. Neither anti-NP IgE nor MOPC bound to any tumour cell line, nor did MOv18 IgE bind to wild type C26 or CC531 tumour cell lines. This suggests that MOv18 IgE and MOv18 IgG1 bind to tumour cell lines through a specific interaction between antibody $F(ab')_2$ regions and FBP.

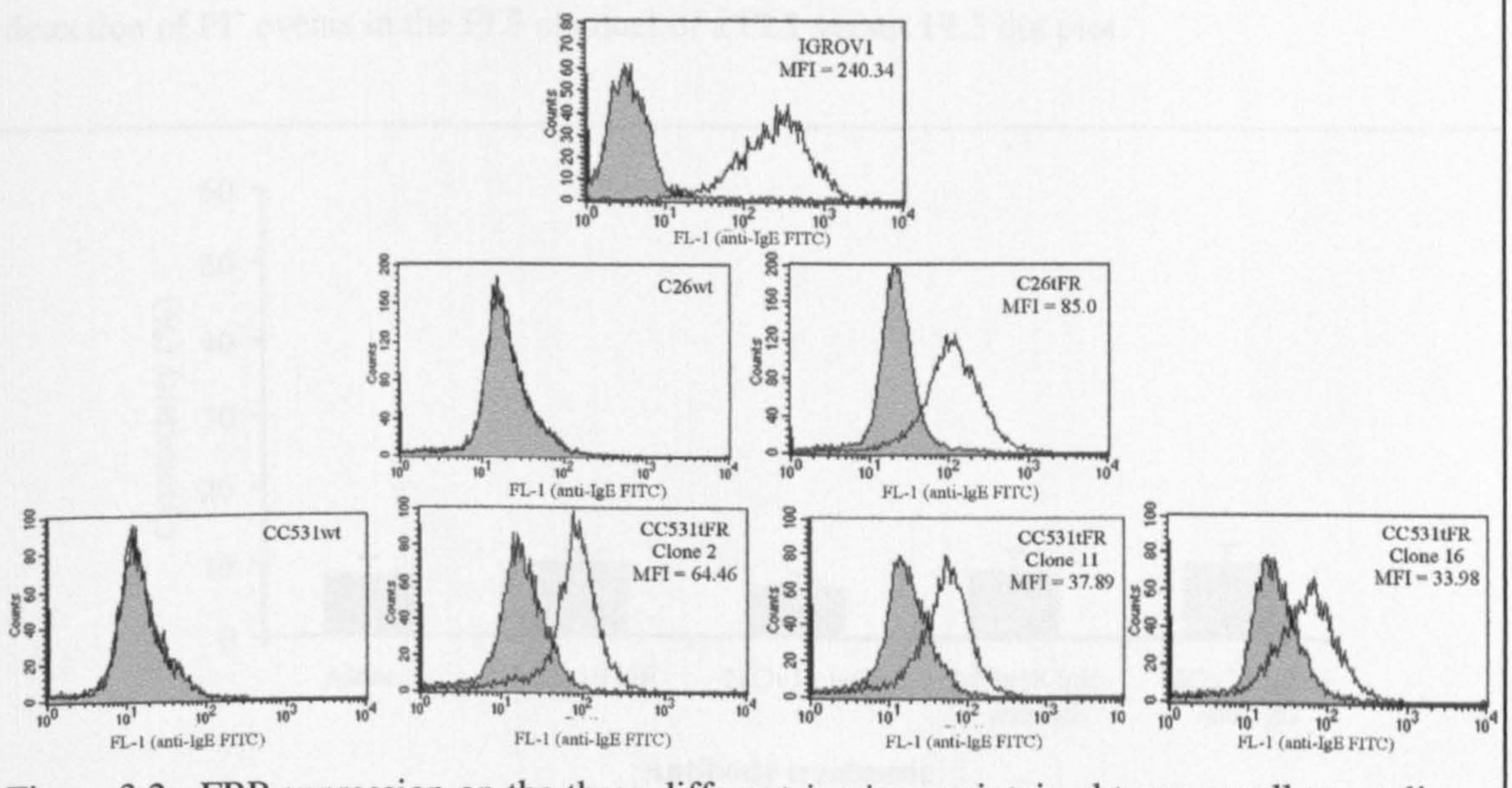

Figure 3.2: FBP expression on the three different *in vitro* maintained tumour cell target lines used for experiments described in this Thesis. The grey shaded area represents the negative control, which in each case is anti-IgE FITC alone binding to the indicated cell line. FBP expression is detected using MOv18 IgE followed by anti-IgE FITC. The MFI given is representative of the difference between the negative control and test antibody. Anti-NP IgE binding to each cell line was negative in each case, as was MOv18 IgE binding to wild type C26 and CC531 cell lines.

3.3.2 Effects of MOv18 binding to FBP

It was first determined whether the binding of MOv18 IgE or MOv18 IgG1 to FBP on tumour target cells was cytotoxic, either alone or when FBP was indirectly aggregated by cross-linking of MOv18 IgE or MOv18 IgG1 Fc regions using anti-IgE or anti-IgG antibodies, respectively. The purpose of this was to confirm that any death of tumour cell targets that was seen in the presence of effector cells and MOv18 in later Chapters, was a result of effector cell activity, and not cytotoxic effects of the MOv18 antibody. As described in section 2.3.2 tumour cells were incubated in FACS tubes at 37 °C (130 000 cells / tube) for 2.5 hours with either MOv18 IgE or MOv18 IgG1 (2 μg), alone or in combination with an excess of whole, bivalent anti-IgE or anti-IgG respectively (antibodies used have reference numbers 18 and 21 in Table 2.2). Testing MOv18 IgE and MOv18 IgG1 in this way replicates the conditions of the *in vitro* killing assay, used in Chapters 4 and 5, but with the exclusion of effector cells. Results using IGROV1 cells, show both MOv18 IgE and MOv18 IgG1 to have no significant effect on the viability of IGROV1 cells above background levels when incubated together for 2.5 hours (Figure 3.3). In addition, it appears that aggregation of FBP on IGROV1 cells by cross-linking either FBP-bound MOv18 IgE or MOv18 IgG1, does not cause cell death. Dead cells were quantified by staining with propidium iodide (PI) and detection of PI^+ events in the FL3 channel of a FL1 versus FL3 dot plot.

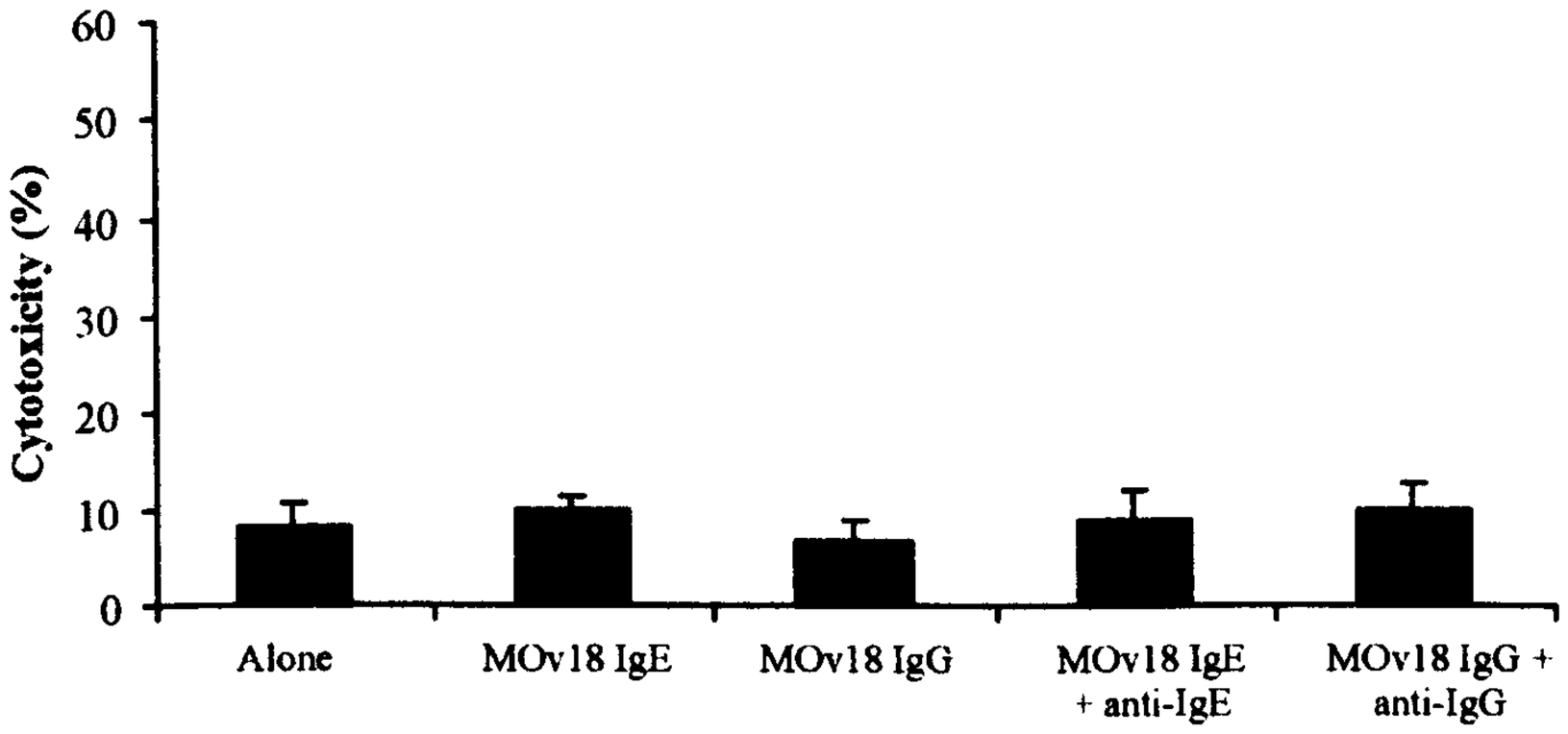

Figure 3.3: Effect of MOv18 IgE and MOv18 IgG1 alone on IGROV1 viability. IGROV1 tumour cell targets (130 000 cells / FACS tube) were treated with either PBS, 2 μg MOv18 IgE or 2 μg MOv18 IgG1, and incubated for 2.5 hours at 37 °C. Where indicated, cells were additionally incubated with bivalent anti-IgE or anti-IgG antibody for the 2.5 hour incubation at 37 °C. Dead cells were detected by flow cytometry as PI^+ events on a FL1/FL3 dot plot.

Results with IGROV1 cells contrast from those obtained with C26tFR cells, shown in Figure 3.4 below. MOv18 IgE alone has a substantial cytotoxic effect on C26tFR cells, with greater than 50 % of the population being killed in a 2.5 hour period. MOv18 IgE had no effect on wild type C26 cells, and anti-NP IgE no effect on C26tFR cells. However, not only was an equivalent effect not seen with MOv18 IgG1, but pre-treatment of C26tFR cells with MOv18 IgG1 before MOv18 IgE incubation, was able to substantially inhibit MOv18 IgE-mediated cytotoxicity (Figure 3.4A). Incubation of C26tFR cells with MOv18 IgG1 in the presence of anti-IgG, did not induce cytotoxicity, and anti-IgE also did not increase MOv18 IgE-mediated cytotoxicity any further (Figure 3.4B).

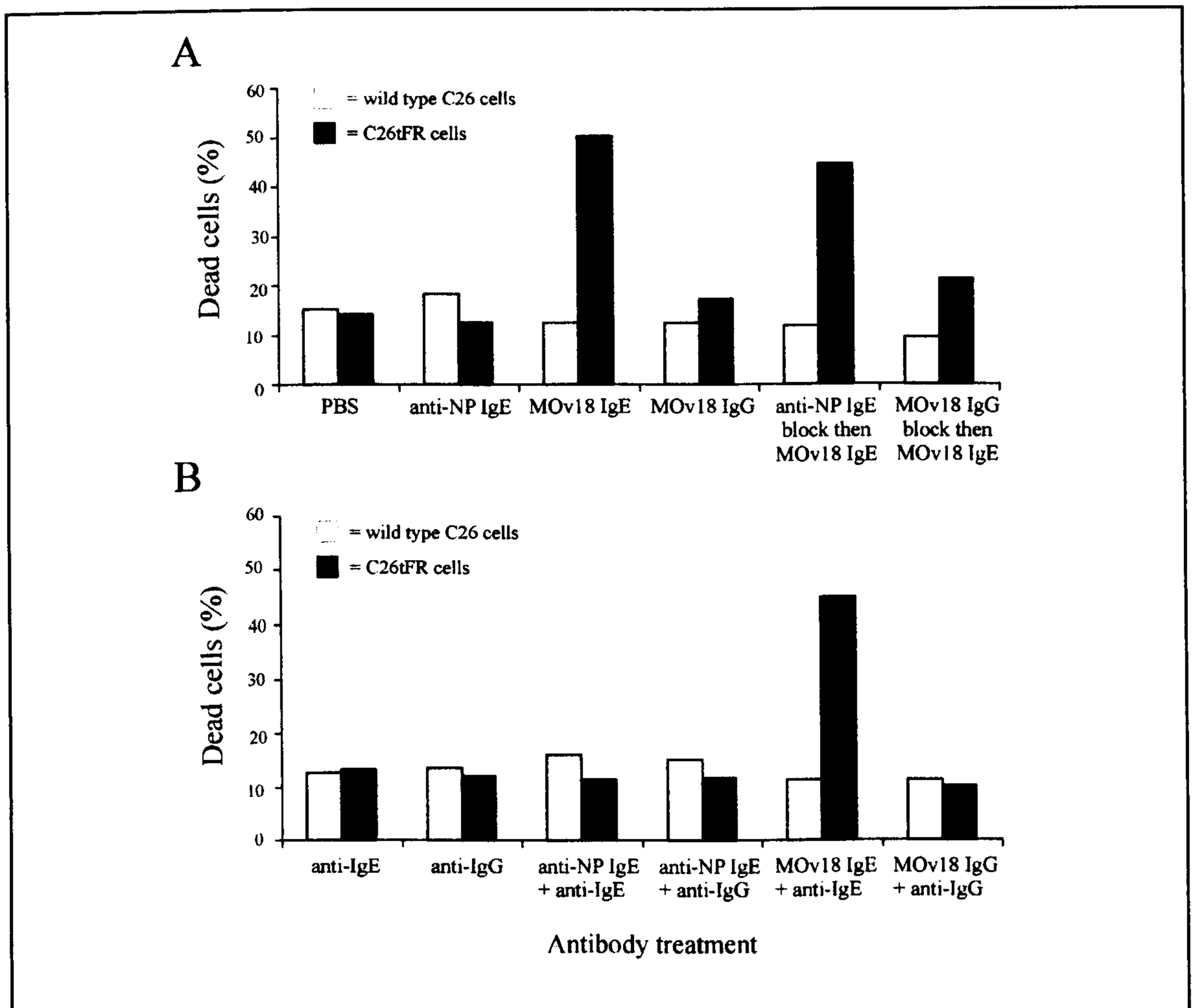

Figure 3.4: Effect of MOv18 IgE, anti-NP IgE, and MOv18 IgG1 alone on wild type and FBP-transfected C26 cell viability; (A) also shows the effect of MOv18 IgE following pre-treatment of cells with anti-NP IgE or MOv18 IgG; (B) shows the effect on cell viability when whole, bivalent anti-IgE or anti-IgG was additionally included for the duration of the 2.5 hour incubation at 37 °C. Dead cells were detected by flow cytometry as PI^+ events in the FL3 channel of a FL1/FL3 dot plot.

A cytotoxic effect of MOv18 IgE alone was also tested for on FBP-transfected CC531 cells (Figure 3.5). Results of MOv18 IgE cytotoxicity on each clone of FBP-transfected CC531 cells, suggest that killing through FBP by MOv18 IgE is proportional to the level of FBP expression (see Figure 3.2 for FBP expression levels). However, IGROV1 cells express levels of FBP substantially higher than that of CC531tFR clone 2 and C26tFR (see Figure 3.2), but do not show the same susceptibility to MOv18 IgE mediated cytotoxicity. Therefore, it appears the effect is either specific for cells expressing high FBP levels gained through transfection, or, for rodent cell types expressing human FBP.

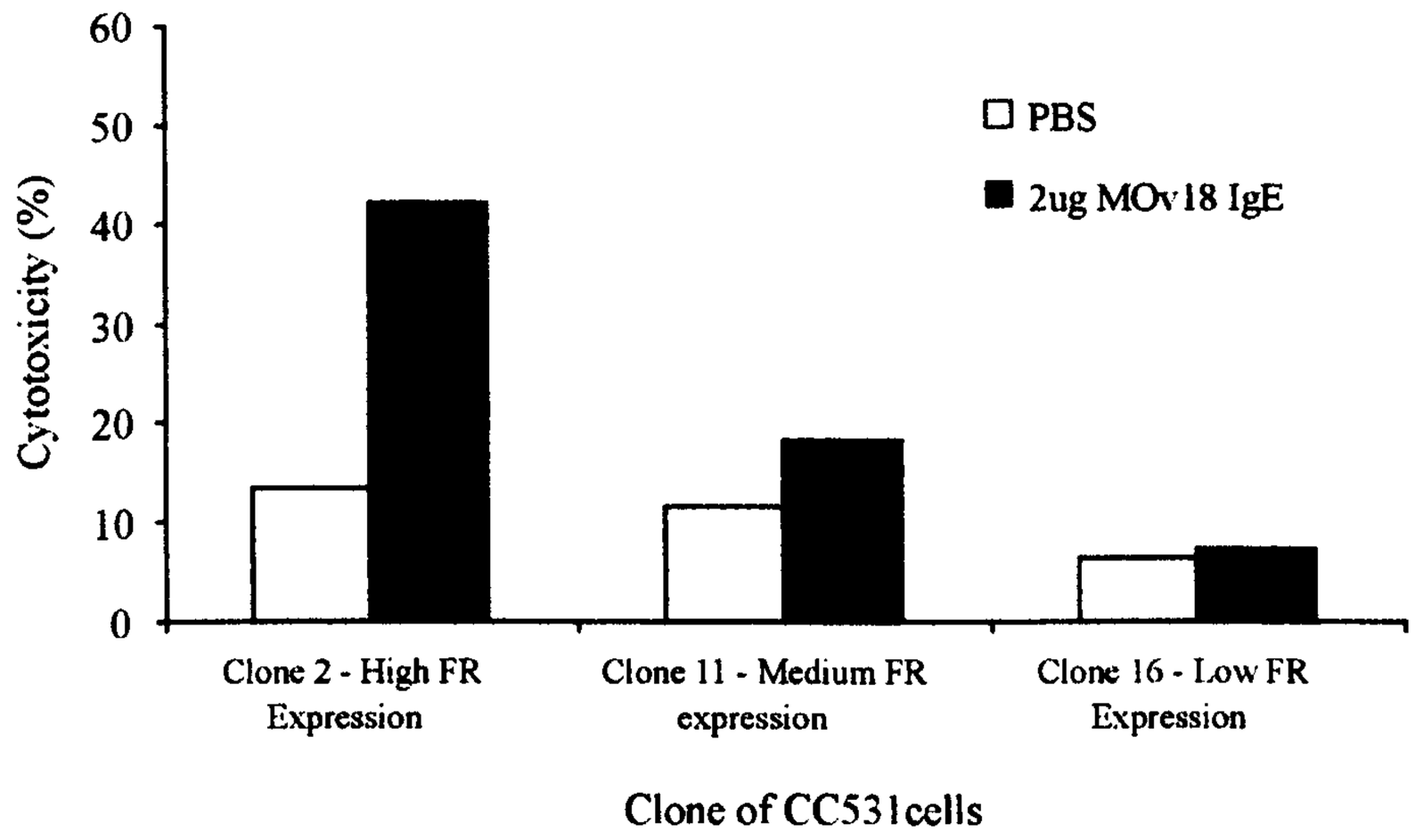

Figure 3.5: Cells of each clone of CC531 were incubated with either PBS or 2 μg MOv18 IgE for 2.5 hours at 37 °C. Dead cells were stained with PI and detected by flow cytometry on a FL1/FL3 dot plot.

3.4 Effector cell populations

Of the cell populations implicated in IgE-mediated immune responses (and discussed in section 1.3.5), those demonstrated to possess IgE-mediated cytotoxic effector functions include mast cells, basophils, monocytes and eosinophils. In addition, they are primary tumour-infiltrating leukocyte populations (as discussed in section 1.1.2). If monocytes and eosinophils could perform MOv18 IgE-mediated tumour cell death *in vitro* and or *in vivo*, this would suggest that it might be possible to manipulate those monocytes or eosinophils, either resident within tumours or actively recruited to tumour sites, to perform anti-tumour effector functions in human patients following treatment with MOv18 IgE. Monocytes have already been shown to have the ability to kill FBP-expressing human tumour cells in a MOv18 IgE-

dependent manner, both alone and as part of a population of PBMC (Karagiannis *et al.*, 2003). In this project, purified monocytes have been studied further; the ability of purified human eosinophils to act as effector cell populations in MOv18 IgE-mediated killing of tumour cells both *in vitro* and *in vivo*, has also been studied.

3.4.1 Monocytes

Monocytes are the blood-circulating developmental stage of the mononuclear phagocyte lineage. This lineage originates from a granulocyte-macrophage colony-forming unit in the bone marrow under the influence of the lineage-determining cytokines M-CSF and GM-CSF, in addition to IL-3, KIT and TNF-family members, to form pro-monocytes. Once mature, pro-monocytes leave the bone marrow to circulate in the blood with a half-life of approximately 3 days. These blood circulating mature monocytes are also known as 'immature macrophages' as they either constitutively, or upon receipt of specific signals (as discussed in section 1.3.5), are induced to migrate out of the blood to become tissue-dwelling macrophages. In tissues, macrophages may live for months, with characteristics specific to the particular tissue in which they reside (Johnston, 1988). Tissue-dwelling macrophages may mature further, into terminally differentiated multi-nucleated giant cells. The cells of the mononuclear lineage perform roles critical in host defence, including cytotoxicity, phagocytosis and secretion of soluble factors to co-ordinate the activities of other cells. They also play roles in tissue turnover and wound repair. Furthermore, as discussed in section 1.1.2, monocytes and macrophages may have the ability to recognise and kill tumour cells *in vivo*; but this function appears to be suppressed as part of the successful evolution of a developing tumour (Pollard, 2004). The ability of monocytes and macrophages to defend the host by rapid phagocytosis is conferred by their expression of complement receptors and Fc receptors for IgG and IgE.

As mentioned in section 1.3.2, the first description of FcεRI expression on monocytes purified from human peripheral blood came from Maurer and co-workers in 1994. However, the methods used in this study, acid stripping of endogenous pre-bound IgE followed by detection of receptors using the anti-FcεRI antibody, 15-1, meant that FcεRI was only detected on monocytes from atopic donors. Experiments performed since this time have shown FcεRI to be detectable also on monocytes from healthy human donors (Reischl *et al.*, 1996), although this required removal of carbohydrate from the cell membrane by neuraminidase digestion. In 2003, Karagiannis *et al.*, reported the level of FcεRI expression to be in the region of 2550 molecules per CD14-positive cell. They also showed that MOv18 IgE-mediated tumour-cell killing by monocytes is proportional to their level of free FcεRI

expression; monocytes from non-atopic individuals, which express a greater number of free FcεRI than atopic individuals (where FcεRI is occupied by endogenous allergen-specific IgE), are more effective in MOv18 IgE-mediated tumour cell killing. Therefore, donors used in *in vitro* assays in this Project, were chosen on the basis of having no history of allergic symptoms. Monocytes used in *in vivo* experiments were taken only from individuals characterised as non-atopic by skin prick testing.

FcεRI and CD23 expression levels were analysed by indirect immunofluorescence and flow cytometry on monocytes from all donors whose monocytes were used in killing assays described in this Thesis. FcεRI expression from a representative donor is shown in Figure 3.6. Monocytes were identified using an anti-CD14-PE antibody. Total IgE receptor expression on monocytes was determined by saturation of free IgE receptors with human IgE (MOv18 IgE or NP IgE) and detection of total IgE (endogenous and added IgE) by secondary staining with anti-IgE FITC (antibody reference 18 in Table 2.2). A mean of 31.2 % (n = 3) of CD14-positive cells gave a positive anti-IgE-FITC signal (range was 27.6 – 36.2 %). The percentage of cells expressing free IgE receptors was determined by subtracting the percentage of cells with pre-bound endogenous IgE from the number of cells staining positive for IgE following saturation with IgE. This gave a mean of 14.8 % of cells with free FcεRI (range was 14.6 – 15 %). The mean number of CD14-positive cells expressing free IgE receptors, when detected with 15.1 and anti-IgG1-FITC, was roughly consistent at 24.25 % (range 11.5 – 37 %). These results are in accordance with those reported in Karagiannis *et al.*, 2003.

CD23 is not constitutively expressed by primary monocytes freshly purified from the peripheral blood of normal human donors. However, they may be induced to express CD23b in response to specific signals, most importantly, IL-4 (Vercelli *et al.*, 1988 and Yokota *et al.*, 1988). Stimulation of monocytes with IL-4 may be associated with their activation and maturation into tissue-dwelling macrophages. Accordingly, no CD23 expression was detected on monocytes from any of the three blood donors tested. CD14-positive cells from each donor were demonstrated to be CD23-negative using the anti-CD23 antibody, BU38, in conjunction with anti-IgG1-FITC.

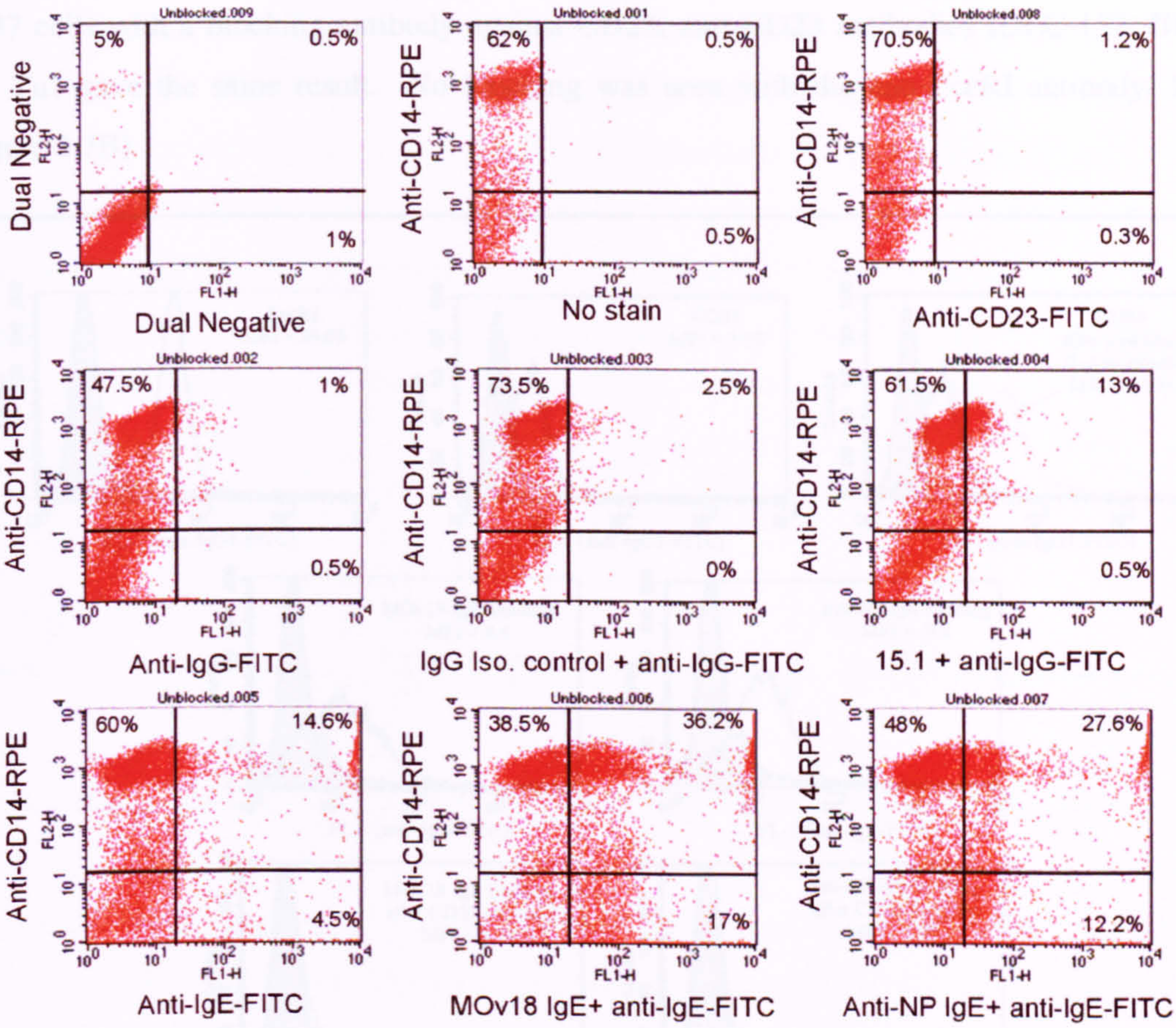

Figure 3.6: Monocyte expression of IgE receptors. These data, from one blood donor, are representative of those obtained for the three non-allergic monocyte donors used in this project. Monocytes are defined as $CD14^{+}$ cells. CD23 expression was negative by BU38 and anti-IgG-FITC staining. Unoccupied FcεRI were detected using the anti-FcεRI antibody, 15-1, in conjunction with anti-IgG1-FITC. Occupied and free FcεRI were detected by anti-IgE-FITC detection of endogenous IgE, compared to anti-IgE FITC staining of monocytes pre-treated with an excess of human IgE (MOv18 IgE or anti-NP IgE).

The IgE receptor expression status of U937 monocytes was also determined. A uniformly high expression of both FcεRI and CD23 was found (Figure 3.7A). FcεRI was detected using 15-1 and anti-IgG1-FITC, giving a mean fluorescence intensity of 39.05. CD23 was detected using BU38 and anti-IgG1-FITC, to give a mean fluorescence intensity of 3.98. As has often been reported since the original evidence was provided by Kawabe *et al.*, 1988, treatment of U937 cells with IL-4 upregulates CD23 expression (Figure 3.7A; far right histogram) with an increase in mean fluorescence intensity from 3.98 for untreated U937 cells to 31.91 for IL-4-treated U937 cells. Surprisingly, it was observed that both MOv18 IgE and NP IgE binding to U937 monocytes could be completely blocked by pre-treatment of the

U937 cells with a blocking antibody against CD23; anti-CD23 antibodies IDEC-152, BU38 and Tu1 gave the same result. No blocking was seen with the anti-FcεRI antibody, 15-1 (Figure 3.7B).

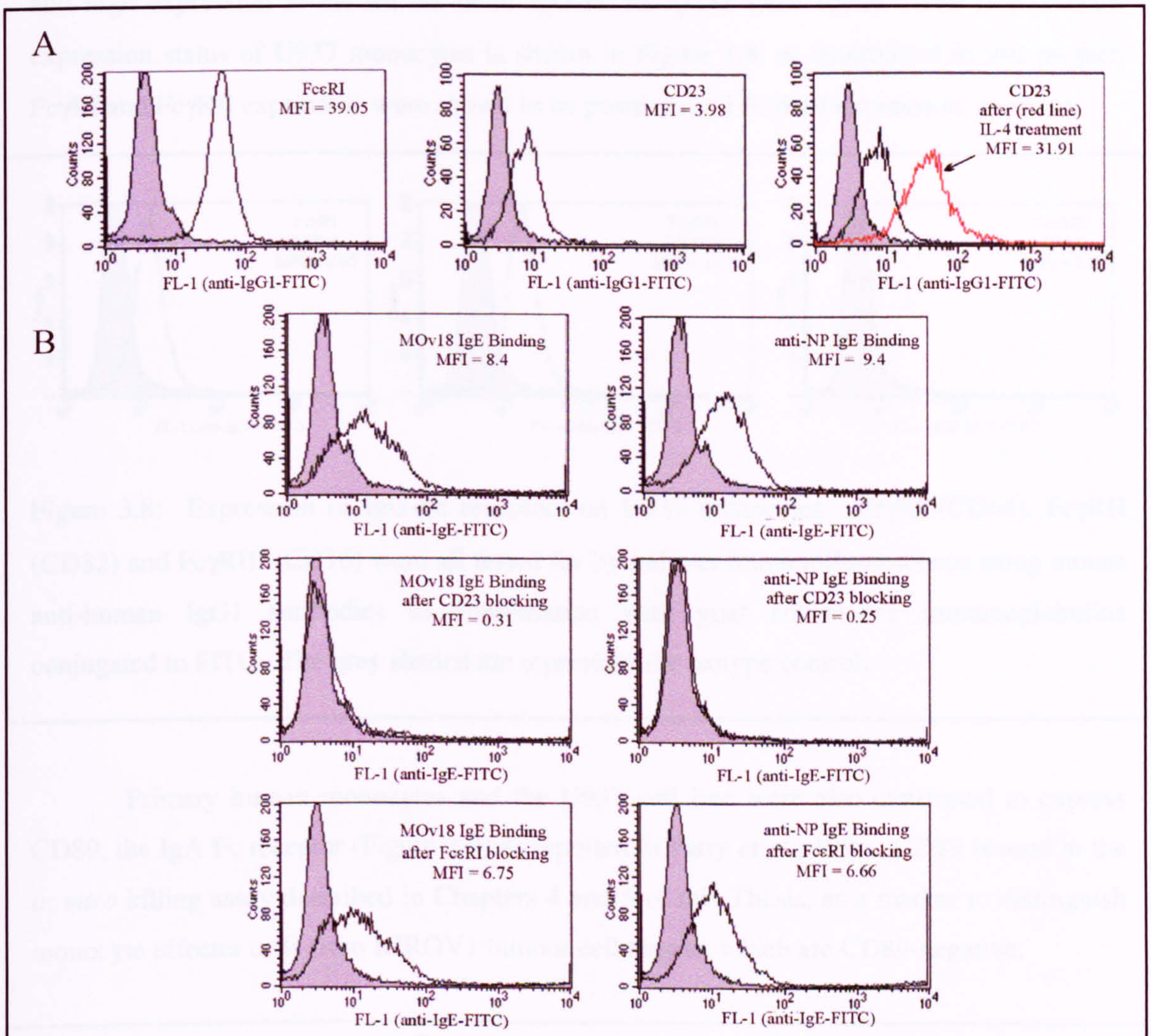

Figure 3.7: IgE receptor expression by U937 monocytes. (A) Left histogram; FcεRI expression detected by 15-1 and anti-IgG1-FITC. Middle histogram; CD23 expression detected by BU38 and anti-IgG1-FITC. Right histogram; CD23 expression (again detected using BU38 and anti-IgG1-FITC) on untreated cells (black line) and the increase in CD23 expression after 4 days culture in IL-4-supplemented medium (red line). The grey shaded area in each histogram represents the negative control. (B) Binding of MOv18 IgE and anti-NP IgE to U937 monocytes as detected by anti-IgE FITC, and effect on IgE binding of pre-treatment of cells with anti-CD23 (IDEC-152) or anti-FcεRI (15-1) blocking antibodies.

There are three different classes of Fcγ-receptor, FcγRI (CD64), FcγRII (CD32) and FcγRIII (CD16). Details of these Fc receptors for IgG are given in Table 1.1. Their expression by primary monocytes was extensively characterised in Karagiannis *et al.*, 2003, and high expression levels for all three IgG-Fc receptors were found. The Fcγ receptor expression status of U937 monocytes is shown in Figure 3.8, as determined in this project. FcγRI and FcγRII expression were shown to be positive, and FcγRIII expression, negative.

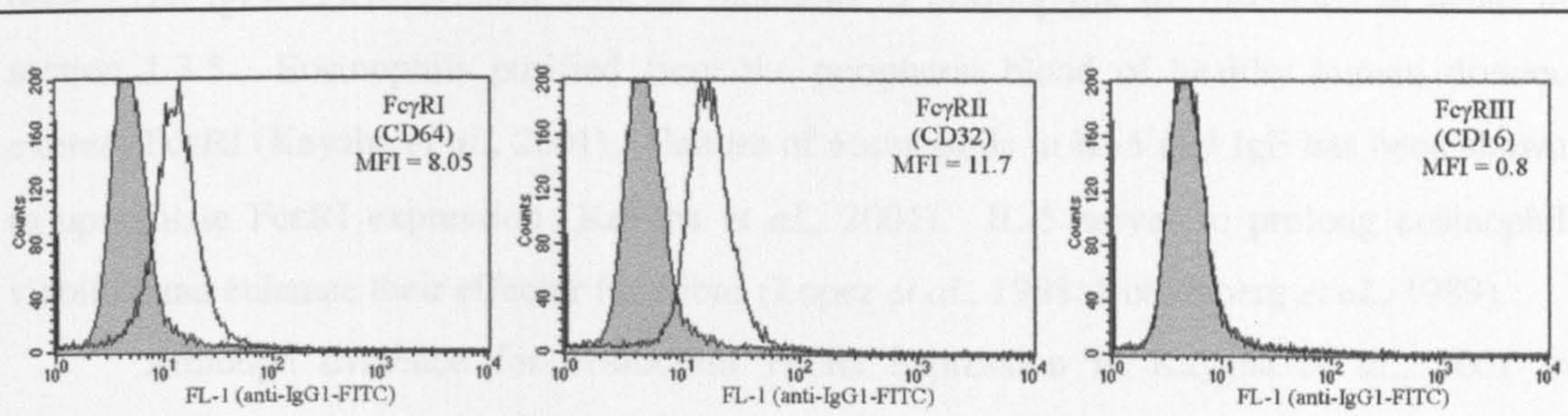

Figure 3.8: Expression of IgG-Fc receptors on U937 monocytes. FcγRI (CD64), FcγRII (CD32) and FcγRIII (CD16) were all tested for by indirect immunofluorescence using mouse anti-human IgG1 antibodies in combination with goat anti-mouse immunoglobulins conjugated to FITC. The grey shaded are represents the isotype control.

Primary human monocytes and the U937 cell line were also confirmed to express CD89, the IgA Fc receptor (Figure 3.9) as reported in Patry *et al.*, 1996. CD89 is used in the *in vitro* killing assay described in Chapters 4 and 5 of this Thesis, as a marker to distinguish monocyte effector cells from IGROV1 tumour cell targets, which are CD89-negative.

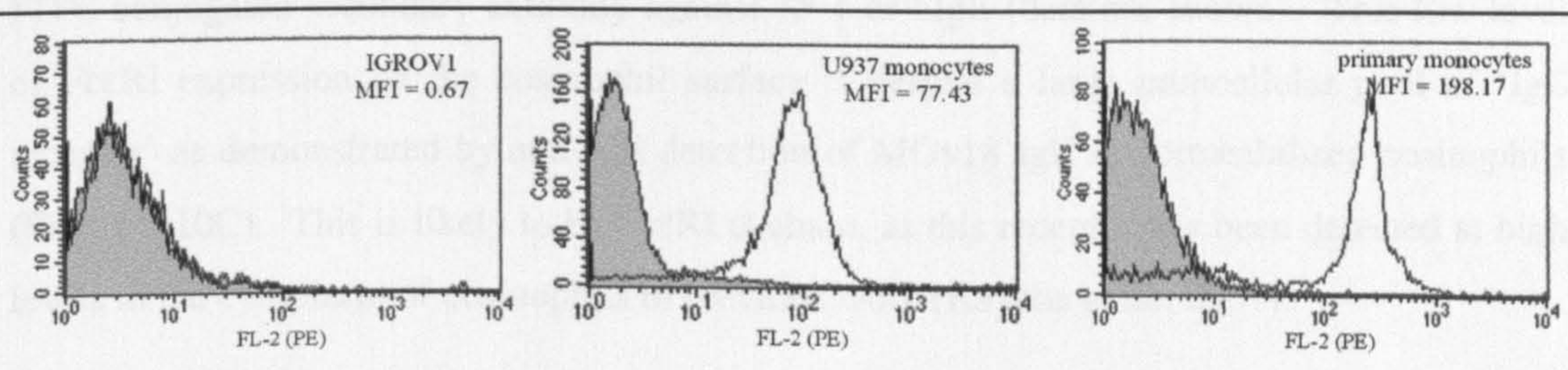

Figure 3.9: FACS histograms of primary and U937 monocytes cells showing CD89 expression to be absent on IGROV1 tumour cells, and positive on both U937 and primary monocytes, using a PE-conjugated anti-CD89 antibody. Thee grey shaded area represents the isotype control.

3.4.2 Eosinophils

Eosinophils develop from $CD34^+$ progenitors in the bone marrow under the influence of IL-5, which promotes their maturation and movement into the circulation. Their precise function in the human immune system is not clearly understood. They are the most abundant infiltrating cell population in many parasitic and allergic diseases and, although they are associated with some host protection in the former, they cause significant host pathology in both. The IgE-FcεRI-mediated effector functions of eosinophils are discussed in detail in section 1.3.5. Eosinophils purified from the peripheral blood of healthy human donors, express FcεRI (Kayaba *et al.*, 2001). Culture of eosinophils in IL-5 and IgE has been shown to upregulate FcεRI expression (Kayaba *et al.*, 2001). IL-5 serves to prolong eosinophil viability and enhance their effector functions (Lopez *et al.*, 1988; Rothenberg *et al.*, 1989).

Although evidence for eosinophil FcεRI expression in Kayaba *et al.*, 2001 is convincing, expression is very low, and in other studies, FcεRI expression has been deemed to be absent (Sihra *et al.*, 1997; Seminario *et al.*, 1999). Therefore, FcεRI expression was analysed on freshly purified human eosinophils from one of the donors used as a source of eosinophils for cytotoxicity assays documented in Chapter 5. Using indirect immunofluorescence and flow cytometry, a positive signal for FcεRI expression was obtained with the anti-hFcεRIα antibody, 15-1, in conjunction with an anti-IgG1-PE secondary antibody. Although the positive signal for FcεRI is very low in Figures 3.10A and B, its specificity is demonstrated in two ways. Firstly, 15-1 binding could be blocked by pre-treatment of the cells with IgE and, similarly, IgE binding could be blocked by pre-treatment of the cells with 15-1. When MOv18 IgE was replaced with anti-NP IgE, the same result was achieved (data not shown). For no donor tested was FcεRI expression detectable using a FITC-conjugated secondary antibody against 15-1 or hIgE (data not shown). This low level of FcεRI expression on the eosinophil surface is despite a large intracellular pool of 'IgE receptor' as demonstrated by anti-IgE detection of MOv18 IgE in permeabilised eosinophils (Figure 3.10C). This is likely to be FcεRI α-chain, as this receptor has been detected at high levels in the cytoplasm of eosinophils in previous work (Kayaba *et al.*, 2001).

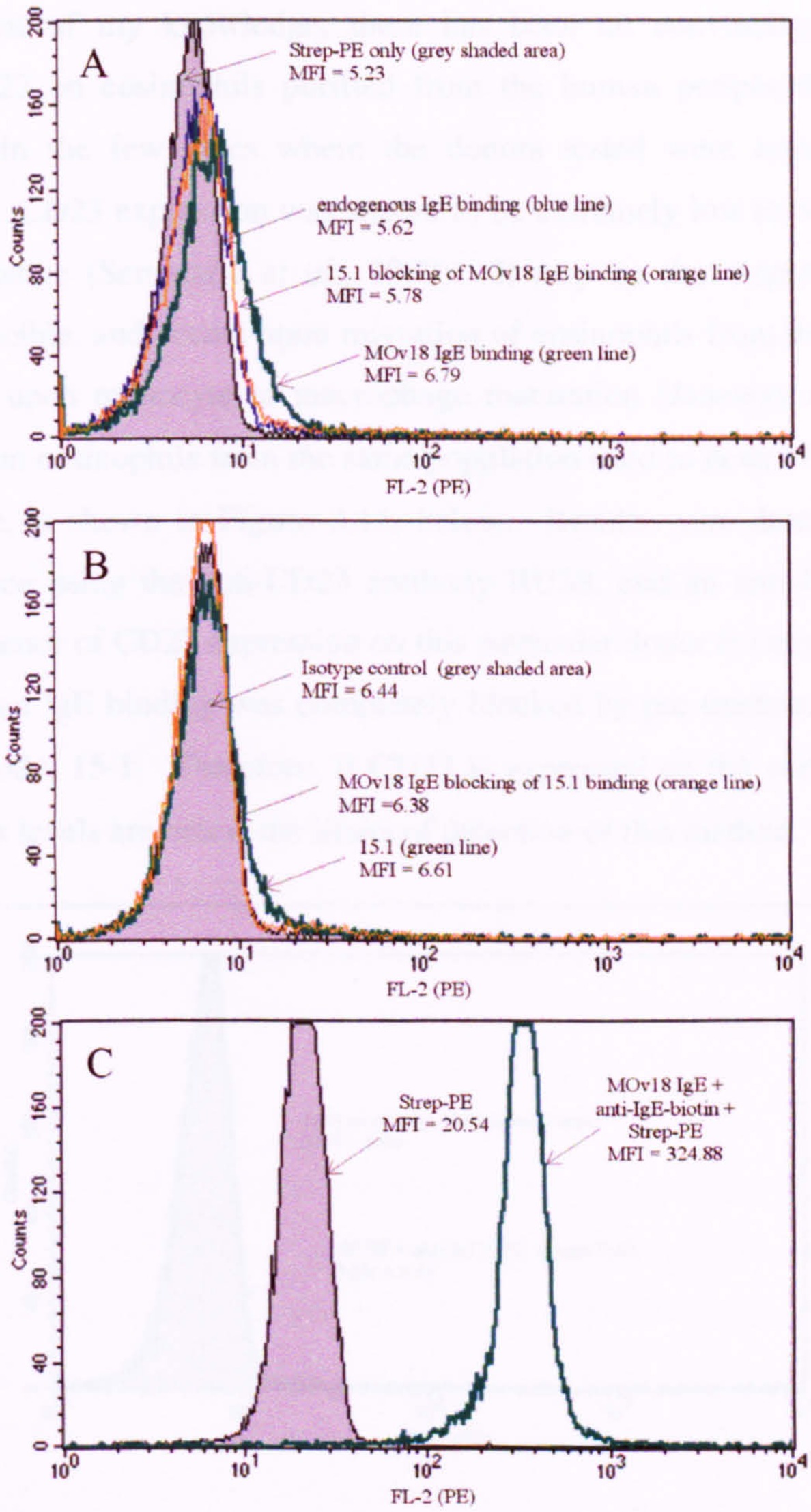

Figure 3.10: Surface and intracellular IgER expression by human peripheral blood eosinophils from a normal donor. (A) FcεRI expression. The grey shaded area represents Strep-PE staining alone. Endogenous IgE binding is detected using anti-IgE biotin + Strep-PE. The total number of FcεRI expressed (both unoccupied and bound with endogenous IgE) was detected by treatment of cells with MOv18 IgE followed by anti-IgE biotin and strep-PE staining. MOv18 IgE binding could be blocked with 15-1. (B) FcεRI expression detected with 15-1 and anti-IgG1-PE. 15-1 binding was blocked by pre-treatment of cells with MOv18 IgE. (C) Intracellular IgER-expression as detected with MOv18 IgE in conjunction with anti-IgE biotin and strep-PE in permeabilised eosinophils.

To the best of my knowledge, there has been no convincing evidence for the expression of CD23 on eosinophils purified from the human peripheral blood of normal donors to date. In the few cases where the donors tested were normal (not atopic or hypereosinophilic), CD23 expression was shown to be extremely low to negative (Lantero *et al.*, 2000), or negative (Seminario *et al.*, 1999). It may be that expression of CD23 on eosinophils is inducible, and occurs upon migration of eosinophils from the circulation to the tissues, as occurs upon monocyte to macrophage maturation (Janeway *et al.*, 4th Edition). CD23 expression on eosinophils from the same population used to detect FcεRI expression in Figure 3.10 above, is shown in Figure 3.11, below. Results were determined by indirect immunofluorescence using the anti-CD23 antibody BU38, and an anti-IgG1-PE secondary antibody. The absence of CD23 expression on this particular donor is consistent with the data showing that human IgE binding was completely blocked by pre-treatment of cells with the anti-FcεRIα antibody, 15-1. Therefore, if CD23 is expressed on the surface of eosinophils from this donor, its levels are below the limits of detection of this method.

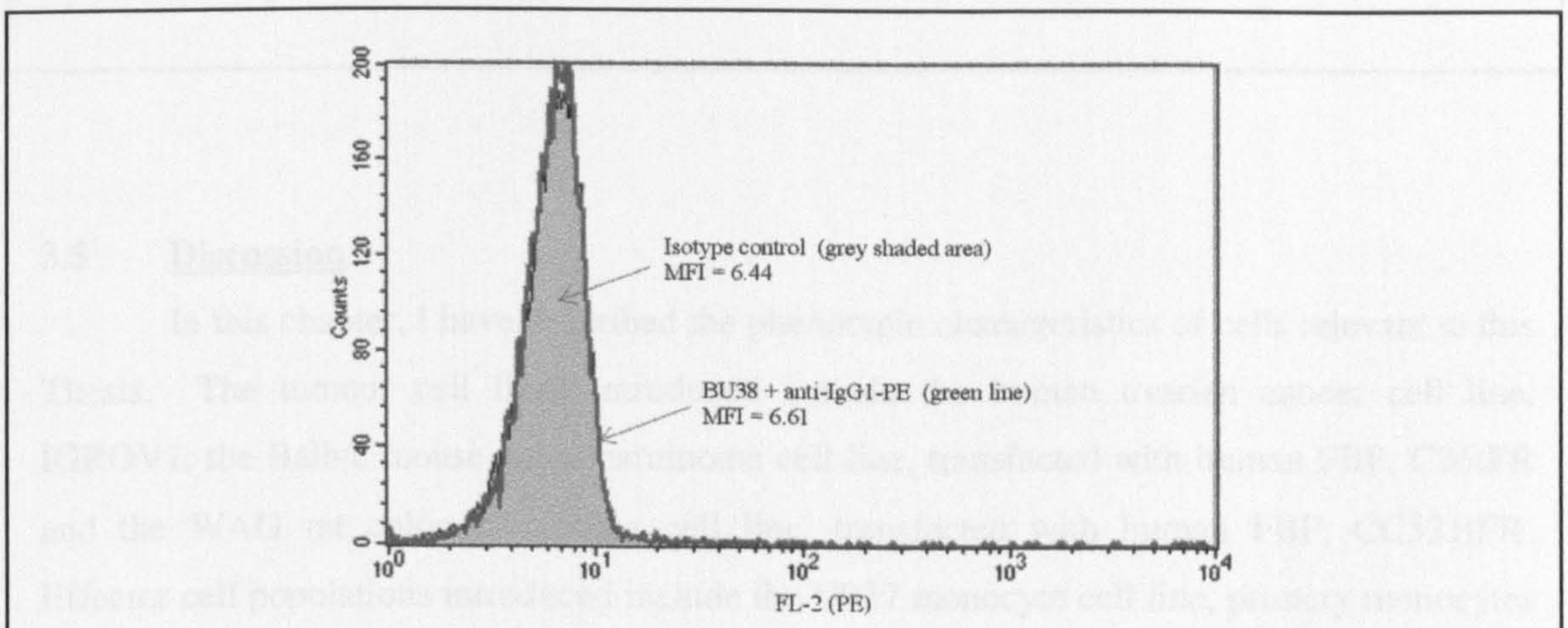

Figure 3.11: Expression of CD23 on the surface of human peripheral blood eosinophils from a normal donor. CD23 was detected using the anti-CD23 antibody, BU38, and anti-IgG1-PE.

Eosinophils also express on their surface FcR γ-chain (Seminario *et al.*, 1999), a component of FcγRIII, in addition to FcεRI. Surface expression of FcγRIII has been reported to occur on approximately 6 % of eosinophils purified from the human peripheral blood of normal donors (Zhu *et al.*, 1998). Like FcεRI, a sizeable pool of FcγRIII can be detected in the cytoplasm of all eosinophils. Furthermore, eosinophils express high levels of the IgG Fc receptor, FcγRII, but are negative for FcγRI (Grazanio *et al.*, 1989; Koenderman *et al.*, 1993; Kita *et al.*, 1999). Also relevant to work described in later Chapters of this Thesis is the expression of CD49d (an integrin) by eosinophils. CD49d was chosen as a marker to

distinguish eosinophils from IGROV1 tumour target cells due to its high expression level on the former, and absence of the latter (Figure 3.12).

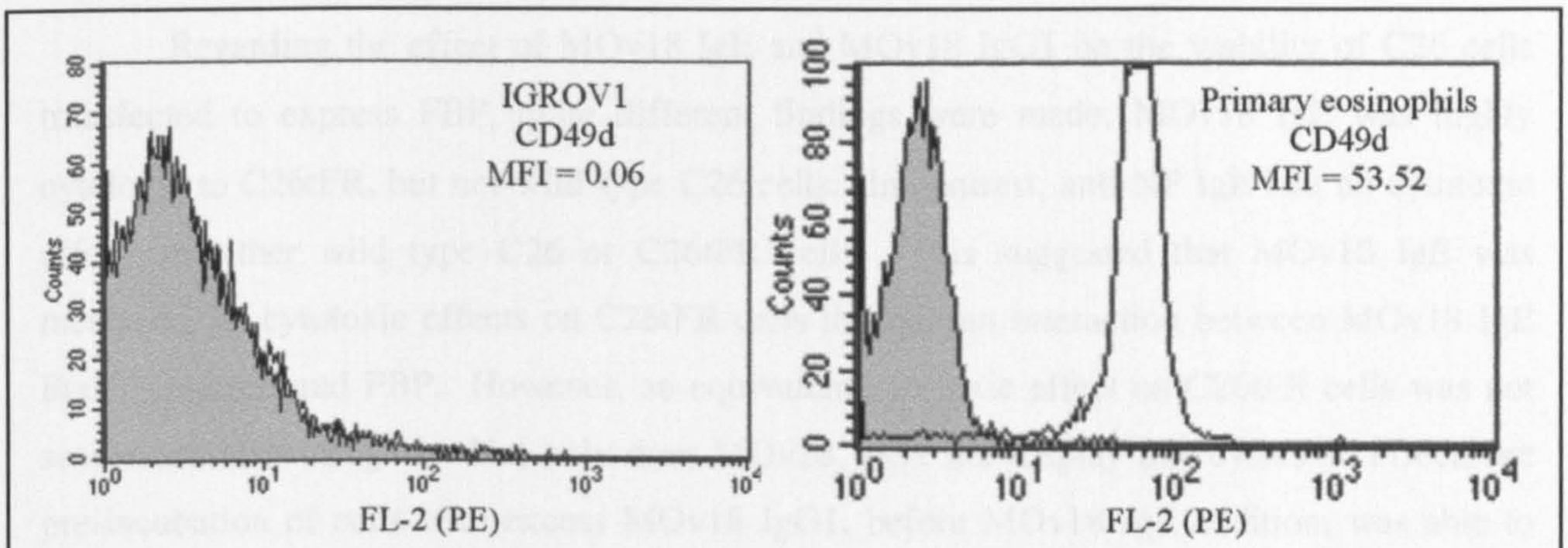

Figure 3.12: CD49d was found to be negative on IGROV1 tumour cells and positive on primary eosinophils, as detected with a PE-conjugated anti-CD49d antibody. The grey shaded area represents the isotype control.

3.5 Discussion

In this chapter, I have described the phenotypic characteristics of cells relevant to this Thesis. The tumour cell lines introduced include the human ovarian cancer cell line, IGROV1, the Balb/c mouse colon carcinoma cell line, transfected with human FBP, C26tFR and the WAG rat colon carcinoma cell line, transfected with human FBP, CC531tFR. Effector cell populations introduced include the U937 monocyte cell line, primary monocytes and primary eosinophils, purified from human peripheral blood.

In section 3.3.2, I describe experiments performed to determine whether MOv18 IgE or MOv18 IgG1 alone cause cytotoxicity to each tumour cell line through binding to and cross-linking FBP. For IGROV1 cells this has been tested previously and no cytotoxicity has been seen (Gould *et al.*, 1999; Karagiannis *et al.*, 2003). No reports of this kind for C26tFR cells have been made, and these are the first studies to be performed with CC531tFR cells. In summary, what has been found in this chapter is that, as expected, neither MOv18 IgE nor MOv18 IgG1 binding to FBP on IGROV1 cells is cytotoxic, either alone or when cross-linked by anti-IgE or anti-IgG antibodies, respectively. This makes the IGROV1 tumour cell line a suitable target for exclusive measurement of (antibody-dependent) cell-mediated killing. Furthermore, the high level of FBP expression on this cell line has previously been shown to enhance susceptibility to ADCC *in vitro* (Coney *et al.*, 1994), a significant finding when taken

with the association of high FBP expression with poor prognosis in human ovarian cancer patients (Campbell *et al.*, 1991 and Toffoli *et al.*, 1994). As such, IGROV1 cells are used as the tumour target cell line in the *in vitro* killing assays described in Chapters 4 and 5.

Regarding the effect of MOv18 IgE and MOv18 IgG1 on the viability of C26 cells transfected to express FBP, quite different findings were made: MOv18 IgE was highly cytotoxic to C26tFR, but not wild type C26 cells. In contrast, anti-NP IgE had no cytotoxic effect on either wild type C26 or C26tFR cells. This suggested that MOv18 IgE was mediating its cytotoxic effects on C26tFR cells through an interaction between MOv18 IgE $F(ab')_2$ regions and FBP. However, an equivalent cytotoxic effect on C26tFR cells was not seen from MOv18 IgG1. Not only does MOv18 IgG1 not display this cytotoxic effect, but pre-incubation of cells with excess MOv18 IgG1, before MOv18 IgE addition, was able to significantly reduce the cytotoxic effects of MOv18 IgE. Anti-NP IgE, with its structurally identical Fc region to MOv18 IgE but no FBP-binding $F(ab')_2$ region, was unable to confer a similar blocking effect, supporting the apparent mediation of MOv18 IgE cytotoxicity through FBP. This phenomenon will be investigated further as part of the continuing MOv18 IgE project. Indeed, differential effects of some, but not other IgEs on the survival and activation of different cell lines are not unprecedented (Asai *et al.*, 2001; Kalesnikoff *et al.*, 2001; Kitaura *et al.*, 2003). Work described in this Thesis has been performed under conditions where this effect does not apply, by using the IGROV1 tumour cell line for *in vitro* studies, and clone 16 of the CC531tFR cell line for an *in vivo* model (Chapter 6). Experiments using the C26tFR cell line (or clones 2 and 11 of CC531tFR) in the future, will require additional controls to account for the contribution of killing coming from MOv18 IgE-alone binding; suitable controls are suggested in the relevant parts of later Chapters.

Expression of Fc-receptors, to which MOv18 IgE or MOv18 IgG1 could bind on effector cells, were also characterised. U937 monocytes have been shown to be able to bind both anti-NP IgE and MOv18 IgE via CD23, and not FcεRI, despite expression of the latter at a higher level. This phenomenon has not previously been reported for FcεRI on U937 monocytes, although it has for primary monocytes (as discussed in section 2.2.3 and Reischl *et al.*, 1996), where it was found that treatment of primary monocytes with neuraminidase was able to restore IgE-binding capacity through the removal of sialic acid residues that were blocking IgE binding. However, treatment of U937 monocytes with neuraminidase by Dr. Sophia Karagiannis, was found to have no effect on IgE binding to FcεRI. It may be that FcεRI expressed by U937 monocytes is blocked by a different carbohydrate, requiring a different enzyme for its removal. To see if it was in fact carbohydrate groups in IgE that were preventing binding, Dr. Rebecca Beavil deglycosylated some anti-NP IgE and MOv18 IgE

(using PGNase), which Dr. Sophia Karagiannis found were still unable to bind FcεRI (Dr. Rebecca Beavil and Dr. Sophia Karagiannis, personal communication). The consequence of the inability of this U937 clone to bind human IgE, for work described in this Thesis, is that they can be used to assess contribution of CD23 alone to MOv18 IgE-mediated killing of tumour cells by U937 monocytes.

In confirmation of previous reports, approximately one third of primary human monocytes, purified from the peripheral blood of non-atopic donors, were shown to express FcεRI, of which typically half were occupied with endogenous IgE (Reischl *et al.*, 1996). Furthermore, as generally accepted (and discussed in Reischl *et al.*, 1996) CD23 appeared not to be expressed by freshly purified human peripheral blood monocytes from the three normal donors tested in this Project. Primary human eosinophils, from a single donor, were also shown to express very low levels of FcεRI, but no detectable CD23. Finally, it was shown that CD89 expression on monocytes (primary and U937) and CD49d expression on eosinophils occurred at sufficiently high levels on these cell types that they could be used to clearly distinguish them from IGROV1 tumour cells, on which these antigens are absent. Such a marker was required for the killing assay described in Chapter 4 of this Thesis.

Expression of Fc receptors for IgG on primary human monocytes and eosinophils has previously been well characterised, with primary monocytes expressing high levels of FcγRI, FcγRII and FcγRIII (Karagiannis *et al.*, 2003) and eosinophils expressing only FcγRII at high levels (Seminario *et al.*, 1999). Eosinophils are known to additionally express FcγRIII at low levels on approximately 6 % of cells, but the procedure used for eosinophil purification in this Thesis (section 2.2.3) involves their negative selection from a population of neutrophils, by use of anti-CD16 (FcγRIII) magnetic beads, and therefore any FcγRIII-expressing eosinophils are removed. It is important to note that FcγRII exists in a number of functionally heterogeneous subsets (see Table 1.1), including activatory ITAM-coupled isoforms (FcγRIIa) and inhibitory ITIM-coupled isoforms (FcγRIIb). FcγRII on primary monocytes has been shown to include both inhibitory and activatory isoforms. To the best of my knowledge, it is not known which isoform(s) of FcγRII is expressed by eosinophils, although FcγRIIa expression is typically associated with granulocytes (Table 1.1). As expected, the U937 clone used for studies reported in this Thesis showed expression of both FcγRI and FcγRII (U937 expression of FcγRI was originally demonstrated by Allen and Seed in 1989 and of FcγRII, by Stuart *et al.*, 1987). It has previously been demonstrated (Cameron *et al.*, 2002) that the isoform of FcγRII expressed on U937 monocytes is FcγRIIa. Cameron *et al.* also detected transcripts for FcγRIIb, but expression of the protein was shown to be dependent

on differentiation of the U937 monocytes into a more macrophage-like phenotype upon stimulation with dibutyryl cyclicAMP.

CHAPTER 4:

Development of a novel flow cytometric antibody-dependent cell-mediated cytotoxicity / phagocytosis assay (ADCCP)

4.1 Introduction

In this Chapter, I describe the development of a novel method for quantifying tumour cell death, triggered by Fc-receptor-expressing effector cells armed with a tumour-specific antibody. When an effector cell is conferred with antigen-specificity in this way, it is able to kill cells either by phagocytosis (internally) and or by cytotoxicity (externally): the mode(s) of killing used depends on the properties of both effector and target cells, the isotype of the antibody and the immune context of the interaction. The parameter used to quantify cell death in the most commonly used cytotoxicity assays, such as chromium (Brunner *et al.*, 1968) or LDH (Korzeniewski *et al.*, 1983) release assays, is based on the loss of membrane integrity which occurs as a cell dies. In the ^{51}Cr-release assay, this requires the target cells to be loaded with ^{51}Cr prior to incubation with effector cells and antibody. This ^{51}Cr is released from the targets as they die, into the extracellular medium, where it is measured. In the LDH assay, release of the cytosolic enzyme lactate dehydrogenase from dying cells catalyses the conversion of lactate and NAD^+ into pyruvate and NADH, following which a sample of the extracellular medium is mixed with diaphorase for conversion of NADH and the tetrazolium salt INT (2-p-iodophenyl-3-p-nitrophenyl-5-phenyl tetrazolium chloride) into a red formazan product (and NAD^+), which is measured in a colorimeter. Clearly, measuring cell death on the basis of a change in a component of the extracellular media resulting from release of a substance from the cell cytosol, will not take into account any tumour cells which have been phagocytosed, as the markers of cell death will instead be released from the damaged target cell into the phagocyte (as shown previously to be the case by Munn and Cheung, 1989).

Previous *in vitro* assessment of MOv18 IgE-mediated tumour cell death has been made using both chromium (Gould *et al.*, 1999) and LDH-release methods, in addition to a flow cytometric (FCM) method based on the same principle (uptake of the DNA-binding dye, EthD1 through damaged cell membrane) (Karagiannis *et al.*, 2003). However, immunofluorescence imaging of MOv18 IgE-mediated tumour cell killing by monocytes (Karagiannis *et al.*, 2003) suggests phagocytosis may also play a prominant role as a mechanism of tumour cell killing. Indeed, CD23 has a recognised role in mediating phagocytosis (as discussed in section 1.3.6). Therefore, it may be that a proportion of cell death is unaccounted for in this system. Although the FCM assay mentioned above (and described in Karagiannis *et al.*, 2003) is based on the same principle as chromium and LDH release, like other FCM assays of ADCC, it has the advantage that dead cells are directly quantified on a single cell basis. Direct visualisation of all cells in this way and the ability to measure additional fluorescent markers in the flow cytometer allows for potential measurement of further parameters of cell death in the same assay population.

In this chapter, I explain the set-up of a new flow cytometric approach for quantifying antibody-mediated tumour cell death occurring by both cytotoxicity and phagocytosis. This assay is based on the same principle as those FCM assays used in Karagiannis *et al.*, 2003, Radosevic *et al.*, 1990 and Lee-MacAry *et al.*, 2001, as just a few examples. What makes the assay described in this chapter different from those previously used is the inclusion of a third fluorophore that allows quantification of phagocytosis in addition to cytotoxicity.

4.2 Principle of assay

A schematic representation of the principle of this assay is shown in Figure 4.1, below, for reference throughout the remainder of this chapter. Each individual step involved in this assay is described in detail below. In summary, this flow cytometric assay involves the use of three different fluorophores. Before the assay is begun, tumour target cells are stained with the green fluorescent dye, CFSE (for more details, see section 4.2.1); this is step one. Tumour cells are then incubated with unstained effector cells (step two) and antibody (MOv18 IgE or the control antibody, anti-NP IgE). After effector and target cell incubation, effector cells are labelled with the fluorescent dye, Phycoerythrin (PE), against an antigen expressed only on effector but not target cells; following this, all dead cells are labelled with Propidium Iodide (PI) (step 3). The change in the viability of the cells is then assessed by flow cytometry (step 4). Five different (useful) cell populations can be distinguished in total. These include (1) live tumour targets ($CFSE^+$, PE^-, PI^-), (2) live effector cells ($CFSE^-$, PE^+, PI^-), (3) dead tumour targets ($CFSE^+$, PE^-, PI^+), (4) dead effector cells ($CFSE^-$, PE^+, PI^+), and (5) tumour cells which have been phagocytosed ($CFSE^+$, PE^+, $PI^{- \text{ or } +}$). The set-up of this assay was begun by first separately optimising the single staining of individual cell types. Staining intensity was later adjusted such that the three fluorophores could be used in combination.

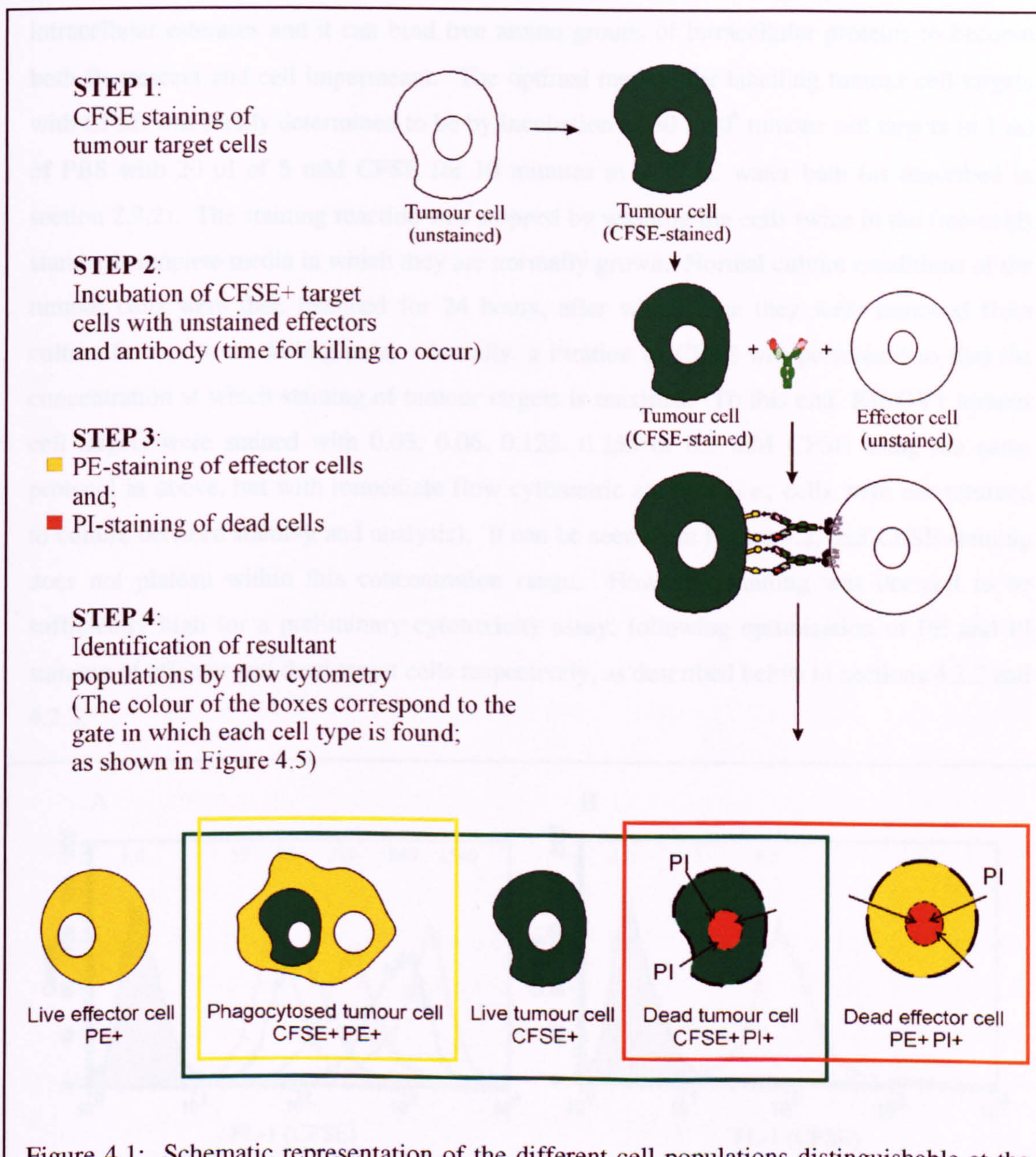

Figure 4.1: Schematic representation of the different cell populations distinguishable at the beginning and end of the ADCCP assay described in this chapter. The coloured boxes are for cross-reference with Figure 4.5B (at a later stage of reading this chapter); the green box corresponds to Region 1, the yellow box to Region 2, and, the red box to Region 3.

4.2.1 Target cell preparation

The tumour cell target line chosen was IGROV1 (the reasons for which are described in Chapter 3), and the target-cell fluorescent label chosen was CFSE. CFSE is cell permeant and non-fluorescent until inside the cell, whereupon its acetate groups are cleaved by intracellular esterases and it can bind free amino groups of intracellular proteins to become both fluorescent and cell impermeant. The optimal method for labelling tumour cell targets with CFSE was finally determined to be by incubation of 50 x 10^6 tumour cell targets in 1 ml of PBS with 20 µl of 5 mM CFSE for 10 minutes in a 37 °C water bath (as described in section 2.3.2). The staining reaction was stopped by washing the cells twice in the (ice-cold) standard complete media in which they are normally grown. Normal culture conditions of the tumour cells were then resumed for 24 hours, after which time they were removed from culture for use in the killing assay. Initially, a titration of CFSE was performed to find the concentration at which staining of tumour targets is maximal. To this end, IGROV1 tumour cell targets were stained with 0.03, 0.06, 0.125, 0.255 or 0.5 mM CFSE using the same protocol as above, but with immediate flow cytometric analysis (*i.e.*, cells were not returned to culture between staining and analysis). It can be seen from Figure 4.2, that CFSE staining does not plateau within this concentration range. However, staining was deemed to be sufficiently high for a preliminary cytotoxicity assay, following optimisation of PE and PI staining of effector and dead target cells respectively, as described below in sections 4.2.2 and 4.2.3.

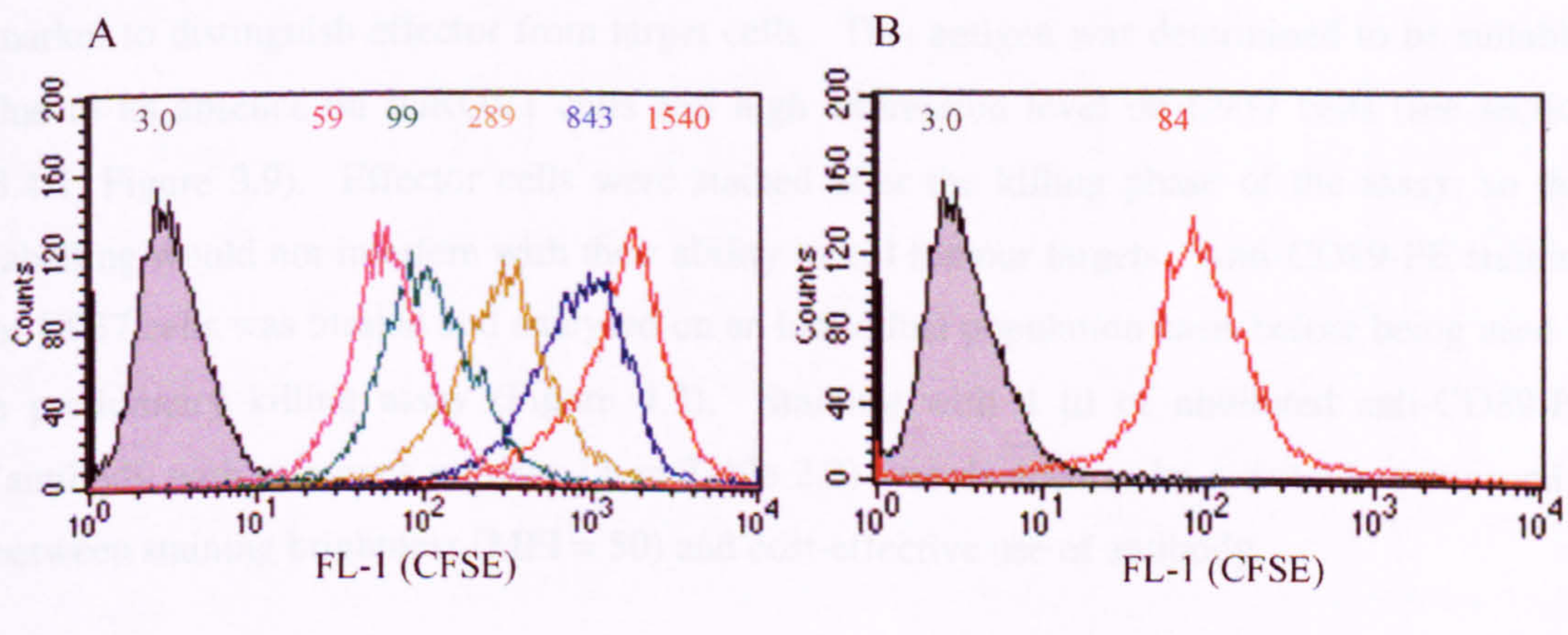

Figure 4.2: (A) Titration of IGROV1 CFSE staining. The grey shaded are represents unstained IGROV1 cells ('treated as stained', where CFSE was replaced with PBS), followed in order of increasing CFSE staining intensity with 0.03 (pink line), 0.06 (green line), 0.125 (brown line), 0.25 (blue line) or 0.5 mM (red line) CFSE staining. (B) The $FL1^+$ population on this plot represents IGROV1 cells stained with 5 mM CFSE 24 hours before analysis (and returned to culture between staining and analysis).

Preliminary killing assays showed that there was leakage of CFSE fluorescence into the FL2 channel that was too high to be compensated for, and therefore the staining intensity needed to be reduced. It was decided that instead of using a lower CFSE concentration, it would be better to follow staining with a 24 hour culture period, before using the cells in a killing assay. This would allow the excess CFSE to be quenched, but the tenacious retention of fluorescent CFSE dye means that cells should remain sufficiently bright (even in those that have divided). It can be seen from comparison of the red line on each of the histograms in Figure 4.2A and B that an overnight incubation of IGROV1 tumour cells stained with 0.5 mM CFSE lead to a reduction in CFSE mean fluorescence intensity from 1540 to 84; the uniform nature of this reduction suggests it is due to catabolism and not cell division. The advantage of this culture period (in addition to reducing CFSE staining intensity) is that the tumour cells have time to recover from the staining procedure, potentially reducing background cell death in the ADCCP assay.

4.2.2 Effector cell preparation

The effector cell population used in the set-up of this killing assay was the U937 monocyte cell line. This choice was based on its IgE receptor expression, uniform nature and virtually limitless availability, removing the need for time-consuming cell purification procedures, and the variability associated with using single cell populations from different donors. CD89 (the IgA Fc receptor), expressed on the surface of U937 cells, was chosen as a marker to distinguish effector from target cells. This antigen was determined to be suitable, due to its absence on IGROV1 cells and high expression level on U937 cells (see section 3.4.1, Figure 3.9). Effector cells were stained after the killing phase of the assay, so that labelling would not interfere with their ability to kill tumour targets. Anti-CD89-PE staining of U937 cells was titrated and analysed on an individual population basis before being used in a preliminary killing assay (Figure 4.3). Staining with 4 µl of undiluted anti-CD89-PE (antibody with reference number 11 in Table 2.2) was deemed to be a suitable compromise between staining brightness (MFI = 50) and cost-effective use of antibody.

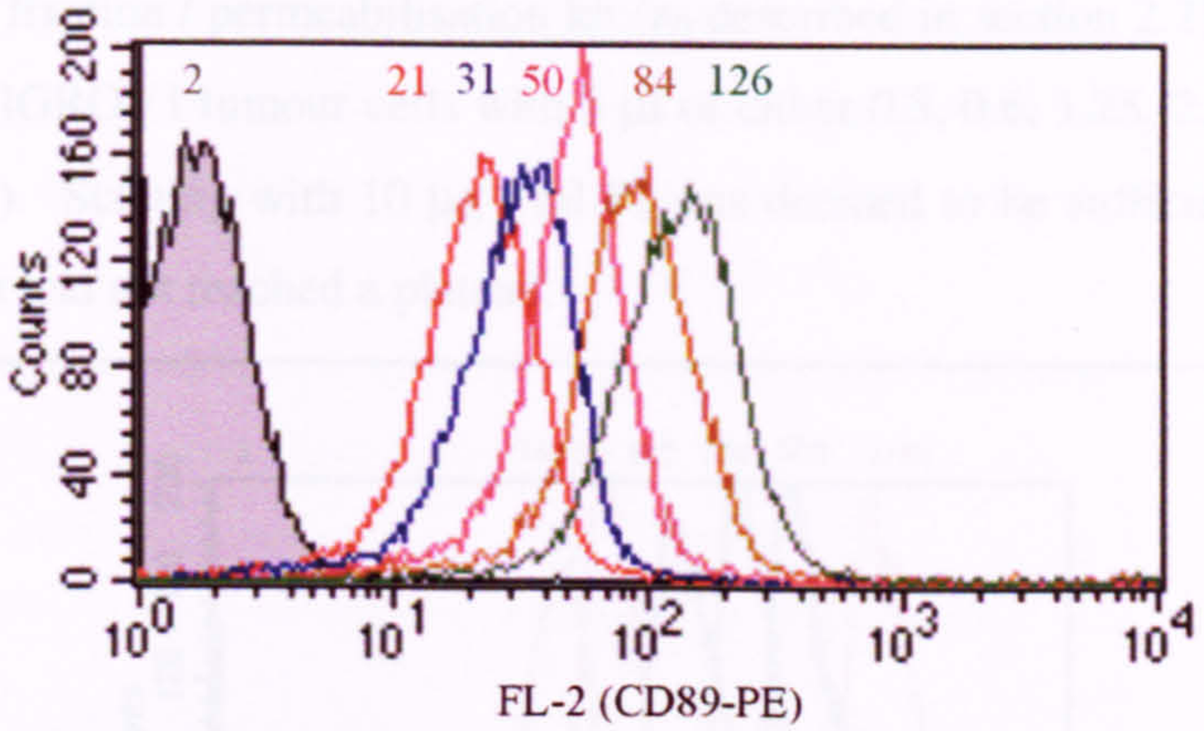

Figure 4.3: Titration of CD89-PE staining of U937 monocytes. The grey shaded area represents unstained U937 monocytes, followed by order of increasing FL2 MFI by staining with 1 µl (red line), 2 µl (blue line), 4 µl (pink line), 8 µl (brown line) and 10 µl (green line) of anti-CD89-PE, per 130 000 cells.

4.2.3 Cytotoxicity / phagocytosis assay

Labelled IGROV1 tumour target cells ($CFSE^+$) were incubated in triplicate in 12 x 75 mm FACS tubes (Falcon, Becton Dickinson) with unstained effector cells and antibody (MOv18 IgE, MOv18 IgG, anti-NP IgE, MOPC or 'no-antibody control' tubes) at 37 °C, 5 % CO_2. The total number of cells in each tube was 260 000 in a 400 µl volume (these figures were based on those used for the flow cytometric killing assay used in Karagiannis *et al.*, 2003). These three components were always added in immediate succession in the order of targets, effectors then antibody, although a change in this order had no effect on killing (results not shown). Following the incubation at 37 °C (for 2.5 hours unless otherwise indicated) during which killing is expected to occur, the contents of each FACS tube was washed once in 2 ml of ice cold FACS buffer, and then U937 effector cells were labelled with anti-CD89-PE. Subsequent to this staining step, cells were again washed in 2 ml ice cold FACS buffer, following which any dead cells were labelled with PI. Cells were washed again, and then resuspended to 250 µl in ice-cold FACS buffer for immediate analysis, during which they were kept on ice.

PI was chosen as a suitable dead-cell marker due to the ability to view its emitted fluorescence in the FL3 channel. PI cannot cross an intact plasma membrane, and therefore dead cells are labelled when membrane integrity is lost to the extent to which PI entry is allowed. PI intercalates between bases in the double stranded DNA and emits red fluorescence when excited by blue light. Cells were killed and membranes permeabilised

using the DAKO fixation / permeabilisation kit (as described in section 2.2) for titration of PI in dead ($CFSE^+$) IGROV1 tumour cells with 5 µl of either 0.3, 0.6, 1.25, 2.5, 5 or 10 µg / ml of PI (Figure 4.4). Staining with 10 µg / ml PI was deemed to be sufficiently high (MFI = 1186), although it had not reached a plateau.

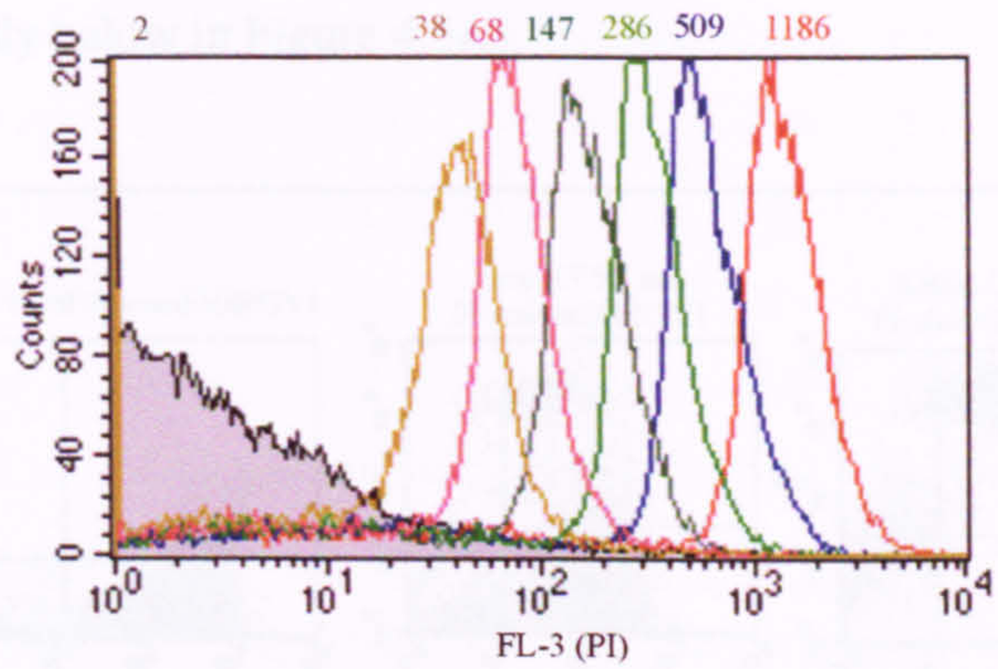

Figure 4.4: Optimisation of PI staining of killed $CFSE^+$ IGROV1 cells. The grey shaded area represents dead $CFSE^+$ IGROV1 cells not stained with PI. Populations with $FL3^+$ fluorescence, represent (beginning with the lowest MFI) cells stained with 0.3 (brown line), 0.6 (pink line), 1.25 (dark green line), 2.5 (light green line), 5 (blue line) and 10 (red line) µg / ml of PI.

4.2.4 Flow cytometry

Cells were analysed on a dual laser FACSCalibur™ (Becton Dickinson). A threshold was set on a forward and side scatter plot to exclude the minimum amount of cell debris. Cells were excited by an Argon ion laser emitting at 488 nm. CFSE-labelled cells were detected in the FL1 channel (530/30 nm band pass filter). PE-labelled cells were detected in the FL2 channel (585/42 nm band pass filter). PI used to identify dead cells was detected in the FL3 channel (670 nm LP band pass filter). Photomultiplier voltages were set to place the CFSE-labelled cells predominantly in the third log decade of the FL1 channel and the first log decade of the FL2 channel. Following this, voltage and compensation adjustments were made using a series of control tubes, such that PE^+ cells were placed predominantly in the second log decade of the FL2 channel and the first log decade of both FL1 and FL3 channels, and that PI^+ cells were placed in the fourth log decade of the FL3 channel and first log decade of both FL1 and FL2 channels. Control tubes used to achieve this included live unstained effectors, live PE^+ effectors, live $CFSE^+$ effectors and killed (using Dako fixation / permeabilisation kit, see Table 2.1) $CFSE^+$ targets either subject, or not, to PI staining (PI^- / $CFSE^+$ and PI^+ / $CFSE^+$ respectively).

4.2.5 Calculation of cytotoxicity and phagocytosis

Acquisition was stopped after 20 000 events had been acquired and two dot plots were created from which to calculate the proportion of killing coming from both cytotoxicity and phagocytosis (Figure 4.5B). The gates shown in Figure 4.5B were set using the same series of control tubes used to optimise instrument settings as described above in section 4.2.4 (and shown individually below in Figure 4.5A).

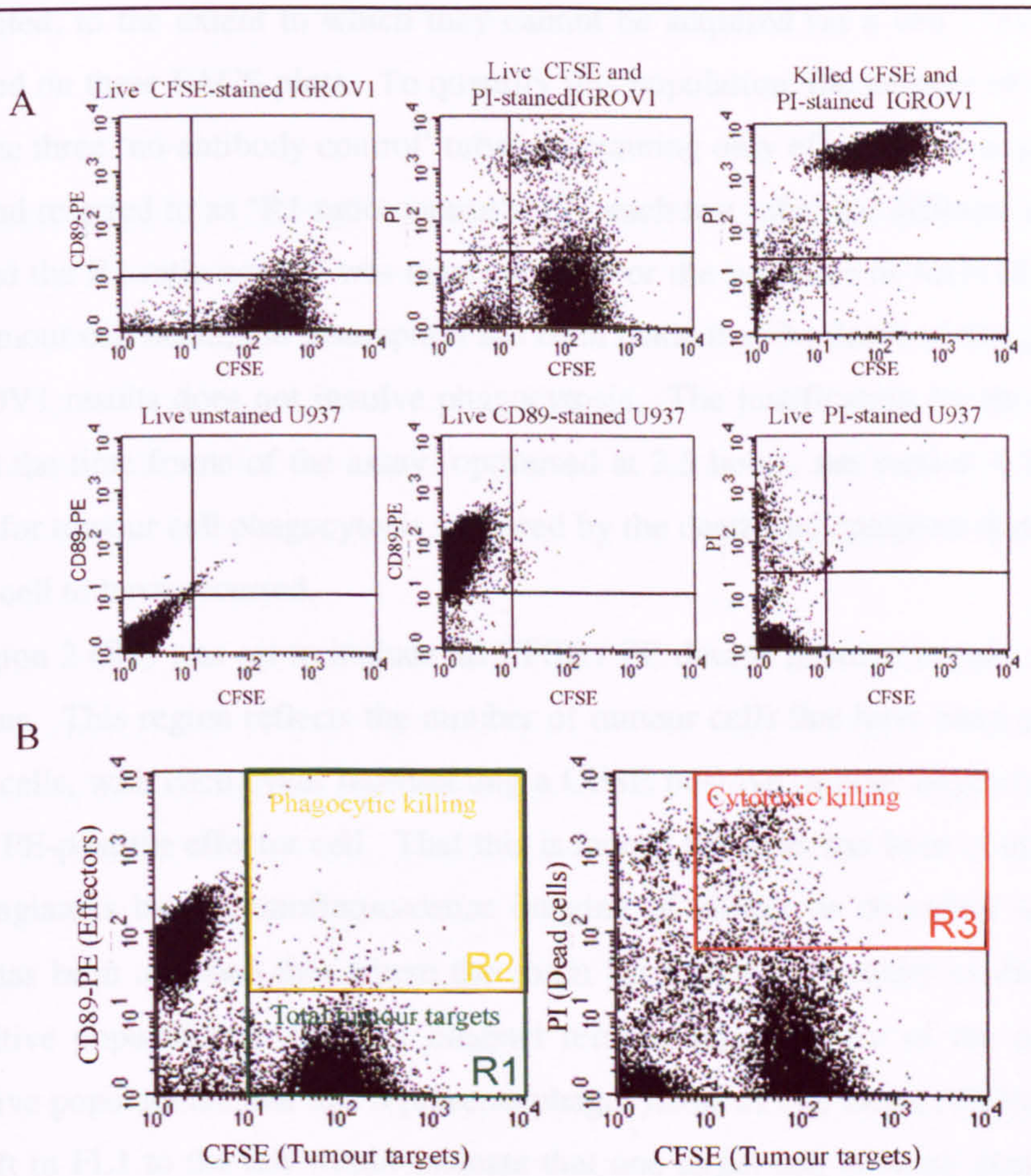

Figure 4.5: (A) Control tube populations used for instrument settings and determination of where quadrants should be set. (B) Dot plots from which calculations were made: Region 1 (R1) includes events representing $CFSE^+$ tumour cell targets alone. The $CFSE^+$ tumour cell targets may be present within PE-stained effector cells (where they have been phagocytosed); these events are found in Region 2 (R2). Region 3 (R3) contains those tumour targets which have been killed externally of effector cells (cytotoxicity) and are thus $CFSE^+/PI^+$. Schematic representations of those cells found within these gates can be found in Figure 4.1.

Region 1 (R1) was set to include all CFSE-positive events acquired, regardless of their PI and PE status. When effectors and targets were mixed at an original ratio of 1:1, R1 was expected to contain approximately 10 000 events, representing half of the 20 000 events acquired in total. Due to both background death and additional antibody-mediated death (where relevant), the number of events in R1 was consistently lower than 10 000, reflecting the increase in ratio of live effectors to targets, in the tube. The amount by which the number of events in R1 is reduced, represents the proportion of tumour cells which had been killed and fragmented, to the extent to which they cannot be acquired (as a cell / 'event') and go unrepresented on these FACS plots. To quantify this population, the number of events in R1 of each of the three 'no-antibody control' tubes (containing only effector and target cells) was averaged, and referred to as 'R1 ratio control'. For each test tube, the difference between its R1 value and the R1 ratio control was determined. For the purposes of MOv18 IgE / U937-mediated tumour cell death, the assumption has been made that the death of this population of killed IGROV1 results does not involve phagocytosis. The justification for this is based on the fact that the time frame of the assay (optimised at 2.5 hours, see section 4.3 below) was insufficient for tumour cell phagocytosis followed by the death and complete disintegration of the effector cell to have occurred.

Region 2 (R2) was set to include all CFSE / PE double positive events, regardless of their PI status. This region reflects the number of tumour cells that have been phagocytosed by effector cells, with each event representing a CFSE positive tumour target (or proportion of) inside a PE-positive effector cell. That this is indeed the case, has been confirmed by Dr. Sophia Karagiannis by immunofluorescence imaging of killing, as described in section 4.4 below. It has been assumed that where the mean fluorescence intensity of the CFSE / PE double positive population in the FL1 channel remains equal to that of the corresponding single positive populations, that this represents phagocytosis of one target cell by one effector cell. A shift in FL1 to the left would indicate that one target cell is being phagocytosed by more than one effector cell.

Region 3 (R3) was set to include CFSE / PI double positive events. This reflects the population of IGROV1 tumour target cells ($CFSE^+$) which have been killed by cytotoxicity such that their membranes have lost integrity sufficient to allow PI to enter and fluoresce, but have not fragmented such that they have become undetectable as single events (and formed part of the population responsible for deviations in the R1 value from the 'R1 ratio control'). The final calculation for determination of cells killed by cytotoxicity and or phagocytosed, was therefore as follows:

Percentage of original IGROV1 cells in the assay which were killed by cytotoxicity:

$$R1 \text{ ratio control} - R1 = X.$$

$$(X + R3) / R1 \text{ ratio control} \times 100$$

Percentage of original IGROV1 cells in the assay which are phagocytosed:

$$R2 / R1 \text{ ratio control} \times 100$$

4.3 Optimisation of U937/MOv18 IgE mediated killing of IGROV1 tumour cells

To determine the IgE concentration, effector to target ratio and time point at which MOv18 IgE-mediated killing of IGROV1 cells by U937 effectors was optimal, titrations were performed. The effector to target ratio was performed first, using a time-point of 2.5 hours and 2 μg antibody. It can be seen from Figure 4.6A, that a 1:1 effector to target ratio was optimal. A timecourse demonstrated 2.5 hours to be optimal (Figure 4.6B). Using the optimal time-point of 2.5 hours, and effector to target ratio of 1:1 at which cytotoxicity is maximal, MOv18 IgE (and anti-NP IgE) were titrated (Figure 4.6C), and 2 μg of MOv18 IgE was shown to give optimal killing. These results are discussed in more detail in chapter 5, where primary monocytes and eosinophils are compared to U937 monocytes for their ability to act as effectors of MOv18 IgE-mediated tumour cell killing.

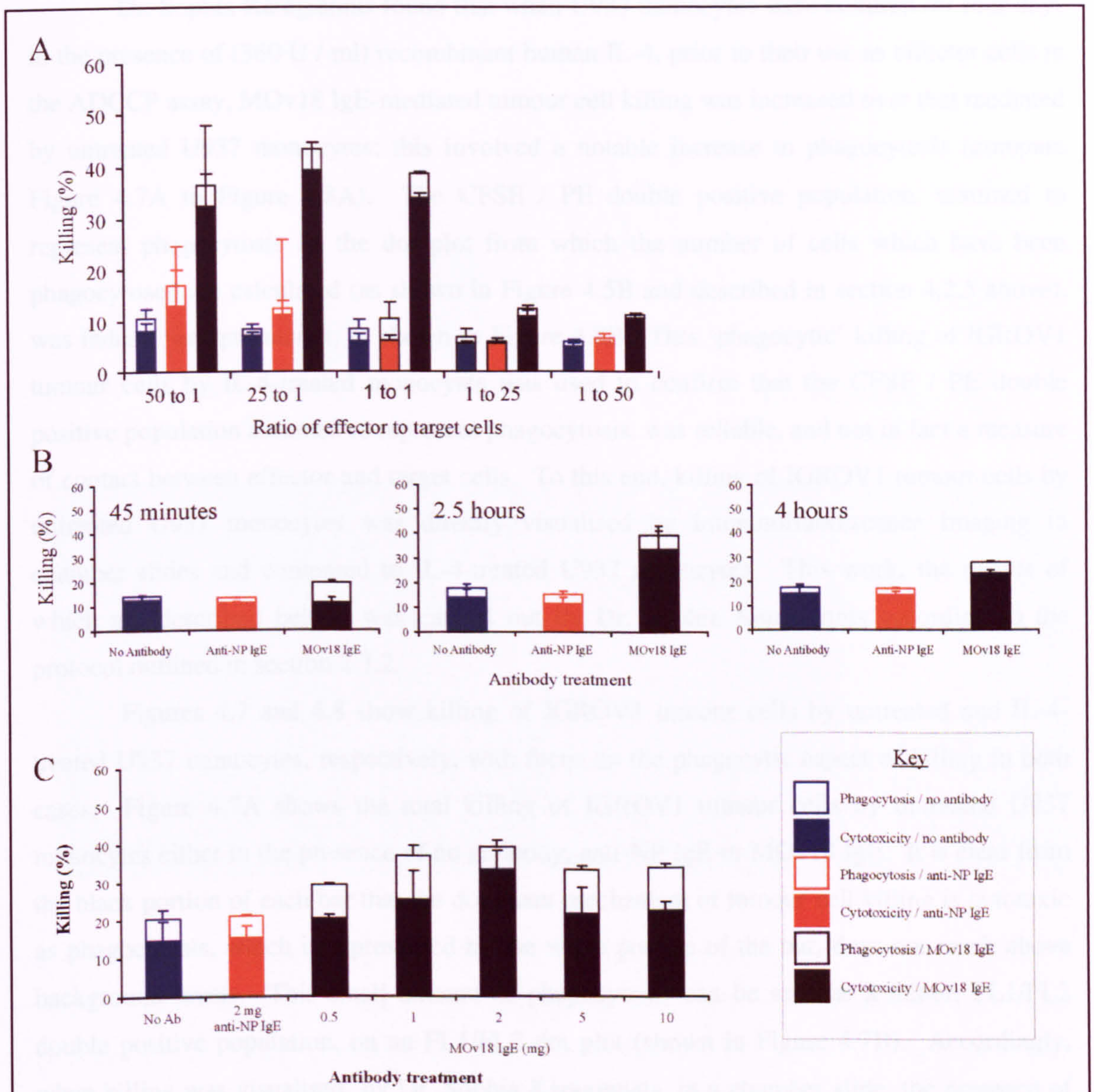

Figure 4.6: Titrations to determine optimal (A) effector to target ratio (B) timepoint and (C) amount of MOv18 IgE (per 260 000 cells / 400 µl / tube). Blue bars represents effector and target cells incubated together in the presence of no MOv18 IgE or anti-NP IgE, red bars represent effector and target cells incubated together in the presence of anti-NP IgE and black bars represent effector and target cells incubated together in the presence of MOv18 IgE. Filled bars represent killing by cytotoxicity and hollow bars, phagocytosis.

4.4 Immunofluorecence imaging of killing

Dr. Sophia Karagiannis found that when U937 monocytes were cultured for four days in the presence of (360 U / ml) recombinant human IL-4, prior to their use as effector cells in the ADCCP assay, MOv18 IgE-mediated tumour cell killing was increased over that mediated by untreated U937 monocytes; this involved a notable increase in phagocytosis (compare Figure 4.7A to Figure 4.8A). The CFSE / PE double positive population, assumed to represent phagocytosis on the dot plot from which the number of cells which have been phagocytosed are calculated (as shown in Figure 4.5B and described in section 4.2.5 above), was indeed very prominent, as shown in Figure 4.8B. This 'phagocytic' killing of IGROV1 tumour cells by IL-4-treated monocytes was used to confirm that the CFSE / PE double positive population assumed to represent phagocytosis, was reliable, and not in fact a measure of contact between effector and target cells. To this end, killing of IGROV1 tumour cells by untreated U937 monocytes was directly visualised by immunofluorescence imaging in chamber slides and compared to IL-4-treated U937 monocytes. This work, the results of which are described below, was carried out by Dr. Sophia Karagiannis according to the protocol outlined in section 2.3.2.

Figures 4.7 and 4.8 show killing of IGROV1 tumour cells by untreated and IL-4-treated U937 monocytes, respectively, with focus on the phagocytic aspect of killing in both cases. Figure 4.7A shows the total killing of IGROV1 tumour cells by untreated U937 monocytes either in the presence of no antibody, anti-NP IgE or MOv18 IgE. It is clear from the black portion of each bar that the dominant mechanism of tumour cell killing is cytotoxic as phagocytosis, which is represented by the white portion of the bar, does not reach above background levels. This small amount of phagocytosis can be seen as a minor, FL1/FL2 double positive population, on an FL1/FL2 dot plot (shown in Figure 4.7B). Accordingly, when killing was visualised, by Dr. Sophia Karagiannis, in a chamber slide, the presence of any green IGROV1 tumour cells within U937 effector cells (after incubation of effector and target cells together with MOv18 IgE), was rarely seen (Figure 4.7C). In contrast, as shown in Figure 4.8, when U937 cells were treated with IL-4 for four days prior to their use as effector cells in this assay, the dominant mechanism of IGROV1 tumour cell killing was by phagocytosis, as indicated by the white portion of the bars in Figure 4.8A. The phagocytosis could be clearly seen as a prominent FL1/FL2 double-positive population, on the FL1 versus FL2 dot plot shown in Figure 4.8B. In accordance, when killing was visualised after incubation of effector plus target cells and MOv18 IgE in a chamber slide, green $CFSE^+$ IGROV1 tumour cells could regularly seen to be present within U937 effector cells (appearing orange); this was not seen when control antibody, anti-NP IgE, was used instead of MOv18 IgE (Figure 4.8C).

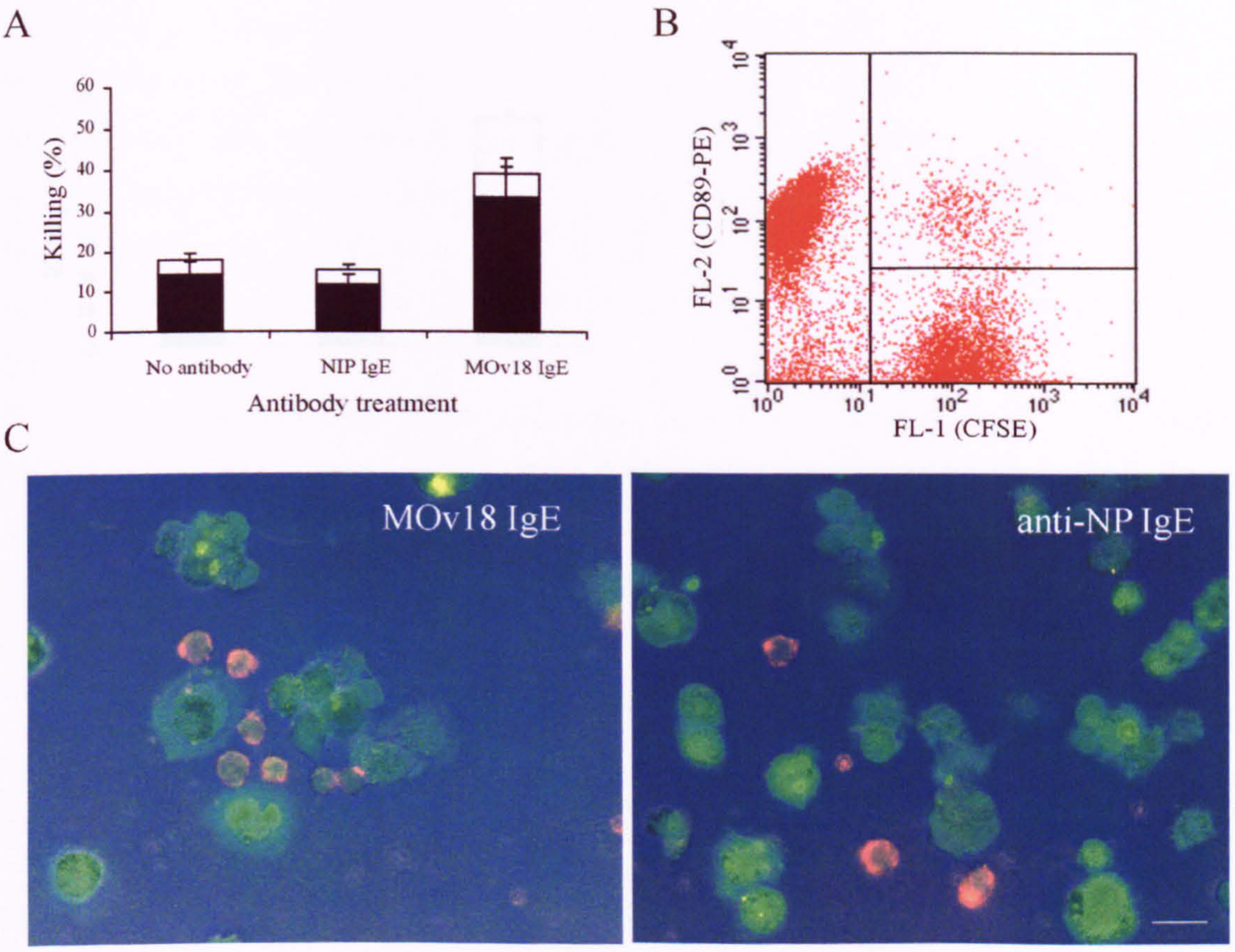

Figure 4.7: This figure shows killing of IGROV1 tumour target cells by untreated U937 effector cells. (A) Graph to show quantified killing of IGROV1 tumour cells as it occurs by both cytotoxicity (black portion of bars) and phagocytosis (white portion of bar). The white portion of the bar, representing the low, background level of MOv18 IgE-mediated phagocytosis of IGROV1 cells is shown in (B) on a FL1 versus FL2 dot plot. In accordance, when killing was visualised by Dr. Sophia Karagiannis, as shown in (C), phagocytosis was rarely seen in the presence of either MOv18 IgE, or control antibody, anti-NP IgE.

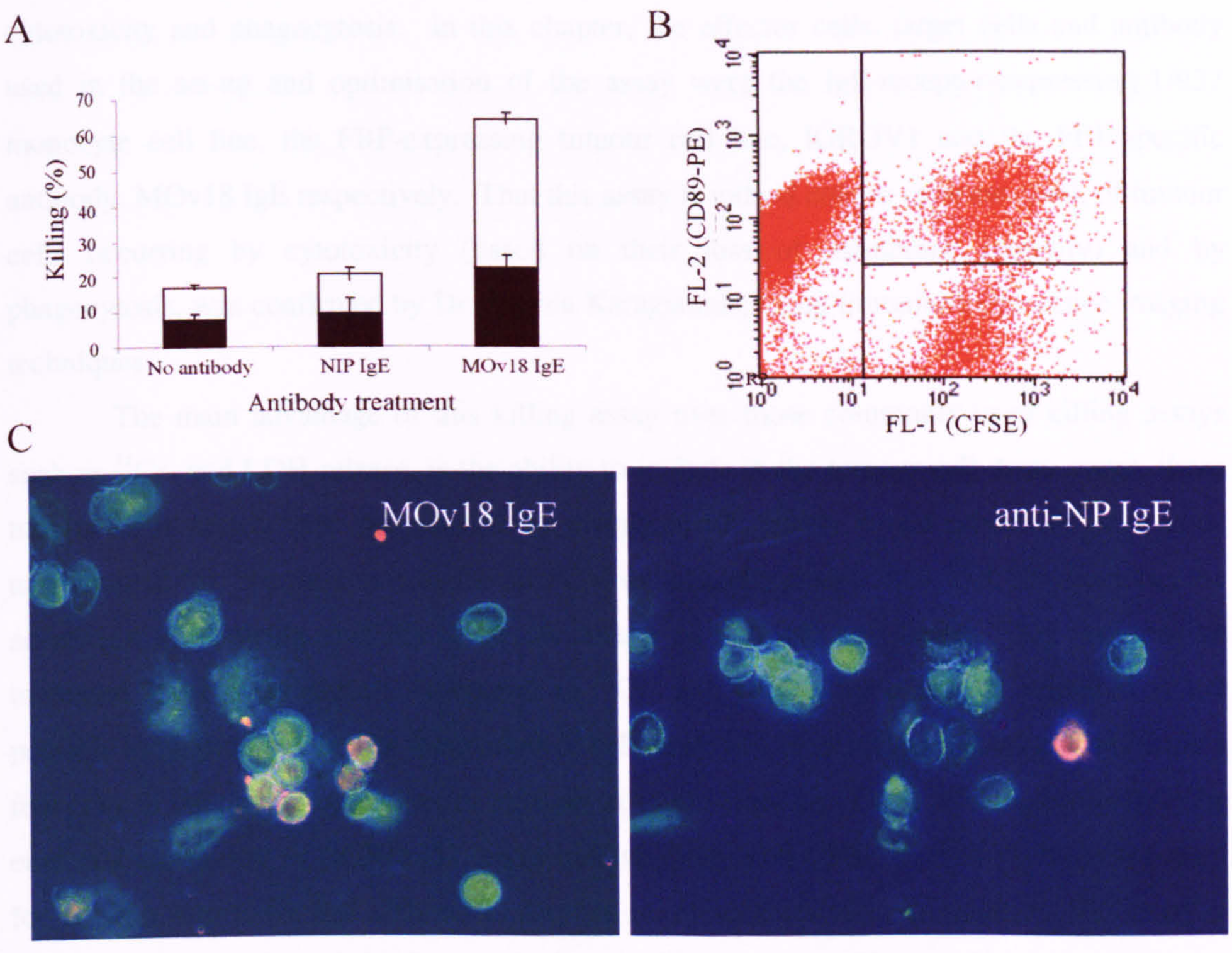

Figure 4.8: This figure shows killing of IGROV1 tumour target cells by IL-4-treated U937 effector cells. Results shown in this figure (ADCCP assay and immunofluorescence imaging) are from experiments performed by Dr. S. Karagiannis. (A) Graph to show quantified killing of IGROV1 tumour cells as it occurs by both cytotoxicity (black portion of bars) and phagocytosis (white portion of bar). The white portion of the bar representing the high level of MOv18 IgE-mediated phagocytosis of IGROV1 cells is shown in (B) on a FL1 versus FL2 dot plot. In accordance, when killing was visualised by Dr. Sophia Karagiannis and shown in (C), $CFSE^+$ IGROV1 tumour cells could frequently be seen inside U937 effector cells. $CFSE^+$ tumour cells phagocytosed by PE-stained effector cells, appeared orange.

4.5 Discussion

Work described in this chapter documents the procedures leading to the development of a novel flow cytometric assay with which to quantify antibody-dependent cell-mediated cytotoxicity and phagocytosis. In this chapter, the effector cells, target cells and antibody used in the set-up and optimisation of the assay were the IgE-receptor-expressing U937 monocyte cell line, the FBP-expressing tumour cell line, IGROV1 and the FBP-specific antibody, MOv18 IgE respectively. That this assay is indeed able to measure death of tumour cells occurring by cytotoxicity (based on their loss of membrane integrity) and by phagocytosis, was confirmed by Dr. Sophia Karagiannis, using immunofluorescence imaging techniques.

The main advantage of this killing assay over those commonly used killing assays such as ^{51}Cr- and LDH-release, is the ability to include in the tumour cell death count, those tumour cells which have been killed by phagocytosis, which would otherwise have gone unaccounted for. Furthermore, as for all FCM cytotoxicity assays, this ADCCP assay has the advantage of allowing analysis to be conducted on a single cell basis. This provides an increased level of sensitivity compared to ^{51}Cr- and LDH-release assays, where it is not possible to determine whether the marker of cell death has been released in its entirety from a few cells of the target population, or partially released from all. Other advantages include the ease and uniformity of (IGROV1) target cell labelling with CFSE (which excludes the need for volatile, expensive and difficult to dispose of, radiochemicals). In addition, this assay is cost-effective, requires minimal manual labour and is quick to perform and analyse.

A disadvantage of this assay is the inability to determine whether cells were phagocytosed alive or dead, *i.e.*, whether phagocytosis is being used as a mechanism of cell killing or for clearance of dead cells. It may be possible to re-optimise the assay to include PI within the culture during effector and target cell incubation with antibody, such that target cells may take up PI immediately after death but before phagocytosis, and be represented as a population of cells triple-positive for CFSE, PI and PE. An additional disadvantage of this ADCCP assay is that compensation of the overlap of CFSE emission into the FL2 channel can be challenging; although this has been optimised for the experiments described in this Thesis, it would have to be re-optimised if cell types or cell-staining procedures were changed.

As discussed in Lee-McAry *et al.*, 2001, FCM assays of this kind offer the potential for measurement of up to four different fluorochromes. In the assay described in this chapter, three fluorochromes are used (CFSE, PE and PI) and killing by cytotoxicity and phagocytosis are measured. A similar assay, described in Derby *et al.*, 2001, uses the three fluorochromes PKH 67 (for target cell labelling), 7-AAD (for dead cell labelling) and Annexin V-PE (for labelling of phosphatidyl serine). In this way, they are able to determine whether or not the

mode of cytotoxic death was an apoptotic one or not. In this study, they also pre-treat target cells with Concanamycin A prior to their incubation with effector cells and antibody. Concanamycin A is a perforin inhibitor, and therefore can be used to determine whether tumour target cell death has been mediated by the release of toxic granule proteins from the effector cell. Application of these methods to future work advancing that described in Chapter 5 of this thesis, may help to elucidate the mechanisms of MOv18 IgE-mediated tumour cell death shown to be mediated by eosinophils and monocytes.

CHAPTER 5:

In vitro activity of monocytes and eosinophils as effector cells in MOv18-mediated IGROV1 tumour cell killing

5.1 Introduction

The purpose of this chapter is to assess the ability of monocytes (both primary and the U937 cell line) and eosinophils to act as effector cells in antibody-dependent killing of IGROV1 tumour cells *in vitro*. This is achieved using the ADCCP assay described in the previous chapter and represented schematically in Figure 4.1. Results presented below are divided into three sections. The first, section 5.2, describes MOv18 IgE-mediated killing of IGROV1 cells by the different effector cell populations. Also documented in this section are the attempts made to inhibit MOv18 IgE-mediated tumour cell killing by blocking IgE binding to either FcεRI or CD23, in order to determine which IgE receptor mediates killing. The second, section 5.3, looks at MOv18 IgG1-mediated killing of IGROV1 cells by the different effectors. Thirdly, in section 5.4, the effect of culturing eosinophils in IL-5 either alone or in combination with anti-NP IgE or MOv18 IgE, on their tumouricidal activity, has been assessed. For this chapter, knowledge of IgE and IgG Fc receptor expression by different cell types is useful; this information has been provided in Table 1.1 of Chapter 1.

5.2 MOv18 IgE-mediated tumour cell death

ADCCP assays were performed as described in section 2.3.2. Effector cells used were U937 monocytes, primary monocytes or primary eosinophils (purified as described in section 2.2.3), and target cells were IGROV1 tumour cells, which were introduced in section 3.3. For each effector cell type, three triplicate experiments were performed unless otherwise indicated, each with a different blood donor (where effectors are primary cells). Specificity of MOv18 IgE-mediated tumour cell killing was determined by comparison with anti-NP IgE-mediated killing, and incubation of effector and target cells together in the absence of antibody. As described in section 4.3, the optimal conditions for MOv18 IgE-mediated killing of IGROV1 tumour cells by U937 monocytes were determined to be an effector to target ratio of 1:1, a 2.5 hour incubation period for targets and effectors with antibody, and 2 μg of MOv18 IgE (per 260 000 cells / tube). The results of MOv18 IgE-mediated killing of IGROV1 tumour cells by U937 monocytes under optimal conditions are reproduced from section 4.3 as Figure 5.1A below, to facilitate comparison with equivalent assays using different effector cells, described in this Chapter. Those parameters optimal for MOv18 IgE-mediated killing of IGROV1 tumour cells by U937 monocytes, were also used when effector cells were primary monocytes or eosinophils, for which results are shown below in Figures 5.1B and 5.2, respectively.

As shown in Figure 5.1A, U937 monocytes killed a mean of 40±11 % of the IGROV1 cells (ADCC + ADCP) with which they were incubated in the presence of MOv18 IgE. This is statistically significantly greater ($P = < 0.05$, $n = 3$) than tumour cell killing by U937

monocytes, either in the absence of antibody (18±5 %) or the presence of anti-NP IgE (15±4 %). It is clear from Figure 5.1A, that cytotoxic killing mechanisms (represented by the black portion of each bar) account for the majority of this tumour cell death. Tumour cell death occurring by phagocytosis, in the presence of either no antibody, anti-NP IgE or MOv18 IgE, are all within error of each other (represented by the white portion of each bar).

When effector cells are primary monocytes, total MOv18 IgE-mediated killing leads to death of a mean of 24±5 % of IGROV1 tumour cells, and anti-NP IgE to the death of a mean of 17±4 % of tumour cells. Again, specific killing is mediated by cytotoxic mechanisms as judged by the size of the black portion of the bar. Although tumour killing by primary monocytes in the presence of MOv18 IgE, compared to anti-NP IgE, is low, these results represent the compiled data from three triplicate experiments and therefore, as a trend towards increased killing in the presence of MOv18 IgE is observed, it may be that if more experiments were performed the difference between MOv18 IgE- and anti-NP IgE mediated killing may be greater. Furthermore, it is important to note that not only are the monocytes used in these experiments only 70 to 80 % pure (giving an actual effector to target ratio potentially as low as 0.7 to 1) but the conditions under which these experiments were performed were optimised for U937, not primary, monocytes. Therefore, it may be that that monocytes are able to mediate greater MOv18 IgE-dependent tumour cell killing than these three triplicate experiments suggest.

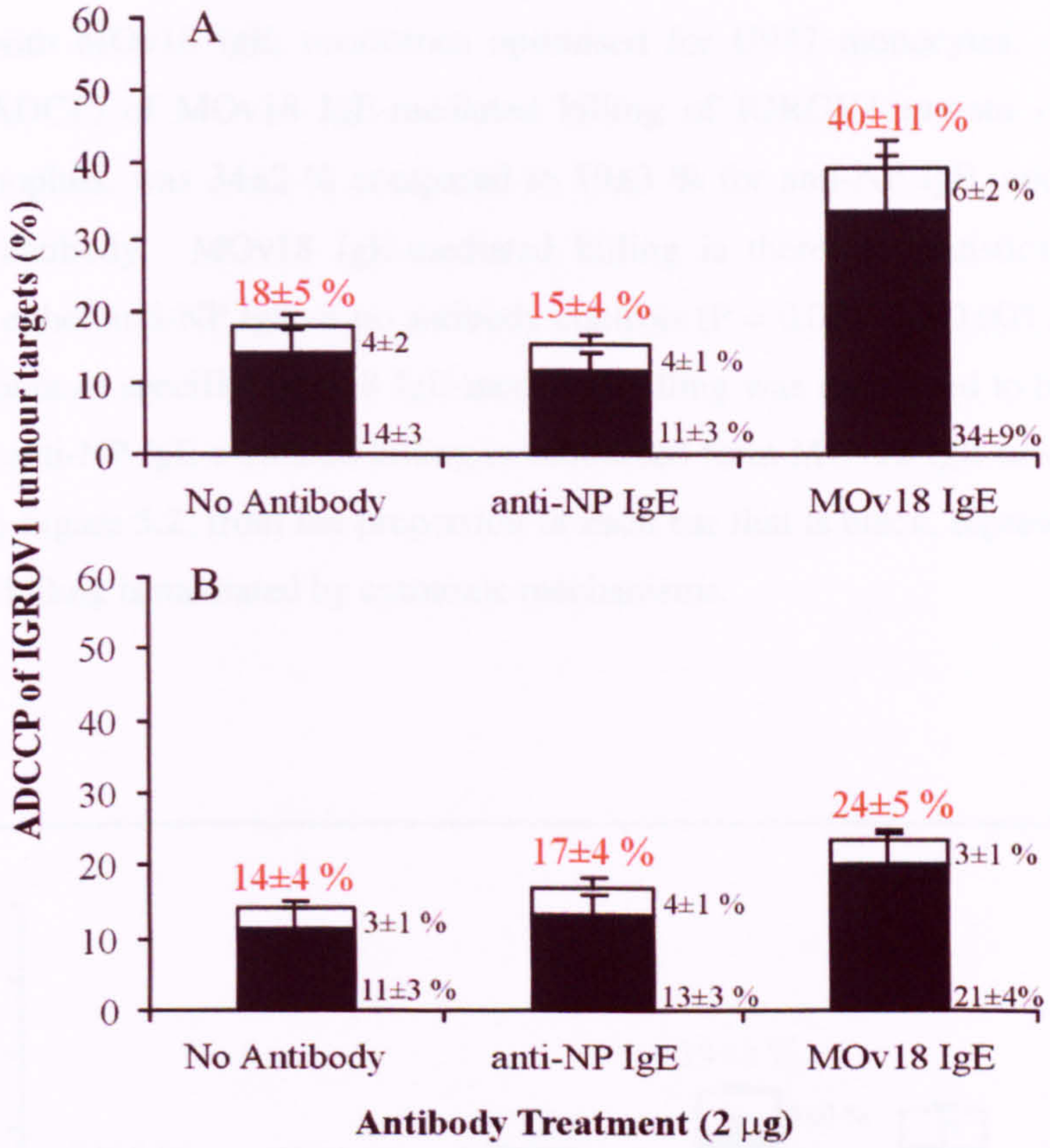

Figure 5.1: Killing of IGROV1 tumour cells by (A) U937 monocytes or (B) Primary monocytes, in the presence of either no antibody, 2 μg anti-NP IgE or 2 μg MOv18 IgE. For each effector cell type, results represent the mean of three separate experiments, each performed in triplicate. The black portion of each bar represents cytotoxic killing, and the white portion, phagocytic killing. The effector to target ratio was 1:1, and the time period of effector, target and antibody incubation was 2.5 hours.

As discussed in section 3.4.2, CD49d, an integrin expressed on eosinophils but not IGROV1 cells, has been used as a marker to distinguish these two cell types in the ADCCP assay. For work described in this Chapter, CD49d staining of eosinophils was first titrated on a single population basis, and then the instrument settings of the flow cytometer were adjusted for use of CD49d-stained eosinophils in combination with CFSE-positive IGROV1 tumour cells and PI-stained dead cells (results not shown). Tumour cell killing by primary human eosinophils in the presence of different concentrations of MOv18 IgE (per 260 000 cells in

total / tube) is shown alongside controls in Figure 5.2 below. Killing was optimal in the presence of 2 μg of MOv18 IgE at an effector to target cell ratio of 1:1, in a 2.5 hour incubation with MOv18 IgE, conditions optimised for U937 monocytes. The mean total (ADCC + ADCP) of MOv18 IgE-mediated killing of IGROV1 tumour cells by primary human eosinophils, was 34±2 % compared to 19±3 % for anti-NP IgE, and 21±6 % in the absence of antibody. MOv18 IgE-mediated killing is therefore statistically significantly greater than either anti-NP IgE or no antibody controls (P = 0.001 and 0.003 respectively, n = 5). The amount of specific MOv18 IgE-mediated killing was calculated to be approximately 15 %, when anti-NP IgE-mediated killing is subtracted from MOv18 IgE-mediated killing. It is clear from Figure 5.2, from the proportion of each bar that is black, representing killing by ADCC, that killing is mediated by cytotoxic mechanisms.

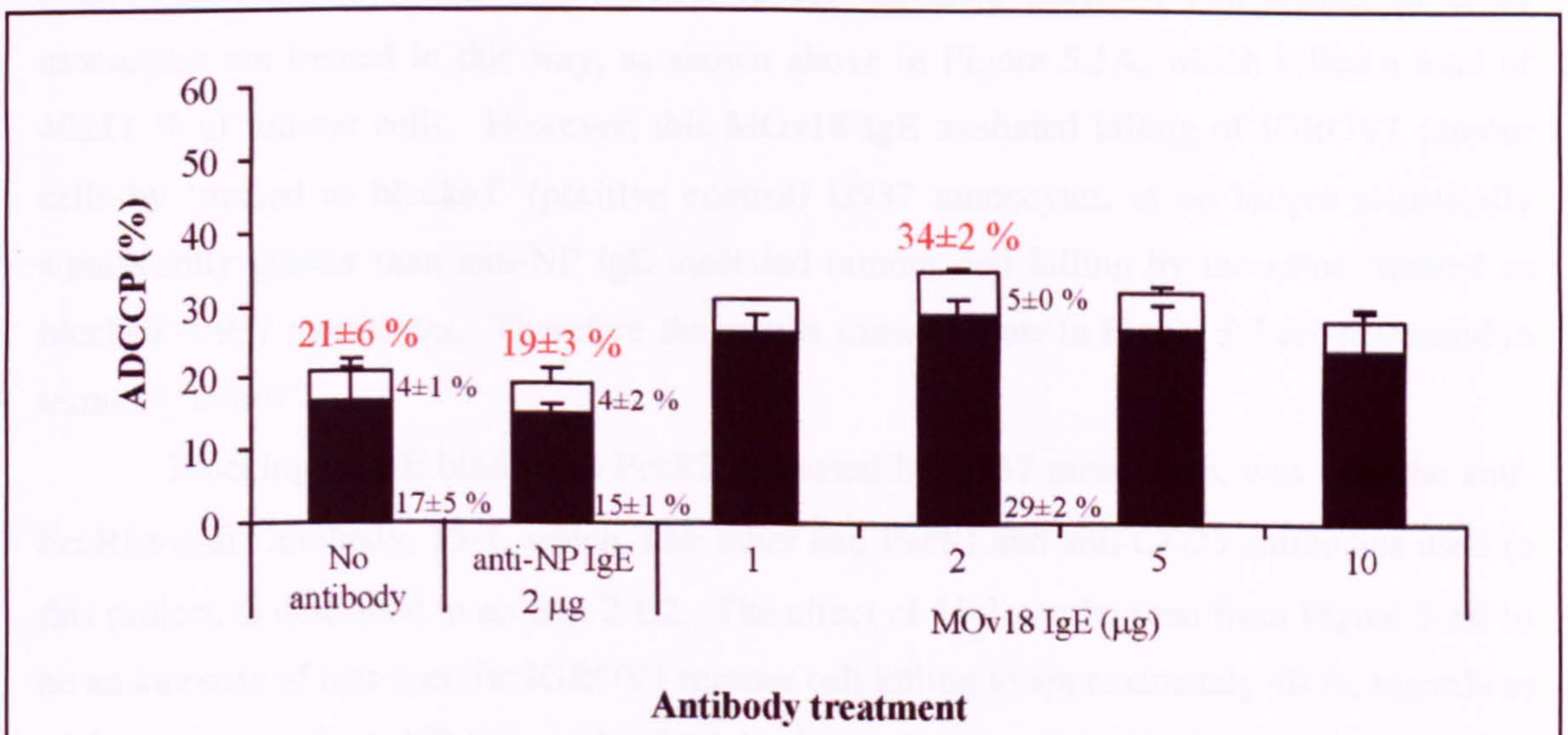

Figure 5.2: Killing of IGROV1 tumour cells by primary eosinophils, in the presence of either no antibody, anti-NP IgE or MOv18 IgE (at indicated μg per 260 000 cells / tube). Results represent the mean of five separate experiments, each performed in triplicate. The black portion of the bar represents cytotoxic killing, and the white portion, phagocytic killing. The effector to target ratio was 1:1, and the time period of effector, target and antibody incubation was 2.5 hours.

Experiments were then performed to determine through which of the IgE receptors, FcεRI or CD23, MOv18 IgE acts to mediate tumour cell killing, for each effector cell type. To this end, as described in section 2.3.2, effector cells were incubated with an excess of anti-FcεRI or anti-CD23 blocking antibody (introduced in section 2.1.2) for 30 minutes prior to their incubation with target cells either alone or in the presence of 2 μg of anti-NP IgE or MOv18 IgE, as in the standard killing assay (section 2.3.2).

Results of attempts to block MOv18 IgE-mediated killing of tumour cells by U937 monocytes are shown in Figure 5.3 below. Figure 5.3A gives the results of MOv18 IgE-mediated killing of IGROV1 cells by U937 monocytes, which were subject to the same protocol used to block IgE receptors, but with replacement of blocking antibody with PBS ('treated as blocked' positive control, performed in every ADCCP assay). These results represent the mean of 7 separate experiments, each performed in triplicate. U937 monocytes treated in this way killed a total of 28±9 % of IGROV1 tumour cells in the presence of MOv18 IgE; this is within error of MOv18 IgE-mediated IGROV1 cell killing by U937 monocytes not treated in this way, as shown above in Figure 5.1A, which killed a total of 40±11 % of tumour cells. However, this MOv18 IgE mediated killing of IGROV1 tumour cells by 'treated as blocked' (positive control) U937 monocytes, is no longer statistically significantly greater than anti-NP IgE-mediated tumour cell killing by the same 'treated as blocked' U937 monocytes. Therefore the results shown below in Figure 5.3 are discussed in terms of 'trends'.

Blocking of IgE binding to FcεRI expressed by U937 monocytes, was with the anti-FcεRIα-chain antibody, 15-1, which, like other anti-FcεRI and anti-CD23 antibodies used in this project, is described in section 2.1.2. The effect of 15-1 can be seen from Figure 5.3B to be an *increase* of non-specific IGROV1 tumour cell killing to approximately 40 %, regardless of the presence of anti-NP IgE or MOv18 IgE. From the size of the black portion or each bar, it is clear that this 15-1-mediated killing occurs through cytotoxic mechanisms. Two different antibodies, each able to block binding of IgE to CD23, BU38 and IDEC-152, were also tested. Pre-treatment of U937 monocytes with 10 μg of BU38 also upregulated non-specific tumour-cell killing (Figure 5.3C), triggering U937 monocytes to kill a mean total of 78±6 % of IGROV1 tumour cells in the absence of either anti-NP IgE or MOv18 IgE; the presence of either anti-NP IgE or MOv18 IgE had no further effect on killing. All tumour cell killing by BU38-treated U937 cells, above that occurring non-specifically by untreated U937 monocytes, was mediated by phagocytic mechanisms. This is in contrast to the MOv18 IgE-independent killing triggered by 15-1. When U937 monocytes were pre-treated with 25 μg of IDEC-152, MOv18 IgE-mediated killing of IGROV1 tumour cells remained, within

experimental error, the same as MOv18 IgE-mediated killing by the positive control 'treated as blocked' U937 cells, with a mean killing total of 24±5 % (Figure 5.3D). $F(ab')_2$ fragments of IDEC-152 mediated a similar effect to whole IDEC-152 (Figure 5.3E), which again was within error of MOv18 IgE-mediated killing by control U937 monocytes. When U937 monocytes were pre-treated with anti-NP IgE, a slight trend towards reduced killing is observable (Figure 5.3F).

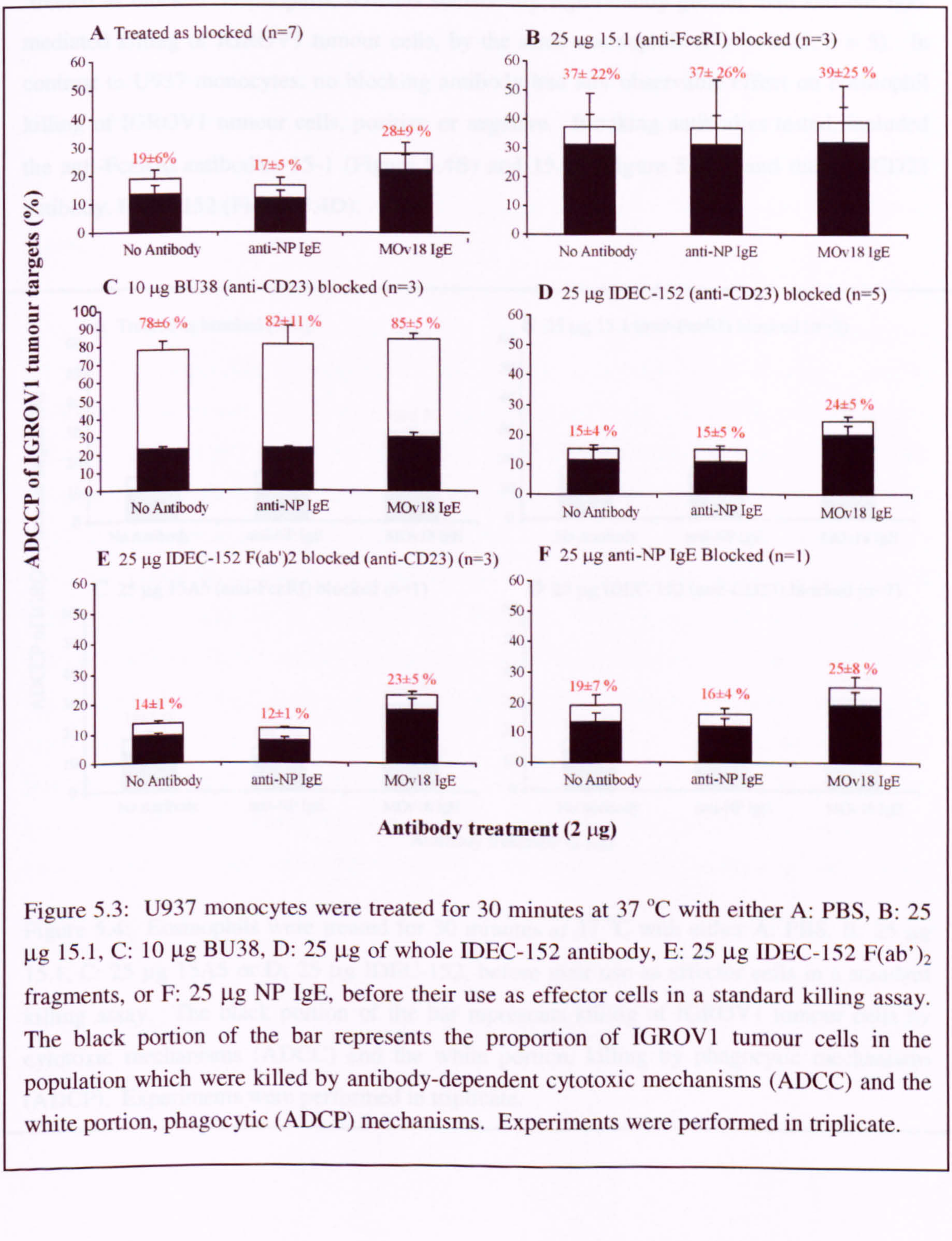

Figure 5.3: U937 monocytes were treated for 30 minutes at 37 °C with either A: PBS, B: 25 µg 15.1, C: 10 µg BU38, D: 25 µg of whole IDEC-152 antibody, E: 25 µg IDEC-152 $F(ab')_2$ fragments, or F: 25 µg NP IgE, before their use as effector cells in a standard killing assay. The black portion of the bar represents the proportion of IGROV1 tumour cells in the population which were killed by antibody-dependent cytotoxic mechanisms (ADCC) and the white portion, phagocytic (ADCP) mechanisms. Experiments were performed in triplicate.

Similar experiments involving pre-treatment of eosinophils with PBS, anti-FcεRI or anti-CD23 antibodies before performance of the ADCCP assay, were carried out, and results are shown in Figure 5.4 below. As for U937 monocytes, the eosinophils which were 'treated as blocked' (Figure 5.4A) killed to a level lower than, but within error of (30±5 %), the untreated fresh eosinophils shown in Figure 5.2, which killed a mean of 34±2 % of IGROV1 tumour target cells. However, MOv18 IgE-mediated killing of IGROV1 tumour cells by 'treated as blocked' eosinophils, remains statistically significantly greater than anti-NP IgE-mediated killing of IGROV1 tumour cells, by the same eosinophils ($P = < 0.05$, $n = 5$). In contrast to U937 monocytes, no blocking antibody had any observable effect on eosinophil killing of IGROV1 tumour cells, positive or negative. Blocking antibodies tested, included the anti-FcεRIα antibodies 15-1 (Figure 5.4B) and 15A5 (Figure 5.4C), and the anti-CD23 antibody, IDEC-152 (Figure 5.4D).

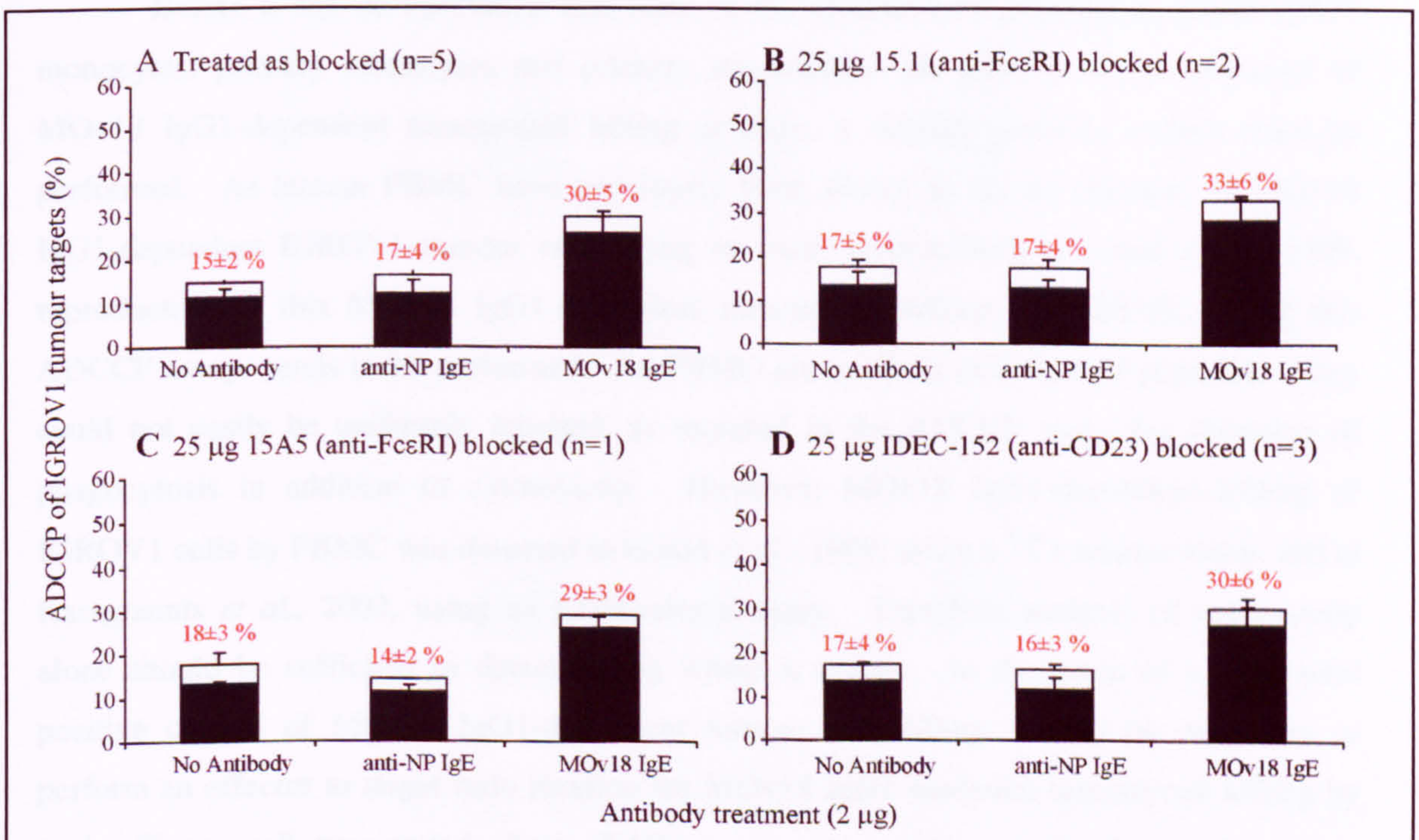

Figure 5.4: Eosinophils were treated for 30 minutes at 37 °C with either A: PBS, B: 25 µg 15.1, C: 25 µg 15A5 or D: 25 µg IDEC-152, before their use as effector cells in a standard killing assay. The black portion of the bar represents killing of IGROV1 tumour cells by cytotoxic mechanisms (ADCC) and the white portion, killing by phagocytic mechanisms (ADCP). Experiments were performed in triplicate.

5.3 MOv18 IgG1-mediated tumour cell death

The ability of monocytes and eosinophils to perform MOv18 IgG1-mediated tumour cell killing was tested. As can be seen from Figure 5.5, neither U937 monocytes, primary monocytes nor primary eosinophils were able to kill IGROV1 tumour cells by MOv18 IgG1-mediated mechanisms above background levels. The results shown in Figure 5.5 are representative of those performed using an effector to target ratio of 1:1, incubation time of effector and target cells together with antibody of 2.5 hours, and 2 μg of MOv18 IgG1 or MOPC antibody per tube; these are the conditions determined to be optimal for MOv18 IgE-mediated IGROV1-killing by U937 monocytes. However, for each effector cell type, negative results were also found over a range of MOv18 IgG1 concentrations (1, 2, 5 and 10 μg per 260 000 cells / tube) and time points (45 minutes, 4, 6 and 8 hours), the results of which are not shown. Different ratios of effector to target cells were not tried due to insufficient time.

Before it can be concluded that none of the effector cell populations tested (U937 monocytes, primary monocytes and primary eosinophils) are able to act as effectors of MOv18 IgG1-dependent tumour-cell killing *in vitro*, a suitable positive control must be performed. As human PBMC have previously been shown to act as effectors of MOv18 IgG1-dependent IGROV1 tumour cell killing *in vitro*, as described in Gould *et al.*, 1999, reproduction of this MOv18 IgG1-dependent tumour-cell killing with PBMC, using this ADCCP assay, needs to be performed. As PBMC are a mixed effector cell population they could not easily be uniformly labelled, as required in the ADCCP assay for detection of phagocytosis in addition to cytotoxicity. However, MOv18 IgG1-dependent killing of IGROV1 cells by PBMC was detected in Gould *et al.*, 1999, using a ^{51}Cr-release assay, and in Karagiannis *et al.*, 2003, using an LDH-release assay. Therefore analysis of cytotoxicity alone should be sufficient to detect killing where it occurs. In the event of a successful positive control of MOv18 IgG1-dependent tumour cell killing, it will be necessary to perform an effector to target ratio titration for MOv18 IgG1-mediated tumour cell killing by each effector cell type tested above (U937 monocytes, primary monocytes and primary eosinophils), in addition to testing longer time periods of effector and target cell incubation together with antibody.

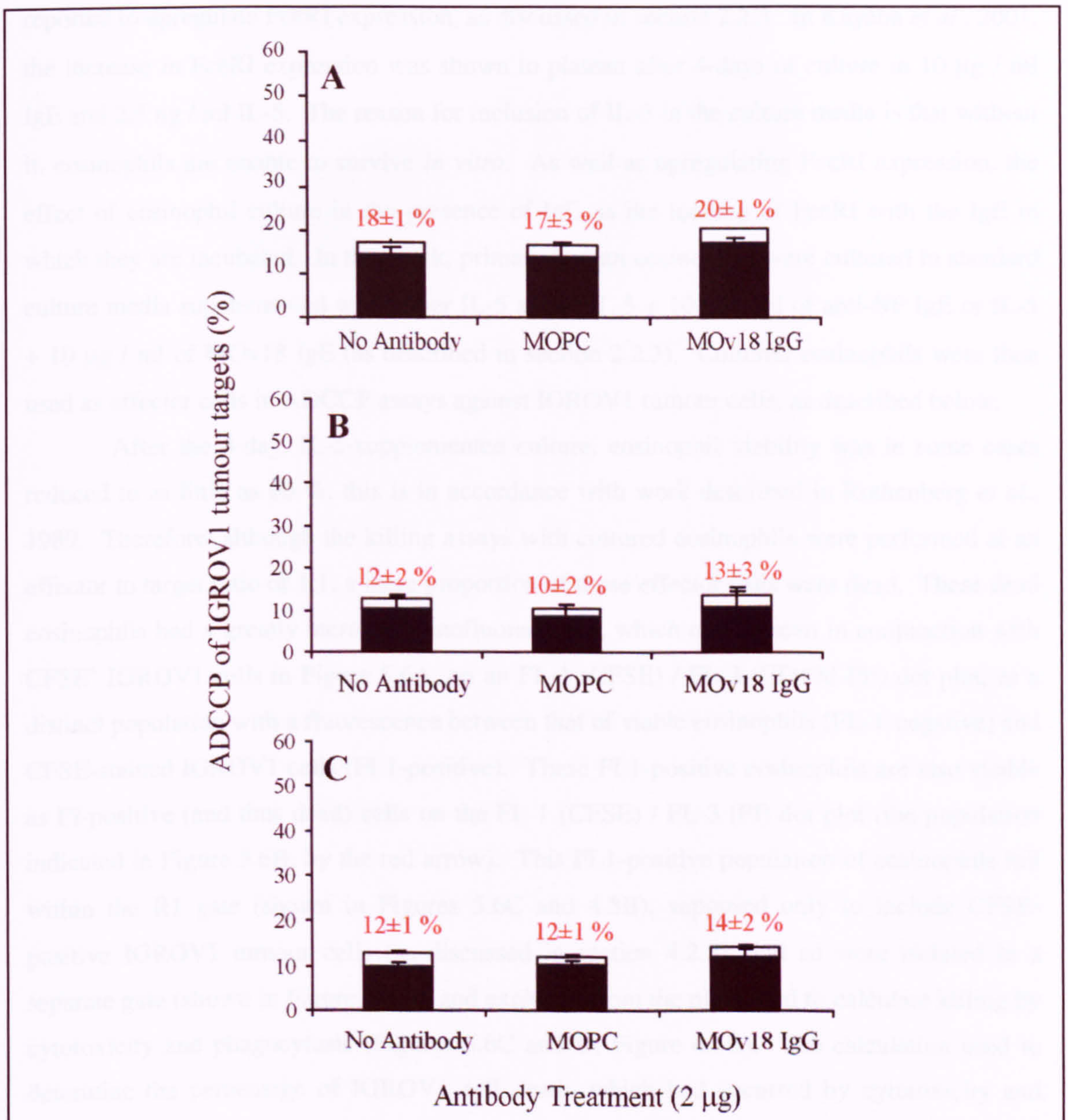

Figure 5.5: MOv18 IgG1 mediated killing of tumour cell targets compared to MOPC isotype control and no antibody controls with A; U937 monocyte effectors, B; primary monocyte effectors and C; primary eosinophil effectors. For each cell type, three triplicate experiments were performed.

5.4 Effect of IL-5 and IgE culture on eosinophil tumouricidal activity

Culture of human eosinophils in media supplemented with human IgE has been reported to upregulate FcεRI expression, as discussed in section 2.2.3. In Kayaba *et al.*, 2001, the increase in FcεRI expression was shown to plateau after 4-days of culture in 10 μg / ml IgE and 2.5 ng / ml IL-5. The reason for inclusion of IL-5 in the culture media is that without it, eosinophils are unable to survive *in vitro*. As well as upregulating FcεRI expression, the effect of eosinophil culture in the presence of IgE, is the loading of FcεRI with the IgE in which they are incubated. In this work, primary human eosinophils were cultured in standard culture media supplemented with either IL-5 alone, IL-5 + 10 μg / ml of anti-NP IgE or IL-5 + 10 μg / ml of MOv18 IgE (as described in section 2.2.3). Cultured eosinophils were then used as effector cells in ADCCP assays against IGROV1 tumour cells, as described below.

After the 4-day, IL-5-supplemented culture, eosinophil viability was in some cases reduced to as little as 60 %; this is in accordance with work described in Rothenberg *et al.*, 1989. Therefore, although the killing assays with cultured eosinophils were performed at an effector to target ratio of 1:1, a large proportion of these effector cells were dead. These dead eosinophils had a greatly increased autofluorescence, which can be seen in conjunction with $CFSE^+$ IGROV1 cells in Figure 5.6A, on an FL-1 (CFSE) / FL-2 (CD49d-PE) dot plot, as a distinct population with a fluorescence between that of viable eosinophils (FL-1-negative) and CFSE-stained IGROV1 cells (FL1-positive). These FL1-positive eosinophils are also visible as PI-positive (and thus dead) cells on the FL-1 (CFSE) / FL-3 (PI) dot plot (the population indicated in Figure 5.6B, by the red arrow). This FL1-positive population of eosinophils fell within the R1 gate (shown in Figures 5.6C and 4.5B), supposed only to include CFSE-positive IGROV1 tumour cells (as discussed in section 4.2.5), and so were isolated in a separate gate (shown in Figure 5.6A), and excluded from the plots used to calculate killing by cytotoxicity and phagocytosis (Figures 5.6C and D; Figure 4.5B). The calculation used to determine the percentage of IGROV1 cell death, which had occurred by cytotoxicity and phagocytosis, was then performed as normal (as described in sections 2.3.2 and 4.2.5), using a theoretical effector to target ratio of 1:1. However, as approximately 40 % of the eosinophils effectors were dead, this equates to a functional effector to target ratio of only ~ 0.6:1.

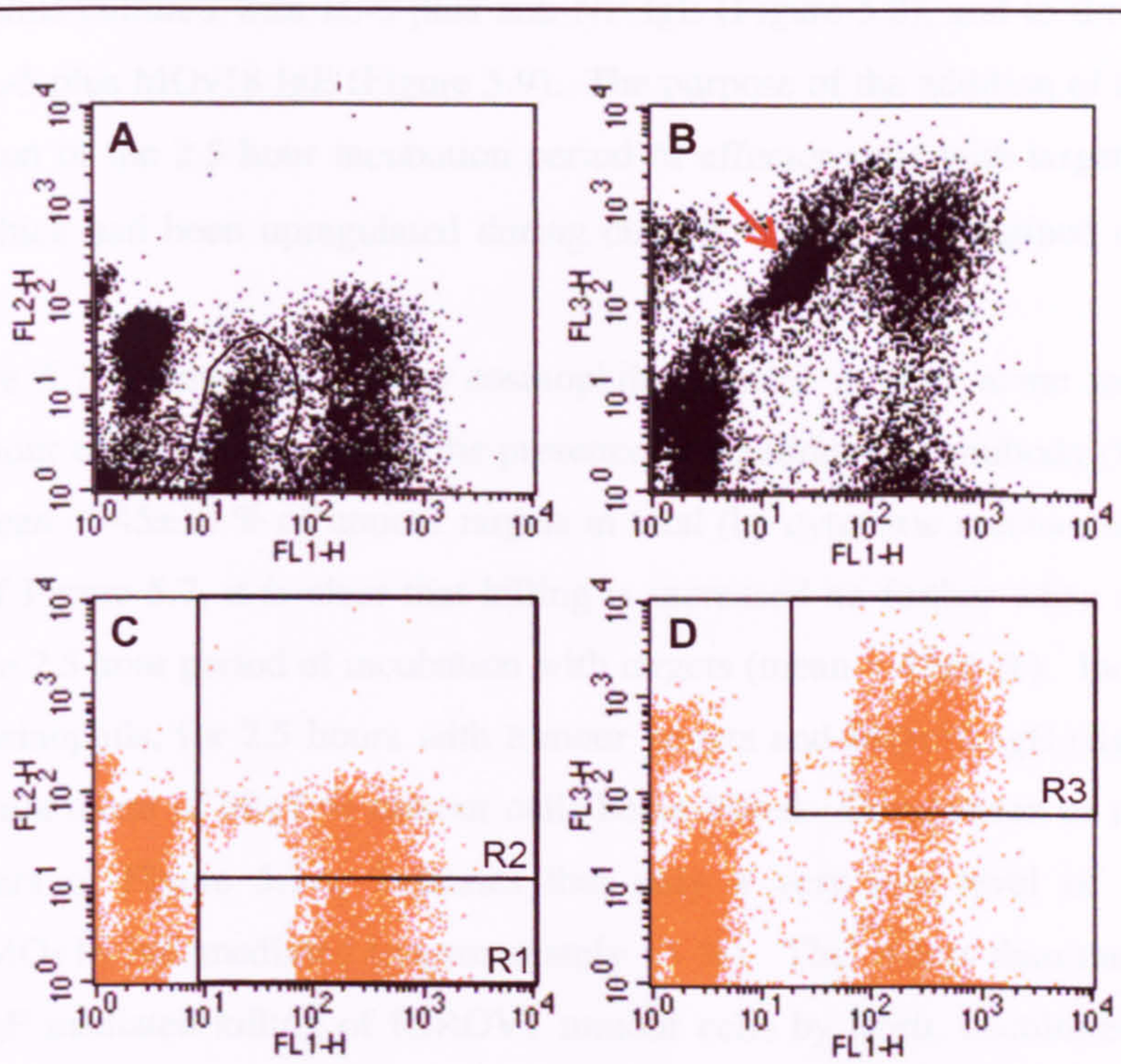

Figure 5.6: Dot plots showing how a population of dead, cultured eosinophils, were removed from the 'R1' gate, shown on plot (C) which is used to determine the number of IGROV1 cells remaining in the sample after incubation with effector cells and antibody has occurred. (A) FL1/FL2 dot plot showing the (gated) highly autofluorescent population of dead eosinophils between CD49d-PE$^+$ (FL2) viable eosinophils on the left, and CFSE$^+$ IGROV1 cells on the right. The same population is confirmed to be dead by its uptake of PI, shown in (B) on an FL1/FL3 dot plot, as the population indicated with the red arrow. Events falling within the gate made on the FL1/FL2 dot plot shown in (A), were excluded from the two dot plots (shown in this figure as C and D) which are used to normally calculate killing by cytotoxicity (events within R3 on plot D) and phagocytosis (events within R2 of plot C).

As discussed above, eosinophils were cultured for four days in culture media supplemented with either (A) IL-5, (B) IL-5 plus anti-NP IgE, or, (C) IL-5 plus MOv18 IgE, and then used as effector cells in ADCCP assays. For the ADCCP assay, eosinophils from each culture condition were mixed with IGROV1 target cells (at an effector to target ratio of '1:1', for 2.5 hours), either in the presence of no additional antibody, 2 μg of anti-NP IgE or 2 μg of MOv18 IgE. Therefore, eosinophils cultured in IL-5 for four days, were then mixed with IGROV1 tumour cells at a 1:1 ratio, and either no antibody (Figure 5.7; left bar), or, 2 μg of anti-NP IgE (Figure 5.7; middle bar), or, 2 μg of MOv18 IgE (Figure 5.7; right bar), for the

2.5 hour duration of the culture period with effector cells. The same method was applied to those eosinophils cultured with IL-5 plus anti-NP IgE (Figure 5.8), and to those eosinophils cultured in IL-5 plus MOv18 IgE (Figure 5.9). The purpose of the addition of fresh antibody, for the duration of the 2.5 hour incubation period of effector cells with targets, was to load any FcεRI which had been upregulated during culture, but which remained unoccupied by IgE.

Figure 5.7 (below) shows that eosinophils cultured in IL-5 alone and mixed with IGROV1 tumour cells for 2.5 hours in the presence of no additional antibody (Figure 5.7; left bar), kill a mean of 45±10 % of tumour targets in total (by cytotoxic mechanisms). From the middle bar of Figure 5.7, it is clear that killing is increased no further when anti-NP IgE is present for the 2.5 hour period of incubation with targets (mean = 45±6 %). Incubation of IL-5-cultured eosinophils, for 2.5 hours with tumour targets and MOv18 IgE (right bar; Figure 5.7), results in a mean of 58±7 % tumour cells being killed. Comparison of the middle and right-hand bars of Figure 5.7A, indicates that only a very low level of this killing is specifically MOv18 IgE-mediated (approximately 13 %). This is less than the specific level of MOv18 IgE-mediated killing of IGROV1 tumour cells by fresh, uncultured, eosinophils, shown in Figure 5.2.

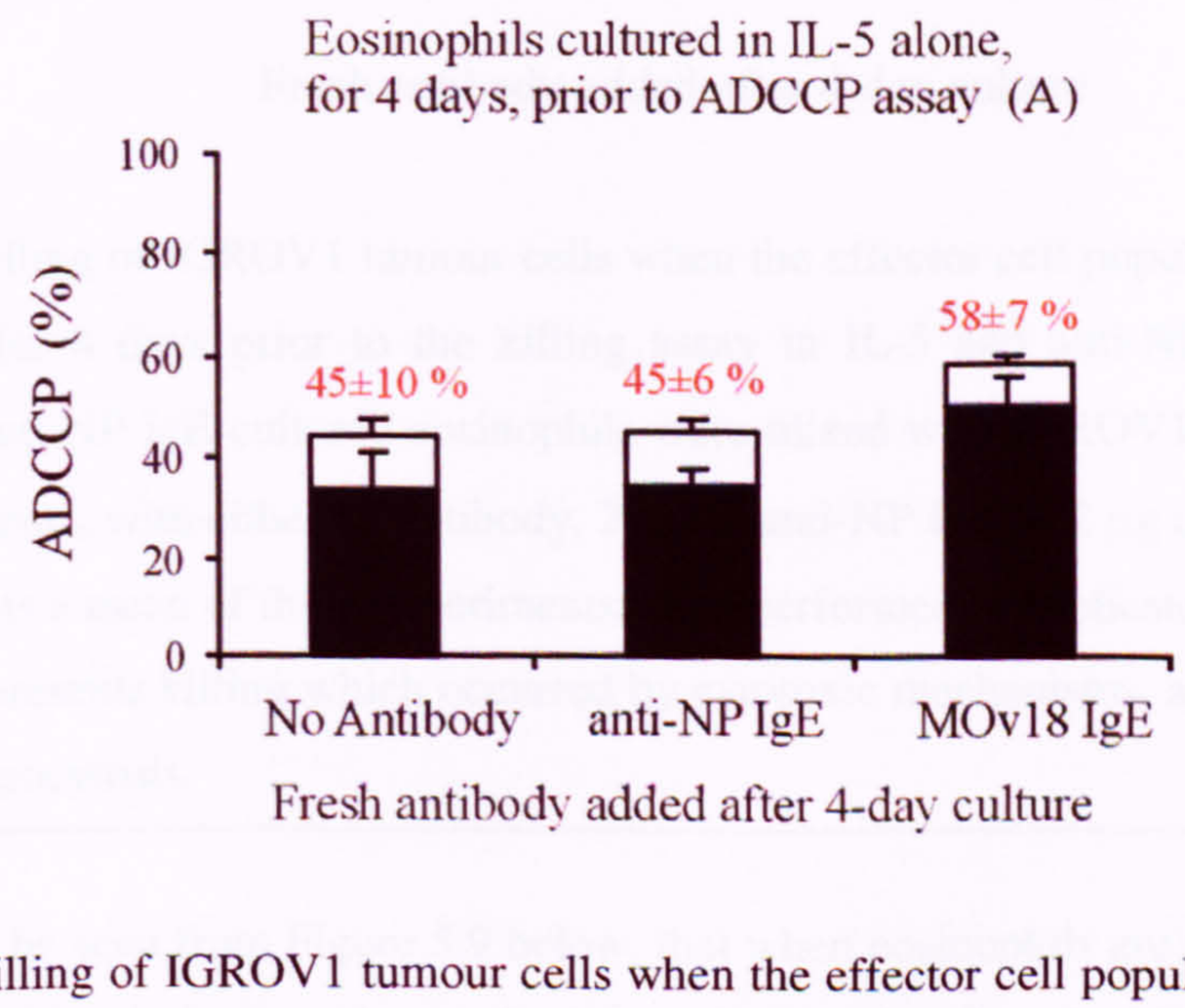

Figure 5.7: Killing of IGROV1 tumour cells when the effector cell population of eosinophils was cultured for 4 days prior to the killing assay in IL-5-supplemented media. IL-5 cultured eosinophils were mixed with IGROV1 target cells at a 1:1 ratio, for 2.5 hours, with either no antibody, 2 μg of anti-NP IgE or 2 μg of MOv18 IgE. This graph represents a mean of three experiments, each performed in triplicate. The black portion of each bar represents killing which occurred by cytotoxic mechanisms, and the white portion of the bar, phagocytosis.

Figure 5.8 below shows that eosinophils cultured in IL-5 + anti-NP IgE and mixed with IGROV1 tumour cells for 2.5 hours in the presence of no additional antibody kill a mean of 61±24 % of tumour cells (Figure 5.8; left bar). Killing remains within error of this, when additional anti-NP IgE (Figure 5.8; middle bar) or MOv18 IgE (Figure 5.8; right bar) is added for the 2.5 hour incubation period of the assay (61±27 and 70±20 % respectively). This non-specific killing by IL-5 + anti-NP IgE cultured eosinophils of IGROV1 tumour targets (Figure 5.8; left bar) is greater than specific killing mediated by either fresh eosinophils and MOv18 IgE (Figure 5.2) or IL-5-cultured eosinophils and MOv18 IgE (Figure 5.7).

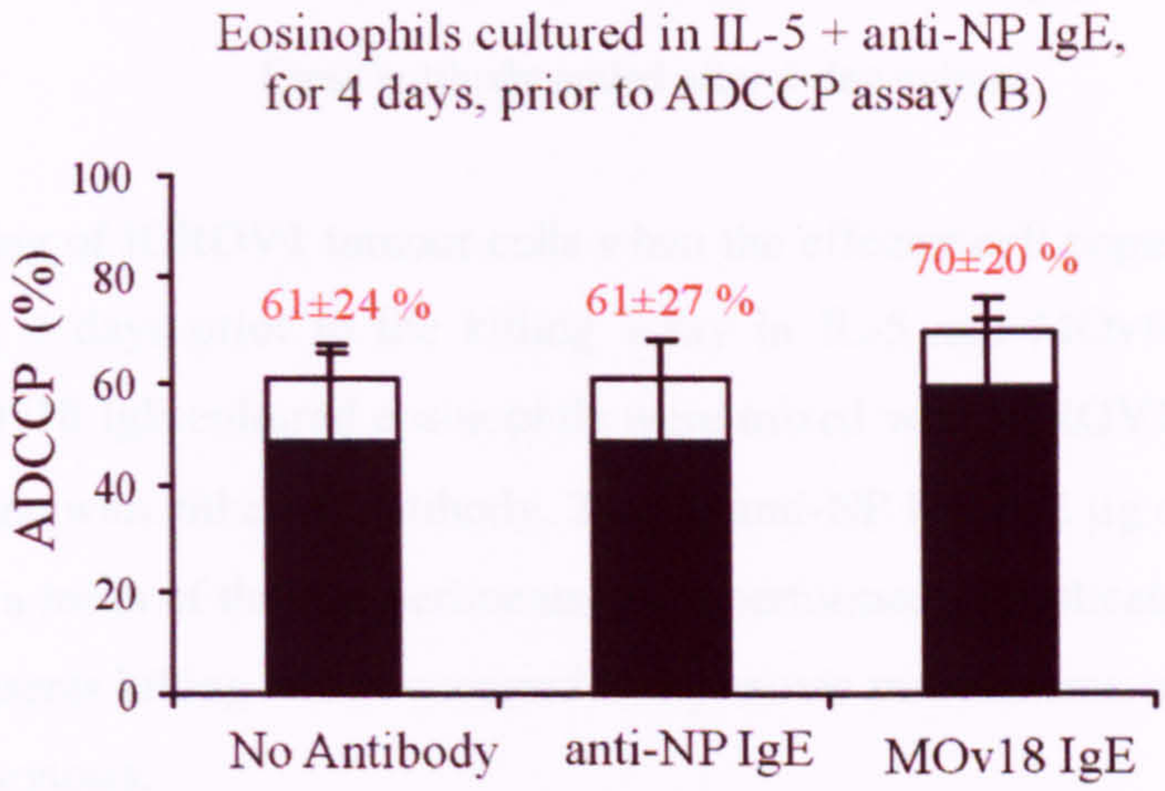

Figure 5.8: Killing of IGROV1 tumour cells when the effector cell population of eosinophils was cultured for 4 days prior to the killing assay in IL-5 and anti-NP IgE-supplemented media. IL-5/anti-NP IgE-cultured eosinophils were mixed with IGROV1 target cells at a 1:1 ratio, for 2.5 hours, with either no antibody, 2 μg of anti-NP IgE or 2 μg of MOv18 IgE. This graph represents a mean of three experiments, each performed in triplicate. The black portion of each bar represents killing which occurred by cytotoxic mechanisms, and the white portion of the bar, phagocytosis.

It can be seen from Figure 5.9 below, that when eosinophils are cultured with IL-5 + MOv18 IgE, killing is increased even further over those incubated with IL-5 + anti-NP IgE (Figure 5.8); in the absence of additional antibody, killing by IL-5 + MOv18 IgE-cultured eosinophils is 74±38 % (Figure 5.9; left bar). This is within error of the IGROV1 tumour-killing mediated by eosinophils cultured in IL-5 + MOv18 IgE and then incubated for the duration of the assay with 2 μg of anti-NP IgE (Figure 5.9; middle bar) or MOv18 IgE (Figure 5.9; right bar), which kill 74±39 and 78±31 % respectively.

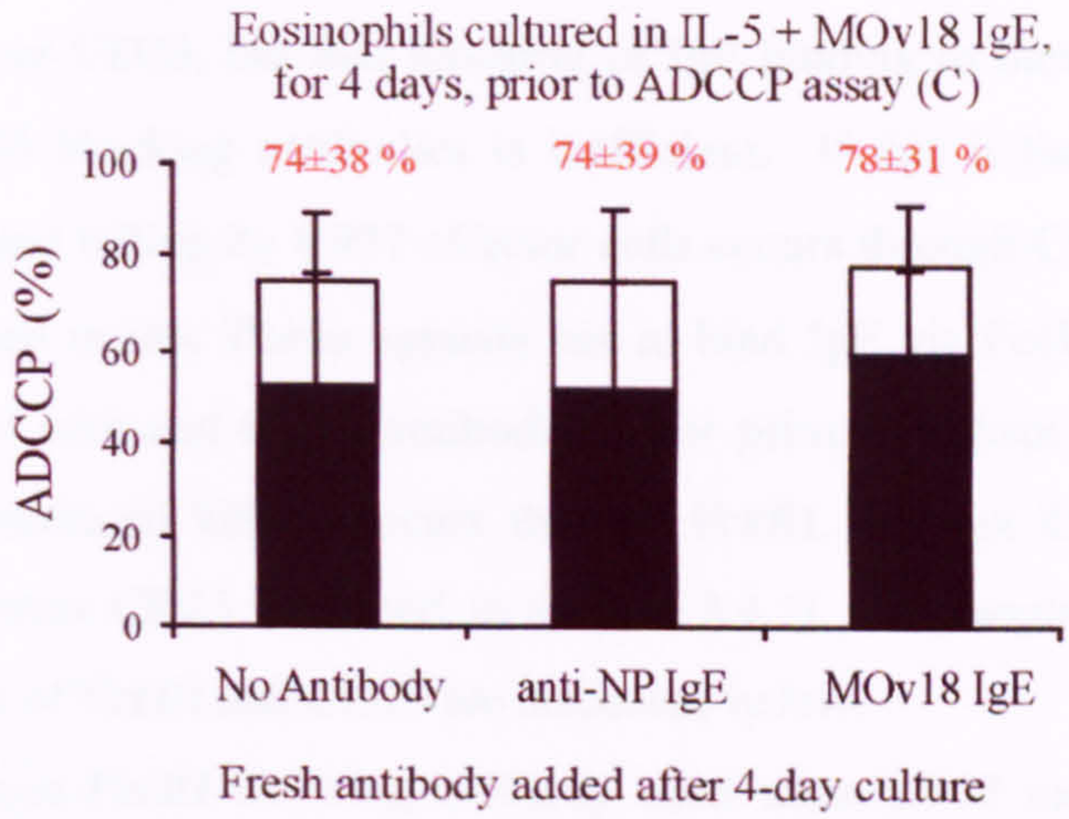

Figure 5.9: Killing of IGROV1 tumour cells when the effector cell population of eosinophils was cultured for 4 days prior to the killing assay in IL-5 and MOv18 IgE-supplemented media. IL-5/MOv18 IgE-cultured eosinophils were mixed with IGROV1 target cells at a 1:1 ratio, for 2.5 hours, with either no antibody, 2 μg of anti-NP IgE or 2 μg of MOv18 IgE. This graph represents a mean of three experiments, each performed in triplicate. The black portion of each bar represents killing which occurred by cytotoxic mechanisms, and the white portion of the bar, phagocytosis.

5.5 Discussion

Results in this Chapter demonstrate that U937 monocytes, primary monocytes and primary eosinophils are effective at killing IGROV1-tumour cells by ADCC when the tumour-specific antibody is of the IgE isotype (MOv18 IgE). These results show that IgE can effectively mediate tumour cell death *in vitro* when the effector cells are IgE receptor-expressing effector cells (demonstrated in Chapter 3). In contrast, at an effector to target ratio of 1:1, neither U937 monocytes, primary monocytes nor primary eosinophils were able to perform MOv18 IgG1-mediated killing of tumour cells, at the antibody concentrations and time periods of effector and target cell incubation with MOv18 IgG1, which were tested. Also shown in this Chapter is the effect of culturing eosinophils in IL-5 and IgE; the result was a high level of non-specific IGROV1 tumour cell killing that occurred independently of MOv18 IgE.

In section 5.2, the attempts that were made to block MOv18 IgE-mediated tumour cell killing by U937 monocytes and primary eosinophils are described. Pre-treatment of effector cells (U937 monocytes or eosinophils) with a selection of different antibodies to block IgE binding to either FcεRI or CD23 failed to prevent subsequent MOv18 IgE-mediated

tumour cell killing. It is possible that MOv18 IgE-dependent killing can be mediated through either FcεRI and / or CD23, but that blocking of IgE binding to these receptors using anti-FcεRI or anti-CD23 blocking antibodies is inefficient. If this is the case, it is likely that MOv18 IgE-mediated killing by U937 effector cells occurs through CD23, and not FcεRI, as the U937 clone used in this Thesis appears not to bind IgE via FcεRI; IgE binding can be completely blocked with anti-CD23 antibodies. For primary human monocytes, it is likely that MOv18 IgE-mediated killing occurs through FcεRI, and not CD23, as this cell type appears not to express CD23 (reported in section 3.4.1). Explanations for the potentially inefficient blocking of FcεRI and CD23 are discussed below.

The only anti-FcεRI blocking antibody used when U937 monocytes were effector cells, was 15-1. Regardless of whether or not 15-1 efficiently prevented IgE binding, the fact that it non-specifically activated effector cells (with the effect of mediating high levels of cytotoxicity towards tumour cells) means that a role for this receptor in MOv18 IgE-dependent tumour cell killing (with monocyte or eosinophil effectors), cannot be excluded. In fact, no conclusions can be drawn about the role of this receptor in U937/MOv18 IgE-mediated killing of IGROV1 tumour cells, except that 15-1 is able to induce the U937 cells to kill tumour cells. This MOv18 IgE-independent killing by 15-1 might be mediated by 'bystander killing', resulting from the cross-linking of FcεRI by the bivalent antibody, activating the U937s to release mediators cytotoxic to IGROV1 cells. Indeed the 15-1 antibody has been shown previously to activate primary human basophils to release histamine (Riske *et al.*, 1991), and activate human monocytes to mediate sustained cytosolic calcium increases (Maurer *et al.*, 1994). Use of monovalent Fab fragments of 15-1 in the future may therefore provide effective blocking in the absence of non-specific cellular activation. 15-1 did not, however, activate eosinophils to kill tumour cells non-specifically; it is possible that the very low number of FcεRI expressed on the eosinophil cell surface prevented a similar cross-linking of FcεRI, by bivalent 15-1.

The other FcεRI-blocking antibody tested, 15A5, also failed to block MOv18 IgE-mediated killing of tumour cells, when eosinophils were the effectors. The 15A5 antibody also did not activate the eosinophils to kill tumour cells in a MOv18-IgE-independent fashion. It is possible that MOv18 IgE-mediated killing by eosinophil effectors is very sensitive, and that only a few IgE receptors are required to be occupied by MOv18 IgE for killing to occur. Therefore, if a small number of IgE receptors are able to escape blocking, and MOv18 IgE is able to bind, the cross-linking of these few receptors by a FBP-expressing tumour target may be sufficient to mediate tumour cell killing. This high level of sensitivity may also explain the inability of anti-NP IgE to effectively out-compete MOv18 IgE, and completely block

IGROV1 tumour cell killing by U937 monocytes. As an alternative to blocking FcεRI with Fab fragments of anti-FcεRI blocking antibodies, blocking of FcεRI-mediated effector cell activation may be a better approach. This might be performed with the anti-FcεRIα-chain antibody, 5H5F8, which does not block IgE binding to FcεRIα, but instead prevents downstream signalling (Nechansky *et al.*, 2001).

Similar explanations may be applied to the failure of anti-CD23 antibodies to block any MOv18 IgE-mediated killing, which might be triggered through this receptor. Like 15-1, regardless of whether or not BU38 effectively blocked IgE binding to CD23, no conclusions can be drawn as to the role of CD23 in killing from these experiments as BU38 treatment of U937 monocytes activated them to kill IGROV1 cells in a MOv18 IgE-independent manner. As with 15-1, this is likely to be a result of CD23 cross-linking by bivalent BU38 antibody. Similarly, use of BU38 monovalent Fab fragments may be effective in blocking IgE binding and thus any CD23-mediated killing. The inability of IDEC-152 to block killing may be explained by this antibody having a lower affinity for CD23 than IgE; the affinity of IDEC-152 for CD23 is not known. It might therefore be displaced by MOv18 IgE during the ADCCP assay, allowing killing to occur as normal. The relatively low affinity of IgE for CD23 (compared to FcεRI) may also allow for displacement of anti-NP IgE with MOv18 IgE, preventing killing being effectively blocked in this way.

Finally, it may be that MOv18 IgE-mediated killing is mediated through neither FcεRI nor CD23. This would explain the inability of either anti-NP IgE, anti-FcεRI or anti-CD23 antibodies, used separately or together, to block subsequent MOv18 IgE-mediated killing; the attempted blocking of U937-mediated tumour cell killing using anti-FcεRI and anti-CD23 blocking antibodies simultaneously, has been performed by Dr. S. Karagiannis (results not shown). It is unlikely that MOv18 IgE-dependent killing is acting non-specifically, firstly, as cell-mediated killing of (FBP-expressing) IGROV1 tumour cells cannot be mediated in either the presence of anti-NP IgE nor MOv18 IgG1, suggesting that both FBP and IgE-receptor specificities are required. That MOv18 IgE is indeed binding FBP on IGROV1 cells, and not non-specifically to another antigen, is unlikely due to two reasons. Firstly, anti-NP IgE does not bind to IGROV1 cells (shown in Figure 3.1B). Secondly, MOv18 IgE binds to FBP-transfected C26 or CC531 tumour cells, but not to their wild type counterparts (Figure 3.2). That MOv18 IgE is indeed binding to IgE receptors on effector cells, is demonstrated by the ability to block its binding with anti-IgE receptor antibodies; anti-CD23 blocks MOv18 IgE and anti-NP IgE binding to U937 cells and anti-FcεRI blocks MOv18 IgE and anti-NP IgE binding to primary eosinophils. The interesting possibility therefore remains, that a third IgE receptor may be involved in mediating MOv18 IgE-

dependent tumour cell killing; the most likely candidate for this role is epsilon binding protein (introduced in section 1.3.8).

Results described in this chapter show MOv18 IgE-mediated tumour cell killing by both primary and U937 monocytes to be mediated by cytotoxic and not phagocytic mechanisms. This is in contrast to previous immunofluorescent imaging of IGROV1 tumour cell killing reported in Karagiannis *et al.*, 2003, which showed monocytes to be phagocytosing tumour cells in a MOv18 IgE-dependent manner. However, experiments described in both these studies (Karagiannis *et al.*, 2003; this Thesis), were performed under quite different conditions. Experiments described in Karagiannis *et al.*, 2003, were performed in chamber slides, to which the monocytes adhere; experiments described in this Thesis, were performed in FACS tubes, to which the cells do not adhere; adherance of monocytes to a plastic substrate has been shown to impact positively on their activation state (Maurer *et al.*, 1994). In addition, a different effector to target ratio was used in each study, 50:1 (Karagiannis *et al.*, 2003) compared to 1:1 (this study), as was a different time period for which effector and target cells were incubated together with antibody (90 minutes compared to 2.5 hours, respectively). Furthermore, the monocytes seen to phagocytose tumour cells in the study by Karagiannis *et al.*, 2003, were doing so as part of a mixed effector cell population (PBMC), whereas monocytes used for experiments described in this Thesis, were 70 to 80 % pure.

The earlier time point at which monocytes were detected phagocytosing tumour cells as described in Karagiannis *et al.*, 2003, might be explained by the fact that in these studies, monocytes composed a smaller proportion of the total cell population, which were whole PBMC. Therefore, it may be that a different cell type which is present in PBMC, but less prevalent in the 70 – 80 % pure population of monocytes used in experiments described in this Thesis, is in fact mediating tumour cell death, with monocytes merely acting to clear the tumour cell debris by phagocytosis. One potential candidate for this role are basophils, which were frequently observed in contact with tumour cells in the presence of MOv18 IgE, but not control antibody, anti-NP IgE, in the immunofluorescent imaging described in Karagiannis *et al.*, 2003.

In this Thesis, the 'cytotoxic' mechanism by which monocytes mediate MOv18 IgE-dependent tumour cell death, may be through the secretion of the pro-inflammatory cytokine TNF-α, which is secreted upon FcεRI cross-linking (Kraft *et al.*, 2002). As suggested by its name 'tumour necrosis factor', this cytokine has well characterised anti-tumour activity. Also secreted upon cross-linking of FcεRI on monocytes, are MCP-1, MIP-1β and IL-6 (Kraft *et al.*, 2002; von Bubnoff *et al.*, 2002) in addition to the immunomodulatory cytokine, IL-10

(Novak *et al.*, 2001). Cross-linking of CD23 expressed by U937 monocytes may lead to tumour cell killing through the secretion of IL-6, TNF-α and or IL-1β (Ouaaz *et al.*, 1993), as occurs following cross-linking of CD23 on primary monocytes (Paul-Eugene *et al.*, 1992; Borish *et al.*, 1991). The IgE-dependent cytotoxic mechanisms by which eosinophils might be activated to kill tumour cells include the release of granule proteins and eosinophil peroxidase (Gounni *et al.*, 1994). It would be interesting to assay for the presence of any of these soluble mediators of tumour cell killing in the culture media in which the killing assay was performed.

Human eosinophils cultured for 4 days in IL-5-supplemented media, were shown to mediate high levels of MOv18 IgE-independent tumour cell killing. The original purpose of including IL-5 in the eosinophil culture media was to allow these cells to survive *in vitro*, so that the effect of their culture in anti-NP IgE or MOv18 IgE on their ability to perform MOv18 IgE-dependent ADCC of tumour cells could be assessed. The reason for including IgE in the culture media was in response to the reported demonstration of the ability of IgE culture of eosinophils to increase their level of (IgE-loaded) FcεRI at the cell surface (Kayaba *et al.*, 2001). However, what were 'control' eosinophils cultured in IL-5 alone were significantly more cytotoxic to tumour cells than fresh, uncultured eosinophils, regardless of the presence of IgE in the culture media.

The enhancement of human eosinophil viability during *in vitro* culture, using IL-5, is well recognised; in the absence of IL-5 less than 10 % of eosinophils typically survive 3 days, and none survive 4 days of culture in enriched medium (Lopez *et al.*, 1988; Rothenberg *et al.*, 1989). IL-5 culture of eosinophils is also associated with a change in eosinophil density. Eosinophils freshly purified from 'normal' (not hypereosinophilic or allergic) donors have a 'normodense' phenotype, but after 3 days of culture in IL-5-supplemented media they become 'hypodense', similar to eosinophils freshly purified from hypereosinophilic donors. Eosinophils with the hypodense phenotype in patients with hypereosinophilia associated with chronic helminthic infection, have been shown to be 'functionally enhanced', with enhanced effector function in ADCC (Rothenberg *et al.*, 1989; Rivoltini *et al.*, 1993). This reduction in eosinophil density (normodense to hypodense) may also be associated with an increase in concentration of cytotoxic eosinophil-derived products in the cell culture media (Rothenberg *et al.*, 1989); it is possible that such increased toxicity of the culture media accounts for the high levels of antibody-independent tumour cell killing seen in experiments described in this chapter.

The ability of eosinophils to act as effector cells in IgG-mediated ADCC of either parasite (Khalife *et al.*, 1989) or tumour cell (Rivoltini *et al.*, 1993) targets *in vitro*, is

dependent on their activation status; eosinophils purified from normal donors (normodense), are ineffective, and those purified from hypereosinophilic donors (hypodense), are effective. Therefore, the lack of MOv18 IgG1-mediated killing of IGROV1 tumour cell targets by freshly purified human eosinophils from normal donors reported in this chapter, is in accordance with these previous studies. In view of the fact that eosinophils primarily express only FcγRII of the three FcγR (Seminario *et al.*, 1999) and that this receptor could be of either the inhibitory or stimulatory isotype, these results may not be surprising. Interestingly, eosinophils from cancer patients receiving IL-2 therapy acquire the hypodense phenotype and accordingly, are able to act as effectors of IgG-mediated cytotoxicity against tumour cells *in vitro*, in contrast to the normodense eosinophils purified from the same patients before treatment (Rivoltini *et al.*, 1993). This acquired, IgG-mediated, cytotoxicity was comparable to that mediated *in vitro* with IL-5 cultured eosinophils (Rivoltini *et al.*, 1993).

In Chapter 3, Fcγ-receptors expressed by U937 monocytes were shown to include FcγRI, and of FcγRII, the non-inhibitory FcγRIIa isoform (Cameron *et al.*, 2002). Primary monocytes express FcγRI, FcγRII (both inhibitory and stimulatory isoforms) and FcγRIII (Ravetch and Kinet, 1991; Woof *et al.*, 2004). Cross-linking of stimulatory IgG Fc receptors, including FcγRI, FcγRIIa and FcγRIIIa, is associated with the phagocytosis, cytotoxicity and release of inflammatory mediators by expressing cell types (see Table 1.1). In contrast, cross-linking of FcγRIIb is associated with inhibitory signals (Ravetch and Kinet, 1991). Co-aggregation of the inhibitory FcγRIIb with a stimulatory Fc receptor (including FcγR, FcαR, FcεR and also the TCR and BCR) is also associated with the suppression of signalling initiated by these receptors (Ravetch and Kinet, 1991).

Primary (and U937) monocytes were unable to act as effectors of MOv18 IgG1-dependent tumour cell killing under the conditions tested. Previously, primary monocytes freshly purified from normal donors have proved to be effective in IgG1-dependent tumour cell killing (Steplewski *et al.*, 1988). However, this cytotoxicity required long time periods of effector and target cell incubation together with tumour specific IgG and high effector to target ratios. Experiments described in Steplewski *et al.*, 1988, using an [^{111}In]indium oxine-release assay, show a ratio of 10 monocyte effectors to 1 tumour cell target incubated with tumour-specific chimaeric IgG1 to mediate ~ 13 % tumour cell lysis after 18 h, and ~ 30 % lysis after 18 h when the E:T ratio was increased to 50:1. It may be that MOv18 IgG1-dependent cytotoxicity by primary monocytes in this work could be mediated if these longer timepoints were used alongside a higher ratio of effector to target cells. The longest timepoint

tested in work described in this chapter was 8 hours, and the only effector to target ratio tried was 1:1; there was insufficient time to perform additional experiments.

It must also be noted that there have been studies performed in which IgG-dependent killing of tumour cells by primary monocytes was poor, even using high effector to target ratios and long timepoints. It has been found that treatment of primary monocytes with cytokines including M-CSF, GM-CSF or IFN-γ, known to stimulate the maturation of monocytes into a more macrophage-like phenotype, increases their capacity to act as effectors of IgG-dependent tumour-cell killing (Munn and Cheung, 1989; Keler *et al.*, 2000). M-CSF-cultured monocytes have been shown to mediate FcγRII and FcγRIII-dependent phagocytosis of tumour cells, and IFN-γ-cultured monocytes to be efficient mediators of FcγRI-dependent ADCC (Van Schie *et al.*, 1992; Munn and Armstrong, 1993). Indeed, the (significant, but low levels of) tumour-cell killing by unstimulated monocytes shown in Steplewski *et al.*, 1988 was increased significantly by pre-treatment of the monocytes for 2 days prior to the assay in IFN-γ-supplemented-media. Dr. S. Karagiannis is currently performing experiments to assess the ability of IL-4-stimulated monocytes to act as MOv18 IgE-dependent effectors of tumour cell killing, as IL-4 is known to upregulate the expression of CD23 by primary monocytes.

It is also interesting to note that MOv18 IgG1-dependent killing of IGROV1 cells by a mixed effector population, PBMC, determined using a chromium-release assay in experiments described in Gould *et al.*, 1999, required an effector to target ratio of 50:1, and an incubation period of effector and target cells together with MOv18 IgG1, of at least 5 hours. Experiments using an LDH-release assay to assess MOv18 IgG1-dependent killing of IGROV1 cells by PBMC, described in Karagiannis *et al.*, 2003, required an effector to target ratio of 50 – 100:1, and an incubation period of effector and target cells together with MOv18 IgG1 of 20 hours. Although it is not known which cell type(s) amongst this mixed effector cell population were mediating MOv18 IgG1-dependent killing of IGROV1 cells, these results support the idea that IgG1-dependent tumour cell killing requires a higher effector to target ratio, and incubation period of cells with MOv18 IgG1, than those tested in experiments described in this chapter.

In summary, whether or not conditions can be optimised such that U937 monocytes, primary monocytes or primary eosinophils could act as MOv18 IgG1-dependent effectors of IGROV1 tumour cell killing, the relative simplicity with which monocytes and eosinophils can be triggered to act as MOv18 IgE-dependent effectors of tumour cell killing gives support to the hypothesis that tumour-specific antibodies of the IgE isotype may be more effective than IgG1 in triggering an anti-tumour immune response.

CHAPTER 6:

In vivo models of MOv18 activity

6.1 Introduction

In this chapter I describe how the *in vivo* modelling of MOv18 activity is being pursued in the most physiologically relevant ways possible. This requires the dual modelling of both human cancer and a functional IgE-mediated immune response in one system. As discussed in section 1.3.2, mouse FcεRIα chain is unable to associate with γ_2-dimers in the absence of β-chain. This means that mice can only express tetrameric FcεRI, consequently limiting the expression of this receptor to mast cells and basophils. This is in contrast to the human FcεRI expression profile, which additionally includes expression of an FcεRI-$\alpha\gamma_2$ trimer on Langerhans cells, dendritic cells, monocytes, eosinophils and platelets. For tumour-bearing animals to be treated with chimaeric MOv18 IgE, tumours used in animal models are required to express human folate binding protein (FPB).

The two models previously described for this project have overcome these problems by creating 'human' mouse models of cancer (Gould *et al.*, 1999; Karagiannis *et al.*, 2003). Both models involve engraftment of immunocompromised mice with human tumour and treatment of these tumour-bearing mice with human immune cells and chimaeric-human MOv18 (see section 1.4.2). The first model (Gould *et al.*, 1999) involved growth of the human (FBP-expressing) ovarian cancer cell line, IGROV1 (introduced in sections 2.2.1 and 3.3.1), as a solid, subcutaneous tumour in SCID mice. Treatment was by intravenous injection of human PBMC effector cells and MOv18, and efficacy was determined by comparing the size of subcutaneous tumours in treated to untreated control mice at time-points after engraftment. The second model (Karagiannis *et al.*, 2003), involves transplant and growth of the human (FBP-expressing) ovarian tumour, HUA, in the peritoneal cavity of nude mice in the form of ascities. Therefore, the anatomical location of the HUA tumour in the nude mouse model mimics human ovarian cancer more closely than the SCID mouse model.

6.2 Nude mouse model

The nude mouse model mentioned above has been used in a series of experiments described below. In summary, four different human immune (effector) cell populations have been tested for their ability to mediate improved survival of HUA-tumour-bearing nude mice when given alone or in combination with MOv18 IgE. In addition, MOv18 IgE has been compared to MOv18 IgG1 where the effector cell population is human PBMC. MOv18 IgE has previously been compared to MOv18 IgG1 in the SCID mouse model, also mentioned above (Gould *et al.*, 1999). The result was a superior efficacy of MOv18 IgE, compared to MOv18 IgG1, in inhibiting tumour growth. This contrasted with *in vitro* results in Gould *et al.*, 1999, which showed MOv18 IgG1 to be more effective than MOv18 IgE in triggering

PBMC to kill IGROV1 tumour cell targets in a chromium-release assay. These results support the hypothesis that *in vitro* activity of tumour-specific IgE does not reflect its potential *in vivo*. The purpose of comparing MOv18 IgE to MOv18 IgG1 in the nude mouse model, was to see if this enhanced effect of MOv18 IgE over MOv18 IgG1 could be replicated in a disparate, and more physiological, *in vivo* system.

A standard protocol was used for survival experiments in nude mice, described in this chapter, whereby mice were transplanted with the human ovarian cancer, HUA, on day 1 and received treatments of human effector cells and antibodies on specific dates thereafter, as described in detail in section 2.3.3. In all experiments survival was measured in terms of the number of days between the transplant of the tumour and sacrifice of the mouse. Sacrifice was performed when the swelling of the peritoneal cavity, due to growth of the tumour, was such that the weight of the mouse was increased by approximately 10 % (Home Office limits).

In the first nude mouse experiment discussed below, each mouse was treated, on days 1, 7, 14 and 21, with either (A) PBS, (B) PBS containing 4 million human PBMC, (C) PBS containing 4 million human PBMC plus 100 μg MOv18 IgE or (D) PBS containing 4 million human PBMC plus 100 μg MOv18 IgG1. The first three of these treatment groups (A-C) have been compared before, in Karagiannis *et al.*, 2003, but those mice received only two treatment doses, on days 1 and 15, and this was sufficient to confer upon mice in the third treatment group (C), a significant survival advantage over the first two groups (A and B). In addition, results of experiments comparing MOv18 IgE to MOv18 IgG1 in the SCID mouse model described in Gould *et al.*, 1999, showed that only one dose of MOv18 IgE was needed for it to be more effective than MOv18 IgG1. This was proposed to be a reflection of the long IgE-FcεRI binding half-life. The purpose of the increased dosing in the first nude mouse experiment described in this chapter, was to ensure MOv18 IgG1 had the maximum chance of producing an effect equivalent to, or better than, MOv18 IgE.

As expected, control mice receiving tumour alone died within approximately 20 days. Mice receiving PBMC in conjunction with MOv18 IgE survived significantly longer than control mice receiving PBS alone ($P = 0.002$; $n = 9$), and closely approached statistical significance compared to mice receiving PBMC alone ($P = 0.056$; $n = 9$). Mice receiving PBMC alone (Figure 6.1) did not survive significantly longer than mice receiving PBS ($P = 0.067$; $n = 9$). Survival of mice receiving PBMC in conjunction with MOv18 IgG1 also did not survive significantly longer than either group of control mice ($P = 0.3$; $n = 8$ in both cases). These P-values are obtained using a two-tailed student's T-test. However, it is justifiable to use a one-tailed T-test based on the fact that treated mice are not expected to

survive a shorter period of time than control mice. In this case, the survival of mice receiving PBMC plus MOv18 IgE do survive statistically significantly longer than mice receiving PBMC alone, P = 0.028. In the similar experiment, shown as Figure 1A in Karagiannis *et al.*, 2003, and mentioned above, the mean survival of group A was 22±0.4, group B was 30±1.1 and group C, 40±3.4 days (these results represent the mean ± the standard error). In Figure 6.1, these equivalent three treatment groups showed no further improvement in survival as a result of the increased treatment doses, with mean survival times of 19±2, 26±11 and 40±17 respectively (these values represent the mean ± the standard deviation).

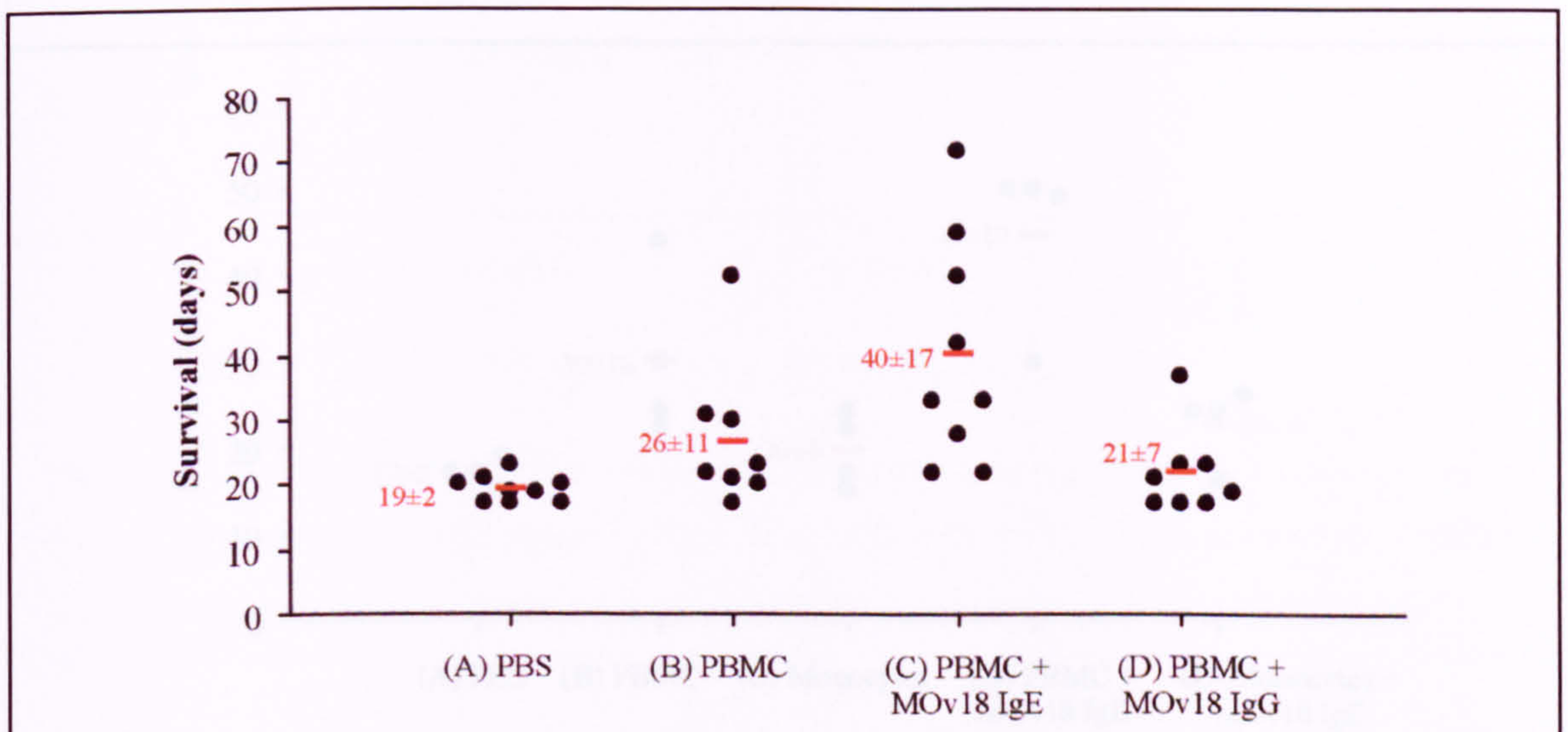

Figure 6.1: Survival of nude mice bearing HUA ovarian cancer xenografts and receiving on days 1, 7, 14 and 21 the following intra-peritoneal treatments: Group A = PBS alone, Group B = PBS containing 4 million PBMC, Group C = PBS containing 4 million PBMC plus 100 µg MOv18 IgE and Group D = PBS containing 4 million PBMC plus 100 µg MOv18 IgG1.

In Karagiannis *et al.*, 2003, it is described how immunohistochemistry was performed on the HUA tumour sections taken from mice that received treatments of PBS, PBMC or PBMC in combination with MOv18 IgE. The results showed large numbers of human $CD68^+$ monocytes / macrophages to be infiltrating the tumour islands in sections taken from mice that received MOv18 IgE with PBMC, in contrast to those that received PBMC alone. In addition to this, immunofluorescence visualisation of tumour cell killing by PBMC (also described in Karagiannis *et al.*, 2003) and *in vitro* cytotoxicity assay data, described in this Thesis (Figure 5.1B), suggested human $CD14^+$ monocytes could act as effector cells in this system. In response to this information, a population of monocyte-enriched human PBMC

(70 to 80 % pure) were tested for their ability to improve the survival of HUA-xenograft-bearing nude mice in conjunction with MOv18 IgE. Due to the fact that no survival advantage was conferred by increasing the number of treatment doses from two to four in Figure 6.1, mice in this experiment received only two treatment doses. Treatments included either (A) PBS alone, (B) PBS containing 4 million monocytes, or (C) PBS containing 4 million monocytes plus 100 µg MOv18 IgE, per mouse. As a positive control, one group of mice each received treatment of PBS containing 4 million PBMC in combination with MOv18 IgE, and one group each received PBS containing 4 million PBMC alone.

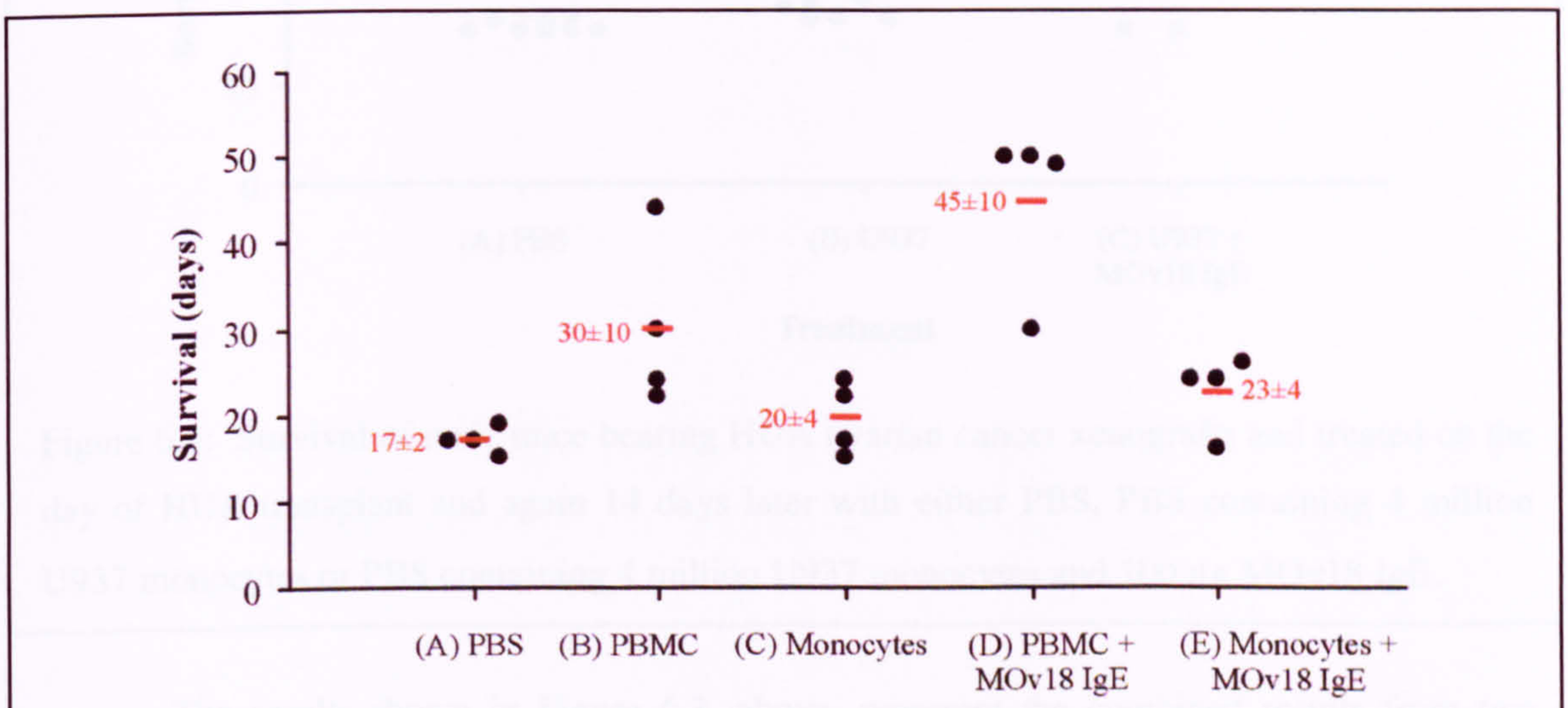

Figure 6.2: Survival of groups of nude mice bearing HUA ovarian cancer xenografts and receiving the following treatments on days 1 and 15: (A) PBS alone, (B) PBS containing 4 million PBMC, (C) PBS containing 4 million monocytes, (D) PBS containing 4 million PBMC plus 100 µg MOv18 IgE or (E) PBS containing 4 million monocytes plus 100 µg MOv18 IgE.

It can be seen from Figure 6.2, that mice receiving monocytes alone, or in combination with MOv18 IgE, failed to show a trend of increased survival over control groups. The positive control group of PBMC plus MOv18 IgE did show a trend towards increased survival, as observed in the previous experiment (see Figure 6.1). However, as only four mice per condition have been used in this experiment, survival differences are not statistically significant. To see if the U937 monocyte cell line could improve survival of these tumour-bearing mice, a similar experiment was set up. Tumour-bearing nude mice each received treatments on days 1 and 15 of either (A) PBS alone, (B) PBS containing 4 million

U937 monocytes or (C) PBS containing 4 million U937 monocytes in combination with 100 µg MOv18 IgE.

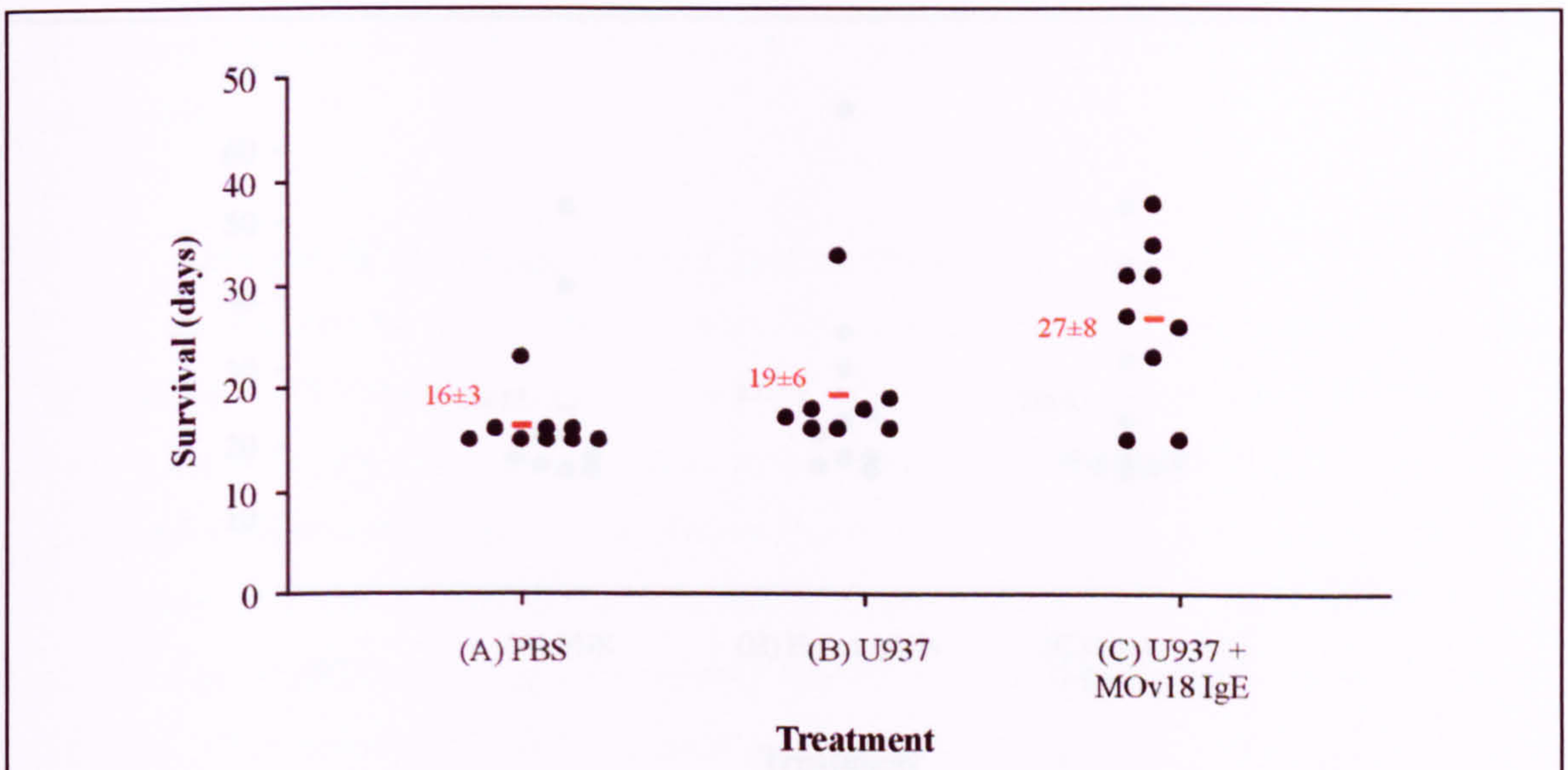

Figure 6.3: Survival of nude mice bearing HUA ovarian cancer xenografts and treated on the day of HUA transplant and again 14 days later with either PBS, PBS containing 4 million U937 monocytes or PBS containing 4 million U937 monocytes and 100 µg MOv18 IgE.

The results shown in Figure 6.3, above, represent the combined results from two identical experiments, one of which was performed by Dr. Sophia Karagiannis. It can be seen from Figure 6.3 that mice treated with U937 monocytes, in combination with MOv18 IgE, survive for 27±8 days; this is statistically significantly longer than the survival of mice receiving treatments of either U937 monocytes alone (19±6 days; $P = 0.042$, $n = 8$) or PBS alone (16±3 days; $P = 0.002$, $n = 9$). As expected, mice receiving treatment with U937 cells alone did not survive significantly longer than mice receiving PBS treatment ($P = 0.19$, $n = 9$).

Due to the efficacy of eosinophils in killing tumour cells *in vitro* (shown in the previous Chapter), and their documented anti-tumour activity *in vivo* (Tepper *et al.*, 1992), the capacity of a purified population of eosinophils to enhance the survival of HUA-tumour-bearing nude mice in combination with MOv18 IgE was tested. Tumour-bearing nude mice were treated on day 1 each with (A) PBS, (B) PBS containing 3.6 million eosinophils or (C) PBS containing 3.6 million eosinophils plus 100 µg MOv18 IgE. On day 15 these treatments were repeated, but when eosinophils were included, they were reduced to 2.36 million per mouse (due to a lower eosinophil yield per ml of blood from the same donor). It can be seen from Figure 6.4 that eosinophils either alone or in combination with MOv18 IgE, conferred

no survival advantage upon HUA-tumour-bearing nude mice, with negligible differences between the mean survival values of all three groups.

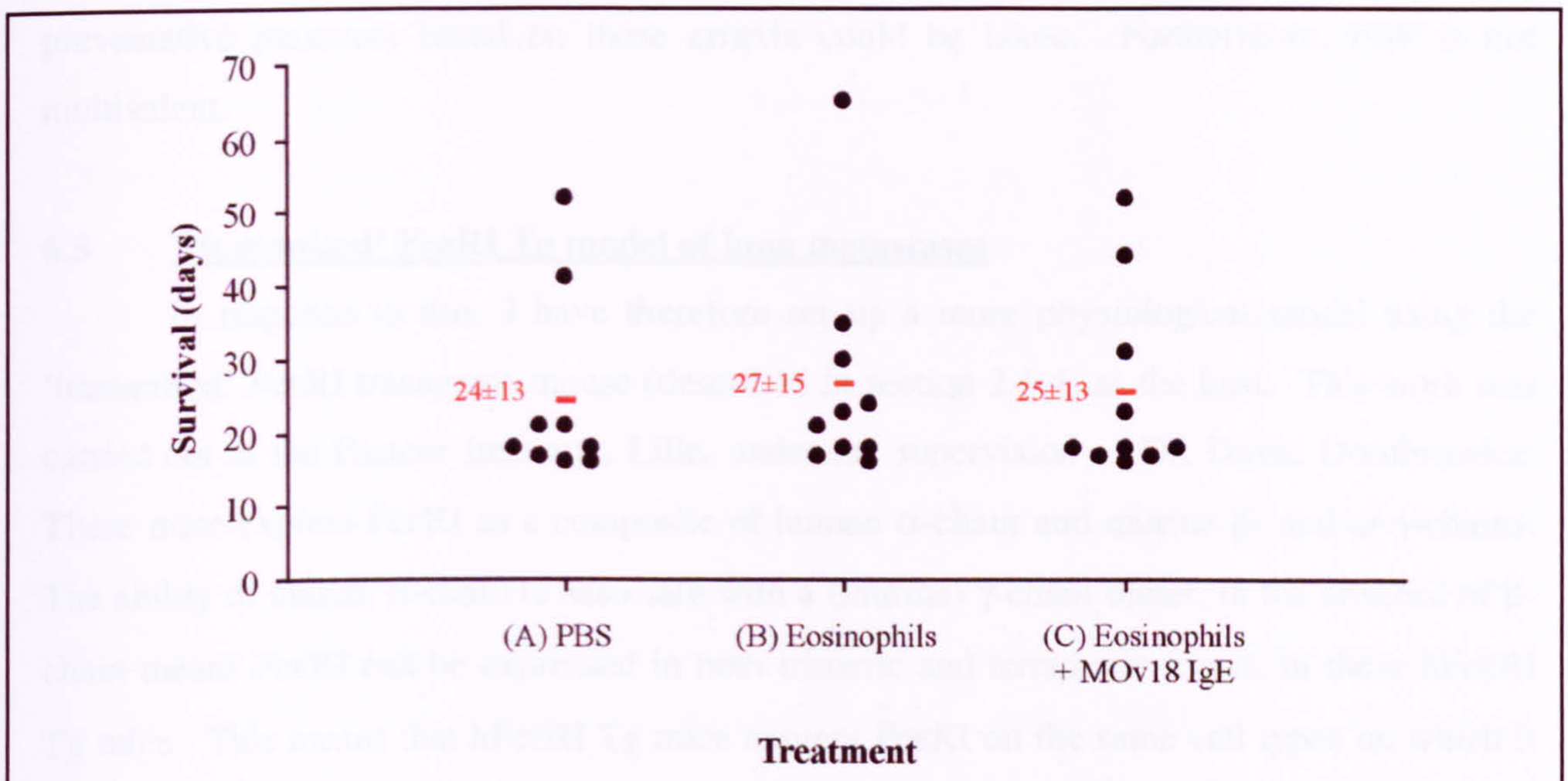

Figure 6.4: Survival of nude mice bearing HUA ovarian cancer xenografts and treated on the day of HUA transplant with either (A) PBS, (B) PBS containing 3.6 million eosinphils or (C) PBS containing 3.6 million eosinophils and 100 µg MOv18 IgE. On day 15, each mouse received a second treatment dose, but where eosinophils were included, they were reduced to 2.36 million per mouse.

The disadvantage of the nude and SCID mouse xenograft models is that treatment relies on the persistence of human effector cells in mice, while in humans the supply of effector cells would be constant, and so treatment with MOv18 IgE is likely to be more effective. Furthermore, these models rely on the activity of a restricted population of IgE receptor-expressing cells that are responsible for only a minor component of the allergic immune response, which in effect, is the immune response we are trying to target to the tumour cells. The absence of the additional IgE receptor-expressing effector cells in these immunodeficient models is likely to result in an underestimation of the beneficial effects conferred by treatment with MOv18 IgE. However, use of an animal model which underestimates the efficacy of MOv18 IgE treatment for cancer, may also not give a reliable indication of whether or not treatment with MOv18 IgE will trigger systemic anaphylaxis. This highlights the need for an immunocompetent host, including functional mast cells and basophils, to model anti-tumour activity of MOv18 IgE. Anaphylaxis resulting from MOv18 IgE treatment would require the secretion of large amounts of multivalent IgE-specific tumour

antigen into the circulation, and a serum IgE concentration above ~10^7 M^{-1}, the threshold required to induce FcεRI expression on circulating IgE effector cells (Gould *et al.*, 1999). Therefore as a treatment for patients, in the unlikely event of anaphylaxis occurring, preventative measures based on these criteria could be taken. Furthermore, FBP is not multivalent.

6.3 'Humanised' FcεRI Tg model of lung metastases

In response to this, I have therefore set up a more physiological model using the 'humanised' FcεRI transgenic mouse (described in section 2.1.4) as the host. This work was carried out at the Pasteur Insititute, Lille, under the supervision of Dr. David Dombrowicz. These mice express FcεRI as a composite of human α-chain and murine β- and or γ-chains. The ability of human α-chain to associate with a (murine) γ-chain dimer, in the absence of β-chain means FcεRI can be expressed in both trimeric and tetrameric forms, in these hFcεRI Tg mice. This means that hFcεRI Tg mice express FcεRI on the same cell types on which it is found in humans. The Balb/c colon carcinoma, C26, transfected with human FBP (C26tFR), was chosen for the tumour target in this model (Rodolfo *et al.*, 1998) and was provided by Dr. Silvana Canevari, of the Isituto Nazionale Tumori, Milan, Italy, as part of a collaboration on this model. As hFcεRI Tg mice are backcrossed to a Balb/c background, the C26tFR cell line was likely to be syngeneic. Intravenous injection of C26 cells leads to their growth as artificial lung metastases. The combination of human-IgE-binding FcεRI, and human FBP-expression means these mice can be treated with chimaeric-human MOv18 IgE.

The suitability of this model for assessing MOv18 IgE activity is supported by work documented in both Rodolfo *et al.*, 1996 and 1998. Work in these publications demonstrates the susceptibility of the C26tFR cell line (growing as artificial lung metastases in Balb/c mice) to eradication by induction of a humoral immune response (of the IgG isotype). Most importantly, they show that passive treatment, intravenously, with MOv18 IgG1 and MOv19 (an IgG2a antibody specific for an epitope of FBP different from that of MOv18), markedly reduces the number of metastases on the lungs of these mice. The difference between this Balb/c-C26tFR model described in Rodolfo *et al.*, 1998, and the model being set-up here is that the Balb/c host mouse is replaced with the hFcεRI Tg mouse, allowing an IgE-mediated immune response, closer to that of humans, to be examined.

Reported in Chapter 3, is the observation that C26tFR cells are susceptible to death induced by MOv18 IgE alone. Therefore, an additional control group will need to be included to allow for adjustment of results from MOv18 IgE-alone killing. This control group would involve injection of C26tFR tumour into two separate groups of Balb/c mice, one of

which would subsequently receive treatment with MOv18 IgE, while the other would remain untreated. The inability of human IgE to bind to murine FcεRI (Conrad *et al.*, 1983) in Balb/c mice means that any increase in survival of these mice over untreated tumour-bearing Balb/c mice will be due to non-effector cell mediated effects of human chimaeric MOv18 IgE. Therefore, four groups of tumour-bearing mice would be needed in total: (1) a group of C26tFR tumour-bearing hFcεRI Tg mice, to be treated with MOv18 IgE; (2) a group of C26tFR tumour-bearing hFcεRI Tg mice, to receive no treatments; (3) a group of C26tFR tumour-bearing Balb/c mice, to be treated with MOv18 IgE; and (4) a group of C26tFR tumour-bearing Balb/c mice, to remain untreated.

Following confirmation that C26tFR tumour cells were able to grow in humanised FcεRIα Tg mice, I investigated whether human FcεRIα-chain expression in the transgenic mice had any effect on the rate of tumour growth. To this end, survival was compared between mice of four different genotypes each injected on day 1 with 10^4 C26tFR tumour cells. The genotypes included Balb/c (n = 5), FcεRIα $h^{+/+}m^{-/-}$ (n = 4), FcεRIα $h^{-/-}m^{+/+}$ (n = 3), and FcεRIα $h^{-/+}m^{-/+}$ (n = 5), (Dombrowicz *et al.*, 1996). This number of tumour cells (10^4) was chosen for injection based on work documented in Rodolfo *et al.*, 1998. Mice were sacrificed when they showed dyspnea. As can be seen in Figure 6.5, survival in the syngeneic Balb/c strain was identical to all hFcεRI Tg strains, demonstrating that FcεRI is not involved in tumour growth or spread. In addition, mice treated with 10^4 tumour cells survived for the expected duration of approximately 20 days, suggesting this to be an appropriate number of tumour cells for injection, since survival duration is the parameter used to determine treatment efficacy.

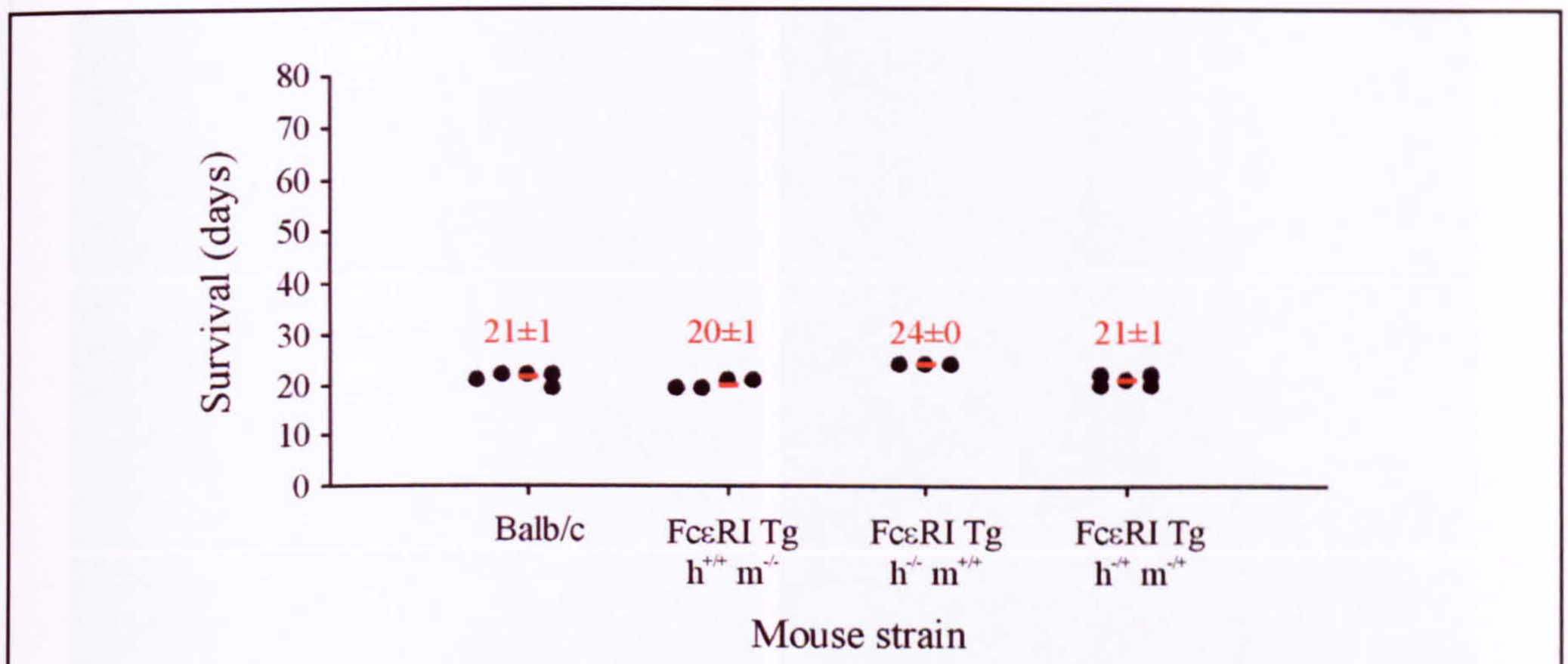

Figure 6.5: Survival of different strains of mouse syngeneic with the C26tFR tumour cell line. Balb/c mice and three strains of hFcεRI Tg mice received intravenous injection of 10^4 C26tFR tumour cells. Results plotted represent the number of days between tumour injection and sacrifice upon development of dyspnea.

An alternative method for quantifying MOv18 IgE activity in this model is by counting the number of metastases on the lungs of each mouse in every group, on one specific day after tumour injection. For this method, injection of a higher number of tumour cells is required for the development of extensive superficial lungs metastases. Determination of the average number of metastases on the lungs of mice from each group is possible by following sacrifice with a lung infusion of India ink before their removal *en bloc* and placement in Fekete solution (Fekete, 1939; sections 2.1.3 and 2.3.3). Fekete solution bleaches tumour metastases, but not normal lung tissue, causing metastases to show up as white nodules on a black background of healthy lung tissue. For determination of the optimum number of tumour cells to be injected and optimum day for sacrifice in metastases-counting experiments, mice were divided into 3 groups of 15. Group A received an intravenous injection (on day 1) of 5 x 10^3 C26tFR tumour cells in 400 µl PBS; group B, 10^4 and group C, 10^5. Three mice from each group were then sacrificed on each of days 15, 17, 19, 21 or 23 (see section 2.3.3). Balb/c mice were used for this experiment, justified on the basis of there being no strain-related differences in tumour growth when compared as described above (shown in Figure 6.5). The purpose of this was to conserve the more limited numbers of hFcεRI Tg mice available. A selection of lungs bearing metastases were photographed, and are shown below in Figure 6.6; these results are discussed in detail, below.

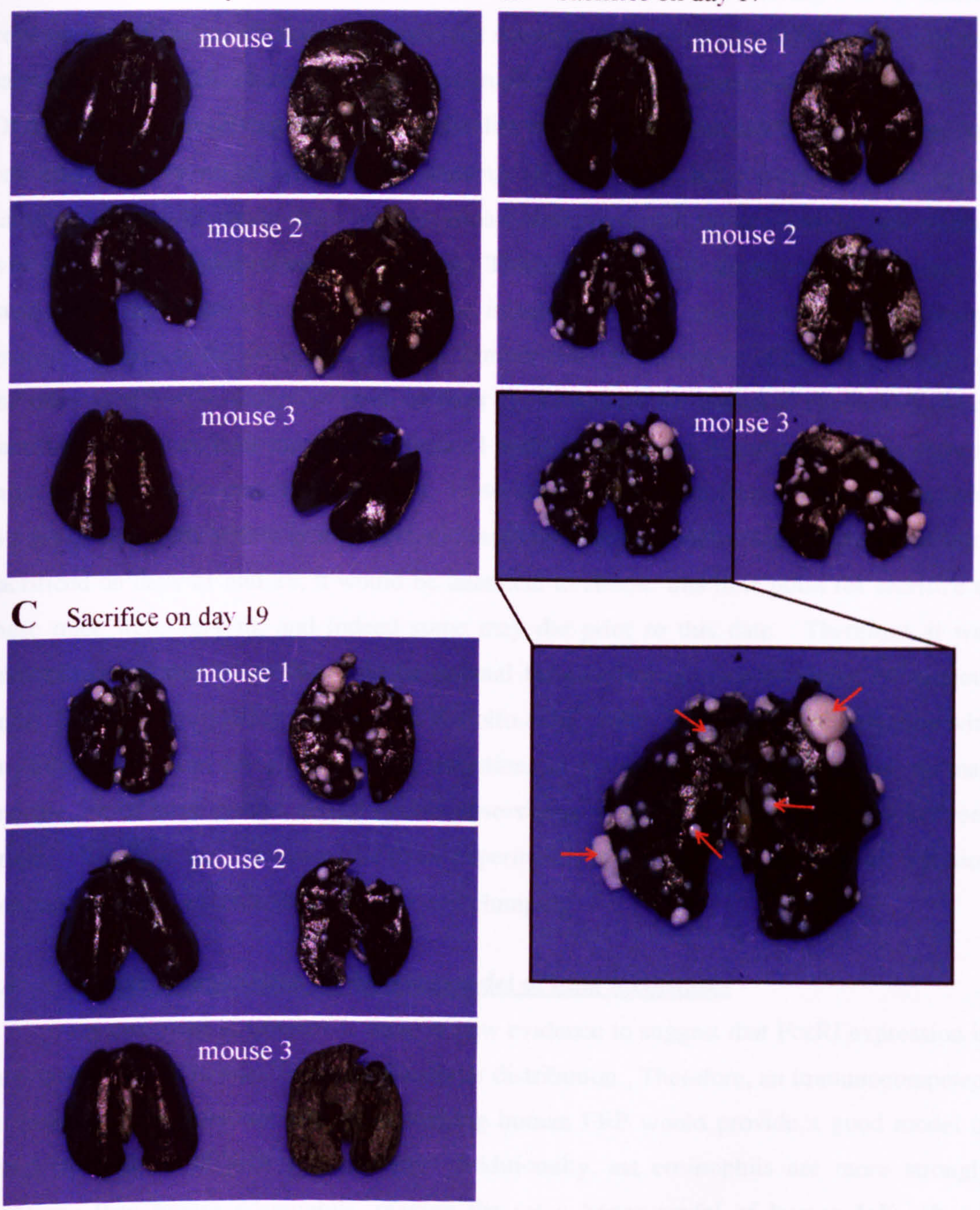

Figure 6.6: Images of tumour growth in metastases counting experiments. All three blocks (A-C) represent lungs from mice injected with 10^5 C26tFR tumour cells in 400 µl PBS on day 1. Front and back views of lungs from each of three different mice sacrificed on day 15, (A), day 17, (B), and day19, (C). One lung image (the front view of lungs from mouse 3, sacrificed on day 17) has been enlarged, and a few of the many metastases have been indicated with red arrows. The black areas represent normal lung tissue.

There was no evidence of metastases on the lungs of mice receiving 5 x 10^3 tumour cells on any of the sacrifice dates (results not shown). Mice receiving 10^4 tumour cells and sacrificed on days 15, 17 and 19 were also completely free of metastases (results not shown). Of the three mice receiving 10^4 tumour cells that were sacrificed on day 21, one of them had one small tumour nodule (results not shown). Of the three mice from the same group sacrificed on day 23, again there was one mouse with one small tumour nodule, and another with two small nodules (results not shown). This correlates with the mean survival time of mice shown in Figure 6.5, which were also injected with 10^4 tumour cells. Most tumour growth was seen in the group receiving 10^5 tumour cells; photographs of the lungs of each of the mice sacrificed in groups of three on days 15, 17 and 19 are shown in Figure 6.6. Mice sacrificed at the two later time points (days 21 and 23) were very ill and accordingly showed large tumour nodules (results not shown). However, it can be seen from Figure 6.6 that there is a lot of variability within groups, and, although the tumour nodules were extensive in mice sacrificed on days 21 and 23, it would be unethical to choose this time point for sacrifice as these mice were very ill, and indeed some may die prior to this date. Therefore, it was determined that day 17 or 19 would be optimal for sacrifice of mice receiving 10^5 tumour cells. This is in accordance with data in Rodolfo *et al.*, 1998. Personal communication with Dr. Silvana Canevari revealed that wide variations in the growth of this tumour are normal, and the use of large groups should enable observation of differences in metastases between groups. Variation was minimised for these experiments by using a large intravenous injection volume of 400 µl, which reduces tumour cell clumping.

6.4 Wistar Albino Glaxo (WAG) rat model of lung metastases

As discussed in Chapter 1, there is now evidence to suggest that FcεRI expression in rats mirrors that of humans in terms of cellular distribution. Therefore, an immunocompetent rat bearing a syngeneic rat tumour expressing human FBP would provide a good model in which to look at MOv18 IgE activity. Additionally, rat eosinophils are more strongly cytotoxic than mouse eosinophils, making the rat a better model of human IgE effector mechanisms (Dr. David Dombrowicz, personal communication). A suitable rat model has therefore been optimised, as described below. Again, this work was carried out at the Pasteur Insititute, Lille, under the supervision of Dr. David Dombrowicz. Dr. Jianguo Shi cloned and expressed murine MOv18 IgE, with which to treat these tumour-bearing rats. Murine MOv18 IgE differs in only a few amino acid positions from rat IgE and interacts with the same affinity as rat IgE binding to rat FcεRI (Sterk and Ishizaka, 1982). This model is also likely to include CD23 function (as discussed in section 1.3.6). The rat colon carcinoma line CC531, was transfected to express human FBP by Dr. Silvana Canevari for the purpose of this work,

so that CC531 tumour cells can be cross-linked to IgE receptor-expressing immune cells by murine MOv18 IgE. The CC531 tumour line is syngeneic with the WAG strain rat, and grows as lung metastases when injected intravenously. This transfected line had not previously been used in the WAG rat, but results below show that expression of human FBP did not prevent tumour growth. Clone 16 of the CC531tFR cell line was chosen over clones 11 and 2 due to results described in section 3.3.2 of Chapter 3, which show that the higher level of FR expression on clones 11 and 2 makes them susceptible to death by treatment with MOv18 IgE alone.

Firstly, an experiment was performed to determine the number of CC531tFR tumour cells that would cause death of the rats within approximately one month of tumour injection. This time scale was intended to provide a short enough experimental time frame for production of results at a reasonable rate, whilst allowing time for the treatments to have an effect. Previous studies documenting growth of the untransfected CC531 line in WAG rats have pre-treated rats first with cyclophosphamide in order to reduce immune activity and give more rapid tumour growth from injection of fewer cells. As the rats in this model were to be treated with an immunotherapeutic agent, with which we hoped to trigger their own immune systems to kill the tumour cells, we wanted to keep the rats as healthy and immunocompetent as possible and so avoid the use of cyclophosphamide. One reference to rats intravenously injected with CC531 cells without prior cyclophosphamide treatment (Marquet *et al.*, 1984) used 5×10^5 CC531 cells to produce lung metastases that resulted in death of the rats within 5 months. Clearly injection of a significantly higher number of tumour cells was necessary to produce tumour growth within the shorter time frame required for these experiments. As a starting point, 2.5 million CC531 cells were injected. When 2.5 million tumour cells were injected in cyclophosphamide pre-treated rats in work of both Kuppen *et al.*, 1994 and Hagenaars *et al.*, 2000, macroscopically visible lung metastases developed after approximately two weeks. In my experiment however, this number of tumour cells was not sufficient to produce lung metastases even by day 100 (Figure 6.7). Doubling the number of tumour cells injected, to 5×10^6, led to sacrifice (due to dyspnea) of one of the two rats injected on day 40 and the other on day 59; extensive lung metastases were seen upon autopsy in both rats.

A

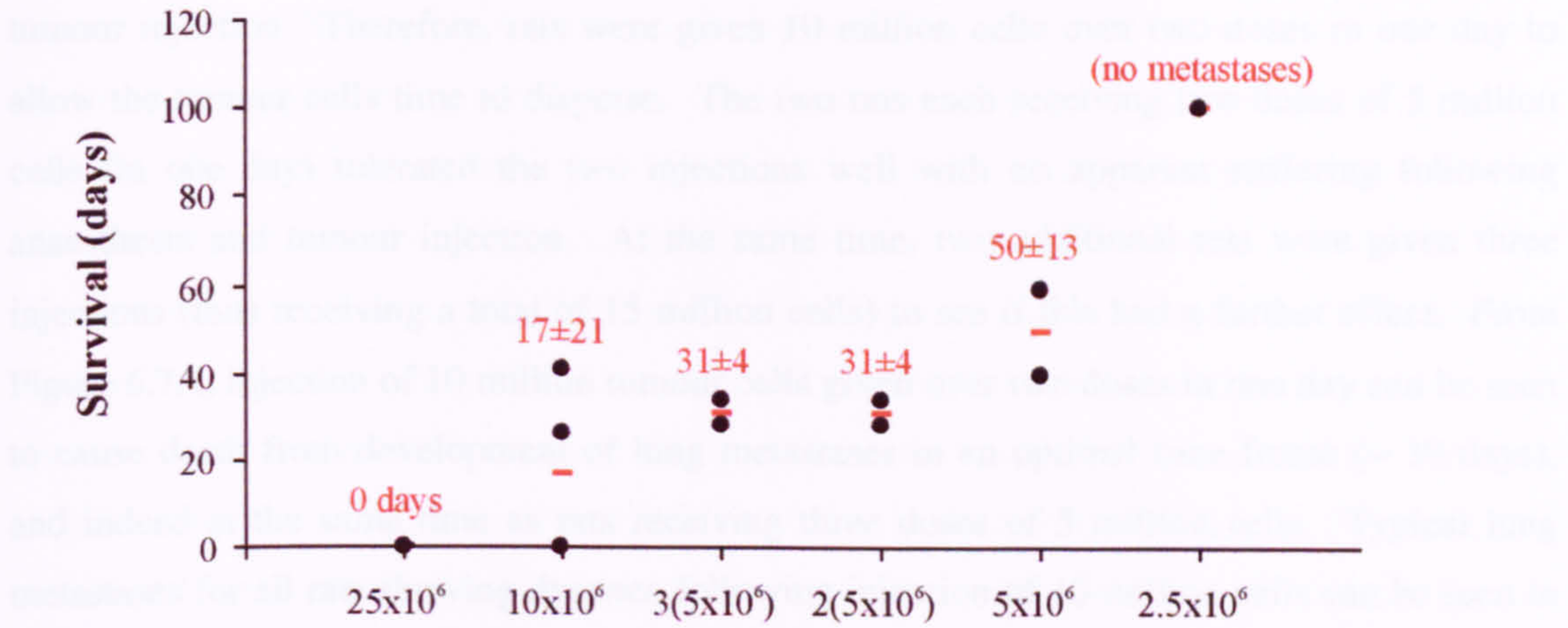

B

Figure 6.7: (A) Time-course of WAG rat development of lung metastases following intravenous injection of CC531tFR tumour cells. Rats under isofluorane anaesthesia received intravenous injection in 1 ml PBS of CC531tFR tumour cells: 25 million, 10 million, 2 injections of 5 million, 3 injections of 5 million, 1 injection of 5 million or 1 injection of 2.5 million cells. (B) Typical lung metastases seen following sacrifice after development of dyspnea; these lungs were taken from a rat that received a single dose of 10 million CC531tFR tumour cells. The peritoneal and chest cavities were opened and lungs infused with India ink by injection via the mouth and trachea. Lungs were then removed *en bloc* and placed in Fekete solution for a minimum of 24 hours.

However, survival durations under these conditions were still long, and so to reduce them, higher numbers of tumour cells were used. Two rats were injected with 25 million tumour cells intravenously. However, rats receiving this many tumour cells died under anaesthesia immediately following tumour injection, possibly due to blockage of the vasculature by the large numbers of tumour cells. The dose was then decreased to 10 million tumour cells. Four rats received this dose, two of which died under anaesthesia. However,

the two surviving rats showed lung metastases at an optimal time point, 30 – 40 days after tumour injection. Therefore, rats were given 10 million cells over two doses in one day to allow the tumour cells time to disperse. The two rats each receiving two doses of 5 million cells (in one day) tolerated the two injections well with no apparent suffering following anaesthesia and tumour injection. At the same time, two additional rats were given three injections (thus receiving a total of 15 million cells) to see if this had a further effect. From Figure 6.7A, injection of 10 million tumour cells given over two doses in one day can be seen to cause death from development of lung metastases in an optimal time frame (~ 30 days), and indeed at the same time as rats receiving three doses of 5 million cells. Typical lung metastases for all rats showing dyspnea following injection of 10 million cells can be seen in Figure 6.7B. It can be seen that the metastases are small and evenly spread making this injection number also suitable for 'metastases counting' experiments.

6.5 Discussion

Experiments described above using the nude mouse model originally used for this project, as described in Karagiannis *et al.*, 2003, demonstrate that treatment of HUA tumour-bearing mice with human PBMC in conjunction with MOv18 IgE, but not MOv18 IgG1, mediates improved survival of mice. Mice treated with 4 million PBMC in conjunction with 100 μg MOv18 IgE each survived for a mean of 40±17 days compared to 26±11 for mice treated with PBMC alone, or 21±7 for mice treated with 4 million PBMC plus 100 μg MOv18 IgG1. These results are in accordance with those using the SCID mouse model of human ovarian cancer (Gould *et al.*, 1999), which also demonstrate increased *in vivo* efficacy of MOv18 IgE over MOv18 IgG1. In the SCID model, mice were injected subcutaneously with 2.5×10^6 IGROV1 tumour cells, which in control mice leads to development of a subcutaneous tumour greater than 200 mm^2 in size by day 35. Treatment was once, one day after tumour challenge, and involved intravenous injection with chimaeric MOv18 IgE or MOv18 IgG1 (100 μg) in combination with human PBMC (3×10^6), per mouse. MOv18 IgG1 did have some activity, inhibiting tumour growth for 19 days after one treatment dose. However, MOv18 IgE was able to provide the same protection as MOv18 IgG1, but for longer, with tumour growth still being inhibited by 62 % on day 35. Together, these results support the proposal that the efficacy of MOv18 IgE in mediating tumour cell death by human PBMC effector cells is underestimated using *in vitro* cytotoxicity assays.

In the nude mouse model used above (section 6.2), antibody and effector cell treatment doses are given directly into the peritoneal cavity, where the tumour grows as ascities; tumour islands amongst tumour cells in suspension. Some solid tumour is observable in late stage disease attached to the peritoneal organs. Therefore, unlike the SCID mouse

model where treatments are given intravenously and the tumour grows subcutaneously, effector cells and antibody are not required to penetrate tissues from the blood. Additionally, four once-weekly doses of effector cells and antibody were given to maximise chances of MOv18 IgG1 activity compared to MOv18 IgE. Therefore, it was surprising that MOv18 IgG1 in conjunction with PBMC mediated no improvement in the survival of HUA-bearing mice whatsoever. One explanation may be that the nude mouse model is a less sensitive method for assessing anti-tumour activity than the SCID mouse model, which allows for continuous measurement of tumour growth over a longer period of time. As HUA tumour-growth in the nude mouse model, at the dose used in these experiments, is life threatening within approximately 20 days, MOv18 IgG1 may temporarily inhibit tumour cell growth, but overall the tumour growth could be overwhelming, such that any effect does not lead to enhancement of mouse survival.

The longer half-life for which IgE binds to FcεRI-expressing effector cells compared to IgG1 binding to any FcγR, is likely to be a significant contributory factor in the enhanced ability of MOv18 IgE over MOv18 IgG1, to provide protection against tumour growth (see section 1.3.4). That survival of mice receiving four doses of PBMC in combination with MOv18 IgE (Figure 6.1) is no longer than in previous similar experiments (Karagiannis *et al.*, 2003), where mice survived for the same length of time after only two doses of the treatment, supports this proposal. These results correlate with the dramatic effect on tumour growth with PBMC and MOv18 IgE, mediated with only one single dose in the SCID mouse model (Gould *et al.*, 1999). The inability of MOv18 IgG1 to improve the survival of tumour-bearing nude mice even with weekly treatment doses may therefore be explained by its inability to remain bound to FcγR-expressing effector cells for sufficient time to confer them with anti-tumour activity. Indeed, the half-life of receptor-bound IgG is in the order of days, compared to weeks for IgE bound to FcεRI on mast cells in tissues (see section 1.3.4). The results with MOv18 IgE also imply good survival of the PBMC-effector cells in these mice, as was expected from results in Mosier *et al.*, 1988, and immunohistochemistry described in Karagiannis *et al.*, 2003.

The human effector cell populations tested above for their ability to kill tumour cells by MOv18 IgE-mediated mechanisms *in vivo* included PBMC, a monocyte-enriched (70 to 80 % pure) population of PBMC, a greater than 95 % pure population of peripheral blood eosinophils and the U937 monocyte cell line. Of the primary cell populations, only whole PBMC were able to mediate an increased duration of survival when given in combination with MOv18 IgE. The U937 monocyte cell line was also able to perform this effect. The inability of an enriched population of primary monocytes to enhance the survival of tumour-bearing mice when injected in combination with MOv18 IgE (Figure 6.2) could be due to one

or more possible reasons. Firstly, monocytes may simply not be the cell type amongst the population of PBMC that mediate tumour cell killing to improve the survival of nude mice. Immunohistochemical demonstration of $CD68^+$ monocytes / macrophages infiltrating tumour cell islands in tumour sections taken from equivalent experiments in Karagiannis *et al.*, 2003, does not mean they are also killing, and may in fact represent macrophage clearance of tumour cell debris following tumour cell-killing by a different effector cell type, such as basophils. Alternatively, it is possible that in the absence of other cell types, the 70 – 80 % pure monocytes did not receive specific signals, normally provided, to enable them to (a) survive (*e.g.*, CSF / M-CSF), (b) mature into activated macrophages which are in fact the tumour-killing cells (*e.g.*, IL-4 or IFN-γ), or (c) mediate effector mechanisms for tumour cell killing (*e.g.*, IL-4-induced upregulation of CD23).

Like monocytes, the inability of a purified population of eosinophils to mediate improved survival of HUA tumour-bearing nude mice may relate to their inability to survive in mice. It is possible that co-injection of eosinophils with recombinant human IL-5 might have aided these cells to survive *in vivo*, as it does *in vitro* (Lopez *et al.*, 1988; Rothenberg *et al.*, 1989). There was insufficient time to analyse tumour sections from these mice by immunohistochemistry to study eosinophil survival. Nude mice are deficient only in αβ T cells, and in fact not even entirely deficient in these, as a subpopulation of αβ T cells that develop extrathymically have been shown to exist (Budzynski and Radzikowski, 1994). This leaves nude mice with a completely intact innate immune system, and so normal numbers of monocytes, macrophages, NK cells and γδ T cells, in addition to a functional humoral immune system. Therefore, nude mice have the capacity to make significant immune responses against both the human tumour xenograft and the human treatment cells. This immune response against the human eosinophils following their injection into the peritoneal cavity of these mice may have led to their immediate degranulation or death, preventing them from having any specific anti-tumour effects.

The experiment looking at the ability of U937 cells in combination with MOv18 IgE to improve the survival of HUA tumour-bearing nude mice was performed before experiments in Chapter 4 determined that IgE was unable to bind FcεRI expressed by this particular U937 clone. Therefore, although originally the experiment intended to address whether or not monocytes *per se*, could improve the survival of mice as a pure population, it also tests what functionally may represent a population of CD23-expressing cells, assuming MOv18 IgE is unable to bind FcεRI on U937s *in vivo*, as *in vitro* data suggests. Although the improved survival of HUA tumour-bearing nude mice by MOv18 IgE and U937 monocytes is statistically significant compared to controls, it may not be physiologically relevant, due to

the fact that U937 cells are a transformed cell line and may not have the same functional ability as primary monocytes.

The improved survival of HUA tumour-bearing nude mice receiving treatments of PBMC alone is likely to be a result of the fact that the PBMC are allogenic with respect to the HUA tumour and indeed murine tissue antigens, such that the lymphocytes ($CD8^+$ T cells and $CD56^+$ NK cells) in the PBMC population recognise these MHC differences and mediate an allo-anti-tumour immune response. However, where enhanced survival is seen in those mice receiving MOv18 IgE in combination with human effector cells, either human PBMC or U937 monocytes, this increased survival can be reasonably judged to be a result of human FcεRI or CD23-expressing effector cells, mediating IgE-antibody-dependent HUA tumour cell-killing. The fact that human IgE does not bind mouse IgE receptors (Conrad *et al.*, 1983), provides further support for these survival effects being due to human rather than mouse cells. It does remain possible that IgE-mediated killing could be enhanced by the effect of activated human effector cells, stimulated by HUA tumour cells releasing chemoattractants and/or cytokines to recruit and activate nude mouse cytolytic effector cells in a bystander fashion.

It is not expected that the increased survival of nude mice receiving treatments containing MOv18 IgE in addition to effector cells, is conferred by direct cytotoxic effects of MOv18 IgE alone. A control group of HUA tumour-bearing mice receiving treatments of MOv18 IgE alone has not been performed yet, but is not expected to have any effects for three reasons. Firstly, SCID mice bearing a subcutaneous IGROV1 tumour showed equivalent tumour growth when mice were treated with PBS or MOv18 IgE alone. Secondly, MOv18 IgE has no effect on IGROV1 tumour cells *in vitro* (see section 3.3.2). Thirdly, effector cell treatments, given in combination with MOv18 IgE, do not always confer a survival advantage, as was the case with both monocytes and eosinophils. If indeed MOv18 IgE acted to induce tumour cell death on its own, then it would likely produce effects in all effector cell treatment groups where it was present.

Xenograft models of human cancer, such as the nude mouse model used above, do not completely replicate the process of tumourigenesis in humans, the human immune system or the dynamic relationship between the two. In this way, they allow direct assessment of whether or not a tumour-specific antibody has the capacity, in the simplest *in vivo* system, to trigger significant tumour cell death. They also allow exposure of any overt toxicities of the treatment. These issues must be addressed directly before it is worth assessing, beyond theoretical speculation, the impact of any more detailed aspects of human cancer and the human immune system on the efficacy of the therapy. A positive result in such models allows

determination of whether or not the time-consuming pursuit of developing a more clinically relevant model is worthwhile. The survival advantage conferred by PBMC in conjunction with MOv18 IgE, but not MOv18 IgG1, in the nude mouse model above, taken with previous *in vivo* results achieved in a SCID mouse model (Gould *et al.*, 1999), and *in vitro* data, suggest that for MOv18 IgE, this pursuit is indeed worthwhile. Using the hFcεRI Tg / C26tFR model, the effect of MOv18 IgE treatment can now be assessed by either measuring the duration of survival in untreated and MOv18 IgE treated mice injected with 10^4 tumour cells on day 1, or by counting metastases on the lungs of all mice at approximately day 17-19 after injection of 10^5 tumour cells. Experiments using the WAG rat / CC531tFR tumour model may also now begin, following the successful cloning and expression of murine MOv18 IgE.

The immunocompetent hFcεRI Tg mouse and WAG rat models have a number of advantages over the xenograft models. Firstly, the IgE systems in both models are much closer to the human immune system, with a similar profile of FcεRI expression found in both hFcεRI Tg mice and rats; the rats additionally have the potential of MOv18 IgE activity through CD23, as discussed in section 1.3.6. Therefore these models are less likely than the xenograft models to underestimate both beneficial MOv18 IgE activity and the potential induction of anaphylactic shock. It would be logical for initial experiments performed in each of the hFcεRI Tg and WAG rat models, to assess whether treatment of tumour-bearing animals with MOv18 IgE is able to mediate any beneficial anti-tumour effects. Then, in the event of a positive effect of MOv18 IgE on the survival of tumour-bearing animals, any toxicity associated with MOv18 IgE treatment should be studied.

My suggestion is that preliminary experiments in these models should be designed to give MOv18 IgE treatment every advantage to mediate anti-tumour activity, and then to work 'backwards' to determine the minimal dosing regimen able to mediate anti-tumour effects. This might involve intravenous injection of a group of WAG rats and or hFcεRI Tg mice with an excess of MOv18 IgE, prior to tumour injection, to saturate all IgE receptor-expressing effector cells with MOv18 IgE, without also saturating FBP expressed by tumours, and preventing ADCC due to equivalence. When excess MOv18 IgE had been cleared, as judged by an absence of free MOv18 IgE in the circulation, tumour-injection could be performed in MOv18 IgE pre-treated and a control group of untreated animals. If the tumour was unable to grow, then this would prove the principle that MOv18 IgE could mediate anti-tumour effector function. In this case, animals could be treated first with tumour, and then at timepoints after tumour injection, treatment with MOv18 IgE could be given. Where a survival advantage is conferred by treatment with MOv18 IgE, it would be interesting to perform histological

analysis of the tumour site to determine which effector cell populations are infiltrating tumour areas in MOv18 IgE-treated compared to untreated control animals.

If MOv18 IgE treatment of tumour-bearing WAG rats or hFcεRI Tg mice was indeed able to confer a survival advantage, then the next step would be to assess whether or not treatment with MOv18 IgE is associated with symptoms of anaphylaxis, if indeed these signs are not already evident. Systemic anaphylaxis manifested by collapse or death of the animals would be apparent immediately after administration of MOv18 IgE. However, a more sensitive measurement of signs of systemic anaphylaxis would be rectal temperature as a function of time after administration of MOv18 IgE. As only very few FcεRI on the mast cell surface are required to be cross-linked for cellular activation, it may be that only very small amounts of tumour-specific IgE are required to effectively mediate tumour cell killing (Metzger, 1992), thus limiting the potential for triggering anaphylaxis. The advantage of treating ovarian cancer with MOv18 IgE is that treatment can be administered locally, directly into the peritoneal cavity.

The ability of a full immune system to take part in a MOv18 IgE-mediated immune response also offers potential for the development of an active immune response against the tumour after MOv18 IgE treatments; the priming of an immune response *in vivo*, by tumour-specific IgE antibodies, has been demonstrated in principle, in Reali *et al.*, 2001. If treatment with MOv18 IgE was found to confer a survival advantage in CC531-tumour bearing WAG rats, which should include both FcεRI and CD23 function, then tumour-specific CTLs and serum antibodies of all isotypes could be assayed to see whether treatment with MOv18 IgE leads to the induction of an acquired immune response compared to control, untreated, tumour-bearing animals.

What the hFcεRI Tg mouse model and the WAG rat model do not allow, is assessment of the impact of the human tumour microenvironment; the effect on MOv18 IgE treatment of the presence of the immune cells which have developed in synergy with the tumour over many years; their activity both influencing and being influenced by the tumour itself. However, positive results of MOv18 IgE activity in these models, alongside a good safety record, may provide sufficient evidence that MOv18 IgE is worth taking into Phase I clinical trials.

CHAPTER 7:

Biological effects of reducing IgE affinity for FcεRI

7.1 Introduction

In the previous two chapters, the potential for using tumour-specific IgE antibodies to trigger immune responses towards tumour cells as a form of cancer immunotherapy was considered. As discussed in section 1.3.4, the high affinity of the interaction between IgE and FcεRI is proposed to confer upon allergen-specific IgE the ability to bind mast cells in the tissues of allergic individuals, such that they are essentially permanently primed for activation immediately upon exposure to specific (multivalent) allergen. This property of the IgE-mediated immune response is also proposed to give tumour-specific IgE antibodies properties advantageous for tumour cell killing. Experiments described in this chapter were performed to determine whether a reduction in the affinity of the IgE-FcεRI interaction was associated with any biological consequences in an *in vivo* model.

7.2 Construction of an anti-NP IgE with reduced affinity for FcεRI

IgE with reduced affinity for FcεRI was constructed by mutation of the arginine residue at position 334 in the N-terminal region of Cε3 of both IgE heavy chains. As discussed in section 1.3.3, R334 is well characterised as a critical binding residue in the IgE-FcεRI interaction, with the R334 residue from both Cε3 domains of IgE forming a direct interaction with FcεRIα (Henry *et al.*, 1997 and Garman *et al.*, 2000); the consequence of an arginine for serine mutation at position 334 in IgE-Fc, is a reduction in IgE Fc affinity for FcεRIα of approximately two orders of magnitude (Henry *et al.*, 1997). This reduction in affinity is primarily a consequence of an increased rate of dissociation of IgE from FcεRI. For the purposes of work described in this chapter, the same R334S mutation was introduced into an anti-NP IgE heavy chain for construction of a whole IgE with reduced affinity for FcεRI. The construction of the mutant R334S anti-NP IgE heavy chain and its permanent transfection into the J558L cell line (a mouse myeloma cell line expressing human λ light chain) was performed by Dr. Jianguo Shi, as described in section 2.2.2.

7.3 Production of wild type and R334S anti-NP IgE

The cell line containing the wild type anti-NP IgE construct was a gift from Dr. Michael Neuberger (the construction of which is documented in Bruggemann *et al.*, 1987). As with R334S anti-NP IgE, this is a permanently transfected J558L cell line. Purification of R334S and wild type anti-NP IgE from cell culture supernatants was performed using the same two-step procedure; affinity chromatography using an α-γ fusion column (see reference 20 in Table 2.2) followed by gel filtration on a Gilson HPLC system using a Superdex™ 200

column. The purity of the final antibody preparations was assessed by both analytical gel filtration and SDS-PAGE.

Figures 7.1 A and B show the analytical gel filtration profiles for wild type and R334S anti-NP IgE respectively, after affinity chromatography but before the gel filtration purification step. From these traces, it was determined that collection of fractions 7-9 in each case would give final preparations free of the aggregated material clearly present in each case as a smaller peak eluting at approximately 10 minutes. After isolation of these fractions, analytical gel filtration was repeated to confirm that the species were indeed entirely monomeric; both wild type and R334S anti-NP IgE displayed the expected gel filtration profile for pure IgE (as seen for both in Figure 7.1C). Figure 7.1D shows the final isolated proteins as single bands, each with an apparent molecular mass of approximately 190 kDa, on a non-reducing 4 - 20 % gradient gel, as expected for human IgE in the native state.

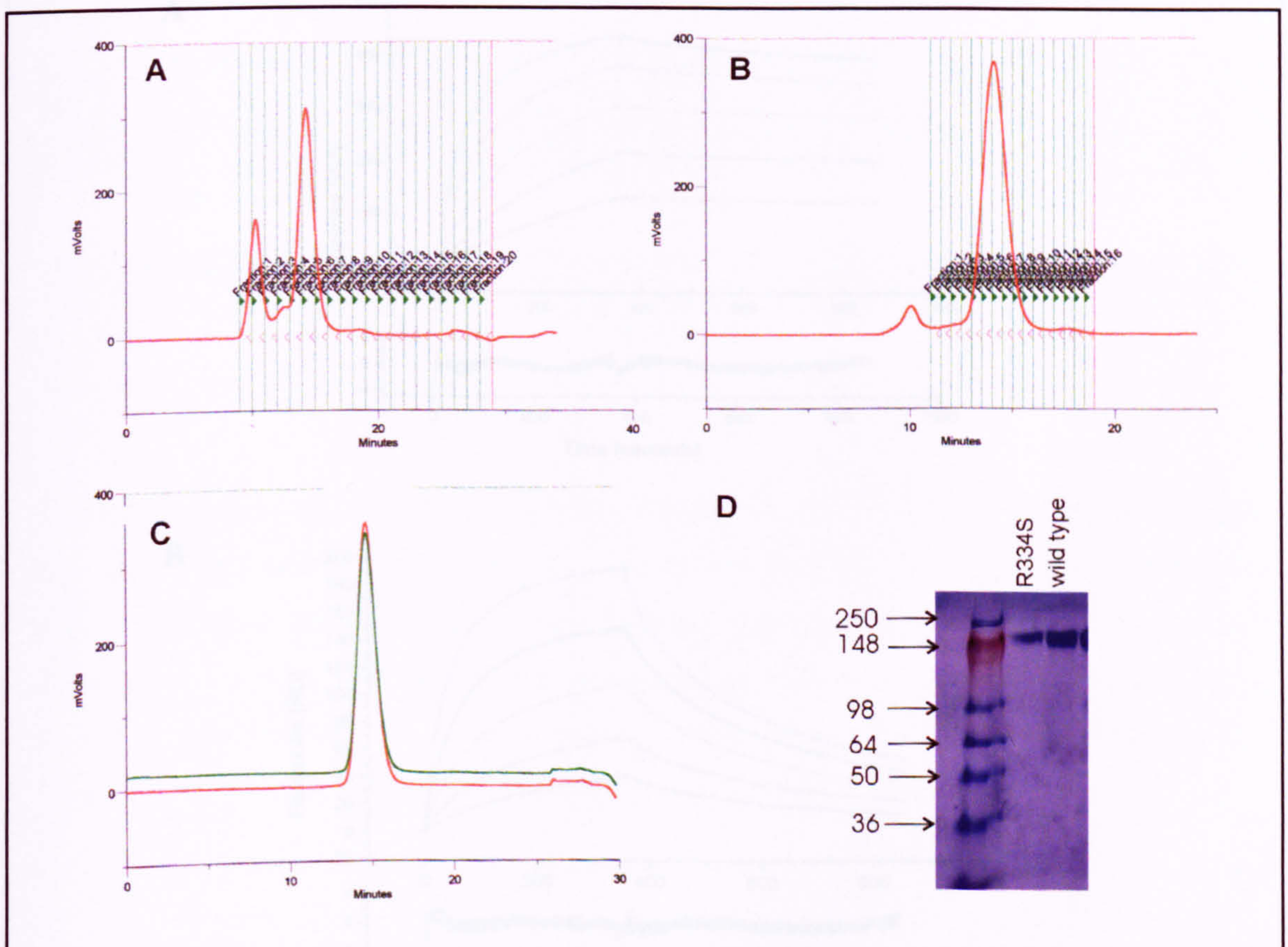

Figure 7.1: Gel filtration profiles for wild type (A) and R334S (B) anti-NP IgE upon affinity chromatography. Purification of fractions 7-9 of both wild type (A) and R334S (B) anti-NP IgE, gave pure and homogeneous preparations: green line = wild type anti-NP IgE and red line R334S anti-NP IgE (C). (D) Non-reducing SDS-PAGE on 4-20 % gradient gel showing final preparations of wild type (right) and R334S (left) anti-NP IgE.

7.4 Kinetics of wild type and R334S IgE interaction with FcεRIα

Experiments to determine the kinetics with which both wild type and R334S anti-NP IgE bound to FcεRIα, were performed by Dr. James Hunt using surface plasmon resonance, according to the protocol described in section 2.3.1. As discussed in section 1.3.3, IgE binding to FcεRI involves a fast and a slow association phase, in addition to a fast and a slow dissociation phase. This biphasic interaction is proposed to reflect the complex nature of the interaction between IgE and FcεRI, involving more than one binding site (in IgE) and the occurrence of a conformational change in IgE, required for FcεRIα chain to access all receptor-binding residues, and generate a high affinity interaction. Therefore the data shown below in Figure 7.2 were obtained by fitting to a biphasic model; the random nature of the residuals indicates that this model provides an adequate description of the interaction.

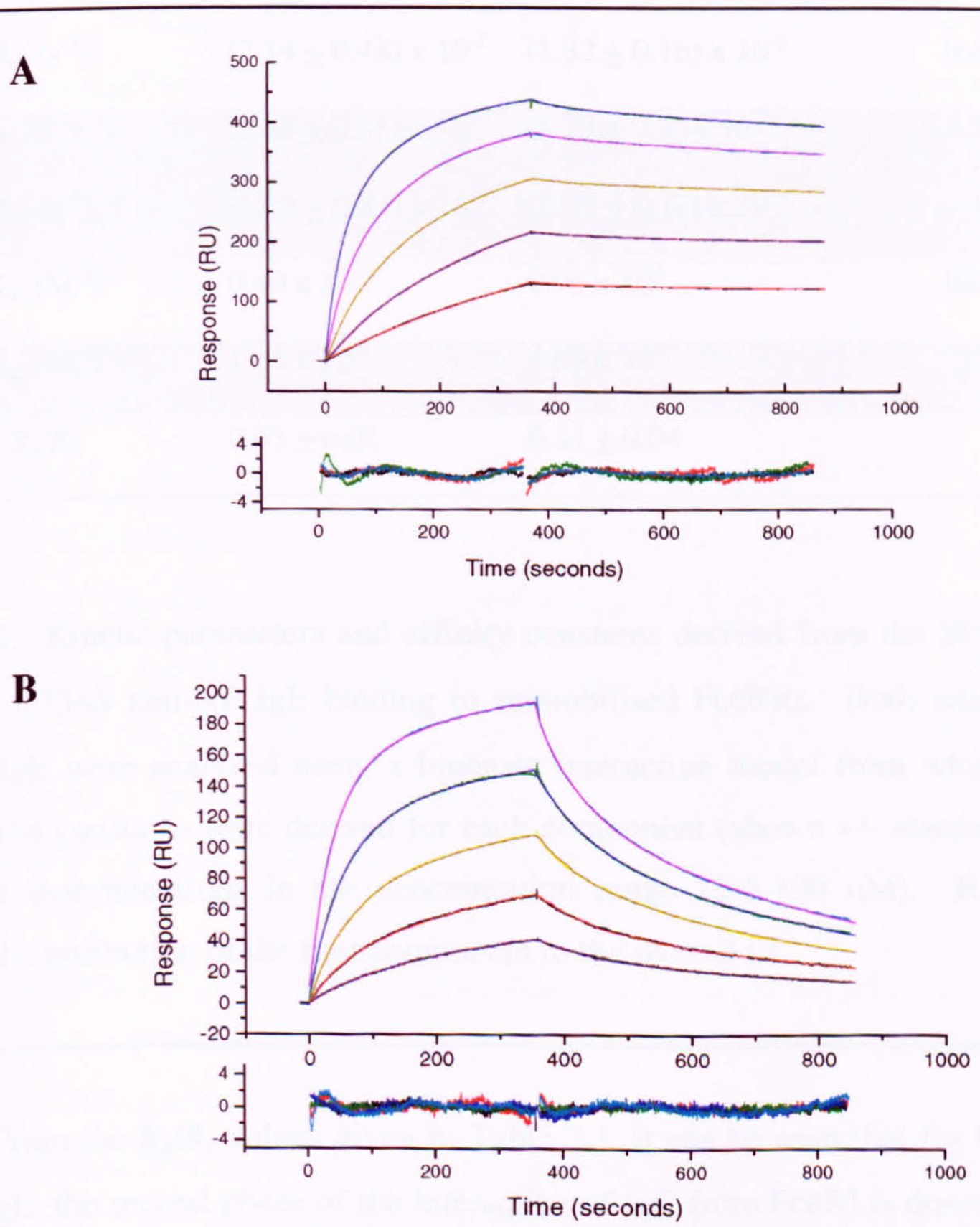

Figure 7.2: Sensorgrams of (A) wild type and (B) R334S anti-NP IgE binding to immobilised IgG_4-Fc-$(sFc\varepsilon RI\alpha)_2$. Anti-NP IgE was injected onto the sensor surface at five different concentrations in the range 12.5 to 100 nM. A 360 s association phase was followed by a 360 s dissociation phase with HBS buffer flowing over the sensor surface at 20 µL / min.

From visual analysis of the sensorgrams in Figures 7.2 A and B it is clear that there is a major difference in the binding properties of wild type and R334S anti-NP IgE for IgG_4-Fc-$(sFc\varepsilon RI\alpha)_2$ (the IgE-binding fusion protein described in section 2.1.2); this difference lies primarily in a significantly faster rate of dissociation of R334S anti-NP IgE from FcεRIα, compared to wild type anti-NP IgE. Table 7.1 below shows the kinetics of both wild type and R334S anti-NP IgE binding to FcεRI; the rate constants for the second phase of both association and dissociation of IgE from FcεRI are highlighted in grey.

constant	IgE wt	IgE R334S	Deviation of R334 from wild type IgE
k_{a1} ($M^{-1}s^{-1}$)	$(0.85 \pm 2.7) \times 10^5$	$(1.27 \pm 0.24) \times 10^5$	Insignificant
k_{d1} (s^{-1})	$(2.14 \pm 0.48) \times 10^{-2}$	$(1.32 \pm 0.16) \times 10^{-2}$	Insignificant
k_{a2} ($M^{-1}s^{-1}$)	$(1.88 \pm 0.51) \times 10^5$	$(8.25 \pm 2.3) \times 10^4$	~ 2 x slower
k_{d2} (s^{-1})	$(1.23 \pm 0.31) \times 10^{-4}$	$(1.71 \pm 0.12) \times 10^{-3}$	~ 10 x faster
K_{a1} (M^{-1})	0.40×10^7	0.96×10^7	Insignificant
K_{a2} (M^{-1})	1.53×10^9	4.68×10^7	33 x lower
R_1/R_0	0.03 ± 0.01	0.31 ± 0.04	-

Table 7.1: Kinetic parameters and affinity constants derived from the SPR analysis of wild type and R334S anti-NP IgE binding to immobilised FcεRIα. Both wild type and R334S anti-NP IgE were analysed using a biphasic interaction model from which association and dissociation constants were derived for each component (shown +/- standard deviation for at least five determinations in the concentration range 12.5-100 nM). R_1/R_0 describes the fractional contribution of the first component to the overall fit.

From the R_1/R_0 values given in Table 7.1, it can be seen that for both wild type and R334S IgE, the second phase of the interaction of IgE from FcεRI is dominant (with the first phase describing the interaction of 3 % of wild type and 31 % of R334S anti-NP IgE with FcεRI); thus the K_{a2} value for both wild type and R334S anti-NP IgE interacting with FcεRI (1.53×10^9 and 4.68×10^7 M^{-1} respectively), is representative of the overall affinity of the majority of IgE molecules interacting with FcεRI. As expected for wild type IgE, the

dominant, second phase of the interaction, is characterised by a slower dissociation rate (k_{d2} ~ 1.23 x 10^{-4} compared to k_{d1} ~ 2.14 x 10^{-2} s^{-1}).

Importantly, the effect of the R334S mutation in IgE is a reduction in its affinity for FcεRI, compared to wild type IgE, of approximately 33-fold (determined by comparing the K_{a2} of wild type and R334S anti-NP IgE; 1.53 x 10^9 / 4.68 x 10^7 = 32.6). From comparison of the k_{d2} values for wild type and R334S anti-NP IgE, which are ~1.23 x 10^{-4} and ~1.71 x 10^{-3} s^{-1} respectively, it is clear that this difference comes primarily from a 10-fold increase in the rate of dissociation of IgE from FcεRI. This is in accordance with the significant difference between the affinity of an R334S IgE-Fc compared to wild type IgE-Fc (Henry *et al.*, 1997).

As discussed in section 1.3.4, the half-life of wild type IgE binding to mast cells is of the order of weeks in tissue, and days in serum. From data in Table 7.1, it is possible to calculate the effect of a 33-fold reduction in IgE-FcεRI interaction affinity (exemplified by R334S IgE), relative to wild type IgE, on the half-life for which IgE remains FcεRI-bound. By taking the reciprocal of the dissociation rate constant for the second (dominant) component of the interaction, k_{d2}, the half-life for IgE binding to FcεRIα can be calculated to be 2.26 hours for wild type IgE, and only 9.7 minutes for R334S IgE. These values are not absolute, but reflect a relative difference in the FcεRI-binding half-lives of wild type compared to R334S IgE, of 13.9 fold. Thus, if the half-life of wild type IgE bound to mast cells in tissues is taken to be 14 days, this equates to approximately 1 day for R334S IgE, making the R334S-FcεRI interaction equivalent to that of IgG1-FcγRIII (see Table 1.1 and section 1.3.4). The effect of a reduction of this magnitude in IgE-FcεRI interaction affinity on allergic reactions could be profound, as it may prevent the normal long-term sensitisation of mast cells and basophils with allergen-specific IgE, and consequently, abolish immediate hypersensitivity. The aim of the experiments described in the following sections was to determine if this affinity change could indeed mediate any biological effects *in vivo*.

7.5 Optimisation of passive cutaneous anaphylaxis model with wild type anti-NP IgE

The *in vivo* model used to compare the biological effects of wild type and R334S anti-NP IgE was a mouse model of passive cutaneous anaphylaxis (PCA). This work was performed in the laboratory of Dr. David Dombrowicz, at the Pasteur Institute, Lille. The mouse host used in this model was the 'humanised' FcεRI transgenic mouse (hFcεRI Tg) described in section 2.1.4, which expresses human α-chain in combination with murine β-chain and γ_2-dimer (or γ_2-dimer alone) to make a functional FcεRI capable of binding human but not murine IgE (Dombrowicz *et al.*, 1996). The minimal amount of wild type anti-NP IgE

required to give maximal passive cutaneous anaphylaxis in these mice was first determined, as PCA experiments had not previously been performed in hFcεRI Tg mice[1].

In summary, as described in section 2.3.3, eighteen mice were divided into 6 groups of 3. Cutaneous mast cells in one ear of each group of three mice were sensitised with a specific (indicated) concentration of wild type anti-NP IgE in PBS by intradermal injection in a total volume of 20 µl (see Figure 7.3A). Equivalent injections containing PBS alone were performed in the other ear such that each mouse acted as its own control. Antigen challenge was performed 48 hours later by intravenous injection via the tail vein, of 100 µg of NIP(5)BSA in 200 µl PBS also containing 2 % Evans blue dye. Mice were sacrificed 1.5 hours after antigen challenge, ears were removed and Evans blue dye extracted and quantified. Evans blue dye extravasated into ear tissue is proportional to anaphylaxis intensity as it is indicative of the increase in vascular permeability characteristic of anaphylaxis. It is clear from Figure 7.3A, that maximal anaphylactic responses are reached when ears are sensitised with 10 µg of wild type anti-NP IgE. The apparent reduced intensity of anaphylaxis seen following injection of 20 µg compared to 10 µg wild type anti-NP IgE is not statistically significant ($p = 0.34$).

Figure 7.3B shows the results from a single mouse; its left ear was sensitised with wild type anti-NP IgE and its right ear with PBS. Challenge was made intravenously 48 hours later, and 1.5 hours subsequently to this the mouse was sacrificed and its ears removed (see inset photo of ears immediately before removal). It is clear from this representative mouse that no transfer of anti-NP IgE occurs between ears as the right ear is completely clear of Evans blue extravasation, except for a small spot at the site of needle damage from PBS injection.

[1] Since the time of writing this Thesis, Zhu *et al.* (March 2005) have reported the use of hFcεRIα Tg mice for PCA experiments using a variation of the method described in this Chapter.

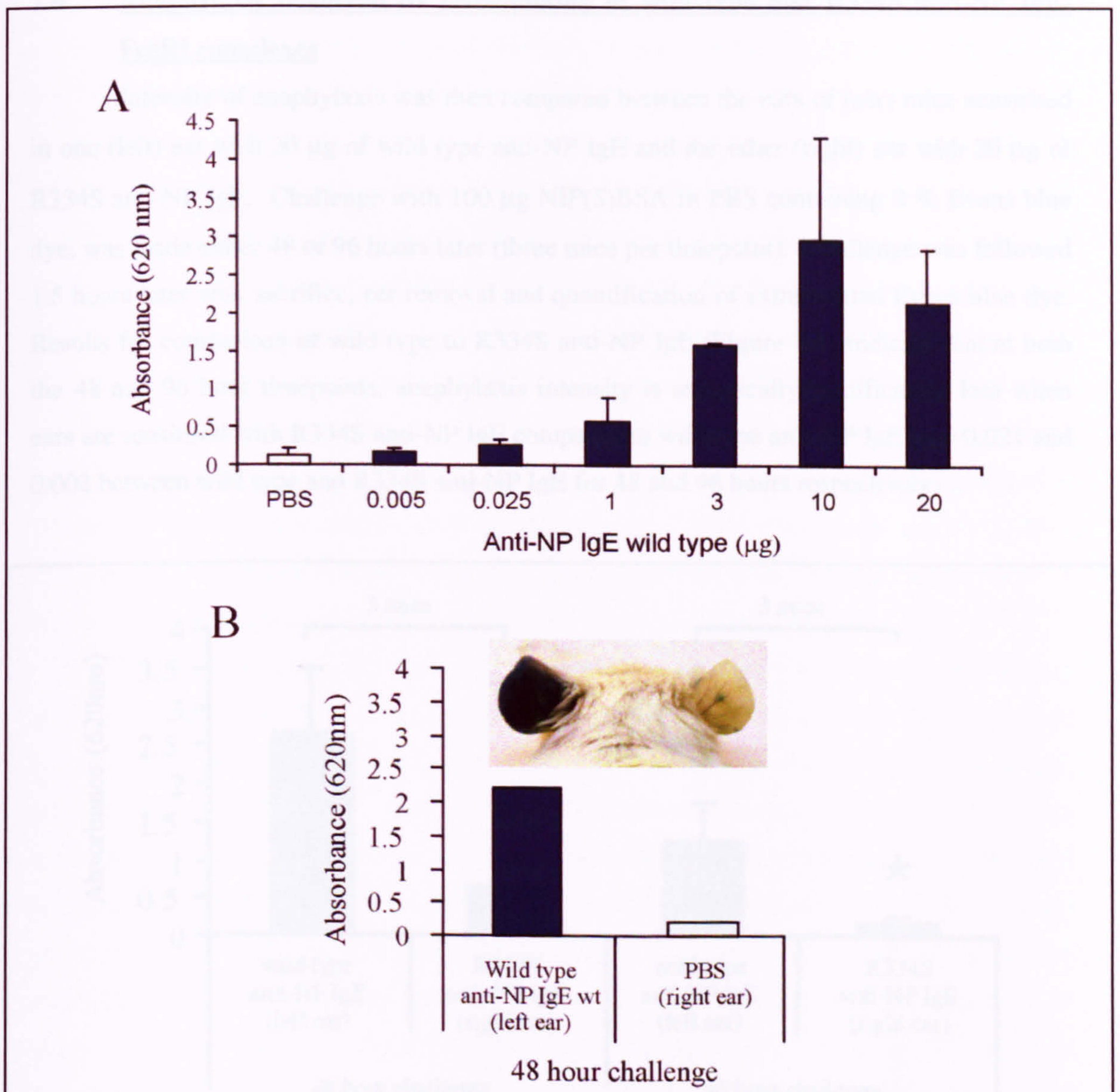

Figure 7.3: (A) Titration of wild type anti-NP IgE in passive cutaneous anaphylaxis in ears of hFcεRI Tg mice. Mouse ears were sensitised with different (indicated) amounts of wild type anti-NP IgE in left ear and PBS in the right ear. Intravenous antigen challenge was performed 48 hours later with NIP(5)BSA and Evans blue dye. (B) Evans blue dye extravasation in the ears of one mouse. This mouse was sensitised in the left ear with wild type anti-NP IgE and in the right ear with PBS. Challenge was made with NIP(5)BSA 48 hours later; this plot shows that no transfer of anti-NP IgE occurs between the two ears of one mouse (the blue spot on the right ear of the photographed mouse is a result of needle damage to ear from injection of PBS).

7.6 Anaphylaxis triggered by cross-linking of wild type and R334S anti-NP IgE-FcεRI complexes

Intensity of anaphylaxis was then compared between the ears of (six) mice sensitised in one (left) ear with 20 μg of wild type anti-NP IgE and the other (right) ear with 20 μg of R334S anti-NP IgE. Challenge with 100 μg NIP(5)BSA in PBS containing 2 % Evans blue dye, was made either 48 or 96 hours later (three mice per timepoint). Challenge was followed 1.5 hours later with sacrifice, ear removal and quantification of extravasated Evans blue dye. Results for comparison of wild type to R334S anti-NP IgE (Figure 7.4) indicate that at both the 48 and 96 hour timepoints, anaphylaxis intensity is statistically significantly less when ears are sensitised with R334S anti-NP IgE compared to wild type anti-NP IgE ($p = 0.021$ and 0.002 between wild type and R334S anti-NP IgE for 48 and 96 hours respectively).

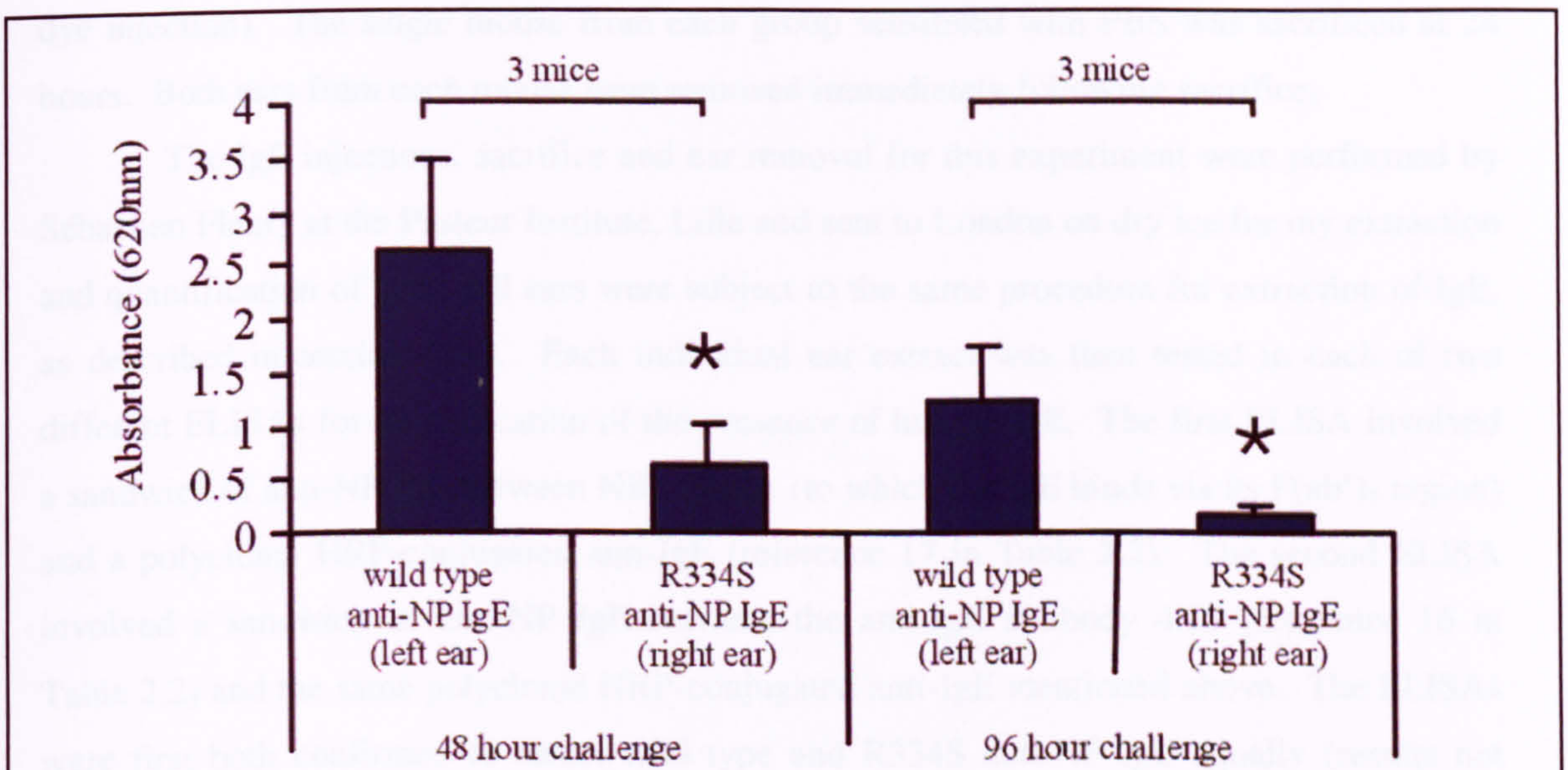

Figure 7.4: Passive cutaneous anaphylaxis in ears of hFcεRI Tg mice. Two sets of 3 mice were used. All 6 mice were sensitised with 20 μg of wild type anti-NP IgE in their left ear, and 20 μg of R334S anti-NP IgE in their right ear. Three mice were challenged intravenously with 100 μg of NIP(5)BSA in PBS containing 2 % Evans blue dye, 48 hours after sensitisation, and the remaining three mice received the same challenge, 96 hours after sensitisation. Challenge in each case was followed 1.5 hours later with sacrifice and ear removal. Ears were cut to identical sizes and Evans blue dye extracted and quantified by absorbance at 620 nm in a spectrophotometer. * indicates a statistically significant difference in anphylaxis intensity between wild type and R334S anti-NP IgE at 48 and 96 hours of $p = 0.021$ and 0.002 respectively.

7.7 Rate of wild type and R334S anti-NP IgE clearance from ear dermis

It was possible that the reduced anaphylaxis intensity in ears sensitised with R334S anti-NP IgE resulted from there being less R334S compared to wild type anti-NP IgE in the ears at all time points of antigen challenge, due to the reduced affinity of binding of R334S anti-NP IgE, potentially allowing a faster rate of clearance from the ear. A control experiment was therefore performed in which the rate of both wild type and R334S anti-NP IgE clearance out of the ear tissue was measured. Twenty mice were divided into two groups of ten, and of the first group nine were each sensitised in both ears with 14 μg wild type anti-NP IgE. The remaining mouse was sensitised in both ears with PBS. Of the second group of ten mice, nine were each sensitised in both ears with 14 μg R334S anti-NP IgE, and the tenth mouse in both ears with PBS. Three mice from each IgE-sensitised group were sacrificed at 24, 48 and 96 hours after sensitisation (in the absence of antigen challenge and Evans blue dye injection). The single mouse from each group sensitised with PBS was sacrificed at 24 hours. Both ears from each mouse were removed immediately following sacrifice.

The IgE injections, sacrifice and ear removal for this experiment were performed by Sébastien Fleury at the Pasteur Institute, Lille and sent to London on dry ice for my extraction and quantification of IgE. All ears were subject to the same procedure for extraction of IgE, as described in section 2.3.3. Each individual ear extract was then tested in each of two different ELISAs for quantification of the presence of human IgE. The first ELISA involved a sandwich of anti-NP IgE between NIP(5)BSA (to which the IgE binds via its $F(ab')_2$ region) and a polyclonal HRP-conjugated anti-IgE (reference 17 in Table 2.2). The second ELISA involved a sandwich of anti-NP IgE between the anti-IgE antibody 4.15 (reference 16 in Table 2.2) and the same polyclonal HRP-conjugated anti-IgE mentioned above. The ELISAs were first both confirmed to detect wild type and R334S anti-NP IgE equally (results not shown). The results in Figures 7.5 A and B indicate that there is no statistically significant difference in the amount of wild type compared to R334S anti-NP IgE present in the ear dermis at the time points indicated, as judged by either ELISA, suggesting that heir clearance from the ear tissue occurs at similar rates.

A ELISA 1: Coating antibody = 4.15 (anti-IgE)
Detection antibody = P 0295 (HRP-anti-IgE)

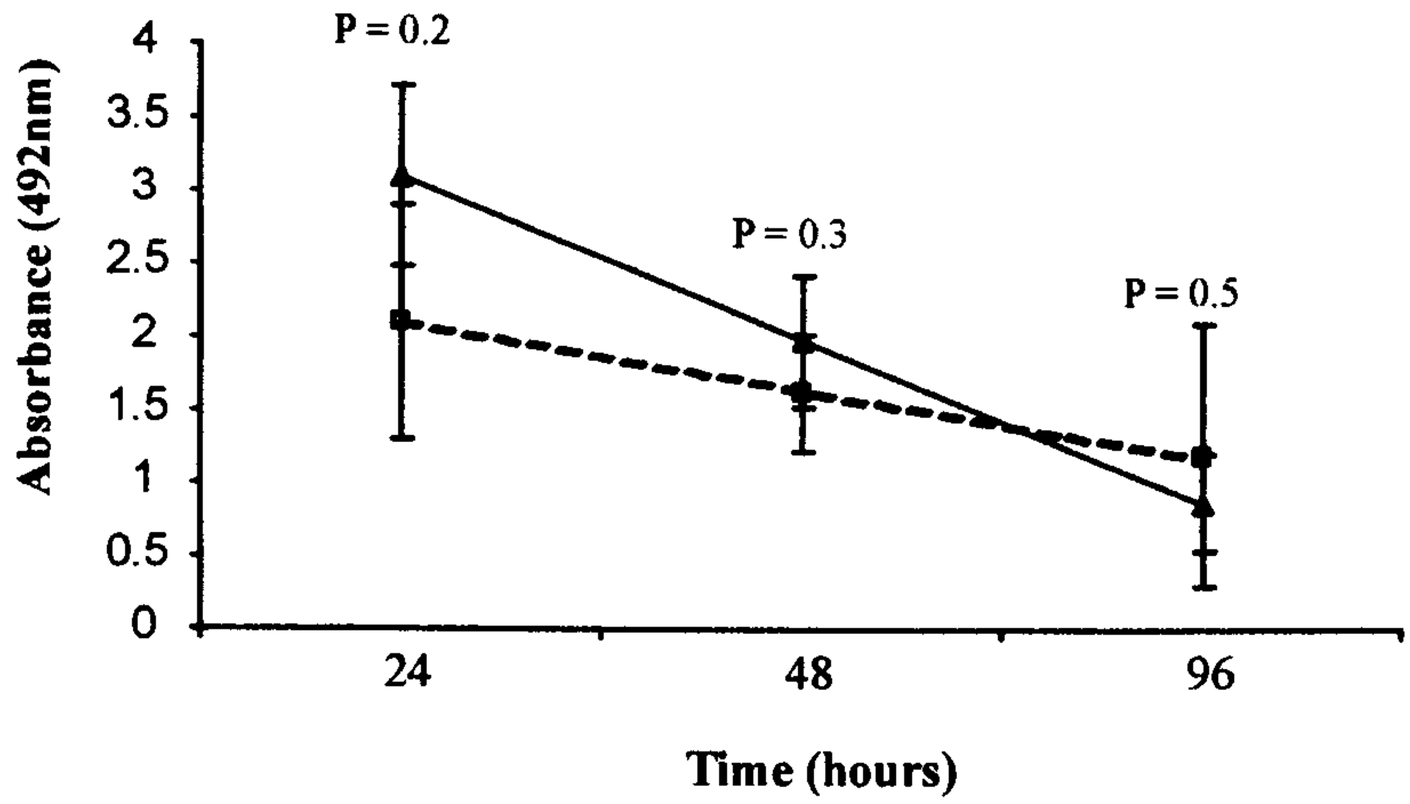

B ELISA 2: Coating antibody = NIP(5)BSA
Detection antibody = P 0295 (HRP-anti-IgE)

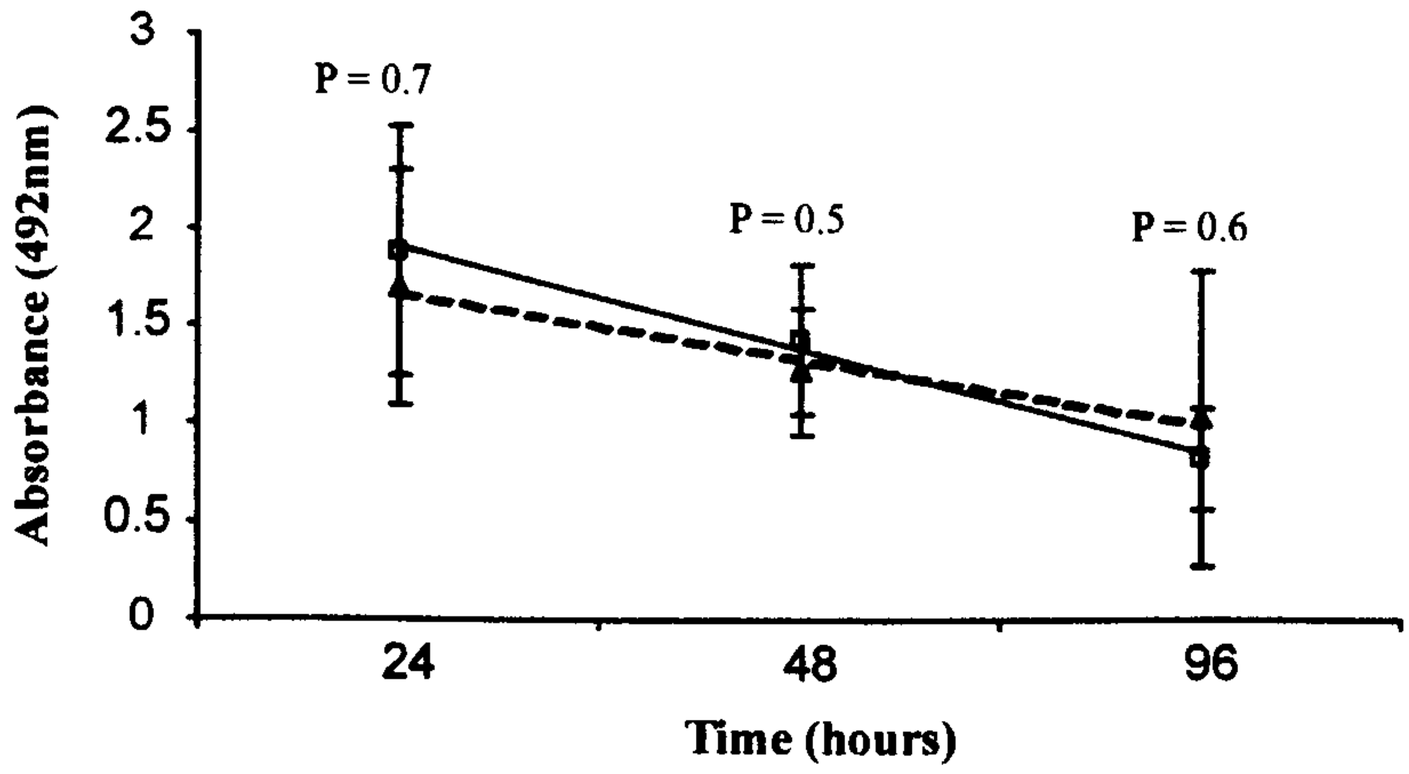

——— = wild type anti-NP IgE
---------- = R334S anti-NP IgE

Figure 7.5: Rate of clearance of wild type versus R334S anti-NP IgE out of mouse ears after intradermal injection. Nine mice each received intradermal injection of 14 μg wild type anti-NP IgE in both ears and another nine mice each received intradermal injection of 14 μg of R334S anti-NP IgE in both ears. Mice were sacrificed in groups of three, at 24, 48 or 96 hours after sensitisation, and anti-NP IgE was extracted from ear tissue and quantified. (A): Quantification of wild type and R334S anti-NP IgE in 4.15 ELISA; (B): Quantification of wild type and R334S anti-NP IgE from same extracts used in A, but on NIP(5)BSA ELISA.

7.8 Discussion

The results of experiments described in this chapter were unexpected. As discussed in Chapter 1, the high affinity of the IgE:FcεRI interaction is proposed to confer upon IgE the ability to sensitise FcεRI-expressing mast cells in tissues for long periods of time. Therefore, it was originally expected that at early time points after sensitisation of mouse ear tissue with either wild type or R334S anti-NP IgE, the intensity of anaphylaxis mediated upon multivalent antigen (NIP(5)BSA) challenge would be similar for both. It was expected that the lower affinity, R334S IgE would be cleared at a faster rate from the ear tissue than wild type IgE, and that this would correlate with a faster rate of reduction in anaphylaxis intensity upon antigen challenge as a function of time following sensitisation, compared to tissue sensitised with wild type IgE.

Instead, what has been found from experiments described in this chapter is firstly, that wild type and R334S IgE appear to be cleared from the ear tissue at equivalent rates (at least within the time points tested). Secondly, despite there being equal amounts of IgE present in the ear tissue at each time point at which antigen challenge was made, the intensity of anaphylaxis mediated through mast cells sensitised with R334S IgE is consistently lower than the intensity of anaphylaxis mediated when mast cells are sensitised with wild type IgE. The equivalent rates of wild type and R334S IgE diffusion out of the ear tissue is likely to be due to the dense, poorly vascularised nature of mouse ear tissue, restricting diffusion of the IgE, and allowing re-binding to IgE receptors. These results provide a different and surprising rationale for the proposal that tumour-specific IgE might be more effective than IgG-subclasses for the immunotherapeutic treatment of cancer, as discussed below. Furthermore, these results have unexpected but extremely important therapeutic implications for allergy and asthma, and these are discussed first.

The IgE-FcεRI interaction plays a central role in allergic immune responses and represents an important molecular target for therapeutic intervention. However, despite the availability of the crystal structure of both IgE-Fc and an IgE-Fcε3-4 fragment in complex with FcεRIα, no therapeutic agent able to effectively abolish the interaction is widely available. The main reason for this is that such a blocking agent is required to bind IgE or FcεRI with a minimum affinity of ~ 10^{10} M^{-1} (equivalent to that between IgE and FcεRI) to have a chance of effectively competing with IgE for receptor binding. However, these results suggest that it is not in fact necessary to abolish the interaction between IgE and FcεRI, as a reduction in affinity of only 33-fold has significant effects *in vivo*.

Results shown in Figure 7.5 suggest that despite the lower affinity of R334S IgE for FcεRI, it is retained as well as wild type IgE in the ear tissue. It is therefore unlikely that the

difference in anaphylaxis intensity seen in Figure 7.4 reflects the presence of different amounts of each IgE in the ear at the time of antigen challenge. Further support for the idea that reduced anaphylaxis is a consequence of reduced IgE-FcεRI interaction affinity and not differences in IgE levels in the ear at the time of antigen challenge, comes from the fact that these results reflect the compiled data from a minimum of three mice per condition at each time point, and that a large excess of IgE has been used for sensitisation.

There was insufficient time in the course of this work to investigate the mechanism behind these results. However, one potential mechanism by which antigen cross-linking of an IgE bound to FcεRI with reduced affinity may lead to a cellular response of reduced intensity is kinetic proof-reading by FcεRI. Kinetic proof-reading is known to be a mechanism used by T cells to discriminate between 'self', and 'non-self' (McKeithan, 1995). However, it has also been shown that IgE bound to FcεRI on RBL-2H3 cells has the capacity to kinetically discriminate between antigens of different affinity, such that ligands with lower affinity for IgE show progressive inefficiency in the phosphorylation of downstream signalling components, to the extent that a complete response is prevented (Torigoe *et al.*, 1998). It is thought that low affinity multivalent antigens are unable to maintain FcεRI aggregation for sufficient time for responses to go to completion. It may be that a similar kinetic proof-reading process applies to FcεRI, whereby a lower affinity IgE causes FcεRI aggregates to dissociate before signalling is complete, leading to a reduced final cellular response. This is supported by data in Table 7.1, which is used in section 7.4 to determine that the half-life of R334S IgE binding to FcεRI is approximately 14 times shorter than binding of wild type IgE to FcεRI. Therefore, it is possible that R334S IgE may bind FcεRI for insufficient time for an FcεRI signalling response to go to completion, when that 'complete' response is likely to take a minimum of 20 minutes, as exemplified by a wheal and flare reaction (Cass and Anderson, 1968).

One way of achieving a reduction in IgE affinity for FcεRI may be to prevent the engagement of one of the two sub-sites of interaction between IgE and FcεRI. This is implied by data in Hunt *et al.*, 2005, in which abolition of the inter-heavy chain disulphide bond of an Fcε3-4 fragment permitted the determination of the binding kinetics of a single sub-site within a fully folded Cε3 domain, and showed it to be in the order of 10^5-10^6 M^{-1}. The reduction in affinity, compared to a wild type IgE Fcε3-4 fragment, comes predominantly from an increased off-rate. This may confer upon IgE a suitably low binding affinity for it to mediate reduced cellular responses similar to R334S IgE. The fact that a conformational change in IgE is required for it to bind FcεRI through both its sub-sites suggests that an inhibitor that prevented this conformational change may have the potential to reduce the ability of IgE to cause allergic reactions.

The central role of IgE (through its interaction with FcεRI) in allergy has recently been demonstrated through the ability of a therapeutic anti-IgE antibody, Omalizumab (Jardieu *et al.*, 1999; Chang *et al.*, 2000), to abrogate the symptoms of both allergy and asthma (for a review see Holgate *et al.*, 2005). Omalizumab is a humanised monoclonal IgG antibody, which binds the Cε3 domains (receptor-binding region) of IgE with sufficiently high affinity (1.5×10^{10} M^{-1}) for it to efficiently block the interaction between free IgE and FcεRI. In addition, it is unable to bind receptor-bound IgE and therefore does not cause cellular activation by cross-linking of FcεRI by itself. Some of its action may also be mediated through direct interaction with membrane IgE on B cells, with the effect of a reduction in the levels of secreted IgE (Sutton *et al.*, 2000). This success of Omalizumab highlights what an excellent target the IgE-FcεRI interaction is, for treatment of allergy.

Despite its success, Omalizumab is unlikely to become a widely available treatment for allergy suffers due to the expense involved in the production of such a large biological molecule, and its need for repeated intravenous administration (Heaney and Robinson, 2005). The development of a small molecule inhibitor of the conformational change required for the binding of both sites in IgE to FcεRIα would therefore be a worthwhile investment. The availability of the crystal structures of IgE-Fc, an IgE-Fcε3-4 fragment and the latter in complex with soluble FcεRIα makes the structure-based design of such an inhibitor possible.

Results of experiments described in this Chapter are now considered in the context of the immunotherapeutic treatment of cancer with tumour-specific IgE antibodies. The results suggest that it is through the high affinity with which IgE binds to FcεRI, that it is able to trigger such a powerful immune response. The corollary might therefore be that the lower affinity binding of IgG subclasses to FcγR leads to a cellular response of lower relative intensity (upon antigen-induced receptor cross-linking). Of course, the cell types to which an antibody binds and activates are dependent on the cellular distribution of its specific Fc receptors, and thus the nature of the immune response triggered depends upon the properties of that cell type. However, the results described in this Chapter imply that immunotherapy for cancer with IgE may mediate immune responses that can cause tumour cell death at lower doses than tumour-specific antibodies of isotypes which bind to Fc receptors with lower affinity. Treatment of cancer with lower doses of tumour-specific IgE is likely to reduce the potential for unwanted side effects. Further support for the theory that only low doses of tumour-specific IgE would be required for effective tumour cell killing, is the well-known sensitivity of cellular activation in response to FcεRI cross-linking with antigen (Metzger, 1992).

This apparent correlation between the affinity of IgE for FcεRI, and the intensity of the cellular response mediated, might explain the more efficient killing of tumour cells seen in *in vivo* models by tumour-specific antibodies of the IgE isotype, compared to IgG (Gould *et al.*, 1999; Karagiannis *et al.*, 2003). In these models, PBMC were used as effector cells, and therefore included cell types expressing FcγR but not FcεRI (*e.g.*, NK cells), in addition to those cell types expressing FcγR and FcεRI (*e.g.*, monocytes). The greater efficacy of IgE over IgG in these models may therefore reflect the activation of fewer FcεRI-expressing cells mediating an anti-tumour immune response of greater intensity and efficacy, rather than the collective anti-tumour activity mediated by IgG1-dependent activation of greater number of cells (each expressing higher levels of FcγR), each responding with lower intensity.

CHAPTER 8:

Final Discussion

8.1 IgE in immunotherapy of cancer?

In this Thesis, MOv18 IgE has been used to assess the proposal that tumour-specific antibodies of the IgE isotype might be able to initiate an immune response able to eradicate tumour cells. MOv18 IgE is a human-mouse chimaeric IgE antibody specific for the tumour antigen associated with ovarian carcinoma, Folate Binding Protein (FBP). The human ovarian carcinoma cell line, IGROV1, was used as the FBP-expressing tumour-target cell population in the study of IgE-mediated killing *in vitro* (Bénard *et al.*, 1985). IGROV1 cells are proposed to provide a suitable target for ADCC by FBP-specific antibodies, due to their high level of FBP expression and the high affinity with which FBP is bound by MOv18 IgE and MOv18 IgG (~ 10^9 M^{-1}) (Coney *et al.*, 1994; Gould *et al.*, 1999). These tumour-antigen properties are known to confer upon tumour cells, susceptibility to antibody-mediated killing.

Although FBP is functionally associated with signalling molecules in the cell membrane (Miotti *et al.*, 2000), the cross-linking (by whole, bivalent antibody) of FBP expressed by IGROV1 cells is not sufficient to initiate signalling responses which negatively affect cell viability (as shown in Chapter 3 of this Thesis, and also in Coney *et al.*, 1994 and Gould *et al.*, 1999). This might be a disadvantage of FBP-specific anti-cancer antibodies, as tumour cell killing mediated through the tumour antigen, independently of the antibody Fc region, is an important determinant of anti-cancer antibody efficacy (Tutt *et al.*, 1998). However, it is important to note that the specificity of an anti-cancer antibody of the IgE (or indeed any) isotype is interchangeable, and MOv18 IgE merely serves as a model to prove the principle that an anti-cancer antibody with an Fc region of the IgE isotype, will recruit an immune response effectively able to mediate tumour cell death, *in vitro* and / or *in vivo*. Therefore, the lack of Fc-independent activity of MOv18 IgE in work described in this Thesis is in fact advantageous.

A novel three-colour flow cytometric antibody-dependent cytotoxicity / phagocytosis assay was designed and set-up, as described in Chapter 4. The main benefit of this killing assay is its ability to quantify those tumour cells that have been killed by cytotoxicity in addition to those that are phagocytosed by effectors during the course of the assay. This ADCCP assay was used to assess the capacity of monocytes and eosinophils to act as MOv18-mediated effector cells of IGROV1 tumour cell killing. The effector to target cell ratio, time period of effector and target cell incubation with MOv18 IgE, and concentration of MOv18 IgE which gave the highest level of IGROV1 tumour cell killing by U937 monocytes were determined. As such, U937 monocytes were able to mediate tumour cell death in the presence of MOv18 IgE, which was significantly higher than in the presence of control antibody, anti-NP IgE. Tumour cell killing was also observed when primary monocytes were used in equivalent assays, in place of U937 monocytes.

Although MOv18 IgE-dependent primary monocyte-mediated killing of IGROV1 tumour cells is low, this ability of primary monocytes to kill IGROV1 tumour cells in a MOv18 IgE-dependent manner was particularly impressive in light of the following reasons. Firstly, as reported previously (Reischl *et al.*, 1996; Karagiannis *et al.*, 2003) and demonstrated in Chapter 3 of this Thesis, only around one third of peripheral blood monocytes express FcεRI, of which a proportion may already be occupied with endogenous IgE, preventing MOv18 IgE binding. Secondly, the population of monocytes used were only 70 – 80 % pure, and as such, used at an actual effector to target ratio of potentially as low as 0.7:1 (when mixed at a ratio of 1:1). Thirdly, the time-period for which effector and target cells were incubated together with MOv18 IgE was only 2.5 hours. Therefore, the level of tumour cell killing by primary monocytes may be significantly improved by optimisation of these parameters.

Using the nude mouse model described in Chapter 6 of this Thesis, a similar population of primary monocytes was unable to improve the survival of tumour-bearing nude mice; potential explanations for this are discussed in section 6.5. In the future, the ability of monocytes to mediate MOv18 IgE-dependent tumour cell killing in this model will be assessed by comparison of monocyte-depleted and reconstituted PBMC, to whole PBMC. However, HUA-bearing nude mice treated with U937 monocytes plus MOv18 IgE did survive longer than control mice. This may reflect the enhanced capacity of these cells to survive in these mice due to the fact that they are a transformed cell line. Alternatively, as the clone of U937 monocytes used for experiments described in this Thesis appear to bind IgE only via CD23 and not FcεRI, these results may reflect the greater efficacy of CD23 over FcεRI, in IgE-dependent activation of monocytes for tumour cell killing *in vivo*.

Supporting a role for CD23 expressed by U937 monocytes in killing of HUA tumour cells in nude mice, is the observation by Dr. Sophia Karagiannis (personal communication) that HUA tumour-bearing nude mice treated with IL-4-stimulated U937 monocytes plus MOv18 IgE survived longer than equivalent mice treated with unstimulated U937 monocytes plus MOv18 IgE. Stimulation of monocytes with IL-4 is known to upregulate expression of CD23. This potential involvement of CD23 in mediating IgE-dependent tumour cell killing *in vivo* is significant, as associated with monocyte migration into tissue (or tumours) is their maturation into macrophages, a process which involves an upregulation in CD23 expression; tissue-dwelling macrophages may then be activated by IL-4, which stimulates further expression of CD23 (Gordon, 2003).

Also shown in Chapter 5, was the ability of a pure population of peripheral blood eosinophils to effectively mediate IGROV1 tumour cell killing. This is the first report of IgE-dependent tumour cell killing by freshly purified human peripheral blood eosinophils *in vitro*.

Previously, a number of mouse models of cancer have shown eosinophil-dependent tumour cell killing (Tepper *et al.*, 1989; Tepper *et al.*, 1992; Reali *et al.*, 2001; Mattes *et al.*, 2004) in response to IL-4. As discussed in section 1.1.1, eosinophils are commonly found to infiltrate human tumours. Together, these results suggest that it might be possible to manipulate these eosinophils in human patients; mast cells located in and around the tumour area would become sensitised with tumour-specific IgE following treatment, and cross-linking of FcεRI-bound IgE by tumour antigen would lead to mast cell degranulation, involving the release of IL-4 and IL-5. The inflammation associated with mast cell and subsequent eosinophil activation might then lead to recruitment of additional eosinophils and other effector cell types, including basophils, monocytes and T cells and an enhancement of the anti-tumour inflammatory response. In addition, IL-4 treatment of eosinophils may drive their differentiation and expansion into 'Th2-cytokine' producers (Pericle *et al.*, 1994; Chen *et al.*, 2004); the effect of this would be further IL-4 production, and positive feedback.

Unfortunately, like primary monocytes, purified human eosinophils were unable to mediate the improved survival of nude mice, as described in Chapter 6 of this thesis. As discussed in section 6.6, these negative results may relate to the failure of primary monocytes and eosinophils to survive in the mice for sufficient time to mediate an anti-tumour effector function. The *in vivo* survival of eosinophils may have been improved by co-injection of IL-5. The role of eosinophils in mediating killing of HUA tumour cells in the nude mouse model is currently being determined by Dr. S. Karagiannis, by assessing the ability of a population of eosinophil-supplemented PBMC plus MOv18 IgE, compared to whole PBMC plus MOv18 IgE, in mediating the improved survival of HUA-tumour-bearing nude mice.

In contrast to IgE, neither monocytes (U937 and primary) nor eosinophils were able to kill tumour cells in a MOv18 IgG1-dependent manner, within the parameters used in experiments described in this Thesis. A suitable positive control is now required to confirm these results. Although it is possible that given the right conditions *e.g.*, a greater effector to target ratio and increased duration of incubation of effector and target cells with MOv18 IgG1, that MOv18 IgG1-dependent killing of IGROV1 tumour cell targets may be increased, results of experiments described in this Thesis suggest that IgE is a more sensitive trigger than IgG for initiating ADCC of tumour cell targets. Similarly, treatment of HUA-bearing nude mice with PBMC plus MOv18 IgE but not MOv18 IgG1, was able to confer a survival advantage (Karagiannis *et al.*, 2003). Tumour-bearing mice treated with human PBMC in combination with MOv18 IgE survived for a mean of 40±17 days compared to 26±11 days for mice treated with PBMC alone, and 21±7 days for mice treated with PBMC and MOv18 IgG. This ability of PBMC plus MOv18 IgE, but not MOv18 IgG, to mediate improved survival of nude mice replicates (in a different system) those results obtained in Gould *et al.*,

1999, where MOv18 IgE was more effective than MOv18 IgG (in combination with PBMC) in prolonging inhibition of growth of a subcutaneously growing (IGROV1) ovarian cancer xenograft in SCID mice. These results provide further support for the ability of tumour-specific IgE to mediate a more effective anti-tumour immune response than IgG against tumour cells *in vivo*.

One disadvantage of the nude mouse xenograft model described in Chapter 6 (and discussed above), is that the IgE-mediated anti-tumour immune response is limited to those human cellular effector cells injected, and by the duration for which these cells survive in the mice. Injected human effector cells included either PBMC (which lack eosinophils), an enriched population of monocytes, or a pure population of eosinophils. Therefore mast cells, the primary mediators of an allergic immune response, have been excluded. These experiments are therefore likely to underestimate the beneficial effects of treatment of cancer with MOv18 IgE. The corollary, however, is that this model also does not provide an accurate assessment of the potential that treatment with MOv18 IgE might cause anaphylactic shock. Therefore, two new, more physiological models were set up, each using an immunocompetent host, the 'humanised' hFcεRIα transgenic mouse and the WAG rat. This involved the optimisation of the growth of the syngeneic FBP-expresssing tumour cell lines, C26tFR and CC531tFR, to cause death of the animals within a suitable time frame. The ability of MOv18 IgE to mediate beneficial effects on the survival of C26tFR tumour-bearing hFcεRI Tg mice, and or CC531tFR tumour-bearing WAG rats, can now be assessed. Furthermore, any toxicity that might be associated with MOv18 IgE therapy can be studied. More detailed suggestions for preliminary experiments have been made in Chapter 6; in brief, the suggested experiments were intended to address both the efficacy of MOv18 IgE treatment in mediating the improved survival of tumour-bearing animals, in addition to assessing the potential of MOv18 IgE therapy in causing anaphylactic shock.

Tumour-bearing WAG rats treated with MOv18 IgE that show a survival advantage, could be studied for the presence of tumour-specific $CD4^+$ or $CD8^+$ T cells, and serum tumour-specific antibodies of different isoytpes, as a sign of the generation of an active anti-tumour immune response. As discussed in section 1.4.3, the acquisition of anti-tumour immunity by treatment with MOv18 IgE has been proved in principle, in experiments described by Reali *et al.*, 2001. Presentation of tumour-antigen is likely to be enhanced by treatment of tumours with IgE, in part due to the inflammatory environment created by activation of innate immune responses at the tumour site, but also due to the known role of both FcεRI (expressed by Langerhans cells in tissues) and CD23 (on macrophages and B

cells) in antigen presentation. In addition CD23 expression on macrophages would be upregulated in response to IL-4, potentially amplifying presentation of tumour antigen further.

Alongside *in vivo* studies of MOv18 IgE activity, future work on this project should include further *in vitro* studies to determine the mechanisms by which each effector cell type mediates tumour cell killing, beyond simply stating 'cytotoxicity' or 'phagocytosis'. Tumour-cell killing mechanisms may include the secretion of oxidative metabolites, nitric oxide or cytokines such as TNF-α. Furthermore, it is necessary to determine which IgE receptor it is, FcεRI and / or CD23, through which killing is triggered with each cell type, to be sure that at least one of these receptors is involved in mediating tumour-cell death, and to exclude a role for a third IgE receptor (*e.g.*, εBP, briefly introduced in section 1.3.8). It would also be useful to determine the capacity of both mast cells and basophils, primary mediators of the allergic response, to act as MOv18 IgE-dependent effectors of tumour cell killing *in vitro*. Furthermore, the capacity of different cell type combinations, *e.g.*, basophils and monocytes, to mediate MOv18 IgE-dependent tumour cell killing, could also be studied.

Experiments described in this Thesis, provide support, further to that provided by Gould *et al.*, 1999 and Karagiannis *et al.*, 2003, for the proposal that tumour-specific IgE antibodies might be efficaciously used for the immunotherapy of cancer. Results of experiments described in this thesis suggest that IgE receptor-expressing cells, including monocytes and eosinophils (which infiltrate tumours), may be conferred with tumouricidal activity when activated with a tumour-specific IgE antibody. Harnessing this arm of the immune system and re-directing it towards tumour cells, may result in the successful induction of a passive immune response against tumours of solid tissues. Treatment of cancer with tumour-specific monoclonal antibodies allows for the specific killing of tumour cells with minimal cross-reactivity with normal cells; this is in great contrast to the unwanted cell killing occurring with traditional chemotherapy and radiation therapy. Manipulation of the predominantly tissue-based IgE-mediated immune response by use of tumour-specific antibodies of the IgE isotype may improve the success of monoclonal antibody therapy for the treatment of solid tumours, as long as the side effects can be shown to be preferable to the cancer itself.

8.2 Implications of the high affinity interaction between IgE and FcεRI

As discussed in Chapter 1 of this Thesis, the high affinity with which IgE binds FcεRI is proposed to be responsible for the ability of IgE to tenaciously bind FcεRI-expressing mast cells in tissues, and basophils in blood. In this way, the allergen-specific IgE produced by B cells of allergic individuals is able to sensitise these cell types, leaving the individual essentially permanently primed to make an immediate response upon allergen challenge. In Chapter 7 of this Thesis, experiments were performed to see if IgE could be made less anaphylactogenic by reducing its affinity for FcεRI; it was expected that the lower affinity of R334S IgE for FcεRI would cause it to diffuse out of the tissue faster, correlating with a reduction in anaphylaxis upon antigen challenge. To this end, Dr. Jianguo Shi cloned and expressed a human anti-NP IgE which was mutated in both its Cε3 domains (an arginine for serine substitution at position 334, R334S), to give it a 33-fold reduced affinity FcεRI, compared to wild type IgE. 'Humanised' FcεRI transgenic mice (which bind human IgE) were then sensitised in one ear with wild type IgE, and in the other with R334S IgE, for binding to resident mast cells; mice received intravenous antigen challenge at timepoints thereafter.

These experiments show that despite there being identical amounts of wild type and R334S anti-NP IgE in the ears of these mice, the intensity of anaphylaxis occurring in mouse ears sensitised with R334S anti-NP IgE was consistently lower than in those sensitised with wild type IgE. These results suggest that the intensity of the (mast cell) response, mediated by cross-linking of FcεRI at the cell surface, is proportional to the affinity of the IgE-FcεRI interaction. These are particularly interesting results, which support the proposal that IgE might be more successfully used than IgG in immunotherapy of cancer. The IgE-receptor-expressing cells found in and around tumour areas might be triggered to kill tumour cells by sensitisation with relatively less antibody (IgE) than would be required for another antibody isotype (IgG), which binds its Fc receptors with lower affinity.

It is interesting to note that studies are currently underway to enhance the affinity of IgG binding to FcγRIII, relative to FcγRII; the rationale for this work, is that if tumour-specific antibodies of the IgG isotype could be manipulated to bind preferentially to the stimulatory receptor FcγRIII over FcγRIIb, then they may be able to trigger effector cells expressing both these FcγR, to mediate more effective tumour cell killing responses (reviewed in Weiner and Carter, 2005). Clynes *et al.*, 2000, have used mouse models to demonstrate the benefits of reducing FcγRIIb involvement in IgG-mediated anti-tumour immune responses. These studies assessed the efficacy of Rituximab and Trastuzumab in enhancing the survival of tumour-bearing mice either deficient, or not, in FcγRIIb. Results showed a survival

advantage in mice treated with either anti-cancer antibody, in FcγRII-deficient mice, over wild type controls. Interestingly, it was thought that the increased effector cell activity was contributed primarily by monocytes (which express both FcγRII and FcγRIII), highlighting the importance of monocyte manipulation in antibody-mediated tumour cell killing, a cell type which may be more successfully manipulated using IgE.

These results also have unexpected, but highly significant implications for the design of a therapeutic agent for the treatment of allergy and asthma. The IgE-FcεRI interaction represents a fundamental therapeutic target for inhibition of the allergic immune response. The beneficial effects of inhibiting the interaction between IgE and FcεRI, have recently been demonstrated with the therapeutic anti-IgE antibody Omalizumab, by its ability to abolish the symptoms of allergy and asthma. However, a major barrier to the successful production of such a therapeutic agent has been the requirement for it to compete with the extremely high affinity of the interaction between IgE and FcεRI. Moreover, it must do so with such efficacy that even a small number of FcεRI do not become occupied with IgE; the formation of FcεRI dimers has been shown to be sufficient for mast cell activation (Segal, 1977). Work described in Chapter 7 of this Thesis has shown that it may not in fact be necessary to completely block IgE binding to FcεRI, but only to reduce the affinity of the interaction by approximately 33-fold to achieve a reduction in the intensity of IgE-mediated immune responses *in vivo*. As discussed in Chapter 7, the design of a small molecule allosteric inhibitor of IgE may be one way by which the affinity of the interaction can be suitably decreased. The advantage of a small molecule allosteric inhibitor compared to the therapeutic antibody, Omalizumab, is that it would be cheaper to produce and also able to be administered orally or topically; it could therefore be widely available to all allergy sufferers.

It would be interesting to determine the mechanism by which IgE binding to FcεRI with lower affinity leads to anaphylactic responses of reduced intensity. The faster off-rate of R334S compared to wild type IgE from FcεRIα (shown in Table 7.1) suggests that in the tissue R334S anti-NP IgE might be associating, dissociating and re-associating faster than wild type anti-NP IgE does with FcεRI; this may be responsible for the reduced intensity of anaphylaxis through a kinetic proof reading mechanism (as speculated in section 7.8). If this were the case, the reduced intensity of anaphylaxis could be explained by an inability of R334S anti-NP IgE to hold together the FcεRI aggregate for sufficient time for the response to go to completion (full degranulation of the mast cell) (Torigoe *et al.*, 1997 and 1998).

In vitro experiments could be used to determine whether or not a 'kinetic proofreading' mechanism is the reason for the reduced intensity of anaphylactic responses

seen when mast cells are sensitised with lower affinity IgE. One method that might be used to test this, is to use either a cell line expressing human FcεRI (*e.g.*, RBL cells transfected with human FcεRI α-chain) or bone marrow derived mast cells from hFcεRI Tg mice, to compare hexosaminidase release following aggregation of an equal number of FcεRI at the cell surface with R334S compared to wild type IgE. Alternatively, following aggregation of (an equal number of) FcεRI by either R334S or wild type IgE, the various components of the downstream signalling pathway could be immunoprecipitated, and their phosphorylation status compared. Experiments of this type are currently being performed by Dr. James Hunt, to test the kinetic proofreading hypothesis.

If indeed the reduced intensity of anaphylaxis triggered by a lower-affinity IgE (R334S) was based on a mechanism of kinetic proofreading, another potential way of manipulating this mechanism as a therapy for allergy and asthma, may be to treat patients with a low affinity IgE (such as R334S IgE) with an irrelevant specificity, such that it will persist in the tissue and quickly associate and dissociate from FcεRI on mast cells faster than wild type allergen-specific IgE. The effect of this may be the 'hoarding' of Lyn kinase, preventing wild type IgE signalling responses from going to completion in response to allergen challenge. One disadvantage of such treatment however, is likely to be an upregulation of FcεRI on the cells in response to the higher serum IgE levels.

8.3 Final comment

In section 1.5 of Chapter 1, the aims of this Thesis were indicated as being two-fold:

- To assess the efficacy of MOv18 IgE in triggering immune responses against tumours, both *in vitro* and *in vivo*.

- To address how the affinity of the IgE-FcεRI interaction impacts on the intensity of IgE-mediated immune responses *in vivo*.

Both of these aims have been accomplished. As a result, this Thesis illustrates that tumour-specific IgE antibodies might be successfully used to harness an immune response, typically encountered towards innocuous antigens in allergic individuals, to instead kill tumour cells in cancer patients.

References:

Allen,J.M. and Seed,B. (1989). Isolation and expression of functional high-affinity Fc receptor complementary DNAs. Science *243*, 378-381.

Asai,K., Kitaura,J., Kawakami,Y., Yamagata,N., Tsai,M., Carbone,D.P., Liu,F.T., Galli,S.J., and Kawakami,T. (2001). Regulation of mast cell survival by IgE. Immunity. *14*, 791-800.

Bayon,Y., Alonso,A., and Sanchez,C.M. (1998). IgE/DNP complexes induce nitric oxide synthesis in rat peritoneal macrophages by a mechanism involving CD23 and NF-κB activation. Biochem. Biophys. Res. Commun. *242*, 570-574.

Beavil,A.J., Edmeades,R.L., Gould,H.J., and Sutton,B.J. (1992). Alpha-helical coiled-coil stalks in the low-affinity receptor for IgE (FcεRII/CD23) and related C-type lectins. Proc. Natl. Acad. Sci. U.S.A *89*, 753-757.

Benard,J., Da Silva,J., De Blois,M.C., Boyer,P., Duvillard,P., Chiric,E., and Riou,G. (1985). Characterization of a human ovarian adenocarcinoma line, IGROV1, in tissue culture and in nude mice. Cancer Res. *45*, 4970-4979.

Bieber,T., de la,S.H., Wollenberg,A., Hakimi,J., Chizzonite,R., Ring,J., Hanau,D., and de la,S.C. (1992). Human epidermal Langerhans cells express the high affinity receptor for IgE (FcεRI). J. Exp. Med. *175*, 1285-1290.

Bennich,H.H., Ishizaka,K., Johansson,S.G., Rowe,D.S., Stanworth,D.R., and Terry,W.D. (1968). Immunoglobulin E. A new class of human immunoglobulin. Immunochemistry. *5*, 327-328.

Bettler,B., Hofstetter,H., Rao,M., Yokoyama,W.M., Kilchherr,F., and Conrad,D.H. (1989). Molecular structure and expression of the murine lymphocyte low-affinity receptor for IgE (FcεRII). Proc. Natl. Acad. Sci. U. S. A *86*, 7566-7570.

Bingle,L., Brown,N.J. and Lewis,C. (2002). The role of tumour-associated macrophages in tumour progression: implications for new anticancer therapies. Journal of Pathology. *196*,254-265.

Blank,U., Ra,C., Miller,L., White,K., Metzger,H., and Kinet,J.P. (1989). Complete structure and expression in transfected cells of high affinity IgE receptor. Nature *337*, 187-189.

Blank,U. and Rivera,J. (2004). The ins and outs of IgE-dependent mast cell exocytosis. Trends in Immunology. *25*, 266-273.

Bonnefoy,J.Y., Henchoz,S., Hardie,D., Holder,M.J., and Gordon,J. (1993). A subset of anti-CD21 antibodies promote the rescue of germinal centre B cells from apoptosis. Eur. J. Immunol. *23*, 969-972.

Borkowski,T.A., Jouvin,M.H., Lin,S.Y., and Kinet,J.P. (2001). Minimal requirements for IgE-mediated regulation of surface FcεRI. J. Immunol. *167*, 1290-1296.

Bottaro,F., Tomassetti,A., Canevari,S., Miotti,S., Ménard,S., Colnaghi,M., (1993). Gene transfection and expression of the ovarian carcinoma marker folate binding protein on NIH/3T3 cells increases cell growth *in vitro* and *in vivo*. Cancer Res. *53*, 5791-5796.

Borish,L., Mascali,J.J., and Rosenwasser,L.J. (1991). IgE-dependent cytokine production by human peripheral blood mononuclear phagocytes. J. Immunol. *146*, 63-67.

Bruggemann,M., Williams,G.T., Bindon,C.I., Clark,M.R., Walker,M.R., Jefferis,R., Waldmann,H., and Neuberger,M.S. (1987). Comparison of the effector functions of human immunoglobulins using a matched set of chimeric antibodies. J. Exp. Med. *166*, 1351-1361.

Bruggemann,M. and Neuberger,M.S. (1996). Strategies for expressing human antibody repertoires in transgenic mice. Immunol. Today *17*, 391-397.

Brunner,K.T., Mauel,J., Cerottini,J.C., and Chapuis,B. (1968). Quantitative assay of the lytic action of immune lymphoid cells on 51-Cr-labelled allogeneic target cells *in vitro*; inhibition by isoantibody and by drugs. Immunology *14*, 181-196.

Buist,M., Molthoff,C., Kenemans,P. and Meiger,C. (1985). Distribution of OV-TL 3 and MOv18 in normal and malignant ovarian tissue. J. Clin. Pathol. *48*, 631-636.

Budzynski,W. and Radzikowski,C. (1994). Cytotoxic cells in immunodeficient athymic mice. Immunopharmacol. Immunotoxicol. *16*, 319-346.

Cameron,A.J., McDonald,K.J., Harnett,M.M., and Allen,J.M. (2002). Differentiation of the human monocyte cell line, U937, with dibutyryl cyclicAMP induces the expression of the inhibitory Fc receptor, FcγRIIb. Immunol. Lett. *83*, 171-179.

Campbell,I.G., Jones,T.A., Foulkes,W.D., and Trowsdale,J. (1991). Folate-binding protein is a marker for ovarian cancer. Cancer Res. *51*, 5329-5338.

Campbell,A.M., Vignola,A.M., Chanez,P., Godard,P., and Bousquet,J. (1994). Low-affinity receptor for IgE on human bronchial epithelial cells in asthma. Immunology *82*, 506-508

Carter,P. (2001). Improving the efficacy of antibody-based cancer therapies. Nat. Rev. Cancer *1*, 118-129.

Cass,R.M. and Andersen,B.R. (1968). The disapperance rate of skin-sensitizing antibody activity after intradermal administration. J. Allergy *42*, 29-35.

Chen,B.H., Ma,C., Caven,T.H., Chan-Li,Y., Beavil,A., Beavil,R., Gould,H., and Conrad,D.H. (2002). Necessity of the stalk region for IgE interaction with CD23. Immunology *107*, 373-381.

Chang,T.W. (2000). The pharmacological basis of anti-IgE therapy. Nat. Biotechnol. *18*, 157-162.

Chang,H.L., Gillett,N., Figari,I., Lopez,A.R., Palladino,M.A., and Derynck,R. (1993). Increased TGF-β expression inhibits cell proliferation *in vitro*, yet increases tumorigenicity and tumor growth of Meth A sarcoma cells. Cancer Res. *53*, 4391-4398.

Clynes,R., Takechi,Y., Moroi,Y., Houghton,A., and Ravetch,J.V. (1998). Fc receptors are required in passive and active immunity to melanoma. Proc. Natl. Acad. Sci. U. S. A *95*, 652-656.

Clynes,R.A., Towers,T.L., Presta,L.G., and Ravetch,J.V. (2000). Inhibitory Fc receptors modulate *in vivo* cytoxicity against tumor targets. Nat. Med. *6*, 443-446.

Coney,L.R., Tomassetti,A., Carayannopoulos,L., Frasca,V., Kamen,B.A., Colnaghi,M.I., and Zurawski,V.R., Jr. (1991). Cloning of a tumor-associated antigen: MOv18 and MOv19 antibodies recognize a folate-binding protein. Cancer Res. *51*, 6125-6132.

Coney,L.R., Tomassetti,A., Carayannopoulos,L., Frasca,V., Kamen,B.A., Colnaghi,M.I., and Zurawski,V.R., Jr. (1991). Cloning of a tumor-associated antigen: MOv18 and MOv19 antibodies recognize a folate-binding protein. Cancer Res. *51*, 6125-6132.

Conrad,D.H., Wingard,J.R., and Ishizaka,T. (1983). The interaction of human and rodent IgE with the human basophil IgE receptor. J. Immunol. *130*, 327-333.

Conrad,D.H. (1990). FcεRII/CD23: the low affinity receptor for IgE. Annu. Rev. Immunol. *8*, 623-645.

Cragg,M.S., French,R.R., and Glennie,M.J. (1999). Signaling antibodies in cancer therapy. Curr. Opin. Immunol. *11*, 541-547.

Denkers,E., Badger,C., Ledbetter,J. and Bernstein,I. (1985). Influence of antibody isotype on passive serotherapy of lymphoma. J. Immunol. *135*, 2183-2186.

Derby,E., Reddy,V., Kopp,W., Nelson,E., Baseler,M., Sayers,T., and Malyguine,A. (2001). Three-color flow cytometric assay for the study of the mechanisms of cell-mediated cytotoxicity. Immunol. Lett. *78*, 35-39.

Dombrowicz,D., Flamand,V., Brigman,K.K., Koller,B.H., and Kinet,J.P. (1993). Abolition of anaphylaxis by targeted disruption of the high affinity IgE receptor α-chain gene. Cell *75*, 969-976.

Dombrowicz,D., Brini,A.T., Flamand,V., Hicks,E., Snouwaert,J.N., Kinet,J.P., and Koller,B.H. (1996). Anaphylaxis mediated through a humanized high affinity IgE receptor. J. Immunol. *157*, 1645-1651.

Dombrowicz,D., Lin,S., Flamand,V., Brini,A.T., Koller,B.H., and Kinet,J.P. (1998). Allergy-associated FcRβ is a molecular amplifier of IgE- and IgG-mediated *in vivo* responses. Immunity. *8*, 517-529.

Dombrowicz,D., Quatannens,B., Papin,J.P., Capron,A., and Capron,M. (2000). Expression of a functional FcεRI on rat eosinophils and macrophages. J. Immunol. *165*, 1266-1271.
Dombrowicz,D. and Capron,M. (2001). Eosinophils, allergy and parasites. Curr. Opin. Immunol. *13*, 716-720.

Donnadieu,E., Jouvin,M.H., and Kinet,J.P. (2000). A second amplifier function for the allergy-associated FcεRIβ subunit. Immunity. *12*, 515-523.

Donnadieu,E., Jouvin,M.-H., Rana,S., Moffatt,M., Cookson,W. and Kinet,J.-P. (2003). Competing functions encoded in the allergy-associated FcεRIβ gene. Immunity. *18*, 665-674.

Dunn,G.P., Bruce,A.T., Ikeda,H., Old,L.J., and Schreiber,R.D. (2002). Cancer immunoediting: from immunosurveillance to tumor escape. Nat. Immunol. *3*, 991-998.

Dyer,M., Hale,G., Hayhoe,F. and Waldmann,H. (1989). Effects of Campath-1 antibodies *in vivo* in patients with lymphoid malignancies: influence of antibody isotype. Blood. *73*, 1431-1439.

Eiseman,E. and Bolen,J.B. (1992). Engagement of the high-affinity IgE receptor activates src protein-related tyrosine kinases. Nature *355*, 78-80.

Elovic,A., Galli,S.J., Weller,P.F., Chang,A.L., Chiang,T., Chou,M.Y., Donoff,R.B., Gallagher,G.T., Matossian,K., McBride,J., and . (1990). Production of TGF-α by hamster eosinophils. Am. J. Pathol. *137*, 1425-1434.

Fekete,E. (1938). A comparative morphological study of the mammary gland in a high and a low tumour strain of mice. Amer. J. Path. *14*. 557-578.

Garman,S.C., Wurzburg,B.A., Tarchevskaya,S.S., Kinet,J.P., and Jardetzky,T.S. (2000). Structure of the Fc fragment of human IgE bound to its high-affinity receptor FcεRI alpha. Nature *406*, 259-266.

Garman,S.C., Sechi,S., Kinet,J.P., and Jardetzky,T.S. (2001). The analysis of the human high affinity IgE receptor FcεRIα from multiple crystal forms. J. Mol. Biol. *311*, 1049-1062.

Geha,R.S., Helm,B., and Gould,H. (1985). Inhibition of the Prausnitz-Kustner reaction by an IgE fragment synthesized in E. coli. Nature *315*, 577-578.

Glennie,M.J. and Van de Winkel,J.G. (2003). Renaissance of cancer therapeutic antibodies. Drug Discov. Today *8*, 503-510.

Goldsmith,M.M., Cresson,D.H., and Askin,F.B. (1987). The prognostic significance of stromal eosinophilia in head and neck cancer. Otolaryngol. Head Neck Surg. *96*, 319-324.

Gordon,S. (2003). Alternative activation of macrophages. Nat. Rev. Immunol. *3*, 23-35.

Gould,H., Beavil,R., Reljić,R., Shi,J., Ma,C., Sutton,B. and Ghirlando,R. (1997). IgE homeostasis: is CD23 the safety switch? IgE Regulation: Molecular Mechanisms. John Wiley and Sons Ltd, pages 37-59.

Gould,H.J., Mackay,G.A., Karagiannis,S.N., O'Toole,C.M., Marsh,P.J., Daniel,B.E., Coney,L.R., Zurawski,V.R., Jr., Joseph,M., Capron,M., Gilbert,M., Murphy,G.F., and Korngold,R. (1999). Comparison of IgE and IgG antibody-dependent cytotoxicity *in vitro* and in a SCID mouse xenograft model of ovarian carcinoma. Eur. J. Immunol. *29*, 3527-3537.

Gould,H.J., Sutton,B.J., Beavil,A.J., Beavil,R.L., McCloskey,N., Coker,H.A., Fear,D., and Smurthwaite,L. (2003). The biology of IgE and the basis of allergic disease. Annu. Rev. Immunol. *21*, 579-628.

Gounni,A.S., Lamkhioued,B., Ochiai,K., Tanaka,Y., Delaporte,E., Capron,A., Kinet,J.P., and Capron,M. (1994). High-affinity IgE receptor on eosinophils is involved in defence against parasites. Nature *367*, 183-186.

Graziano,R.F. and Fanger,M.W. (1987). FcγRI and FcγRII on monocytes and granulocytes are cytotoxic trigger molecules for tumor cells. J. Immunol. *139*, 3536-3541.

Hagenaars,M., Ensink,N.G., Eggermont,A.M., van der Velde,E.A., van de Velde,C.J., Fleuren,G.J., and Kuppen,P.J. (2000). Endogenous natural killer cells do not play a role in antitumor effects induced by IL-2 in a syngeneic rat colon tumor model. Cancer Immunol. Immunother. *48*, 561-568.

Hale,G., Clark,M. and Waldmann,H. (1985). Therapeutic potential of rat monoclonal antibodies: Isotype specificity of antibody-dependent cell-mediated cytotoxicity with human lymphocytes. J. Immunol. *134*, 3056-3061.

Hanahan,D. and Weinberg,R. (2000). The hallmarks of cancer. Cell. *100*, 57-70

Hassner,A. and Saxon,A. (1984). Isotype-specific human suppressor T cells for IgE synthesis activated by IgE-anti-IgE immune complexes. J. Immunol. *132*, 2844-2849.

Heaney,L.G. and Robinson,D.S. (2005). Severe asthma treatment: need for characterising patients. Lancet *365*, 974-976.

Henry,A.J., Cook,J.P., McDonnell,J.M., Mackay,G.A., Shi,J., Sutton,B.J., and Gould,H.J. (1997). Participation of the N-terminal region of Cε3 in the binding of human IgE to its high-affinity receptor FcεRI. Biochemistry *36*, 15568-15578.

Herlyn,D. and Koprowski,H. (1982). IgG2a monoclonal antibodies inhibit human tumour growth through interaction with effector cells. Proc. Natl. Acad. Sci. USA. *79*, 4761-4765.

Holgate,S., Casale,T., Wenzel,S., Bousquet,J., Deniz,Y., and Reisner,C. (2005). The anti-inflammatory effects of omalizumab confirm the central role of IgE in allergic inflammation. J. Allergy Clin. Immunol. *115*, 459-465.

Horiuchi,K., Mishima,K., Ohsawa,M., Sugimura,M., and Aozasa,K. (1993). Prognostic factors for well-differentiated squamous cell carcinoma in the oral cavity with emphasis on immunohistochemical evaluation. J. Surg. Oncol. *53*, 92-96.

Hudson,P. and Souriau,C. (2003). Engineered antibodies. Nat. Med. *9*, 129-134.

Hung,K., Hayashi,R., Lafond-Walker,A., Lowenstein,C., Pardoll,D., and Levitsky,H. (1998). The central role of $CD4^+$ T cells in the antitumor immune response. J. Exp. Med. *188*, 2357-2368.

Hunt,J., Beavil,R.L., Calvert,R.A., Gould,H.J., Sutton,B.J., and Beavil,A.J. (2005). Disulfide Linkage Controls the Affinity and Stoichiometry of IgE Fcε3-4 Binding to FcεRI. J. Biol. Chem. *280*, 16808-16814.

Ishizaka,T., Helm,B., Hakimi,J., Niebyl,J., Ishizaka,K., and Gould,H. (1986). Biological properties of a recombinant human IgE fragment. Proc. Natl. Acad. Sci. U. S. A *83*, 8323-8327.

Jain,R.K. and Baxter,L.T. (1988). Mechanisms of heterogeneous distribution of monoclonal antibodies and other macromolecules in tumors: significance of elevated interstitial pressure. Cancer Res. *48*, 7022-7032.

Janeway,C. and Travers,P. Immunobiology: the immune system in health and disease. 4th Edition.

Jardieu,P.M. and Fick,R.B., Jr. (1999). IgE inhibition as a therapy for allergic disease. Int. Arch. Allergy Immunol. *118*, 112-115.

Johnston,R.B., Jr. (1988). Current concepts: immunology. Monocytes and macrophages. N. Engl. J. Med. *318*, 747-752.

Johnston,R. (1988). Monocytes and macrophages. The New England Journal of Medicine. *318*, 747-752

Jugens,R. (1997). Finally! The Brambell receptor (FcRB). Mediator of transmission of immunity and protection from catabolism for IgG. Immunol. Res. *16*:29-57.

Kalesnikoff,J., Huber,M., Lam,V., Damen,J.E., Zhang,J., Siraganian,R.P., and Krystal,G. (2001). Monomeric IgE stimulates signaling pathways in mast cells that lead to cytokine production and cell survival. Immunity. *14*, 801-811.

Kaminski,M., Kitamura., Maloney,D., Campbell,M. and Levy,R. (1986). Importance of antibody isotype in monoclonal anti-idotype therapy of a murine B cell lymphoma. A study of hybridoma class switch variants. J. Immunol. *136*, 1123-1130.

Kapp,D.S. and LiVolsi,V.A. (1983). Intense eosinophilic stromal infiltration in carcinoma of the uterine cervix: a clinicopathologic study of 14 cases. Gynecol. Oncol. *16*, 19-30.

Karagiannis,S.N., Warrack,J.K., Jennings,K.H., Murdock,P.R., Christie,G., Moulder,K., Sutton,B.J., and Gould,H.J. (2001). Endocytosis and recycling of the complex between CD23 and HLA-DR in human B cells. Immunology *103*, 319-331.

Karagiannis,S.N., Wang,Q., East,N., Burke,F., Riffard,S., Bracher,M.G., Thompson,R.G., Durham,S.R., Schwartz,L.B., Balkwill,F.R., and Gould,H.J. (2003). Activity of human monocytes in IgE antibody-dependent surveillance and killing of ovarian tumor cells. Eur. J. Immunol. *33*, 1030-1040.

Kawabe,T., Takami,M., Hosoda,M., Maeda,Y., Sato,S., Mayumi,M., Mikawa,H., Arai,K., and Yodoi,J. (1988). Regulation of FcεRII/CD23 gene expression by cytokines and specific ligands (IgE and anti-FcεRII monoclonal antibody). Variable regulation depending on the cell types. J. Immunol. *141*, 1376-1382.

Kayaba,H., Dombrowicz,D., Woerly,G., Papin,J.P., Loiseau,S., and Capron,M. (2001). Human eosinophils and human high affinity IgE receptor transgenic mouse eosinophils express low levels of high affinity IgE receptor, but release IL-10 upon receptor activation. J. Immunol. *167*, 995-1003.

Keegan,A.D. and Paul,W.E. (1992). Multichain immune recognition receptors: similarities in structure and signaling pathways. Immunol. Today *13*, 63-68.

Keler,T., Wallace,P.K., Vitale,L.A., Russoniello,C., Sundarapandiyan,K., Graziano,R.F., and Deo,Y.M. (2000). Differential effect of cytokine treatment on FcαRI- and FcγRI-mediated tumor cytotoxicity by monocyte-derived macrophages. J. Immunol. *164*, 5746-5752.

Keown,M.B., Ghirlando,R., Young,R.J., Beavil,A.J., Owens,R.J., Perkins,S.J., Sutton,B.J., and Gould,H.J. (1995). Hydrodynamic studies of a complex between the Fc fragment of human IgE and a soluble fragment of the FcεRI α-chain. Proc. Natl. Acad. Sci. U. S. A 92, 1841-1845.

Keown,M.B., Ghirlando,R., Mackay,G.A., Sutton,B.J., and Gould,H.J. (1997). Basis of the 1:1 stoichiometry of the high affinity receptor FcεRI-IgE complex. Eur. Biophys. J. 25, 471-476.

Khalife,J., Dunne,D.W., Richardson,B.A., Mazza,G., Thorne,K.J., Capron,A., and Butterworth,A.E. (1989). Functional role of human IgG subclasses in eosinophil-mediated killing of schistosomula of Schistosoma mansoni. J. Immunol. *142*, 4422-4427.

Khong,H.T. and Restifo,N.P. (2002). Natural selection of tumor variants in the generation of "tumor escape" phenotypes. Nat. Immunol. *3*, 999-1005.

Kita,H., Kaneko,M., Bartemes,K.R., Weiler,D.A., Schimming,A.W., Reed,C.E., and Gleich,G.J. (1999). Does IgE bind to and activate eosinophils from patients with allergy? J. Immunol. *162*, 6901-6911.

Kitaura,J., Song,J., Tsai,M., Asai,K., Maeda-Yamamoto,M., Mocsai,A., Kawakami,Y., Liu,F.T., Lowell,C.A., Barisas,B.G., Galli,S.J., and Kawakami,T. (2003). Evidence that IgE molecules mediate a spectrum of effects on mast cell survival and activation via aggregation of the FcεRI. Proc. Natl. Acad. Sci. U. S. A *100*, 12911-12916.

Kikutani,H. and Kishimoto,T. (1990). Molecular genetics and biology of two different species of FcεRII. Res. Immunol. *141*, 249-258.

Koenderman,L., Hermans,S.W., Capel,P.J., and Van de Winkel,J.G. (1993). Granulocyte-macrophage colony-stimulating factor induces sequential activation and deactivation of binding via a low-affinity IgG Fc receptor, hFcγRII, on human eosinophils. Blood *81*, 2413-2419.

Kohler,G. and Milstein,C. (1975). Continuous cultures of fused cells secreting antibody of predefined specificity. Nature *256*, 495-497.

Korzeniewski,C. and Callewaert,D.M. (1983). An enzyme-release assay for natural cytotoxicity. J. Immunol. Methods *64*, 313-320.

Kraft,S., Novak,N., Katoh,N., Bieber,T., and Rupec,R.A. (2002). Aggregation of the high-affinity IgE receptor FcεRI on human monocytes and dendritic cells induces NF-κB activation. J. Invest Dermatol. *118*, 830-837.

Kuppen,P.J., Basse,P.H., Goldfarb,R.H., van de Velde,C.J., Fleuren,G.J., and Eggermont,A.M. (1994). The infiltration of experimentally induced lung metastases of colon carcinoma CC531 by adoptively transferred IL-2-activated natural killer cells in WAG rats. Int. J. Cancer *56*, 574-579.

Laemmli,U.K. (1970). Cleavage of structural proteins during the assembly of the head of bacteriophage T4. Nature *227*, 680-685.

Lamers,M.C. and Yu,P. (1995). Regulation of IgE synthesis. Lessons from the study of IgE transgenic and CD23-deficient mice. Immunol. Rev. *148*, 71-95.

Lantero,S., Sacco,O., Scala,C., and Rossi,G.A. (1997). Stimulation of blood mononuclear cells of atopic children with the relevant allergen induces the release of eosinophil chemotaxins such as IL-3, IL-5, and GM-CSF. J. Asthma *34*, 141-152.

Lawson,D., Fewtrell,C., and Raff,M.C. (1978). Localized mast cell degranulation induced by concanavalin A-sepharose beads. Implications for the Ca^{2+} hypothesis of stimulus-secretion coupling. J. Cell Biol. *79*, 394-400.

Lee-MacAry,A.E., Ross,E.L., Davies,D., Laylor,R., Honeychurch,J., Glennie,M.J., Snary,D., and Wilkinson,R.W. (2001). Development of a novel flow cytometric cell-mediated cytotoxicity assay using the fluorophores PKH-26 and TO-PRO-3 iodide. J. Immunol. Methods *252*, 83-92.

Lencer,W. and Blumberg,R. (2004). A passionate kiss, then run: exocytosis and recycling of IgG by FcRn. Trends in cell Biology. *15*:5-9.

Letourneur,F., Hennecke,S., Demolliere,C., and Cosson,P. (1995). Steric masking of a dilysine endoplasmic reticulum retention motif during assembly of the human high affinity receptor for IgE. J. Cell Biol. *129*, 971-978.

Liu,F.-T., Albrandt,K., Mendel,E., Kulczycki,A., Jr., and Orida,N.K. (1985). Identification of an IgE-binding protein by molecular cloning. Proc. Natl. Acad. Sci. U.S.A. *82*, 4100-4104.

Liu,F.-T. (1993). S-type mammalian lectins in allergic inflammation. Immunology Today *14*, 486-490.

Lin,S., Cicala,C., Scharenberg,A.M., and Kinet,J.P. (1996). The FcεRI β-subunit functions as an amplifier of FcεRI γ-mediated cell activation signals. Cell *85*, 985-995.

Liu,Y.J., Cairns,J.A., Holder,M.J., Abbot,S.D., Jansen,K.U., Bonnefoy,J.Y., Gordon,J., and MacLennan,I.C. (1991). Recombinant 25-kDa CD23 and IL-1α promote the survival of germinal center B cells: evidence for bifurcation in the development of centrocytes rescued from apoptosis. Eur. J. Immunol. *21*, 1107-1114.

Lobo,E., Hansen,R. and Balthasar,J. (2004). Antibody pharmacokinetics and pharmacodynamics. J. Pharmaceutical Sci. *93*:2645-2668.

Lopez,A.F., Sanderson,C.J., Gamble,J.R., Campbell,H.D., Young,I.G., and Vadas,M.A. (1988). Recombinant human IL-5 is a selective activator of human eosinophil function. J. Exp. Med. *167*, 219-224.

Lowe,D., Fletcher,C.D., and Gower,R.L. (1984a). Tumour-associated eosinophilia in the bladder. J. Clin. Pathol. *37*, 500-502.

Lowe,D., Fletcher,C.D., Shaw,M.P., and McKee,P.H. (1984b). Eosinophil infiltration in keratoacanthoma and squamous cell carcinoma of the skin. Histopathology *8*, 619-625.

Maenaka,K., van der Merwe,P.A., Stuart,D.I., Jones,E.Y., and Sondermann,P. (2001). The human low affinity FcγRIIa, IIb, and III bind IgG with fast kinetics and distinct thermodynamic properties. J. Biol. Chem. *276*, 44898-44904.

Mantovani,A., Ming,W., Balotta,C., Abdeljalil,B. and Bottazzi,B. (1986). Origin and regulation of tumour-associated macrophages: the role of tumour-derived chemotactic factor. Biochimica et Biophysica Acta. *865*, 59-67.

Mantovani,A., Bottazzi,B., Colotta,F., Sozzani,S. and Ruco,L. (1992). The origin and function of tumour-associated macrophages. Immunology Today. *13*, 265-270.

Marquet,R.L., Westbroek,D.L., and Jeekel,J. (1984). Interferon treatment of a transplantable rat colon adenocarcinoma: importance of tumor site. Int. J. Cancer *33*, 689-692.

Mattes,J., Hulett,M., Xie,W., Hogan,S., Rothenberg,M.E., Foster,P., and Parish,C. (2003). Immunotherapy of cytotoxic T cell-resistant tumors by T helper 2 cells: an eotaxin and STAT6-dependent process. J. Exp. Med. *197*, 387-393.

Matzinger,P. (1998). An innate sense of danger. Semin. Immunol. *10*, 399-415.

Maurer,D., Fiebiger,E., Reininger,B., Wolff-Winiski,B., Jouvin,M.H., Kilgus,O., Kinet,J.P., and Stingl,G. (1994). Expression of functional high affinity IgE receptors (FcεRI) on monocytes of atopic individuals. J. Exp. Med. *179*, 745-750.

Mavromatis,B. and Cheson,B.D. (2003). Monoclonal antibody therapy of chronic lymphocytic leukemia. J. Clin. Oncol. *21*, 1874-1881.

Mavromatis,B.H. and Cheson,B.D. (2004). Novel therapies for chronic lymphocytic leukemia. Blood Rev. *18*, 137-148.

McBride,W.H. (1986). Phenotype and functions of intratumoral macrophages. Biochim. Biophys. Acta *865*, 27-41.

McDonnell,J.M., Calvert,R., Beavil,R.L., Beavil,A.J., Henry,A.J., Sutton,B.J., Gould,H.J., and Cowburn,D. (2001). The structure of the IgE Cε2 domain and its role in stabilizing the complex with its high-affinity receptor FcεRIα. Nat. Struct. Biol. *8*, 437-441.

McKeithan,T.W. (1995). Kinetic proofreading in T-cell receptor signal transduction. Proc. Natl. Acad. Sci. U. S. A *92*, 5042-5046.

Metzger,H., Alcaraz,G., Hohman,R., Kinet,J.P., Pribluda,V., and Quarto,R. (1986). The receptor with high affinity for IgE. Annu. Rev. Immunol. *4*, 419-470.

Metzger,H. (1992). Transmembrane signaling: the joy of aggregation. J. Immunol. *149*, 1477-1487.

Merluzzi,S., Figini,M., Colombatti,A., Canevari,S. and Pucillo,C. (2000). Humanised antibodies as potential drugs for therapeutic use. Adv. Clin. Path. *4*, 77-85.

Miller,L., Blank,U., Metzger,H., and Kinet,J.P. (1989). Expression of high-affinity binding of human IgE by transfected cells. Science *244*, 334-337.

Miotti,S., Canevari,S., Menard,S., Mezzanzanica,D., Porro,G., Pupa,S.M., Regazzoni,M., Tagliabue,E., and Colnaghi,M.I. (1987). Characterization of human ovarian carcinoma-associated antigens defined by novel monoclonal antibodies with tumor-restricted specificity. Int. J. Cancer *39*, 297-303.

Miotti,S., Bagnoli,M., Tomassetti,A., Colnaghi,M.I., and Canevari,S. (2000). Interaction of folate receptor with signaling molecules lyn and Gαi-3 in detergent-resistant complexes from the ovary carcinoma cell line IGROV1. J. Cell Sci. *113 Pt 2*, 349-357.

Mosier,D.E., Gulizia,R.J., Baird,S.M., and Wilson,D.B. (1988). Transfer of a functional human immune system to mice with severe combined immunodeficiency. Nature *335*, 256-259.

Molthoff,C.F., Prinssen,H.M., Kenemans,P., van Hof,A.C., den Hollander,W., and Verheijen,R.H. (1997). Escalating protein doses of chimeric monoclonal antibody MOv18 IgG in ovarian carcinoma patients: a phase I study. Cancer *80*, 2712-2720.

Montagnac,G., Molla-Herman,A., Bouchet,J., Yu,L.C., Conrad,D.H., Perdue,M.H., and Benmerah,A. (2005). Intracellular Trafficking of CD23: Differential Regulation in Humans and Mice by Both Extracellular and Intracellular Exons. J. Immunol. *174*, 5562-5572.

Munn,D.H. and Armstrong,E. (1993). Cytokine regulation of human monocyte differentiation *in vitro*: the tumor-cytotoxic phenotype induced by MCSF is developmentally regulated by IFN-γ. Cancer Res. *53*, 2603-2613.

Munn,D.H. and Cheung,N.K. (1989). Antibody-dependent antitumor cytotoxicity by human monocytes cultured with recombinant MCSF. Induction of efficient antibody-mediated antitumor cytotoxicity not detected by isotope release assays. J. Exp. Med. *170*, 511-526.

Nechansky,A., Aschauer,H., and Kricek,F. (1998). The membrane-proximal part of FcεRIα contributes to human IgE and antibody binding--implications for a general structural motif in Fc receptors. FEBS Lett. *441*, 225-230.

Nechansky,A., Robertson,M.W., Albrecht,B.A., Apgar,J.R., and Kricek,F. (2001). Inhibition of antigen-induced mediator release from IgE-sensitized cells by a monoclonal anti-FcεRI α-chain receptor antibody: implications for the involvement of the membrane-proximal α-chain region in FcεRI-mediated cell activation. J. Immunol. *166*, 5979-5990.

Novak,N., Kraft,S., and Bieber,T. (2001). IgE receptors. Curr. Opin. Immunol. *13*, 721-726.
Ouaaz,F., Paul-Eugene,N., Arock,M., Merle-Beral,H., Huerta,J.M., Debre,P., Kolb,J.P.,

Mossalayi,M.D., and Dugas,B. (1993). Maturation of human myelomonocytic leukemia cells following ligation of the low affinity receptor for IgE (FcεRII/CD23). Int. Immunol. *5*, 1251-1257.

Patry,C., Sibille,Y., Lehuen,A., and Monteiro,R.C. (1996). Identification of FcαR (CD89) isoforms generated by alternative splicing that are differentially expressed between blood monocytes and alveolar macrophages. J. Immunol. *156*, 4442-4448.

Paul-Eugene,N., Kolb,J.P., Abadie,A., Gordon,J., Delespesse,G., Sarfati,M., Mencia-Huerta,J.M., Braquet,P., and Dugas,B. (1992). Ligation of CD23 triggers cAMP generation and release of inflammatory mediators in human monocytes. J. Immunol. *149*, 3066-3071.

Pawankar,R. (2001). Mast cells as orchestrators of the allergic reaction: the IgE-IgE receptor mast cell network. Curr. Opin. Allergy Clin. Immunol. *1*, 3-6.

Payet,M. and Conrad,D.H. (1999). IgE regulation in CD23 knockout and transgenic mice. Allergy *54*, 1125-1129.

Pericle,F., Giovarelli,M., Colombo,M.P., Ferrari,G., Musiani,P., Modesti,A., Cavallo,F., Di Pierro,F., Novelli,F., and Forni,G. (1994). An efficient Th2-type memory follows CD8+ lymphocyte-driven and eosinophil-mediated rejection of a spontaneous mouse mammary adenocarcinoma engineered to release IL-4. J. Immunol. *153*, 5659-5673.

Pollard,J.W. (2004). Tumour-educated macrophages promote tumour progression and metastasis. Nat. Rev. Cancer *4*, 71-78.

Pretlow,T.P., Keith,E.F., Cryar,A.K., Bartolucci,A.A., Pitts,A.M., Pretlow,T.G., Kimball,P.M., and Boohaker,E.A. (1983). Eosinophil infiltration of human colonic carcinomas as a prognostic indicator. Cancer Res. *43*, 2997-3000.

Pribluda,V.S., Pribluda,C., and Metzger,H. (1994). Transphosphorylation as the mechanism by which the high-affinity receptor for IgE is phosphorylated upon aggregation. Proc. Natl. Acad. Sci. U. S. A *91*, 11246-11250.

Ra,C., Jouvin,M.H., and Kinet,J.P. (1989). Complete structure of the mouse mast cell receptor for IgE (FcεRI) and surface expression of chimeric receptors (rat-mouse-human) on transfected cells. J. Biol. Chem. *264*, 15323-15327.

Radosevic,K., Garritsen,H.S., Van Graft,M., De Grooth,B.G., and Greve,J. (1990). A simple and sensitive flow cytometric assay for the determination of the cytotoxic activity of human natural killer cells. J. Immunol. Methods *135*, 81-89.

Ramaswamy,K., Hakimi,J., and Bell,R.G. (1994). Evidence for an IL-4-inducible IgE uptake and transport mechanism in the intestine. J. Exp. Med. *180*, 1793-1803.

Rangarajan,A. and Weinberg,R.A. (2003). Opinion: Comparative biology of mouse versus human cells: modelling human cancer in mice. Nat. Rev. Cancer *3*, 952-959.

Ravetch,J.V. and Kinet,J.P. (1991). Fc receptors. Annu. Rev. Immunol. *9*, 457-492.

Reali,E., Greiner,J.W., Corti,A., Gould,H.J., Bottazzoli,F., Paganelli,G., Schlom,J., and Siccardi,A.G. (2001). IgEs targeted on tumor cells: therapeutic activity and potential in the design of tumor vaccines. Cancer Res. *61*, 5517-5522.

Reischl,I.G., Corvaia,N., Effenberger,F., Wolff-Winiski,B., Kromer,E., and Mudde,G.C. (1996). Function and regulation of FcεRI expression on monocytes from non-atopic donors. Clin. Exp. Allergy *26*, 630-641.

Rigby,L.J., Trist,H., Snider,J., Hulett,M.D., Hogarth,P.M., Rigby,L.J., and Epa,V.C. (2000). Monoclonal antibodies and synthetic peptides define the active site of FcεRI and a potential receptor antagonist. Allergy *55*, 609-619.

Riske,F., Hakimi,J., Mallamaci,M., Griffin,M., Pilson,B., Tobkes,N., Lin,P., Danho,W., Kochan,J., and Chizzonite,R. (1991). High affinity human IgE receptor (FcεRI). Analysis of functional domains of the α-subunit with monoclonal antibodies. J. Biol. Chem. *266*, 11245-11251.

Rivoltini,L., Viggiano,V., Spinazze,S., Santoro,A., Colombo,M.P., Takatsu,K., and Parmiani,G. (1993). *In vitro* anti-tumor activity of eosinophils from cancer patients treated with subcutaneous administration of IL-2. Role of IL-5. Int. J. Cancer *54*, 8-15.

Rodolfo,M., Zilocchi,C., Melani,C., Cappetti,B., Arioli,I., Parmiani,G., and Colombo,M.P. (1996). Immunotherapy of experimental metastases by vaccination with interleukin gene-transduced adenocarcinoma cells sharing tumor-associated antigens. Comparison between IL-12 and IL-2 gene-transduced tumor cell vaccines. J. Immunol. *157*, 5536-5542.

Rodolfo,M., Melani,C., Zilocchi,C., Cappetti,B., Luison,E., Arioli,I., Parenza,M., Canevari,S., and Colombo,M.P. (1998). IgG2a induced by IL-12-producing tumor cell vaccines but not IgG1 induced by IL-4 vaccine is associated with the eradication of experimental metastases. Cancer Res. *58*, 5812-5817.

Rosenwasser,L.J., Busse,W.W., Lizambri,R.G., Olejnik,T.A., and Totoritis,M.C. (2003). Allergic asthma and an anti-CD23 mAb (IDEC-152): results of a phase I, single-dose, dose-escalating clinical trial. J. Allergy Clin. Immunol. *112*, 563-570.

Rothenberg,M.E., Owen,W.F., Jr., Silberstein,D.S., Woods,J., Soberman,R.J., Austen,K.F., and Stevens,R.L. (1988). Human eosinophils have prolonged survival, enhanced functional properties, and become hypodense when exposed to human IL-3. J. Clin. Invest *81*, 1986-1992.

Sampson,H.A., Munoz-Furlong,A., Bock,S.A., Schmitt,C., Bass,R., Chowdhury,B.A., Decker,W.W., Furlong,T.J., Galli,S.J., Golden,D.B., Gruchalla,R.S., Harlor,A.D., Jr., Hepner,D.L., Howarth,M., Kaplan,A.P., Levy,J.H., Lewis,L.M., Lieberman,P.L., Metcalfe,D.D., Murphy,R., Pollart,S.M., Pumphrey,R.S., Rosenwasser,L.J., Simons,F.E., Wood,J.P., and Camargo,C.A., Jr. (2005). Symposium on the definition and management of anaphylaxis: summary report. J. Allergy Clin. Immunol. *115*, 584-591.

Segal,D.M., Taurog,J.D., and Metzger,H. (1977). Dimeric IgE serves as a unit signal for mast cell degranulation. Proc. Natl. Acad. Sci. U. S. A *74*, 2993-2997.

Segota,E. and Bukowski,R.M. (2004). The promise of targeted therapy: cancer drugs become more specific. Cleve. Clin. J. Med. *71*, 551-560.

Seminario,M.C., Saini,S.S., MacGlashan,D.W., Jr., and Bochner,B.S. (1999). Intracellular expression and release of FcεRIα by human eosinophils. J. Immunol. *162*, 6893-6900.

Seto,M., Takahashi,T., Nakamura,S., Matsudaira,Y. and Nishizuka,Y. (1983). *In vivo* antitumour effects of monoclonal antibodies with different Immunoglobulin classes. Cancer Res. *43*, 4768-4773.

Shi,H.Z. (2004). Eosinophils function as antigen-presenting cells. J. Leukoc. Biol. *76*, 520-527.

Shi,J., Ghirlando,R., Beavil,R.L., Beavil,A.J., Keown,M.B., Young,R.J., Owens,R.J., Sutton,B.J., and Gould,H.J. (1997). Interaction of the low-affinity receptor CD23/FcεRII lectin domain with the Fcε3-4 fragment of human IgE. Biochemistry *36*, 2112-2122.

Sihra,B.S., Kon,O.M., Grant,J.A., and Kay,A.B. (1997). Expression of high-affinity IgE receptors (FcεRI) on peripheral blood basophils, monocytes, and eosinophils in atopic and nonatopic subjects: relationship to total serum IgE concentrations. J. Allergy Clin. Immunol. *99*, 699-706.

Simon,H.U. and Blaser,K. (1995). Inhibition of programmed eosinophil death: a key pathogenic event for eosinophilia? Immunol. Today *16*, 53-55.

Smith,S.J., Ying,S., Meng,Q., Sullivan,M.H., Barkans,J., Kon,O.M., Sihra,B., Larche,M., Levi-Schaffer,F., and Kay,A.B. (2000). Blood eosinophils from atopic donors express messenger RNA for the α, β, and γ subunits of the high-affinity IgE receptor (FcεRI) and intracellular, but not cell surface, α-subunit protein. J. Allergy Clin. Immunol. *105*, 309-317.

Smurthwaite,L. and Durham,S.R. (2002). Local IgE synthesis in allergic rhinitis and asthma. Curr. Allergy Asthma Rep. *2*, 231-238.

Steplewski,Z., Sun,L.K., Shearman,C.W., Ghrayeb,J., Daddona,P., and Koprowski,H. (1988). Biological activity of human-mouse IgG1, IgG2, IgG3, and IgG4 chimeric monoclonal antibodies with antitumor specificity. Proc. Natl. Acad. Sci. U. S. A *85*, 4852-4856.

Sterk,A.R. and Ishizaka,T. (1982). Binding properties of IgE receptors on normal mouse mast cells. J. Immunol. *128*, 838-843.

Stuart,S.G., Trounstine,M.L., Vaux,D.J., Koch,T., Martens,C.L., Mellman,I., and Moore,K.W. (1987). Isolation and expression of cDNA clones encoding a human receptor for IgG (FcγRII). J. Exp. Med. *166*, 1668-1684.

Sundstrom,C. and Nilsson,K. (1976). Establishment and characterization of a human histiocytic lymphoma cell line (U-937). Int. J. Cancer *17*, 565-577.
Tada,T., Okumura,K., Platteau,B., Beckers,A and Bazin,H. (1975). Half-lives of two types of rat homocytotropic antibodies in circulation and in the skin. Inter. Archs. Allergy appl. Immun. *48*, 116-131.

Sutton,B., Beavil,R. and Beavil,A. (2000). Inhibition of IgE-receptor interactions. British Medical Bulletin. *56*, 1004-1018.

Tepper,R.I., Pattengale,P.K., and Leder,P. (1989). Murine IL-4 displays potent anti-tumor activity *in vivo*. Cell *57*, 503-512.

Tepper,R.I., Coffman,R.L., and Leder,P. (1992). An eosinophil-dependent mechanism for the antitumor effect of IL-4. Science *257*, 548-551.

Theoharides,T.C. and Conti,P. (2004). Mast cells: the JEKYLL and HYDE of tumor growth. Trends Immunol. *25*, 235-241.

Toffoli,G., Russo,A., Gallo,A., Cernigoi,C., Miotti,S., Sorio,R., Tumolo,S. and Boiocchi,M. (1998). Expression of folate binding protein as a prognostic factor for response to platinum-containing chemotherapy and survival in human ovarian cancer. Int. J. Cancer. *79*, 121-126.

Torigoe,C., Goldstein,B., Wofsy,C. and Metzger,H. (1997). Shuttling of initiating kinase between discrete aggregates of the high affinity receptor for IgE regulates the cellular response. Proc. Natl. Acad. Sci. USA. *94*, 1372-1377.

Torigoe,C., Inman,J.K., and Metzger,H. (1998). An unusual mechanism for ligand antagonism. Science *281*, 568-572.

Tutt,A.L., French,R.R., Illidge,T.M., Honeychurch,J., McBride,H.M., Penfold,C.A., Fearon,D.T., Parkhouse,R.M., Klaus,G.G., and Glennie,M.J. (1998). Monoclonal antibody therapy of B cell lymphoma: signaling activity on tumor cells appears more important than recruitment of effectors. J. Immunol. *161*, 3176-3185.

Van Schie,R.C., Verstraten,R.G., Van de Winkel,J.G., Tax,W.J., and de Mulder,P.H. (1992). Effect of recombinant IFN-γ (rIFN-γ) on the mechanism of human macrophage IgG FcRI-mediated cytotoxicity. rIFN-gamma decreases inhibition by cytophilic human IgG and changes the cytolytic mechanism. J. Immunol. *148*, 169-176.

Vercelli,D., Jabara,H.H., Lee,B.W., Woodland,N., Geha,R.S., and Leung,D.Y. (1988). Human recombinant IL-4 induces FcεRII/CD23 on normal human monocytes. J. Exp. Med. *167*, 1406-1416.

von Bubnoff,D., Matz,H., Cazenave,J.-P., Hanau,D., Beiber,T. and de la Salle,H. (2002). Kinetics of gene induction after FceRI ligation of atopic monocytes identified by suppression subtractive hybridisation. J. Immunol. *169*, 6170-6177.

Waldmann,T.A., Iio,A., Ogawa,M., McIntyre,O.R., and Strober,W. (1976). The metabolism of IgE. Studies in normal individuals and in a patient with IgE myeloma. J. Immunol. *117*, 1139-1144.

Wan,T., Beavil,R.L., Fabiane,S.M., Beavil,A.J., Sohi,M.K., Keown,M., Young,R.J., Henry,A.J., Owens,R.J., Gould,H.J., and Sutton,B.J. (2002). The crystal structure of IgE Fc reveals an asymmetrically bent conformation. Nat. Immunol. *3*, 681-686.

Wang,B., Rieger,A., Kilgus,O., Ochiai,K., Maurer,D., Fodinger,D., Kinet,J.P., and Stingl,G. (1992). Epidermal Langerhans cells from normal human skin bind monomeric IgE via FcεRI. J. Exp. Med. *175*, 1353-1365.

Wank,S.A., DeLisi,C., and Metzger,H. (1983). Analysis of the rate-limiting step in a ligand-cell receptor interaction: the IgE system. Biochemistry *22*, 954-959.

Ward,B.G., Wallace,K., Shepherd,J.H., and Balkwill,F.R. (1987). Intraperitoneal xenografts of human epithelial ovarian cancer in nude mice. Cancer Res. *47*, 2662-2667.

Wardlaw,A.J., Moqbel,R., and Kay,A.B. (1995). Eosinophils: biology and role in disease. Adv. Immunol. *60*, 151-266.

Weiner,L.M. and Carter,P. (2005). Tunable antibodies. Nat. Biotechnol. *23*, 556-557.

Weller,P.F. (1991). The immunobiology of eosinophils. N. Engl. J. Med. *324*, 1110-1118.

Wershil,B.K., Mekori,Y.A., Murakami,T., and Galli,S.J. (1987). ^{125}I-fibrin deposition in IgE-dependent immediate hypersensitivity reactions in mouse skin. Demonstration of the role of mast cells using genetically mast cell-deficient mice locally reconstituted with cultured mast cells. J. Immunol. *139*, 2605-2614.

Wexler,H. (1966). Accurate identification of experimental pulmonary metastases. J. Natl. Cancer Inst. *36*, 641-645.

Winter,G., Griffiths,A.D., Hawkins,R.E., and Hoogenboom,H.R. (1994). Making antibodies by phage display technology. Annu. Rev. Immunol. *12*, 433-455.

Winter,G. and Milstein,C. (1991). Man-made antibodies. Nature *349*, 293-299.

Wong,D.T., Weller,P.F., Galli,S.J., Elovic,A., Rand,T.H., Gallagher,G.T., Chiang,T., Chou,M.Y., Matossian,K., McBride,J., and . (1990). Human eosinophils express TGF-α. J. Exp. Med. *172*, 673-681.

Woof,J.M. and Burton,D.R. (2004). Human antibody-Fc receptor interactions illuminated by crystal structures. Nat. Rev. Immunol. *4*, 89-99.

Wurzburg,B.A. and Jardetzky,T.S. (2002). Structural insights into the interactions between human IgE and its high affinity receptor FcεRI. Mol. Immunol. *38*, 1063-1072.

Xia,M.Q., Hale,G., Lifely,M.R., Ferguson,M.A., Campbell,D., Packman,L., and Waldmann,H. (1993). Structure of the CAMPATH-1 antigen, a GPI-anchored glycoprotein which is an exceptionally good target for complement lysis. Biochem. J. *293 (Pt 3)*, 633-640.

Yamashita,T., Mao,S.Y., and Metzger,H. (1994). Aggregation of the high-affinity IgE receptor and enhanced activity of p53/56lyn protein-tyrosine kinase. Proc. Natl. Acad. Sci. U. S. A *91*, 11251-11255.

Yang,P.C., Berin,M.C., Yu,L.C., Conrad,D.H., and Perdue,M.H. (2000). Enhanced intestinal transepithelial antigen transport in allergic rats is mediated by IgE and CD23 (FcεRII). J. Clin. Invest *106*, 879-886.

Young,R.J., Owens,R.J., Mackay,G.A., Chan,C.M., Shi,J., Hide,M., Francis,D.M., Henry,A.J., Sutton,B.J., and Gould,H.J. (1995). Secretion of recombinant human IgE-Fc by mammalian cells and biological activity of glycosylation site mutants. Protein Eng *8*, 193-199.

Yokota,A., Kikutani,H., Tanaka,T., Sato,R., Barsumian,E.L., Suemura,M., and Kishimoto,T. (1988). Two species of human FcεRII (CD23): tissue-specific and IL-4-specific regulation of gene expression. Cell *55*, 611-618.

Yokota,A., Yukawa,K., Yamamoto,A., Sugiyama,K., Suemura,M., Tashiro,Y., Kishimoto,T., and Kikutani,H. (1992). Two forms of the low-affinity Fc receptor for IgE differentially mediate endocytosis and phagocytosis: identification of the critical cytoplasmic domains. Proc. Natl. Acad. Sci. U. S. A *89*, 5030-5034.

Zhu,X., Hamann,K., Munoz,M., Rubio,N., Mayer,D., Hernrreiter,A. and Leff,A. (1998). Intracellular expression of FcγRIII (CD16) and its mobilisation by chemoattractants in human eosinophils. J. Immunol. *161*, 2574.

Zhu,D., Kepley,C.L., Zhang,K., Terada,T., Yamada,T., and Saxon,A. (2005). A chimeric human-cat fusion protein blocks cat-induced allergy. Nat. Med. *11*, 446-449.